An Investigation of the Role of the ErbB Receptor Family in Chemotherapeutic Drug Resistance and Invasion in Human Breast Cancer

A thesis submitted for the degree of PhD.

By

Sharon Glynn B.Sc. Hons

November 2002

The research work described in this thesis was carried out under the supervision of

Prof. Martin Clynes

National Cell and Tissue Culture Centre
School of Biological Sciences
Dublin City University
Glasnevin
Dublin 9
Ireland

I hereby certify that this material, which I now submit for assessment on the programme of study leading to the award of PhD, is entirely my own work and has not been taken from the work of others save and to the extent that such work has been cited and acknowledged within the text of my work.

Signed: _____

ID No.: 97970425

Date: 24/11/2002

Table of Contents

Table of Contents

Abstract

The purpose of the work described in this thesis was to investigate the effects of upregulation of c-erbB-2 by cDNA transfection and the downregulation by ribozyme transfection on chemotherapeutic drug sensitivity, *in vitro* invasion, and expression of a range of mRNA and proteins.

Four novel multidrug resistant variants of the human breast carcinoma cell line, MDA-MB-435S-F, were established by pulse selection with taxol or adriamycin. *In vitro* toxicity tests revealed that the taxol resistant variants, MDA-MB-435S-F/Taxol-10p and MDA-MB-435S-F/Taxol-10p4p were significantly more resistant to taxol, with cross-resistance to vincristine and taxotere, but not to adriamycin, carboplatin, etoposide or 5-fluorouracil. Adriamycin accumulation studies revealed that both variants displayed increased adriamycin efflux. P-glycoprotein and possibly topoisomerases, but not mrp1, mrp2, mrp4, mrp5, DHFR, thymidylate synthase or GST π, were found to play a role in taxol resistance.

MDA-MB-435S-F cells were resistant to adriamycin selection. MDA-MB-435S-F/Adr-10p gained no significant increase in resistance to adriamycin following 10 rounds of exposure to adriamycin, although it did become resistant to VP-16 and was sensitised to vincristine and 5-fluorouracil. MDA-MB-435S-F/Adr-10p10p was slightly resistant to adriamycin, VP-16, taxotere and vincristine. It was sensitised to taxol, 5-fluorouracil and carboplatin. P-glycoprotein, mrp1, mrp2, mrp4 and mrp5 were not altered at the mRNA level in the adriamycin selected variants. Reduced adriamycin accumulation appears to be the mechanism by which MDA-MB-435S-F/Adr-10p10p became slightly resistant to adriamycin.

Drug selection induced c-erbB-1 expression at protein but not mRNA level in MDA-MB-435S-F. C-erbB-3 protein levels fell dramatically after drug selection. Drug selection of MDA-MB-435S-F induced more aggressively invasive cell lines, as defined by the gain of an ability to invade and relocate. This is a novel discovery for this thesis. The aggressive two-staged invasive phenotype appears to be linked to decreased adhesion and motility and perhaps c-erbB-1 induction and c-erbB-3 repression, but not to increased secretion of a range of proteases. C-erbB-2 was not found to play a role.

C-erbB-2 levels as altered by cDNA and ribozyme transfection were found to be positively associated with invasiveness, and accompanied by decreased adhesion to ECM components and protease secretion in the BT474A ribozyme transfected model. An increase in invasion was observed in two of these MCF-7 H3 c-erbB-2 cDNA transfectants but not the third. This was accompanied by reduction in expression of a serine protease, but not by MMP secretion or changes in adhesive properties.

Alteration of c-erbB-2 expression in BT474A and MCF-7 H3 by cDNA and ribozyme transfection resulted in changes in chemotherapeutic drug resistance. These changes correlated between the two models only for adriamycin and 5-fluorouracil. Changes in drug sensitivity to taxol and carboplatin appeared to be cell line specific. C-erbB-2 upregulation in MCF-7 H3 cDNA transfected cell lines resulted in increased c-erbB-3 protein expression and decreased c-erbB-4 mRNA and protein expression. C-erbB-1 was increased at mRNA level, but not protein. Other ErbB receptors were not found to be affected by c-erbB-2 levels in BT474A except for c-erbB-3 protein, which decreased with decreasing c-erbB-2.

Acknowledgements

I would like to express my very sincere thanks to Professor Martin Clynes, firstly, for giving me the opportunity to do a PhD and secondly, for his support, encouragement, guidance and kindness over the past 5 years.

I wish to acknowledge Dr. Kevin Scanlon and Dr. Dihua Yu for their kind gifts of the plasmids used in this thesis.

A very special thanks goes to Dr. Mary Heenan for her fantastic support, guidance and friendship during the course of this PhD.

Thanks to all my colleagues, past and present, in the NCTCC for all the help and advice given to me over the years. A special thanks goes to Dr. Joanne Keenan, Dr. Robert O'Connor, Dr, Yizheng Liang, Dr. Liz Moran, Dr. Annemarie Larkin, Dr. Padraig Doolan and Dr. Carmel Daly for their help on the various techniques used in this thesis.

To my parents Tony and Mary, for being the best parents in the world, for always being there for me and believing in me. To my sister and brothers, Dawn, David and Daryl, fantastic family. To all my extended family, Aideen, Val, Rona and Erin. To my niece and nephew, Aoife and Conor, for giving me plenty of giggles in the last few months.

Thanks to Dee for being my partner in crime to the bitter end! Told you we'd get there, girl!!! Thanks to Trish, Niamh and Dawn for a fantastic friendship and lots of support, especially all those cinema trips! To Sam for the laughs over the years (Missed you for the last year, enjoyed the trip to Tullamore, may there be many more!). To the toxicology lab, past and present, Mary, Colette, Sam, Joanne, Rob, Laura, Bojana, Paula, Denis, Kieran, Rachel, Mags, Lisa, Vanessa, Petra, Roisin, thank god you weren't all present at once, or we'd be like a tin of baked beans!!!! To Bella, Rasha and Paudie, my coffee and lunch partners, kept me sane and got your ears talked of! To Carol, Yvonne and Mairead for your help. To Annemarie and Aine for calming me down and helping me put the thesis together on that final Friday, and Bella for running around the campus for me, and the courier for waiting! To the girls on my volleyball team, The RedCats, Jenny, Fi, Katy, Goretti, Clare, Jennifer, Helen, Rachelle, Caroline, Gemma and Mitchy, thanks for the hilarious laughs, and the celebration at Enniskillen!

A big thank you to everybody else who I have failed to mention, you have not been forgotten.

This thesis is dedicated to my nephew, Killian Glynn

1.0 Introduction

1.1 Incidence of Breast Cancer and Risk Assessment

Breast cancer remains the most common cancer among women (31% of all cancers) and the second highest cause of cancer deaths (15%, second only to lung cancer). Women are considered to have a high risk of cancer if their risk is greater than that of an average 60-year-old woman. Woman under the age of 39 have a 1 in 225 risk of developing breast cancer, this rises to 1 in 24 between the ages of 40 and 59, 1 in 14 between 60 and 79. A woman's overall risk in their lifetime of developing breast cancer is 1 in 8. These figures can be further broken down into three categories as described in table 1.1.

Age interval (years)	Risk of developing breast cancer (%)	Risk of developing invasive breast cancer (%)	Risk of dying from breast cancer (%)
Birth-110	10.2	9.8	3.6
20-30	0.04	0.04	0.00
20-40	0.49	0.42	0.09
20-110	10.34	9.94	3.05
35-45	0.88	0.83	0.14
35-55	2.53	2.37	0.56
35-110	10.27	9.82	3.56
50-60	1.95	1.86	0.33
50-70	4.67	4.48	1.04
50-110	8.96	8.68	2.75
65-75	3.17	3.08	0.43
65-80	5.48	5.29	1.01
65-110	6.53	6.29	1.53

Table 1.1 Risk of developing and dying from breast cancer (white woman, USA).

Risk of developing breast cancer increases with age, the longer a woman lives without breast cancer, the lower her risk over the rest of her life. Other risks are early menarche and late menopause, which are associated with a 30-50% increased risk. This appears to be related to the number of ovulatory menstrual cycles a woman experiences during a life time. Pregnancy at a young age, especially before the age of 20 reduces the risk,

whereas a woman having her first pregnancy after the age of 30 doubles her risk. Non proliferative benign breast lesions do not carry an increased risk of developing into cancer. Benign lesions characterised by epithelial proliferative changes, especially if associated with atypia, is associated with a 4-5 fold increase in risk of breast cancer, which further rises to 11-fold if accompanied by a first-degree relative with breast cancer. Premalignant lesions such as lobular or ductal carcinoma *in situ* are associated with increased risk of subsequent invasive carcinoma. A patient with a prior history of breast cancer is at increased risk for developing cancer in the contralateral breast. This risk is estimated to be at about 1% per year. Development of breast cancer at a young age may be indicative of an underlying predisposition of breast parenchyma to malignant transformation.

A distinction exists between familial and hereditary breast cancer. Familial breast cancer refers to patients having one or more first- or second- degree relatives with breast cancer. Hereditary breast cancer is a subset of familial breast cancer, in which the incidence of breast cancer is related to autosomal dominant highly penetrant cancer susceptibility such as in the hereditary breast-ovarian cancer syndrome. The cumulative probability of a 30-year-old woman, with a sister or a mother with breast cancer, developing breast cancer by the age of 70 is between 7% and 18%. This increases with number of relative having breast cancer, to a maximum of 30%. A woman with a mother and sister with breast cancer has a 25% risk of developing the disease. Several specific gene loci have been identified that play a role in hereditary breast cancer, including BRCA1, BRCA2, p53, PTEN and ataxia-telangiectasia gene. BRCA1 and BRCA2 are the most common in hereditary disease. Among women who carry germ-line mutations the cumulative risk of breast cancer is thought to range between 40% to 85%, and for ovarian cancer 5% to 60% depending on the population from which the figures are derived (Sakorafas *et al.*, 2002).

1.2 Growth Factor Families and Their Receptors

Growth factors and their receptors have been shown to play a major role in cancer development. Most, if not all, cancer cells contain genetic damage that appears to lie at the heart of tumourigenesis. Malignant cells arise as a result of a stepwise progression of genetic events that include the unregulated expression of growth factors or components of their signalling pathways. Cells of most, if not all, major tissue types are targets of growth factors that mediate their activity by means of receptors with intrinsic tyrosine kinase activity. Signalling pathways that mediate the normal function of growth factors are commonly subverted in cancer, leading to uncontrolled proliferation (Aaronson, 1991).

In multicellular organisms communication between individual cells is essential for their regulation and co-ordination of complex cellular processes such as growth, differentiation, migration and apoptosis. The signal transduction pathways mediating these processes are regulated in part by polypeptide growth factors that generate signals by activating cell surface receptors. The primary mediators of such physiological cell responses are receptor tyrosine kinases (RTKs). RTKs can be divided into 20 subfamilies on the basis of their structural characteristics. All RTKs consist of a single transmembrane domain that separates the intracellular tyrosine kinase domain from the extracellular binding domain. The latter exhibit a variety of conserved elements such as immunoglobulin (Ig)-like or epidermal growth factor (EGF)-like domains, fibronectin type III repeats or cysteine-rich regions that are characteristic for each subfamily. The catalytic domain that displays the highest level of conservation includes the ATP-binding site that catalyses receptor autophosphorylation and tyrosine phosphorylation of RTK substrates. Ligand binding to the extracellular domain leads to conformational changes that induce and stabilise receptor dimerisation leading to increased kinase activity and autophosphorylation of tyrosine residues (Zwich *et al.*, 2001).

Aberrant RTK signalling is a major factor in cancer and other hyperproliferative diseases. Constitutive activation of RTKs can occur by several mechanisms, such as gene amplification, overexpression or mutation. Somatic and germline mutations have been observed in at least 10 different RTK families. These alterations include deletion

or mutation within the extracellular domain or alterations in the catalytic domain, resulting in a constitutively active RTK.

RTK families involved in cancer development include the epidermal growth factor receptor (EGFR/ErbB) family (described further in section 1.3), insulin growth factor receptor (IGFR) family, vascular endothelial growth factor receptor (VEGFR) family, fibroblast growth factor receptor (FGFR) family, hepatocyte growth factor receptor (HGFR) family and platelet-derived growth factor receptor (PDGFR) family.

The IGFR family consists of the insulin receptor (IR) and the insulin-like growth factor (IGF) receptor (IGF-IR). Both receptors consist of two extracellular α subunits, which are responsible for ligand binding and two membrane spanning β subunits bearing the tyrosine kinase domain and autophosphorylation sites. Ligands for these receptors include insulin, IGF-I and IGF-II. While insulin is mostly a metabolic hormone, IGF-I and IGF-II are crucial for normal development and carcinogenesis. IGF-IR and its ligands have been found to play a major role in breast and prostate cancer. In primary breast cancer IGF-I and IGF-II are primarily expressed by the stromal fibroblasts surrounding the normal and malignant tissue, whereas IGF-IR is overexpressed in breast cancer with enhanced tyrosine kinase activity.

VEGF is one of the main inducers of endothelial cell proliferation and permeability of blood vessels. The VEGFR family consists of two receptors VEGFR-1 and VEGFR-2, which are expressed on endothelial cells during embryonic development and are the key regulators of angiogenesis. Expansion of tumours beyond 1-2mm requires *de novo* formation of vascular network to provide the tumour with oxygen and nutrients. Many studies have shown a role for the VEGF-VEHGFR ligand-receptor system in tumour vascularisation and metastasis. Tumours secrete VEGF activating VEGFR-2 and thus inducing proliferation of stromal endothelial cells and sprouting of new blood vessels.

The FGFs represents the largest family of growth factors, with over 20 members identified to date. Two classes of FGFRs have been discovered. The first class comprises the four high affinity FGFRs, whereas the second class is defined by low affinity FGF binding sites. Evidence suggests that the by low affinity FGF binding sites represent heparan sulphate proteoglycan molecules (HSPG) located on the cell surface, which may support the fine tuning of cell responses to FGFs. The family of high

affinity FGFRs is composed of FGFR1 (flg), FGFR2 (bck), FGFR3 and FGFR4. Ligand binding of FGF to FGFRs results in dimerisation and phosphorylation of the cytoplasmic tyrosine residues, but full activation is only achieved in the presence of heparan. A remarkable number of FGFs were discovered as genes isolated from tumours due to their ability to induce proliferation or transformation of fibroblasts. This points to the major role these growth factors play in tumourigensis. Changes in the levels of FGFRs, such as point mutations, elevated expression or different splicing, result in disregulated FGFR signalling, and has been observed in breast, prostate, melanoma, thyroid and salivary gland tumours. Somatic mutations in FGFR-3 similar to the activating mutations in skeletal dysplasias have been identified in bladder cancer and in multiple myeloma.

HGFR is encoded by the proto-oncogene met, and was identified as a regulator of a variety of morphogenic processes like cell migration, cell scattering and invasion of extracellular matrices. It is a disulphide-linked heterodimer with a glycosylated extracellular α-chain and a β-chain, which consists of the transmembrane domain and cytoplasmic tyrosine kinase domain. The ligands for HGFR are HGF and scattering factor (SF), which are expressed by mesenchymal-derived cells. HGR overexpression has been described in a variety of tumours, such as thyroid and colorectal carcinomas, and appears to be prognostically significant for non-small cell lung and breast cancer.

Kit, PDGFR-α and PDGFR-β are members of the PDGFR family. These proteins are characterised by an extracellular domain with five Ig-like domains and an intracellular tyrosine kinase domain split by 1000 amino acids. Two genes have been identified encoding PDGFR-α and PDGFR-β and both receptors are activated by a ligand dimer consisting of PDGF-A and/or PDGF-B. This in turn leads to receptor dimerisation with three possible configurations; αα, ββ, αβ. Co-expression of PDGFR and its ligands has been reported in glioblastoma and other astrocytic brain tumours, whereas normal brain tumours do not express these proteins.

1.3 ErbB Receptor Family of Tyrosine Kinase Receptors

The ErbB receptor family consists of type I growth factor receptors, and is made up of four members, c-erbB-1 (EGFR), c-erbB-2 (HER-2/neu), c-erbB-3 (HER-3) and c-erbB-4 (HER-4). These proteins share a similar structure, with an extracellular domain having two elements contributing to ligand binding and two cysteine-rich regions, followed by a transmembrane region. The cytoplasmic domain consists of a tyrosine kinase domain and a carboxy-terminal domain that contains mapped autophosphorylation sites (Graus-Porta *et al.*, 1997). The receptors share 40-50% sequence identity in their extracellular domains, 60-80% identity in their kinase domains and 10-30% identity in their tails. Although the extracellular domain of c-erbB-3 is homologous to those of the other family members its intracellular domain has diverged significantly (Carraway III and Burden, 1995).

1.3.1 ErbB Receptor Ligands

ErbB ligands can be classified into four groups depending on their receptor affinities and specificities. (1) epidermal growth factor (EGF), amphiregulin (AR) and transforming growth factor α (TGFα) which bind to ErbB-1; (2) betacellulin (BTC), epiregulin and heparin binding EGF-like growth factor (HB-EGF) which bind to c-erbB-1 and c-erbB-4; (3) Neuregulins/heregulins NRG1 and NRG2 which are ligands of c-erbB-3 and c-erbB-4, low and high affinity receptors respectively; NRG3 and NRG4 ligands of c-erbB-4. Common to all these growth factors is the EGF domain with six conserved cysteine residues characteristically spaced to form three intramolecular disulphide bridges (Prenzel *et al.*, 2001). After binding to their receptors, EGF-related peptides induce receptor homodimerisation and heterodimerisation, allowing the receptors to signal. Although none of these ligands bind directly to c-erbB-2, they all induce its tyrosine phosphorylation by triggering heterodimerisation and cross-phosphorylation. ErbB receptors have been shown to compete for dimerisation with c-erbB-2. C-erbB-2 has been shown to enhance EGF-induced tyrosine phosphorylation of c-erbB-1 and NRG-induced tyrosine phosphorylation of c-erbB-3 and c-erbB-4. It also potentiates and prolongs the signal transduction pathways elicited by EGF and NRG. C-erbB-2 also increases the affinity of both EGF and NRG for their receptors. These

results suggest that c-erbB-2 acts as a common receptor sub-unit for all the other ErbB receptors (Graus-Porta *et al.*, 1997).

1.3.2 C-erbB-1

C-erbB-1 is a 170kDa glycoprotein translated from mRNA transcripts encoded by a gene on chromosome 7q21. C-erbB-1 is present at fairly low levels in normal breast epithelial cells. It has been found to be overexpressed in 40% of breast cancers, but rarely due to gene amplification (2%). The overexpression of c-erbB-1 is inversely correlated with the presence of estrogen receptors. Overexpression of c-erbB-1 is associated with short relapse-free interval and survival in multivariate analyses. It is also associated with a lack of response to endocrine therapy (Rajkumar and Gullick, 1994). C-erbB-1 is expressed throughout development and in a variety of cell types (Hung and Lau, 1999). The c-erbB-1 signal transduction occurs through two distinct pathways. One is the phosphatidylinositol pathway, which leads to the activation of protein kinase C and increased intracellular calcium concentration. The other is through the ras protein leading to the activation of the MAP kinase cascade. Both these pathways can trigger a mitogenic response (Suo *et al.*, 1998). C-erbB-1 is frequently overexpressed in non-small cell lung, bladder, cervical, ovarian, kidney and pancreatic cancer, and occurs with very high incidence in squamous cell carcinomas of the head and neck (Zwick *et al.*, 2001). A number of c-erbB-1 deletions have been identified in human cancer and most of these mutations alter the extracellular binding domain of the receptor and result in truncated c-erbB-1 with constitutively active kinase function.

1.3.3 C-erbB-2

C-erbB-2 has been mapped to chromosome 17q21. No ligand for c-erbB-2 has been found. Overexpression due to gene amplification has been found in 10-40% of breast cancers, although some carcinomas overexpress c-erbB-2 in the absence of gene amplification (Suo *et al.*, 1998). Transcription of the c-erbB-2 gene generates two mRNAs, a 4.6 kb transcript encoding the full length 185 kDA transmembrane protein and a truncated 2.3 kb transcript encoding only the extracellular domain of the c-erbB-2 protein. Overexpression of c-erbB-2 has been reported in approximately 35% of

ovarian, 30% of prostate, 20% of gastric and 2% of colorectal cancers (Markogiannakis *et al.*, 1997).

High levels of c-erbB-2 expression have been shown to correlate strongly with poor prognosis in breast cancer (Verbeek *et al.*, 1998). Oncogenic activation of c-erbB-2 can occur by deletion of the extracellular domain or by overexpression as previously mentioned. In rats, but not humans, overexpression can occur through a point mutation in the transmembrane domain (Guy *et al.*, 1992). C-erbB-2 receptor activation stimulates signal transduction leading to increased intracellular calcium and increased plasma membrane potential, rapidly inducing c-fos and c-jun, leading to a mitogenic response (Suo *et al.*, 1998).

C-erbB-2 has intrinsic tyrosine kinase activity. To date, no ligands have been found capable of binding directly to c-erbB-2. However it can be activated by all the erbB ligands through heterodimerisation with other ErbB receptors. C-erbB-2 when activated can interact with various cellular proteins, such as Shc, PLC-γ and GAP, which play significant roles in signal transduction. C-erbB-2 is also capable of dimerising with c-erbB-1, c-erbB-3 and c-erbB-4 (Hung and Lau, 1999).

1.3.4 C-erbB-3

C-erbB-3 is located at chromosome 12q13 and is transcribed as a 6.2 kb mRNA, which translates as a 160-180kDa glycoprotein. The higher weight protein is found in breast tumour cells, while the lower is found in human kidney cells. The size difference is thought to be due to levels of glycosylation. In breast tumour cell lines, variable levels of expression are seen, with the highest levels observed in BT-483, MDA-MB-453 and T47-D, intermediate levels seen in ZR75-1, SKBR-3, MDA-MB-175 and MDA-MB-361. It is absent or present in very low levels in MDA-MB-157 and MCF-7. Non-malignant breast cell lines MTSV-1.7, MRSV-2.1 and HBL100 are negative. Most breast cell lines that overexpress c-erbB-2 also overexpress c-erbB-3. It is also interesting to note that the promoter of c-erbB-2 is very similar to c-erbB-3. In primary tumours overexpression of c-erbB-3 is probably due to up-regulation of gene transcription rather than gene amplification. C-erbB-3 overexpression is associated with the presence of nodal metastasis in breast tumours. The gastric cancer cell line MKN45 has been shown to produce a 1.4kb c-erbB-3 transcript at similar levels to the full length

6.2kb transcript. This transcript corresponds to a secreted receptor extracellular domain. 83% of gastrointestinal tumours overexpress c-erbB-3. Squamous cell carcinoma shows 96% overexpression, while adenocarcinomas and adenomas are at 76%. In the normal pancreas, only the islets of Langerham stain for c-erbB-3. The c-erbB-3 kinase domain has two non-conservative amino acid replacements, Histidine 740 and Asparagine 815, at sites completely conserved as glutamic acid and aspartic acid in all other known tyrosine and serine/threonine kinases. C-erbB-3 is a defective tyrosine kinase and lacks stimulatible tyrosine kinase activity (Rajkumar and Gullick, 1994).

It has been shown that c-erbB-3 can be transphosphorylated by c-erbB-1, resulting in phosphatidylinositide-3'-OH kinase recruitment. However, this heterodimer is incapable of coupling with PLC-γ or GAP, thereby making the c-erbB-3 signalling pathway different to those of the other ErbB family members (Hung and Lau, 1999).

1.3.5 C-erbB-4

The c-erbB-4 protein has a molecular weight of 180kDa and its mRNA is expressed at high levels in normal skeletal muscle, heart, pituitary, parathyroid, spleen, breast, testis, brain and kidney. T47-D, MDA-MB-453, BT-474 and H3396 express high levels of c-erbB-4 mRNA. MCF-7, MDA-MB-330 and MDA-MB-361 express intermediate levels, while MDA-MB-231, MDA-MB-157, MDA-MB-468 and SKBR-3 express low or no levels of c-erbB-4 (Rajkumar and Gullick, 1994). Signal transduction of c-erbB-4 may play an important role in cell growth and differentiation, and its expression may be linked to cell differentiation and favourable prognosis in breast cancer (Suo *et al.*, 1998).

C-erbB-4 is localised to chromosome 2q33.3-34. It encodes a 1283 amino acid protein. The extracellular domain of c-erbB-4 is most similar to c-erbB-3, whereas its cytoplasmic domain exhibits a 79% and 77% identity with EGFR and c-erbB-2, respectively. The NRGs, betacellulin and heparin-binding EGF have been shown to function as ligands for c-erbB-4. Downstream, the c-erbB-4 cytoplasmic domain interacts with SH-2-domain containing proteins such as p120-ras GTPase activating protein, SHC, and the p85 subunit of phophatidylinositol-3'-kinase, which activate the mitogen-activated protein kinase pathway (Srinivasan *et al.*, 1998). The study by Srinivasan *et al.* (1998) investigated the distribution of c-erbB-4 in normal human adult

and fetal tissues and in a sample of common human cancers. There was a widespread distribution in both adult and fetal tissues. In cancers there was a loss of expression in most tumours. Loss of expression was noted in 40-80 per cent of adenocarcinomas and up to 100 per cent of squamous cell carcinomas, whereas overexpression was observed in about 10-20 per cent of adenocarcinomas and astrocytomas. In general, the pattern of c-erbB-4 expression in normal tissues and cancers suggests that it tends to be associated with the differentiated compartment.

1.3.6 ErbB Dimerisation and Signalling

C-erbB-2 is a receptor with high transforming activity, which can be transphosphorylated through heterodimerisation with other ErbB receptors. The orphan c-erbB-2 receptor is the preferred heterodimerisation partner for the ErbB receptor family as it decreases ligand dissociation from the receptor heterodimer thus enhancing and prolonging the activation of signal transduction.

Figure 1.3.6a Receptor dimerisation.

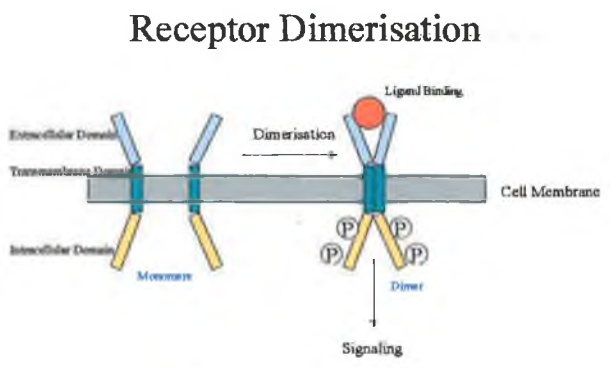

Figure 1.3.6a shows the variety of signals activated by the ErbB receptors depending on their dimerisation partners and the ligand occupying their extracellular domains. C-erbB-2 is the preferred heterodimerisation partner for all other ErbB receptors. By the binding of EGF-like ligands to the extracellular domain of their respective receptors, these peptides can induce both homo- and heterodimerisation. Although none of these ligands bind directly to c-erbB-2, all of them induce its tyrosine phosphorylation by triggering heterodimerisation and cross-phosphorylation. C-erbB-1, c-erbB-3 and c-erbB-4 receptors have been shown to compete for dimerisation with c-erbB-2. C-erbB-2

has been shown to enhance EGF-induced tyrosine phosphorylation of c-erbB-1 and NRG-induced tyrosine phosphorylation of c-erbB-3 and c-erbB-4. It also potentiates and prolongs the signal transduction pathways elicited by EGF and NRG. C-erbB-2 also increases the affinity of both EGF and NRG for their receptors.

Figure 1.3.6b represents the signalling combinations inducible by the ErbB receptor family members.

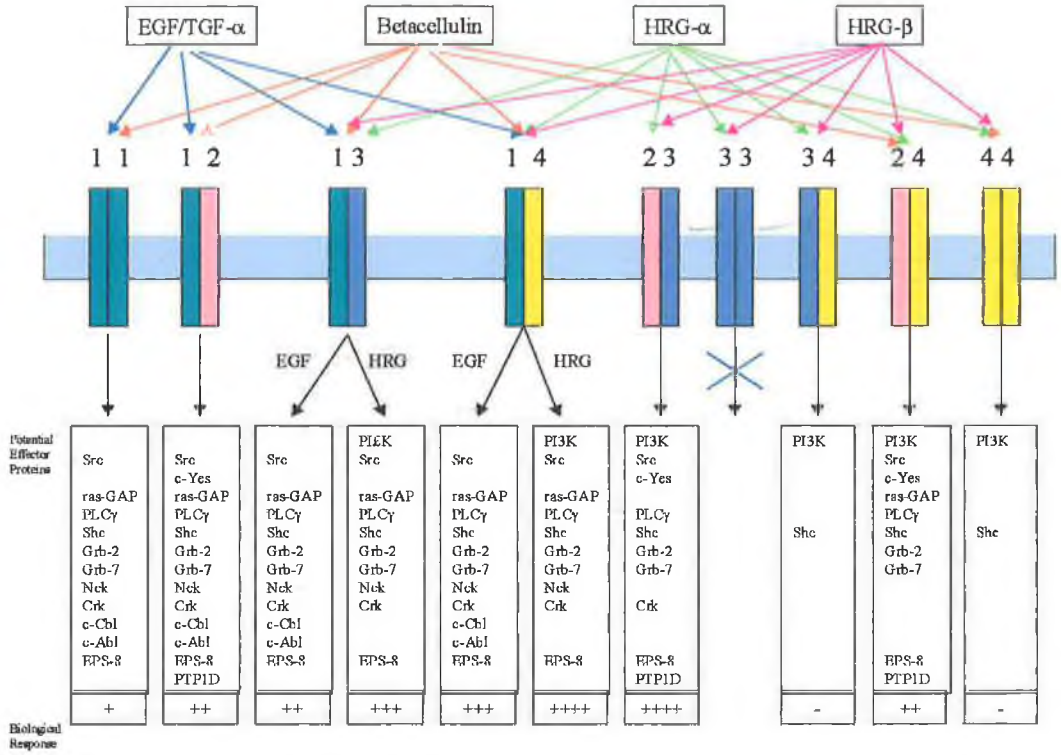

NRG activates c-erbB-3 and c-erbB-4 heterodimerisation with EGFR only when there is no available c-erbB-2. EGF and BTC induced activation of c-erbB-3 is impaired in the absence of c-erbB-2. C-erbB-2 also enhances c-erbB-3 phosphorylation and association with p85, a subunit of phosphatidylinositol-3-kinase. These results suggest that c-erbB-2 acts as a common receptor subunit of all the other ErbB receptors (Graus-Porta *et al.*, 1997).

Gamett *et al.* (1997) provided evidence for a new mechanism of growth factor stimulated receptor dimer formation. They stated that the growth factor induced dimerisation and ensuing receptor trans-phosphorylation results in the disassociation of the original receptor dimer. Each phosphorylated receptor monomer then interacts with a new unphosphorylated receptor to form a secondary dimer. EGF was found to induce c-erbB-2/c-erbB-3 secondary receptors and NRG was found to induce c-erbB-2/EGFR

secondary dimers. This is backed up by the fact that following c-erbB-2/c-erbB-3 heterodimerisation induced by NRG, c-erbB-3 disassociates from c-erbB-2 and forms a complex with p85, the regulatory subunit of phosphatidylinositol-3-kinase.

Olayioye *et al* (1998) constructed NIH3T3 cell lines expressing c-erbB-1 and c-erbB-2 singularly and in pairwise combinations with each of the erbB family members. They found that when c-erbB-1 was activated by EGF it was capable of coupling to both Shc and Grb2, but when activated by NRG (i.e. through heterodimerisation) it was only capable of interacting with Shc. EGF-activated c-erbB-1 was rapidly internalised, whereas NRG -activated c-erbB-1 showed delayed internalisation characteristics. The p85 subunit of phosphatidylinositol-3-kinase associated with EGF-activated c-erbB-1 in a biphasic manner and with NRG -activated c-erbB-1 in a monophasic manner. C-erbB-2 binding to peptides containing the Src homology 2 domain of Grb2 or p85 and the phosphotyrosine binding domain of Shc varied according to the mode of receptor activation. Tryptic phosphopeptide mapping of both c-erbB-1 and c-erbB-2 revealed that receptor phosphorylation is dependent on dimerisation partner. Differential receptor phosphorylation may therefore be the basis for the differences in signalling properties observed. The biological responses triggered by c-erbB-2 are varied. C-erbB-2 can trigger transformation, monoclonal antibody-induced growth inhibition, ligand induced growth stimulation, and apoptosis. Coupling of a given receptor to specific intracellular signalling proteins is modulated by the dimerisation partner and indeed originates from differential receptor phosphorylation. Internalisation of an ErbB receptor is influenced by its ligand and dimerisation partner. The subsets of signalling molecules that couple to an activated receptor undergo time-dependant changes, suggesting that ErbB receptor phosphorylation is not static.

Cohen *et al* (1996) created a collection of NIH3T3 cell lines expressing each member of the ErbB family singularly or in pairs. Transformation (measured by growth in soft agar) occurred only in those clones that expressed two different family members, and the presence of the appropriate ligand. None of the cell lines expressing single erbB members were able to form tumours in mice. C-erbB-2 was tumourigenic when expressed with c-erbB-1 or c-erbB-3, but not with c-erbB-4. They also found that the activation of c-erbB-1 was necessary for the induction of a calcium flux and the phosphorylation of phospholipase Cγ1. In the absence of an added ligand, the steady state level of a c-erbB receptor phosphorylation is affected by the co-expression of other

c-erbB family members. C-erbB-1 phosphorylation is elevated when expressed alone or in combination with c-erbB-3. When it is co-expressed with either c-erbB-2 or c-erbB-4 levels of phosphorylation drop. C-erbB-2 phosphorylation is elevated, except when expressed with c-erbB-3. C-erbB-3 phosphorylation is stimulated when co-expressed with c-erbB-1 or c-erbB-2 but not c-erbB-4. C-erbB-4 is high when expressed alone or with c-erbB-1 but not with c-erbB-2 or c-erbB-3. This would suggest that receptor complexes can form in the absence of the necessary ligands, and the phosphorylation of these complexes is differentially regulated. C-erbB-3, while a defective kinase, does show a weak response to NRG.

Figure 1.3.6c demonstrates the diversity of signalling pathways initiating from c-erbB-2.

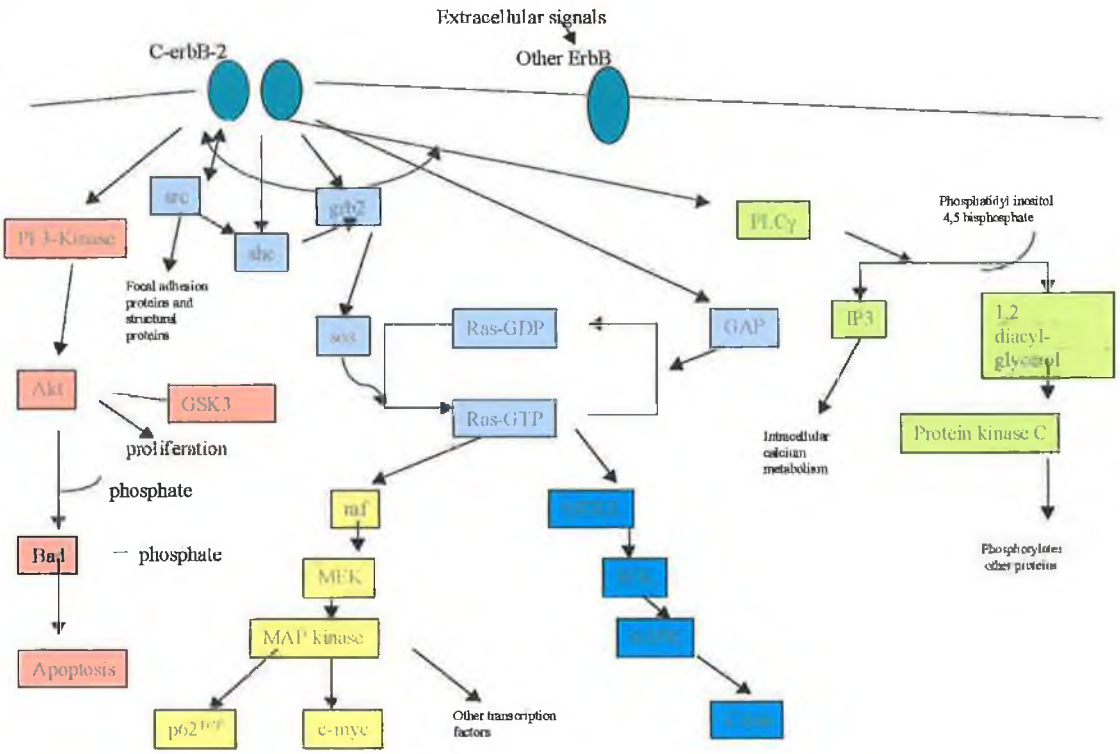

T47D, a breast tumour cell line, expresses all of the ErbB members at moderate levels. Beerli *et al.* (1996) used this cell line to study which of the receptors were activated by the following ligands - EGF, transforming growth factor α (TGFα), amphiregulin (AR), heparin binding EGF (HB-EGF), betacellulin (BTC) and neu differentiation factor (NRG). All except NRG stimulated phosphorylation of c-erbB-1. All except AR were able to stimulate the phosphorylation of c-erbB-2. EGF, TGFα, and AR only had a moderate effect on c-erbB-3. NRG, HB-EGF and BTC significantly stimulated

association of phosphotidylinositol with c-erbB-3. HB-EGF induced low levels of c-erbB-4 tyrosine phosphorylation, while BTC was as efficient as NRG.

Tzahar *et al.* (1997) investigated the mechanism of ligand induced erbB receptor dimerisation. Two molecular mechanisms were compared. (1) Binding of the monomeric ligand induces a conformational change similar to the alteration noted in soluble EGFR after EGF binding, which exposes a cryptic receptor dimerisation site. (2) The second mechanism assumes that EGF-like ligands are bivalent, like in the case of the growth hormone and its receptor. The growth hormone uses two different sites to bind two receptor molecules sequentially. The first binding is diffusion controlled and the second is enhanced by the formation of direct receptor contact areas. Analysis of NRG induced c-erbB-2/c-erbB-3 heterodimerisation shows the use of the second, bivalence model. The ligand simultaneously binds both receptors, but due to its extremely low affinity for c-erbB-2, it only succeeds when the receptors are membrane bound. The full length NRG β2 binds the extracellular domain of c-erbB-3 with a dissociation constant of 26±9nM, while it shows a 1000-fold weaker binding for c-erbB-2 (Horan *et al.*, 1995).

Combinatorial ligand/receptor/effector interactions allow large potential for signal diversification of the ErbB receptor family. Waterman *et al.* (1998) addressed the possibility that turn-off mechanisms enhance the diversification potential. Signalling patterns stimulated by all erbB receptors are all directed through the same MAPK pathway. However unlike the shared rapid MAPK coupling, the kinetics of MAPK inactivation depends on the identity of the stimulating receptor. Concentrating on c-erbB-1 and two of its ligands, EGF and TGF-α, and NRG and one of its receptors, c-erbB-3, they showed that ligand binding variably accelerates endocytosis of the respective ligand-receptor complex. However, unlike the EGF-activated c-erbB-1, which is destined primarily to degradation in lysosomes, NRG and TGF-α direct their receptors to recycling, probably because these ligands dissociate from their receptors earlier along the endocytic pathway. In the case of NRG, structural, as well as biochemical, analyses imply that ligand degradation occurs at a relatively late endosomal stage. Attenuation of receptor down-regulation by this mechanism apparently confers to both NRG and TGF-α more potent and prolonged signalling activity. Alternative endocytic trafficking of ligand-ErbB complexes may tune and diversify signal transduction by EGF family ligands.

1.4 The Role of the ErbB Receptor Family in Cancer

1.4.1.The Role of c-erbB-1 in Human Cancers

Elevated levels of c-erbB-1 and/or its cognate ligands has been identified as a common component of multiple cancer types and appears to promote solid tumour growth. More than 200 studies were identified by Nicholson *et al.* (2001) that analysed relapse-free-interval or survival data directly in relation to c-erbB-1 levels in over 20000 patients. Analysis of the data showed that 10 cancer types both express elevated levels of c-erbB-1 relative to normal tissues and have been studied in sufficient depth to allow sound judgements to be made concerning the association between c-erbB-1 and patient outlook. C-erbB-1 was found to act as a strong prognostic indicator in head and neck, ovarian, cervical, bladder and oesophageal cancers. In these cancers, increased c-erbB-1 expression was associated with reduced recurrence-free or overall survival rates in 70% of studies. In gastric, breast, endometrial and colorectal cancers, c-erbB-1 provided more modest prognostic information, correlating to poor survival rates in 52% of studies, while in non-small cell lung cancer (NSCLC), c-erbB-1 expression only rarely related to patient outlook.

Overexpression and/or amplification of c-erbB-1was observed in 22.00% of infiltrating ductal carcinoma breast tumours (n=315). 16% were grade I, 61% grade II and 23% grade III tumours. Axillary lymph node metastasis had significant correlation with intensified positivity of c-erbB-1 ($p < 0.05$). A significant number of c-erbB-1 positive patients developed local recurrence and distant metastases to brain, liver and bone ($p < 0.05$). c-erbB-1 positivity showed significant correlation with the disease-free and overall survival ($p < 0.05$). At a median follow-up of 48 (4 years) months in c-erbB-1 positive patients, the overall survival was 3.39 years and disease-free survival was 2.86 years. C-erbB-1 negative tumour patients showed a better survival (Aziz *et al.*, 2000). Suo *et al.* (2001) also detected c-erbB-1 expression in 43.9% of primary breast carcinomas (n=107). In contrast they detected no significant associations between the expressions of c-erbB-1 and overall survival.

Immunohistochemical staining for c-erbB-1 was performed on frozen sections of primary breast cancer from 1029 patients with a mean follow-up duration of 46 months.

C-erbB-1 was positive in 26.9% of cases which inversely correlated with the estrogen receptor (ER) status. A univariated analysis indicated that c-erbB-1 had a significant prognostic value in both the disease free survival (DFS) and the overall survival (OS), in both node negative and node positive breast cancer. A multivariate analysis indicated that c-erbB-1 was an independently significant prognostic factor for DFS ($p = 0.0174$) and OS ($p = 0.0105$) in all patients, but that c-erbB-1 demonstrated a prognostic significance only for DFS ($p = 0.0241$) in node negative and only for OS ($p = 0.0333$) in node positive breast cancer. Multivariate analysis indicated that the combination of c-erbB-1(+)/ER(-) was an independently significant factor for both DFS and OS in node negative as well as node positive breast cancer (Tsutsui *et al.*, 2002).

100 breast carcinoma patients with a follow up of 7-11 years were included in a study of ErbB family members, using immunohistochemistry and RT-PCR (Suo *et al.*, 2002). By immunohistochemistry, 36%, 27%, 26%, and 82% of the tumours were positive for c-erbB-1, c-erbB-2, c-erbB-3, and c-erbB-4. All the immunoreactive tumours were confirmed positive by RT-PCR. Statistical analysis of ErbB family members in these tumours showed a significant association between c-erbB-2 expression and reduced disease-free and cancer-specific survival. C-erbB-4 expression was associated with a more favourable outcome. Co-expression of c-erbB-2 and c-erbB-1 was associated with a worse prognosis. C-erbB-4 expression, however, showed an antagonistic effect on the clinical influence of c-erbB-2 expression.

Tumour c-erbB-1 levels were determined by a specific ligand binding assay in 780 consecutive breast cancer patients between 1980 and 1993. All patients had undergone tumour resection with axillary lymph node dissection: 373 patients (47.8%) underwent mastectomy, 37 (5%) subcutaneous mastectomy and 370 (47.2%) tumorectomy. Only a small proportion of patients exhibited a relatively marked c-erbB-1 expression. There was no link between tumour size, grade, node status and c-erbB-1 tumoural levels. There was a constant and significant decrease in c-erbB-1 tumoural levels according to patient age. A significant inverse relationship was found between ER and c-erbB-1 (Ferrero *et al.*, 2001).

Approximately 65% to 70% of human colon carcinomas have been shown to express c-erbB-1. Several investigators have reported that c-erbB-1 expression correlates with more aggressive disease and a poorer prognosis (O'Dwyer *et al.*, 2002). Lee *et al.*

(2002) examined the role of the ErbB family in the neoplastic transformation of the human colon by immunohistochemical analysis in paraffin-embedded specimens from 125 resected colorectal cancers. Data showed that for c-erbB-1 expression, 50% were scored as '+', 2% as '++'. For c-erbB-2 expression, 31% were classified as '+', and 4% as '++'. For c-erbB-3 expression, 34% were scored as '+', and 2% as '++'. A significantly higher percentage of overexpressed c-erbB-3 was observed in early stage carcinomas (Dukes' stage A or B) (50%) than in advanced stage cancers (Dukes' stage C or D) (15%) ($P<0.0001$). For c-erbB-4 expression, 18% were scored as '+', and 4% as '++'. Early stage patients had a lower percentage of c-erbB-4 overexpression than the late stage ones (18% versus 28%). Concomitant overexpression of c-erbB-2 and c-erbB-3 occurred in 21% of the early stage carcinomas, whereas it occurred in only 2% of the late stage ones ($P=0.003$). Conversely, simultaneous overexpression of c-erbB-2 and c-erbB-4 occurred in 17% of the late stage carcinomas but in only 4% of the early stage ones ($P=0.02$). Overexpression of c-erbB-1, c-erbB-2, c-erbB-3 and c-erbB-4 alone was not significantly associated with a shortened survival. However, patients with a simultaneous overexpression of c-erbB-2 and c-erbB-4 had a shorter OS time than others in the univariate analysis ($P=0.01$). This significance disappeared after adjustment for Dukes' staging in the Cox model.

76 paraffin-embedded sections from consecutive stage IIIC-IV ovarian cancer patients with measurable disease after first surgery were examined for expression of COX-2, c-erbB-1, and c-erbB-2. No association was found among COX-2, c-erbB-1, and c-erbB-2. COX-2 positivity was found in a statistically significant higher percentage of unresponsive cases (80.0%) than in patients responding to chemotherapy (35.7%) ($P = 0.0008$) (Ferrandina *et al.*, 2002).

Vered *et al.* (2002) performed a study of 34 samples of formalin-fixed, paraffin-embedded specimens of salivary gland adenoid cystic carcinoma (ACC) and their expression of c-erbB-1. Overlying oral mucosa and adjacent normal salivary ducts served as internal controls. Both membrane and cytoplasmic staining were evaluated. In the final analysis 27 of the 34 specimens were included; 7 were excluded, because the internal control did not reveal any staining. Of these 27 specimens, 85% stained positively for c-erbB-1.

Storkel *et al.* (1993) investigated 100 cases of oral squamous cell carcinomas (SCC) immunohistologically with respect to the expression of c-erbB-1 and the proliferating cell nuclear antigen (PCNA). In conclusion, the amount of antigen expression of both antigens increased with the increasing grade of malignancy of the SCC. Furthermore, there was a statistically significant correlation between the amount of antigen expression and the patient's prognosis. An overexpression of c-erbB-1 and PCNA was associated with a short survival of the patient. Oppositely, c-erbB-1 positivity was protective against locoregional relapse of oral and oropharyngael SCC (Smith *et al*, 2001).

Brabender *et al.* (2001) studied the association between the mRNA expression of c-erbB-1 and c-erbB-2, and survival in primary tumour and matching nonmalignant tissues from 83 patients with NSCLC. Analysis was performed using a quantitative real-time PCR system. C-erbB-1 and c-erbB-2 mRNA expression was detectable in all specimens analysed. 34.9% of patients had high c-erbB-2 expression, and 33.7% of patients had high c-erbB-1 expression. A high c-erbB-1 and c-erbB-2 coexpression was detectable in 16.9% of patients. High c-erbB-2 expression was associated with inferior survival ($P = 0.004$), whereas high c-erbB-1 expression showed a trend toward inferior survival ($P = 0.176$). The impact of c-erbB-1 and c-erbB-2 coexpression on patients' survival was additive ($P = 0.003$). Multivariate analysis determined high c-erbB-1 and c-erbB-2 coexpression ($P = 0.030$) as significant and independent unfavourable prognostic factors.

1.4.2 The Role of c-erbB-2 in Human Cancers

Pfeiffer *et al.* (1996) examined 186 unselected and systemically untreated patients with non-small cell lung cancer (NSCLC) for c-erbB-2 and c-erbB-1 status. C-erbB-1 was found to be highly expressed in 55% of tumours while c-erbB-2 was highly expressed in 26% of tumours. The expression of c-erbB-1 was higher in squamous cell carcinoma, while c-erbB-2 was highest in adenocarcinomas. Overexpression of these receptors was found to have no correlation with prognosis. In contrast, Tsai *et al.* (1996) reported that the intrinsic chemosensitivity of NSCLC cells correlated well with the expression of c-erbB-2, and transfection of c-erbB-2 cDNA into low c-erbB-2 expressing NSCLC significantly enhanced chemoresistance to adriamycin, cisplatin, mitomycin C and VP-16 (Tsai *et al*, 1996).

The majority of normal ovarian tissues express low levels of c-erbB-2. Therefore only tumours that express greater levels of c-erbB-2 can be considered overexpressers. A noted consistency of expression between primary tumours and metastatic sites has been found. No change in expression is seen over time. C-erbB-2 is overexpressed in approximately 30% of ovarian cancers. Some researchers have shown a positive correlation between overexpression and poor prognosis. On the other hand, other reports have shown no adverse prognostic significance for c-erbB-2 overexpression. No correlation was found between c-erbB-2 overexpression and clinicopathological factors such as age, stage, cell type, histological grade, residual tumour after primary cytoreduction or the likelihood of a negative re-exploration after chemotherapy. However, the uniformly poor prognosis for ovarian cancer may effect these results. Clear cell tumours have been found to have an increase in overexpression, with 68% showing overexpression, as opposed to 9% of other cells (Cirisano and Karlan, 1996).

Overexpression of c-erbB-2 has been found in 27% of patients with metastatic disease, as opposed to 4% of patients with disease confined to the uterus. Overexpression correlated with established prognostic variables of grade, stage, depth of invasion, more aggressive disease and disease-related mortality. Heavy staining of cell membrane correlated with 56% 5-year survival, intermediate staining correlated with 83% 5-year survival and negative staining correlated with 95% 5-year survival (Cirisano and Karlan, 1996).

Of 396 adenocarcinomas of the stomach, 10.1% overexpressed c-erbB-2. This overexpression broke down as 15.2% of well differentiated tumours and 3.0% of undifferentiated tumours, showing that c-erbB-2 overexpression is more prevalent in well differentiated gastric tumours. Gene amplification was detected in all the overexpressing tumours (Ooi *et al.*, 1997).

1.4.3 The Role of c-erbB-3 in Human Cancers

C-erbB-3 protein expression was investigated immunohistochemically in a series of 97 malignant breast tumours. 28.8% of cases displayed overexpression, 32% displayed normal levels and 39.2% of cases were c-erbB-3 negative. C-erbB-3 overexpression was positively but not significantly related to negative lymph node status. 21% of lymph

node positive patients as opposed to 41% of lymph node negative patients showed c-erbB-3 overexpression, accompanied by a positive association between c-erbB-3 overexpression and improved survival over a 10-year follow-up period, but it did not achieve statistical significance (Quinn *et al.*, 1994).

Bobrow *et al.* (1997) studied 57 cases of ductal carcinoma *in situ* of the breast (DCIS) by immunocytochemical methods. Staining was either absent (29.8%), present at levels equivalent to that found in adjacent normal tissue (35%) or greater than in normal tissue (35%). In most cases the pattern of staining was cytoplasmic, but in 4 cases with the most intense reaction there was also focal membrane staining. Each of these 4 cases were poorly differentiated. Positive staining was present in 24 poorly differentiated, 8 intermediately differentiated and 8 well differentiated tumours. In the same series of cases, c-erbB-2 protein had previously been shown to be overexpressed in 49% of cases, c-erbB-2 overexpression was correlated with normal level of c-erbB-3, and lack of c-erbB-2 expression was correlated with c-erbB-3 overexpression.

Maurer *et al.* (1998) determined whether c-erbB-3 is found in normal human colon and whether its expression is altered in colorectal cancer in 35 colorectal cancer patients. They also included c-erbB-2 and c-erbB-1 in their analysis to determine their coexpression with c-erbB-3. Normal human colon showed weak c-erbB-3 and c-erbB-2 immunostaining, predominantly in surface epithelial cells. C-erbB-1 immunoreactivity in normal colon varied from weak to strong. In contrast, in 89% and in 83% of colonic cancers, moderate to strong immunoreactivity for c-erbB-3 and c-erbB-2, respectively, was present in most epithelial cancer cells. A concomitant c-erbB-3 and c-erbB-2 immunostaining advantage could be found in 77% of cancerous tissues in comparison with the normal colon. No difference in c-erbB-1 immunostaining was evident between normal colon and cancer. mRNA levels of c-erbB-3 and c-erbB-2 were found to be increased in 64% of cancers in comparison with normal colon samples. 85% of cancers with c-erbB-3 mRNA overexpression showed an increase in c-erbB-2 mRNA. C-erbB-1, however, was decreased in cancer on mRNA level. These findings indicate that c-erbB-2 and c-erbB-3, but not c-erbB-1, may contribute to tumour growth and disease progression in colon cancer.

Funayama *et al.* (1998) studied the overexpression of c-erbB-3 in human SCC. They analysed human SCC cells (A431, SAS and Ca-9-22) for c-erbB-3 gene amplification,

but found no difference between them and normal cells (HFF and TIG-7). Using two sets of primers, one corresponding to the transmembrane form of c-erbB-3 and the other, the secreted form of c-erbB-3, which yields bands of 564bp and 520bp, they found that both types of c-erbB-3 mRNA were overexpressed in oral SCC cell lines and their expression varied in SCC cell lines. Both c-erbB-1 and c-erbB-3 were found to be overexpressed in SCC. C-erbB-3 mRNA was found to be overexpressed at levels 3-5-fold greater in metastatic tumours of nude mice as compared to the primary transplanted tumour.

C-erbB-3 and c-erbB-4 protein expression was analysed using immunohistochemistry in 138 fresh-frozen thyroid tissue samples from 106 patients, including 56 cases of papillary thyroid carcinoma. Increased expression of c-erbB-3 and c-erbB-4 proteins was observed in papillary carcinomas compared to non-neoplastic thyroid tissue. No c-erbB-3 expression was found in any of the normal thyroid tissue samples. Coexisting overexpression of c-erbB-1, c-erbB-2, c-erbB-3, and c-erbB-4 was demonstrated in 64% of papillary thyroid carcinomas. These findings suggest a common regulatory mechanism for the ErbB family of receptors in papillary thyroid carcinomas and provide numerous possibilities for functional receptor interactions (Haugen *et al.*, 1996).

Rajkumar *et al.* (1993) examined the expression of the c-erbB-3 protein in a wide range of tumours of the gastrointestinal (GI) tract using immunocytochemical staining. C-erbB-3 protein was found in normal epithelial cells throughout the GI tract, in squamous epithelium of the oropharanyx and oesophagus, in the parietal cells of the stomach, and in the surface enterocytes of the small and large bowel. 76 tumours arising at these sites were examined for c-erbB-3 protein expression. Widely varying levels of expression were seen, from absent to intense staining with cell membrane accentuation.

1.4.4 The Role of C-erbB-4 in Human Cancers

Merimsky *et al.* (2002) assessed the possible role of c-erbB-4 as a tissue marker for soft-tissue sarcomas (STS) and its correlation with the response to chemotherapy. The histological specimen of 29 patients with STS of a limb who had received pre-operative adriamycin-based chemotherapy were studied for the degree of necrosis and the expression of c-erbB-4. C-erbB-4 expression in the pre-operative tissue samples was compared with the expression in the postchemotherapy resected tumour. The true

objective response rate to pre-operative chemotherapy was 34%. The tumour necrosis was above 90% in 9 patients, 60-90% in 12, and less than 60% in 7 patients. An increase in c-erbB-4 expression was more common in cases with no response to chemotherapy, while no change or a decrease in c-erbB-4 was more common in responsive tumours (P=0.004). No correlation could be found between the degree of necrosis or the chemotherapeutic regimen and the change in expression of c-erbB-4. The median DFS was longer for patients with a decrease or no change in expression of c-erbB-4. It is believed that postchemotherapy new expression or lack of downregulation of the c-erbB-4 molecule represents tumour aggressiveness and increased capability of growth and spread.

Gilmour *et al.* (2001) reported that immunohistochemical expression of c-erbB-4 protein was identified in 93% of ovarian cancers (n=53) using the HFR-1 antibody (targeted to the cytoplasmic domain of the erbB4 receptor) and in 89% of ovarian cancers using the H4.77.16 antibody (targeted to the extracellular domain). Tumours of serous histology were more likely to express a higher level of c-erbB-4 than endometrioid tumours, and for stage III serous tumours, long-term survival was associated with moderate to high coexpression of c-erbB-4 and c-erbB-2. Within ovarian cancer cell lines, high c-erbB-4 expression was associated with cisplatin resistance. Using RT-PCR, the presence of multiple isoforms of c-erbB-4 mRNA was identified in both ovarian primary tumours and cell lines. Splice variants in the juxtamembrane (JM-a and JM-d) and cytoplasmic (CT-a and CT-b) regions were identified in mRNA of both cell lines and primary tumours. Scoccia *et al.* (1998) detected expression of c-erbB-1, c-erbB-2 and c-erbB-3, but failed to detect c-erbB-4 in ovarian carcinomas (17 serous cystadenocarcinomas).

Granulosa cell (GC) tumours represent approximately 7% of all malignant ovarian neoplasms. Ten out of 12 granulosa tumours expressed c-erbB-4 at moderate to high levels in >50% of cancer cells, whereas c-erbB-2 (6 out of 12) and c-erbB-3 (2 out of 12) were expressed less frequently (Furger *et al.*, 1998).

Al Moustafa *et al.* (1999) reported on the differential expression of c-erbB-2, c-erbB-3 and c-erbB-4, and their ligand NRGα, in normal bronchial epithelial, and NSCLC cell lines. Expression of c-erbB-2 and c-erbB-3 vary from very low to a high level in NSCLC cell lines and a low level in normal bronchial cells. In contrast, c-erbB-4 was

detected only in NSCLC cell lines but not in normal bronchial cells. NRGα is expressed at intermediate levels in the normal and cancer cell lines studied. Immunoprecipitation, using antibodies to c-erbB-2, c-erbB-3 or c-erbB-4 receptors, coupled to phosphotyrosine Western blot analysis indicates that these three receptors are constitutively tyrosine phosphorylated in lung cancer cell lines, but only c-erbB-2 and c-erbB-3 are autophosphorylated in normal cells. These data suggest that constitutive activation of c-erbB-2, c-erbB-3 and c-erbB-4 receptors could be induced by NRGα via an autocrine loop mechanism, and that the active forms of c-erbB-4 may cooperate with the other members of the EGF-receptor family in human lung carcinogenesis.

Graber *et al.* (1999) reported that c-erbB-4 mRNA expression decreased 6-fold in the non-metastatic stages of pancreatic cancer when compared to tumours with lymph node or distant metastases or to the normal pancreas. In addition, immunohistochemistry demonstrated that in the normal pancreas, the c-erbB-4 antigen was predominantly present in the cell membrane and cytoplasm of the ductal and acinar cells and at a much lower level, in islet cells. In pancreatic cancer, 61 out of 75 samples exhibited weak to moderate immunoreactivity for c-erbB-4 in the tumour cells. Moreover, in the peri-tumorous region with chronic pancreatitis-like morphological changes, there was weak-to-moderate c-erbB-4 immunostaining in small ductules and degenerating acinar cells.

Co-overexpression of c-erbB-2 and c-erbB-4 was found to be associated with a shorter overall survival time in colorectal cancer patients (Lee *et al.*, 2002).

Bei *et al.* (2001) compared the expression of all four ErbB receptors by immunohistochemistry, using receptor-specific polyclonal antisera, in 32 invasive, 11 *in situ* carcinomas, 6 benign lesions, and 22 samples of histologically normal mucosa adjacent to specimens of carcinoma originating from oral cavity epithelium. Among invasive and *in situ* carcinoma, c-erbB-1 expression was the most prevalent (in 29/32 and 8/11 cases, respectively) followed by c-erbB-2 (17/32 and 2/11) and c-erbB-4 (9/32 and 1/10), while c-erbB-3 was only detected in invasive tumours (12/32). Specific patterns included invasive tumours with expression of c-erbB-1 (8/32) or c-erbB-4 (1/32) alone, as well as different receptor combinations (c-erbB-1+c-erbB-2, c-erbB-1+c-erbB-4, c-erbB-1+c-erbB-2+c-erbB-3, c-erbB-1+c-erbB-2+c-erbB-4, and all four receptors). Simultaneous expression of three or four ErbB receptors correlated with tumour invasion. Some benign lesions and histologically normal mucosa adjacent to

carcinomas showed weak immunostaining of c-erbB-1 (10/28), c-erbB-2 (4/28) or c-erbB-4 (3/28). By comparison, overexpression, as indicated by increased staining intensity, was observed in invasive tumours for c-erbB-1 (18/32), c-erbB-2 (8/32), c-erbB-3 (3/32), and c-erbB-4 (3/32). Statistical evaluation demonstrated a significant association of c-erbB-1 or c-erbB-2 overexpression with invasive carcinoma when compared with benign lesions and apparently normal epithelium.

The expression patterns of ErbB receptors was determined by immunohistochemistry in primary human bladder cancer (n = 245) and compared with conventional biological indicators for their prognostic significance. Expression of c-erbB-1, c-erbB-2, c-erbB-3, or c-erbB-4 receptors was detected in 72.2, 44.5, 56.3, and 29.8% of bladder cancer cases, respectively. Important indicators in association with patient survival were tumour staging (P = 0.017), c-erbB-2 (P = 0.018), c-erbB-1-c-erbB-2 (P = 0.023), and c-erbB-2-c-erbB-3 (P = 0.042) (Chow *et al.*, 2001).

There is a significant relationship between tumour cell expression of c-erbB-4, and aggressive tumour phenotype in childhood medulloblastoma. Two alternative juxtamembrane (JM) isoforms of the c-erbB-4 receptor have been described. Termed JMa and JMb, these variants possess different receptor processing and ligand-binding characteristics. The pattern of c-erbB-4 JM isoform expression in 78 pediatric medulloblastomas was studied. JMa and JMb transcript expression was detected in 53% and 28% of tumour samples, respectively. In addition, two novel c-erbB-4 JM isoforms, subsequently termed JMc and JMd, were isolated from 10% and 36% of tumours, respectively. Sequence analysis revealed the JMc transcript to contain a deletion of the entire JM region. In contrast, JMd includes an extended coding region, retaining both the JMa and JMb sequences. Neither of these novel isoforms was detected in normal human adult cerebellum, but expression of JMd was observed in developing fetal cerebellum, suggesting that this later isoform may represent an c-erbB-4 transcript restricted to primitive neuroectoderm-derived tissue. To confirm that the four c-erbB-4 JM isoforms arise by alternative RNA splicing, the intron-exon junctions of the human c-erbB-4 gene were sequenced within the JM region. This demonstrated the four c-erbB-4 JM variants to be encoded by two short exons containing the JMb and JMa sequences positioned in the order 5' to 3' and separated by a 121 bp intron (Gilbertson *et al.*, 2001).

Knowlden *et al.* (1998) examined c-erbB3 and c-erbB4 mRNA expression in 47 primary breast cancer samples and investigated correlations between these parameters and the expression of both ER and c-erbB-1 and with Ki67 immunostaining. A direct association was found between c-erbB-3 and c-erbB-4, and ER marker status. Inverse associations were seen between c-erbB-3 and c-erbB-4, and c-erbB-1. A significant relationship was seen between Ki67 and c-erbB-4. Measurements of c-erbB-3 protein levels in tumour samples removed from a further 89 patients of known response to endocrine therapy: (i) confirmed the relationship between c-erbB-3 and ER and (ii) identified that patients whose ER positive tumours expressed high levels of c-erbB-3 were most likely to benefit from endocrine measures. These results clearly demonstrate that increased c-erbB-3 and c-erbB-4 expression appears to be associated with the prognostically-favourable ER phenotype.

C-erbB-4 expression was investigated in a range of human tumour cell lines and in normal and malignant breast tissue. Using primers which amplified a 658 base pair (bp) region corresponding to part of the cytoplasmic domain of c-erbB-4, the receptor was found to be expressed in some but not all breast and ovarian tumour cell lines and also in a glioma cell line. The highest level of c-erbB-4 expression was found in the ovarian carcinoma OVCAR-3 and the breast carcinoma T-47D. In all cell lines where the 'full-length' c-erbB-4 was detected, a second previously undescribed c-erbB-4 sequence was also found as a 610 bp PCR product. The alternative PCR product was identical in sequence to c-erbB-4 except for a deletion of 48 bp which encodes a consensus phosphatidylinositol 3-kinase (PI3K) binding site. This suggested that the two forms of c-erbB-4 might interact with different intracellular signalling pathways and therefore influence a wider variety of cellular responses to NRG than previously thought. Expression of both c-erbB-4 variants was found in 7/7 normal breast tissues but only in 9/12 breast tumours analysed. In line with the terminology of Elenius *et al.* (1997b) the two isoforms of the C-terminal transcripts were designated as CT-a (full-length) and CT-b which lacks the P13K binding motif (Sawyer *et al.*, 1998).

Table 1.4 Summary of Effects of ErbB Receptor Expression in Cancer

Author	ErbB Type	Cancer Type	Findings
Nicholson *et al.*, 2001	1	Multiple	Prognostic indicator of poor outcome
Aziz *et al.*, 2000	1	Breast	Prognostic indicator of poor outcome
Tsutsui *et al.*, 2002	1	Breast	Prognostic indicator of poor outcome
Suo *et al.*, 2002	1,2,3,4	Breast	Poor out come for 1,2,3. Favourable outcome for 4
Ferrero *et al.*, 2001	1	Breast	No effect on prognosis
O-Dwyer *et al.*, 2002	1	Colon	Prognostic indicator of poor outcome
Ferrandina *et al.*, 2002	1,2	Ovarian	No effect on prognosis
Vered *et al.*, 2002	1	Salivary gland	85% Positive for overexpression of c-erbB-1
Storkel *et al.*, 1993	1	Oral	Prognostic indicator of poor outcome
Brabender *et al.*, 2001	1,2	NSCLC	Prognostic indicator of poor outcome
Pfeiffer *et al.*, 1996	1,2	NSCLC	No effect on prognosis
Cirisano and Karlan., 1996	2	Ovarian	Prognostic indicator of poor outcome
Ooi *et al.*, 1997	2	Stomach	Overexpressed
Quinn *et al.*, 1994	3	Breast	Prognostic indicator of favourable outcome
Maurer *et al.*, 1998	3	Colon	Increased expression of c-erbB-2 in tumours
Funayama *et al.*, 1998	3	SCC	Overexpression
Haugen *et al.*, 1996	3,4	Thyroid	Overexpression
Rajkumar *et al.*, 1993	3	Gastrointestinal	Inconclusive
Merimsky *et al.*, 2002	4	Soft tissue	Prognostic indicator of poor response to chemotherapy
Gilmour *et al.*, 2001	4	Ovarian	Overexpression
Furger *et al.*, 1998	2,3,4	Ovarian	Overexpression of 2 and 4
Al Moustafa *et al.*, 1999	2,3,4	NSCLC	Overexpression of 4
Graber *et al.*, 1999	4	Pancreatic	Overexpression in metastatic and decreased expression in non-metastatic tumours
Lee *et al.*, 2002	2,4	Colorectal	Prognostic indicator of poor outcome
Bei *et al.*, 2001	1,2,3,4	Oral	C-erbB-1 overexpression most prevalent
Chow *et al.*, 2001	1,2,3,4	Bladder	C-erbB-1 overexpression most prevalent
Gilbertson *et al.*, 2001	4	Medullablastoma	Overexpression
Knowlden *et al.*, 1998	3,4	Breast	Prognostic indicator of favourable outcome

1.5 The Role of C-erbB-2 in Breast Cancer

1.5.1 C-erbB-2 Overexpression as a Prognostic Factor in Breast Cancer

In a study of 166 primary breast cancers by Dittadi *et al.* (1996), 21.6% showed c-erbB-2 overexpression, while 27.1% and 85 51.3% showed intermediate and low level expression. A good correlation was found between DNA content and c-erbB-2 positivity. Overexpressers were associated with DNA aneuploidy. Cirisano and Karlan (1996) reported that the frequency of amplification averages 20-25% of breast cancer cases. The majority of studies have found that overexpression is most common in cancers with positive axillary lymph nodes and is correlated with worse prognosis for both node-negative and node positive tumours. In a study of 122 primary breast tumours and 62 metastases, the frequency of amplification of c-erbB-2 was less in metastases, although not enough to be statistically significant (Driouch *et al.*, 1997).

A study of 163 tumours from patients with different stages of breast cancer were analysed by Marx *et al.* (1990) in order to evaluate the distribution of c-erbB-2. 33% of cases were found to be c-erbB-2 positive. Only 5% of infiltrating lobular carcinomas (small cell carcinomas) showed positivity. Invasive ductal carcinomas show 33% positivity. Non-invasive and early invasive ductal carcinomas, both of the large cell comedo typ,e also showed positivity. C-erbB-2 protein expression was slightly more common in lymph-node positive (37%) than lymph-node negative cancer (30%). 50% of patients with three or more positive lymph-nodes were c-erbB-2 positive. C-erbB-2 overexpression correlated negatively with steroid receptor status and positively with c-erbB-1 expression.

A study by Quenel *et al.* (1995) of 942 invasive ductal carcinomas found 24% with positive membrane staining. They found a significant association between c-erbB-2 and tumour grade. Grading was performed according to Scarff-Bloom-Richardson criteria, with 11.2% of Grade 1, 21.5% of Grade 2 and 35.2% of grade III expressing c-erbB-2. Negative correlation with estrogen and progesterone receptor status was found. No association was found between c-erbB-2 and tumour size, nodal status or patient age. C-erbB-2 positivity correlated with the least differentiated tumours, higher mitotic rate and with the most marked polymorphism. Multivariate analysis showed that c-erbB-2 was

an independent prognostic factor, associated with earlier relapse or metastasis in node-negative patients.

In a study of 33 patients treated for advanced breast cancer, plasma c-erbB-2 levels were determined (this refers to the extracellular domain shed from the cell surface). 30.3% of the metastatic breast cancer were found to be c-erbB-2 positive. 20 of the patients received standard FEC regimen (5-fluorouracil, epirubicin and cyclophosphamide), 8 received a modified FEC regimen, 2 patients received CMF (5-fluorouracil, methotrexate and cyclophosphamide) and 3 patients received vinorelbine. No statistically significant difference was noted in response to chemotherapy between c-erbB-2+ and c-erbB-2- patients. In the 10 c-erbB-2+ patients, two increases and eight decreases were seen in plasma concentrations. Remarkably 5 of 23 c-erbB-2- patients had an increase in plasma c-erbB-2 during treatment. One observation made was that plasma c-erbB-2 positivity is associated with advanced breast cancer. Between 34.6-51% of patients with metastatic breast cancer and 33% of patients with locally recurrent breast cancer show plasma c-erbB-2 positivity, while no patients with locoregional non-inflammatory breast cancer showed positivity (Revillion *et al.*, 1996).

C-erbB-2 gene amplification is associated with poor prognosis in non-inflammatory breast carcinoma, mainly where axillary nodes are invaded and are associated with increased risk of multiple metastases developing simultaneously. In patients with inflammatory breast carcinoma, c-erbB-2 overexpression was not found to be associated with a higher risk of death, suggesting that c-erbB-2 plays different roles in these two cancers (Prost *et al.*, 1994).

123 breast tumour biopsies were examined for c-erbB-2 and c-erbB-1 expression. C-erbB-1 was found to be expressed at lower levels in 975 of tumours. C-erbB-2 was overexpressed in 91% of tumours. Of the c-erbB-2 overexpressing cells, two populations emerged with one having levels of c-erbB-2 from 0.33 to 19 and 45 to 480 times normal. Within the lower group c-erbB-1 expression was inversely related to c-erbB-2 expression. The second population was found to have c-erbB-2 gene amplifications. No inverse correlation was found in this group between c-erbB-2 and c-erbB-1. C-erbB-1 expression was found to correlate indirectly with potential doubling time, but not with the duration of the S-phase. C-erbB-2 showed no correlation with doubling time (Robertson *et al.*, 1996).

Breast carcinoma *in situ* (CIS) is considered to be the earliest form of breast cancer. Although 90% of patients with CIS are cured by surgery, the hypothesis that CIS lesions are precursors of invasive breast cancer is supported by the reports of a significant rate of local reoccurrence in patients who are not treated with mastectomy. Liu *et al.* (1992) assessed the amplification and overexpression of c-erbB-2 in paraffin-embedded specimens from 27 *in situ* carcinomas of the breast and 122 stage II breast cancers. Gene amplification was detected in 48% of *in situ* carcinomas and in 21% of stage II lesions. C-erbB-2 protein levels corresponded with amplification levels. These results suggest that the amplification of c-erbB-2 is an early event in human breast cancer.

Parkes *et al.* (1990) investigated the expression of c-erbB-2 in 70 human primary breast cancers. They found gene amplification in 17.5% of cases. Analysis of c-erbB-2 mRNA levels found overexpression in 30% of tumours associated with those of ductal origin. They demonstrated that enhanced c-erbB-2 expression could occur in the presence or absence of c-erbB-2 gene amplification. *In situ* hybridisation showed that elevated levels of mRNA expression were specific to malignant cells within the breast tumour. A significant correlation was made with poor tumour grade.

C-erbB-2 is overexpressed in 80% of large cell comedo carcinoma *in situ*. It has been postulated that the receptor may be an early event in the genesis of certain types of breast carcinomas, and subsequently may be lost once the tumour becomes invasive. 57.1% of cases of apocrine adenosis were found to be positive for c-erbB-2 overexpression. The staining intensities were classed as strong in 4 cases and weak in 8. Three cases were associated with ductal carcinoma, two with negative staining of both the apocrine adenosis and the carcinoma, while the third showed staining in both. The proliferation rate was increased in some of the lesions and all of the lesions showed some of the cells to be in the cell cycle. The expression of abnormal oncogenes and increased proliferation suggests that there may be an association between these lesions and large cell ductal carcinoma *in situ* and hence invasive carcinoma (Wells *et al.*, 1995).

1.5.2 C-erbB-2 as a Predictor of Response to Chemotherapy in Cell Line Models

Transfection of MDA-MB435 human breast cancer cells with c-erbB-2 resulted in resistance to taxol. The increased taxol resistance was not accompanied by changes in doubling time and S-phase fraction. The MDA-MB-435 cells expressed very low levels of p-glycoprotein and there was no increase of its expression in the c-erbB-2 overexpressing MDA-MB-435 transfectants. Furthermore, these transfectants were not sensitised to taxol treatment by the mdr-1 blocker thioradazine. These data demonstrated that overexpression of c-erbB-2/neu can lead to intrinsic taxol resistance independent of mdr-1 mechanisms (Yu *et al.*, 1996). This overexpression of c-erbB-2 in MDA-MB-435 conferred a 5-9-fold increase in Taxol resistance. A panel of human breast cancer cell lines established from different patients and expressing c-erbB-2 at different levels was examined for their sensitivity to taxol and taxotere. Higher expression of c-erbB-2 in these breast cancer cell lines correlated well with resistance to taxol and taxotere, and the degree of resistance was about 100-fold that in c-erbB-2-overexpressing MDA-MB-435 transfectants, demonstrating that these breast cancer cells are highly resistant to taxol. Higher levels of p-glycoprotein expression were found in several of the breast cancer cell lines. They sought to determine the relative contribution of c-erbB-2 and p-glycoprotein overexpression to taxol resistance in these cell lines. C-erbB-2 was downregulated using anti-c-erbB-2 monoclonal antibodies and the sensitivity of cells to taxol was assayed. P-glycoprotein function was inactivated using thioridazine or verapamil. Both c-erbB-2 down-regulation and p-glycoprotein blockade significantly sensitised the breast cancer cell lines to taxol. These results indicated that overexpression of either c-erbB-2 or p-glycoprotein renders human breast cancer cells resistant to taxol. Furthermore, c-erbB-2 synergised with p-glycoprotein conferring higher degrees of taxol resistance (Yu *et al.*, 1998b).

Studies to elucidate the mechanism of taxol resistance in this model revealed that taxol activated expression of p34Cdc2 kinase in MDA-MB-435 leading to cell cycle arrest at the G2/M phase and, subsequently, apoptosis. A chemical inhibitor of p34Cdc2 and dominant-negative mutant of p34Cdc2 blocked taxol-induced apoptosis in these cells. C-erbB-2 overexpression in MDA-MB-435 cells transcriptionally upregulated p21Cip1, which associates with p34Cdc2, inhibits Taxol-mediated p34Cdc2 activation, delays cell entrance to G2/M phase, and thereby inhibits Taxol-induced apoptosis. In p21Cip1 antisense-transfected MDA-MB-435 cells or in p21-/- MEF cells, c-erbB-2 was unable

to inhibit Taxol-induced apoptosis. Therefore, p21Cip1 participates in the regulation of a G2/M checkpoint that contributes to resistance to Taxol-induced apoptosis in c-erbB-2-overexpressing breast cancer cells (Yu *et al.*, 1998). C-erbB-2 was shown to bind to and colocalise with cyclin B-Cdc2 complexes and phosphorylates Cdc2-Y15. The c-erbB-2 kinase domain is sufficient to directly phosphorylate Cdc2-Y15. Increased Cdc2-Y15-p in c-erbB-2 overexpressing cells corresponds with delayed M phase entry. Expressing a nonphosphorylatable mutant of Cdc2 renders cells more sensitive to taxol-induced apoptosis. Thus, c-erB-2 can confer resistance to taxol-induced apoptosis by directly phosphorylating Cdc2 (Tan *et al.*, 2002).

Chen *et al.* (2000) selected various NIH 3T3 cell lines that specifically expressed c-erbB-1, c-erbB-2, c-erbB-3, c-erbB-1/c-erbB-2, c-erbB-1/c-erbB-3, or c-erbB-2/c-erbB-3. A cytotoxicity assay showed that expression of c-erbB-2 alone did not significantly enhance drug resistance, whereas coexpression of either c-erbB-1 or c-erbB-3 with c-erbB-2 significantly enhanced drug resistance. C-erbB-2 was highly phosphorylated in NIH 3T3 cells that coexpress c-erbB-2 with either ErbB, but not in NIH 3T3 cells that express c-erbB-2 alone. These results suggested that coexpression of c-erbB-1 or c-erbB-3 with c-erbB-2 induces high phosphorylation of c-erbB-2 and renders the cells more resistant to various anti-cancer drugs (Chen *et al.*, 2000). C-erbB-2 overexpression in normal human mammary epithelial cells failed to confer resistance or sensitivity to chemotherapeutic agents (Orr *et al.*, 2000).

A c-erbB-2-targeted ribozyme was used to abrogate c-erbB-2 expression in human SK-OV-3 ovarian cancer cells. SK-OV-3 cells expressing very low residual levels of c-erbB-2 protein, were then assessed for their sensitivity to adriamycin, cisplatin and taxol and compared to control cells. C-erbB-2 expression had no effect on the cytotoxicity of adriamycin or cisplatin in proliferation assays. In contrast, the sensitivity to taxol was increased approximately 70-fold in c-erbB-2 depleted cells (Aigner *et al.*, 2000).

Cell lines transfected with EGFRvIII (activated mutant of c-erbB-1) and c-erbB-2 are more resistant to taxol-mediated cytotoxicity, and tubulin polymerization induced by taxol is suppressed compared with cells expressing wt-EGFR. Montgomery *et al.* (2000) analysed β-tubulin isotypes expressed in cell lines transfected EGFRvIII and c-erbB-2. EGFRvIII- and c-erbB-2-expressing cells demonstrated equivalent total β-tubulin protein compared with cells transfected with wild type receptor or untransfected

controls. EGFRvIII-expressing cells demonstrated increases in class IVα (2.5-fold) and IVβ (3.1-fold) tubulin mRNA, and c-erbB-2-expressing cells showed increases in class IVα (2.95-fold) mRNA. Inhibition of EGFRvIII kinase activity using a mutant allele with an inactivating mutation in the kinase domain decreased expression of class IVα by 50% and partially reversed resistance to taxol.

MCF-10A human mammary epithelial cells transfected with an activated c-Ha-ras gene (MCF-10A Ha-ras cells), the c-erbB-2 gene (MCF-10A c-erbB-2 cells) or both genes (MCF-10A HE cells) were tested for their sensitivity to different cytotoxic drugs (Ciardiello *et al.*, 2000). As compared with parental MCF-10A cells, the transformed cells exhibited an increased sensitivity to topoisomerase I- and topoisomerase II-inhibitors, and to platinum-derivatives with a 2- to 10-fold reduction in IC(50) values. A remarkable difference in sensitivity was observed following treatment with taxanes. While MCF-10A Ha-ras cells showed an increased sensitivity, MCF-10A c-erbB-2 and MCF-10A HE cells exhibited a relative resistance to taxol and taxotere, with an approximately 3.5- to 6.5-fold higher IC(50) as compared with MCF-10A cells suggesting that c-erbB-2 overexpression has a dominant effect compared with an activated c-Ha-ras gene. Inhibition of the type I cAMP-dependent protein kinase (PKAI) by antisense oligonucleotides was able to overcome the effect of c-erbB-2 overexpression on MCF-10A cell sensitivity to taxol and taxotere, with a 20- to 40-fold shift in the IC(50) values for the 2 drugs, indicating a role for PKAI in c-erbB-2 mediated taxol resistance.

Taxol exposure downregulated the expression of c-erbB-2 protein in MCF-7, MDA-MB-435 and MDA-MB-453 (Oldham *et al.*, 2000). 17-allylamino 17-demethoxygeldanamycin was found to sensitise NSCLC cells expressing high levels of c-erbB-2 to taxol-mediated growth arrest and apoptosis. The combination cytotoxic effect was only additive in cells expressing low levels of c-erbB-2. In contrast, pretreatment of cells with 17-allylamino 17-demethoxygeldanamycin, before combined taxol and 17-allylamino 17-demethoxygeldanamycin exposure actually rendered the cells refractory to taxol cytotoxicity (Nguyen *et al.*, 1999). Emodin, a tyrosine kinase inhibitor, suppressed tyrosine kinase activity of c-erbB-2-overexpressing breast cancer cells and preferentially repressed transformation phenotypes of these cells *in vitro*. Emodin significantly inhibited tumour growth and prolonged survival in mice bearing c-erbB-2 overexpressing human breast cancer cells. Furthermore, the combination of

emodin and taxol synergistically inhibited the anchorage-dependent and anchorage-independent growth of c-erbB-2-overexpressing breast cancer cells *in vitro* and synergistically inhibited tumour growth and prolonged survival in athymic mice bearing. Xenografts of human tumour cells expressing high levels of c-erbB-2. Both immunohistochemical staining and Western blot analysis showed that emodin decreases tyrosine phosphorylation of c-erbB-2 in tumour tissue (Zhang *et al.*, 1999).

Using c-erbB-2 transfected MCF-7 cells, Pegram *et al.* (1999) found Herceptin (a c-erbB-2 targeting monoclonal antibody, in clinical use) to be synergistic with cisplatin, thiotepa and VP-16 *in vitro*. Effects were additive with adriamycin, taxol, methotrexate and vinblastine, while 5-fluorouracil was found to be antagonistic. *In vivo*, combinations of Herceptin plus cyclophosphamide, adriamycin, taxol, methotrexate, VP-16, and vinblastine resulted in a significant reduction in xenograft volume compared to chemotherapy alone ($P<0.05$). Xenografts treated with Herceptin plus 5-fluorouracil were not significantly different from those that received solely 5-fluorouracil. Treatment of well established BT-474 breast cancer xenografts in athymic mice with Herceptin resulted in a dose-dependent antitumour activity. In combination studies, treatment with taxol and Herceptin, or adriamycin and herceptin, resulted in greater inhibition of growth than that observed with any agent alone. The combination of taxol and Herceptin resulted in the highest tumour growth inhibition and had a significantly superior complete tumour regression rate when compared with either taxol or Herceptin alone (Baselga *et al.*, 1998).

Adriamycin-selected variants of the human small cell lung carcinoma cell line, GLC4, displayed increased sensitivity to tumour necrosis factor (TNF). Sensitivity to TNF appeared to correlate inversely with the expression and gene copies of topoisomerase IIα and decreases in c-erbB-2 gene copies resulting in decreased c-erbB-2 expression, probably due to linkage between these 2 genes (Sleijfer *et al.* 1998).

NRG β-2 is a naturally occurring ligand that activates c-erbB-2 by inducing its heterodimerisation with c-erbB-4. The ability of this ligand to phosphorylate the c-erbB-2 receptor exogenously allowed Harris *et al.* (1998) to study the effect of c-erbB-2 activation on cancer cell behaviour. MCF-7 NRG β-2 transfected showed markedly increased sensitivity to adriamycin and VP-16. Topoisomerase IIα mRNA and protein (total protein and enzymatic decatenating activity) were found to be upregulated in the

NRG β-2 transfected cells. Because up-regulation of Topoisomerase IIα *in vitro* and in clinical specimens is associated with increased response to adriamycin (presumptively by an increase in drug substrate), this may be the mechanism of the increased sensitivity to adriamycin seen in NRG β-2 transfected cells. This implies that activation of c-erbB-2 or one of the other members of the receptor family may increase sensitivity to adriamycin by up-regulation of Topoisomerase IIα (Harris *et al.*, 1998).

Osmak *et al.* (1997) reported that the selection of SKBR-3 breast cancer cell line with adriamycin, did not result in altered expression of c-erbB-1, c-erbB-2, c-erbB-3, c-Myc, c-H-ras, cathpsin D, cathepsin L, EGF or TGFα.

Fluorescence *in situ* hybridisation was used to study copy number aberrations of both topoisomerase IIα and c-erbB-2 in nine breast cancer cell lines and in 97 clinical breast tumours, which were selected for the study according to their c-erbB-2 status by Southern blotting. Two of the five cell lines with c-erbB-2 gene amplification (SK-BR-3 and UACC-812) showed amplification of topoisomerase IIα. In MDA-361 cells, ErbB-2 amplification (14 copies/cell) was associated with a physical deletion of topoisomerase IIα (four copies of chromosome 17 centromere and two copies of topoisomerase IIα). The topoisomerase IIα amplification in UACC-812 cells was associated with 5.9-fold-increased topoisomerase IIα protein expression and 2.5-fold-increased sensitivity to the topoisomerase II inhibitor, adriamycin, whereas the deletion in MDA-361 leads to decreased protein expression (45% of control) and a 2.4-fold-increased chemoresistance *in vitro*. Of 57 c-erbB-2-amplified primary breast carcinomas, 44% showed c-erbB-2/topoisomerase IIα coamplification and 42% a physical deletion of the topoisomerase IIα gene. No topoisomerase IIα copy number aberrations were found in 40 primary tumours without c-erbB-2 amplification. These findings may explain the altered chemosensitivity to topoisomerase II inhibitors reported in c-erbB-2-amplified breast cancers (Jarvinen *et al.*, 2000).

1.5.3 C-erbB-2 as a Predictor of Response to Chemotherapy in the Clinical Setting

1.5.3.1 Taxanes

Studies of patients with advanced breast cancer disease demonstrate that, despite the association of c-erbB-2 overexpression with poor prognosis, the odds of c-erbB-2-positive patients responding clinically to taxanes were greater than three times those of c-erbB-2-negative patients. Further studies in preclinical models used combination therapy for breast cancer cells that overexpress c-erbB-2, and the use of agents that interfere with c-erbB-2 function plus taxol resulted in significant antitumour effects (Baselga *et al.*, 1997). Plasma levels of the extracellular domain of c-erbB-2 was found to correlate positively with response to weekly taxol in relapsed cancer patients. Weekly taxol treatment was found to be more beneficial to patients with high c-erbB-2 extracellular domain expression, than those with low expression (Kim *et al.*, 2001).

Van Poznak *et al.* (2002) found no association between c-erbB-2 status and response to single-agent taxane chemotherapy in metastatic breast patients.

Formenti *et al.* (2002) performed a study, firstly to identify patients with locally advanced breast cancer (LABC) who will achieve a pathological response to a pre-operative regimen of concurrent taxol and radiation; and secondly, to explore associations between molecular markers from the original tumours and pathological response. A total of 36 patients had pretreatment biopsies and were evaluable for the analysis of the association of molecular markers with pathological response. Pathological response in the mastectomy specimen was achieved in 12 of these 36 patients (33%). Tumours with low c-erbB-2 gene expression and negative estrogen receptors were more likely to respond to the tested regimen ($p = 0.009$ and $p = 0.006$, respectively).

A phase II study by Seidman *et al.* (2001) evaluated weekly Herceptin and taxol therapy in women with c-erbB-2 normal and overexpressing metastatic breast cancer. Efficacy was correlated with immunohistochemical and fluorescent *in situ* hybridisation (FISH) assay results. Up to three prior chemotherapy regimens, including prior anthracycline and taxane therapy, were allowed. Herceptin 4 mg/kg and taxol 90 mg/m^2 were administered on week 1, with Herceptin 2 mg/kg and taxol 90 mg/m^2 administered on subsequent weeks. C-erbB-2 status was evaluated using four different

immunohistochemical assays and FISH. The intent-to-treat response rate for all 95 patients enrolled was 56.8% (95% confidence interval, 47% to 67%). A response rate of 61.4% (4.5% complete response, 56.8% partial response) was observed in 88 fully assessable patients. In patients with c-erbB-2 overexpressing tumours, overall response rates ranged from 67% to 81% compared with 41% to 46% in patients with c-erbB-2 normal expression (ranges reflect the different assay methods used to assess c-erbB-2 status), these differences in response rates between patients were statistically significant for all assay. Therapy was generally well tolerated, although three patients had serious cardiac complications.

Fountzilas *et al.* (2001) treated 34 patients with c-erbB-2 overexpressing advanced breast cancer with weekly taxol immediately followed by Herceptin, for at least 12 weeks. Expression of c-erbB-2 was determined by immunohistochemical analysis on fixed, paraffin-embedded tissues. Eligible patients were required to have > or = 25% stained tumour cells. Thirty-three patients completed at least 12 weeks of combined treatment. After completion of the 12th week of treatment, four patients (12%) achieved complete and 17 (50%) partial response. Median duration of response was 11.6 months. Median time to progression was nine months while median survival had not been reached. The combination of weekly taxol and Herceptin was a safe and active regimen for patients with HER-2/neu overexpressing ABC.

Dieras *et al.* (2001) reported that the taxanes and herceptin have been shown to possess significant clinical activity in metastatic breast cancer. Preclinical testing of taxane/Herceptin combinations demonstrated additive and synergistic interactions with taxol and taxotere, respectively. In a pivotal clinical trial, combination of taxol (3-weekly) and Herceptin was associated with an increased response rate compared with taxol monotherapy (41% vs. 17%; $p = 0.001$). The combination therapy also significantly improved time to disease progression (6.9 vs. 2.7 months; $p < 0.05$). In a phase II study of weekly taxol plus Herceptin in patients with normal or increased tumour c-erbB-2 levels, a response was observed in 60% of patients and the regimen was well tolerated. Responses were more frequent in patients with c-erbB-2-overexpressing tumors (83% vs. 45%). Preliminary results from a phase II study of Herceptin plus taxotere in patients with c-erbB-2 overexpressing tumours indicate significant activity, with a response observed in 7 (44%) of 16 evaluable patients. The

preliminary results of a trial of weekly taxotere and Herceptin demonstrate a response rate of 54% in 13 evaluable patients.

Esteva *et al.* (2002) evaluated the safety and efficacy of weekly taxotere plus Herceptin in women with c-erbB-2 overexpressing metastatic breast cancer. Efficacy was correlated with c-erbB-2 extracellular domain (ECD) levels. Thirty women with metastatic breast cancer were treated with weekly taxotere and Herceptin as first- or second-line therapy. Both taxotere and Herceptin were delivered in 4-week cycles consisting of three weekly treatments followed by 1 week of rest. A loading dose of Herceptin was administered 1 day before the start of the first cycle. The intent-to-treat overall response rate (ORR) was 63% (95% confidence interval [CI], 44% to 80%). The ORR in patients whose tumours were c-erbB-2 positive by FISH was 67% (16 of 24 patients; 95% CI, 45% to 84%). In patients with elevated serum c-erbB-2 ECD at baseline, the ORR was 76% (95% CI, 53% to 92%), compared with 33% (95% CI, 7% to 70%) in patients with low c-erbB-2 ECD levels (P = 0.04). Variations in c-erbB-2 ECD concentrations during treatment correlated with response to treatment.

Hamilton *et al.* (2000) assessed the potential value of the tumour markers p53, c-erbB-2, and Bcl-2 in predicting the clinical response to adriamycin and taxol as single agents in the treatment of metastatic breast cancer. The primary tumours of 114 patients in the European Organization for Research and Treatment of Cancer 10923 trial were assessed by immunohistochemistry using monoclonal antibodies; the results were correlated with clinical response to therapy. C-erbB-2 was positive in 24% of patients, p53 was positive in 25% of patients, and Bcl-2 was positive in 49% of patients. There was no correlation between the expression of any of the markers and the clinical response to either agent. This study does not support the use of p53, c-erbB-2, or Bcl-2 to assist the selection of anthracycline versus taxane in metastatic breast cancer.

1.5.3.2 Anthracyclines

Recent retrospective analyses have suggested that breast cancer patients whose tumours overexpress c-erbB-2 derive preferential benefit from treatment with anthracyclines such as adriamycin. Paik *et al.* (2000) evaluated this recommendation in a retrospective study of National Surgical Adjuvant Breast and Bowel Project Protocol B-15, in which patients received a combination of adriamycin and cyclophosphamide (AC), CMF, or AC followed by CMF. They hypothesised that AC would be superior to CMF only in

the c-erbB-2 positive patients. Immunohistochemical detection of c-erbB-2 was performed on tumour sections from 2034 of 2295 eligible patients. Tumour sections from 29% of patients stained positive for c-erbB-2. AC was superior to CMF in c-erbB-2 positive patients only, although differences in outcomes did not reach statistical significance. In the c-erbB-2 positive cohort, relative risks of failure (i.e, after AC treatment as compared with CMF treatment) were 0.84 for disease-free survival (DFS) (95% confidence interval [CI] = 0.65--1.07; P =.15), 0.82 for survival (95% CI = 0.63--1.06; P =.14), and 0.80 for recurrence-free survival (RFS) (95% CI = 0.62--1.04; P =.10). Tests for interaction between treatment and c-erbB-2 status were suggestive but not statistically significant (P =.19 for DFS, P =.11 for survival, and P =.08 for RFS). These results, together with overview results indicating minor overall superiority for anthracycline-based regimens relative to CMF, indicate a preference for the AC regimen in patients with c-erbB-2 positive tumours. Both AC and CMF regimens may be considered for patients with c-erbB-2 negative tumours.

In the National Surgical Adjuvant Breast and Bowel Project protocol B-11, patients with axillary lymph node-positive, hormone receptor-negative breast cancer were randomly assigned to receive either L-phenylalanine mustard plus 5-fluorouracil (PF) or a combination of L-phenylalanine mustard, 5-fluorouracil, and adriamycin (PAF). Tumour cell expression of c-erbB-2 was determined by immunohistochemistry for 638 out of 682 eligible patients. Overexpression of c-erbB-2 was observed in 37.5% of the tumours studied. Overexpression was associated with tumour size (P=.02), lack of estrogen receptors (P=.008), and the number of positive lymph nodes (P=.0001). After a mean time on study of 13.5 years, the clinical benefit from adriamycin (PAF versus PF) was statistically significant for patients with erbB-2-positive tumours, but it was not significant for patients with c-erbB-2 -negative tumours. Interaction between adriamycin treatment and c-erbB-2 overexpression was statistically significant for disease-free survival (P=.02) and distant disease-free survival (P=.02) but not for survival (P= .15) or recurrence-free survival (P=.06). These data support the hypothesis of a preferential benefit from adriamycin in patients with c-erbB-2-positive breast cancer (Paik *et al.*, 1998).

Jarvinen *et al.* (1998) looked at predictors of response to topoisomerase II inhibitor chemotherapy in advanced breast cancer. Fifty-five patients with advanced breast cancer were treated with weekly epirubicin (30 mg/m^2 weekly up to 1000 mg/m^2), as

first line cytotoxic chemotherapy. Objective response to treatment was analysed according to UICC criteria. The predictive value of topoisomerase IIα, c-erbB-2, p53, estrogen (ER) and progesterone receptor (PR), S-phase fraction and DNA ploidy were analysed from representative formalin-fixed paraffin-embedded primary tumour samples. The proportion of topoisomerase IIα positive cells failed to predict response to epirubicin therapy. Overexpression of c-erbB-2 and hormone receptor negativity were significantly associated with poor response. Response rate in patients with c-erbB-2 overexpressing tumours was 32% compared with 65% in patients with no c-erbB-2 overexpression (P = 0.0058). Accordingly, the response rate for ER-positive patients was 67% compared with 26% in ER-negative patients (P = 0.0021). Histological grade, p53, DNA-ploidy, tumour proliferation rate (S-phase fraction), stage of the disease at diagnosis, age of the patient, previous anti-oestrogen therapy or site of metastasis did not predict the response to epirubicin therapy.

Petit *et al.* (2001) evaluated the predictive value of a tumour's c-erbB-2 status for chemotherapy response in the neoadjuvant setting and the effect of anthracycline dose intensity on this predictive value. C-erbB-2 status was evaluated by immunochemistry on microbiopsy before neoadjuvant chemotherapy in 39 patients (group A) treated with FEC50 (500 mg/m^2 5-fluorouracil, 50 mg/m^2 epirubicin, and 500 mg/m^2 cyclophosphamide) and 40 patients (group B) treated with FEC100 (500 mg/m^2 5-fluorouracil, 100 mg/m^2 epirubicin, and 500 mg/m^2 cyclophosphamide). All tumours were stage II or noninflammatory stage III adenocarcinoma. Patient and tumour characteristics (age, tumour size, clinical nodal status, SBR grade, hormonal receptor status, and c-erbB-2 expression) were similar in the two groups. In univariate analyses, anthracycline dose was the only factor predictive of response (OR = 61.5% with FEC50; OR = 82.5% with FEC100; P = 0.038). When anthracycline dose was correlated with c-erbB-2 status, an OR of 73.9% was demonstrated in c-erbB-2 negative tumours, and an OR of 12.5% was demonstrated in c-erbB-2 positive tumours in group A. In group B, an OR of 69.5% was demonstrated in c-erbB-2 negative tumours, and an OR of 100% was demonstrated in c-erbB-2 positive tumours. There was no difference in OR for c-erbB-2 negative tumours treated with FEC50 or FEC100 (P = 0.74). On the other hand, c-erbB-2 positive tumours treated with FEC100 had a significantly better OR than those treated with FEC50 (P = 0.0003). In a multivariate analysis, the most powerful predictive factor of OR was a conditional variable associating anthracycline dose with c-erbB-2 status. Low-dose anthracycline and c-erbB-2 positivity predicted a

poor OR, low- or high-dose anthracycline and c-erbB-2 negativity predicted an intermediate OR, and high-dose anthracycline and c-erbB-2 positivity predicted a high OR. Vincent-Salomon *et al.* (2000) reported that c-erbB-2 overexpression was not a significant predictive marker of the pathological response to high-dose adriamycin based chemotherapy.

1.5.3.3 Other Agents

Sjostrom *et al.* (2002) assessed whether c-erbB-2 expression is associated with clinical sensitivity taxotere or sequential methotrexate and 5-fluorouracil (MF). A total of 283 patients with metastatic breast cancer were initially enrolled in a randomised multicentre trial comparing taxotere with sequential MF in advanced breast cancer. Paraffin embedded blocks of the primary tumour were available for 131 patients (46%). C-erbB-2 expression was scored immunohistochemically in a semi-quantitative fashion using a 0 to 3+ scale. Staining scores 2+ or greater were considered positive. Overall 54 (42%) patients had c-erbB-2-positive tumours. There was no association between treatment outcome and c-erbB-2 overexpression. The overall response rates (n=128) among c-erbB-2-negative and -positive patients were 35 and 44%, respectively (P=0.359). In the MF arm (n=62), the response rate was somewhat higher in the c-erbB-2 overexpressors (33% versus 18%, P=0.18). In the taxol arm the response rates were very similar, regardless of the c-erbB-2 expression (53% versus 53%).

Konecny *et al.* (2001) examined the association between c-erbB-2 overexpression and the sensitivity to the chemotherapeutic drug combinations of cyclophosphamide, methotrexate and 5-fluorouracil (CMF) and 5-fluorouracil, epirubicin and cyclophosphamide (FEC) of breast cancer cells derived from 140 chemotherapy-naive patients at the time of primary surgery. The data showed that c-erbB-2 overexpression was not associated with *in vitro* drug resistance to CMF or FEC. In contrast, tumours with strong c-erbB-2 overexpression demonstrated increased dose-dependent *in vitro* sensitivity to both the FEC and CMF regimens.

Slamon *et al.* (2001) evaluated the efficacy and safety of Herceptin in women with metastatic breast cancer that overexpressed c-erbB-2. They randomly assigned 234 patients to receive standard chemotherapy alone and 235 patients to receive standard chemotherapy plus Herceptin. Patients who had not previously received adjuvant (postoperative) therapy with an anthracycline were treated with adriamycin (or

epirubicin in the case of 36 women) and cyclophosphamide alone (138 women) or with Herceptin (143 women). Patients who had previously received adjuvant anthracycline were treated with taxol alone (96 women) or taxol with Herceptin (92 women). The addition of Herceptin to chemotherapy was associated with a longer time to disease progression (median, 7.4 vs. 4.6 months; P<0.001), a higher rate of objective response (50 percent vs. 32 percent, P<0.001), a longer duration of response (median, 9.1 vs. 6.1 months; P<0.001), a lower rate of death at 1 year (22 percent vs. 33 percent, P=0.008), longer survival (median survival, 25.1 vs. 20.3 months; P=0.01), and a 20% reduction in the risk of death. Herceptin increases the clinical benefit of first-line chemotherapy in metastatic breast cancer that overexpresses c-erbB-2.

Vargas-Roig *et al.* (1999) reported that c-erbB-2 protein expression was associated with the development of distant metastases in breast cancer patients treated with relatively high doses of anthracyclines in induction chemotherapy (5-fluorouracil, epirubicin or adriamycin, cyclophosphamide).

Bottini *et al.* (1996) found no significance difference in the expression of c-erbB-2, estrogen receptor or progesterone receptor before and after neoadjuvant treatment of operable breast cancer. The study included ninety nine patients who received either CMF (cyclophosphamide, methotrexate and 5-fluorouracil) or epirubicin.

1.5.4 C-erbB-2 as a Predictor of Response to Hormonal Therapy

Overexpression of c-erbB-2 in oestrogen receptor (ER) positive breast tumours is associated with resistance to endocrine therapy. Kumar *et al.* (1996) transfected MCF-7 breast cancer cells, which are strongly ER+ and express low levels of c-erbB-2, with a full-length c-erbB-2 cDNA. Transfection led to the upregulation of bcl-2 (2.5-6 fold) compared to the parental or mock-transfected cell lines. Overexpression also led to enhanced expression of bcl-X_L, with no changes in bcl-X_S. Analysis of cell lines which were ER+, MCF-7 and T47-D and those which are C-erbB-2+, SKBR-3 and MDA-453 showed no difference in bcl-2 expression, the same was also found for bcl-X_L. However analysis of cell lines which overexpress c-erbB-2 and express ER, ZR-75-R and BT-474, showed a 2-5 fold increase in levels of bcl-2 and a 3 fold increase in bcl-X_L. No significant changes in levels of bax were seen in the transfectants. The transfection of the MCF-7 cells with c-erbB-2 led to the suppression of tamoxifen-

induced apoptosis. The result of enhanced bcl-2 expression with c-erbB-2 overexpression is not consistent with previous reports, which show an inverse correlation between c-erbB-2 and bcl-2 expression. These studies however have correlated bcl-2 with either c-erbB-2 or ER but never with the two together. Conversely Krajewski *et al.* (1997) found that the percentage of Bax-immunopositive breast tumour cells correlated positively with c-erbB-2 immunopositivity. The type of breast cancer used in this study was invasive ductal carcinoma.

Giani *et al.* (1998) found that transfection of MCF-7 cells with c-erbB-2 resulted in reduction in the number and size of colonies in a colony formation assay. In hormone-deprived media, the transfectants re-acquired growth capacities, indicating that the transfectants were now hormone independent. However in the presence of hormone, c-erbB-2 overexpression inhibited proliferation by 39-49% and induced differentiation shown by the formation of lipid droplets. This suggests that in the presence of hormones, the c-erbB-2 signalling pathway is switched towards differentiation. They also showed increased MAPK phosphorylation in transfected cells and subsequent upregulation of $p21^{WAF1}$. pRb was found to be hypophosphorylated in the transfected cells. Inhibition of c-erbB-2 with a single chain antibody reversed all changes, proving that changes were c-erbB-2 specific.

Benz *et al.* (1992) also transfected MCF-7 cells with c-erbB-2. Those clones isolated which overexpressed c-erbB-2 were found to possess increased inositol-1,4,5-triphosphate-3'-kinase activity comparable to that of c-erbB-2 overexpressing cell lines SKBR-3 and BT474. The transfectants acquired low-level (2-3 fold) resistance to cisplatin and were no longer sensitive to tamoxifen. The tumourigenicity of the transfectants were found to be estrogen-dependent.

C-erbB-2 overexpression decreases the benefit of adjuvant tamoxifen in early-stage breast cancer without axillary lymph node metastasis. Carlomagno *et al.* (1996) studied the interaction between c-erbB-2 overexpression and adjuvant tamoxifen in node-negative breast cancer patients. 29.5% of early-stage breast cancer without axillary lymph node metastasis were found to overexpress c-erbB-2. C-erbB-2 overexpression correlated with a larger tumour size and decreasing levels of ER. In c-erbB-2 positive cases, adjuvant tamoxifen did not affect disease-free survival or overall survival, while in c-erbB-2 negative cases adjuvant tamoxifen treatment prolonged disease-free survival

and overall survival duration. C-erbB-2 can be used as a marker for lack of efficacy of adjuvant tamoxifen.

A study involving a group of post-menopausal breast carcinoma patients (74) who received neoadjuvant tamoxifen therapy found that c-erbB-2 levels showed no significant variation uduring treatment. C-erbB-2 levels were not significantly modified by hormonal treatment. Those cases that were c-erbB-2 negative initially showed no changes after treatment. There was a slight tendency to decrease in c-erbB-2 positive cases, but in general c-erbB-2 remained stable (Soubeyran *et al.*, 1996).

In contrast, Elledge *et al.* (1998) examined 205 paraffin-embedded blocks of tumours from patients enrolled on Southwest Oncology Group 8228 for c-erbB-2 expression. These patients had metastatic ER positive breast cancer and had not received any prior therapy for metastatic disease. All patients were treated with daily tamoxifen. C-erbB-2 positivity was associated with lower levels of ER and low bcl-2 expression. It was not significantly associated with response rate, time to treatment failure or survival. Therefore, c-erbB-2 expression in ER positive metastatic breast cancer is not associated with poorer response to tamoxifen or a more aggressive clinical outcome, according to this study.

Borg *et al.* (1994) noted a favourable effect of adjuvant tamoxifen on survival for patients with c-erbB-2 negative tumours, while patients who were positive did not benefit from tamoxifen administration. Giai *et al.* (1994) observed that node positive breast cancer patients co-expressing c-erbB-2 and ras had a worse outcome than those patients not co-expressing these oncogenes, when treated with tamoxifen. Wright *et al.* (1992) reported that only 7% of c-erbB-2 positive patients compared to 37% of c-erbB-2 negative patients responded to tamoxifen treatment. The combination of c-erbB-2 and EGFR appears to have an additive effect in reducing the likelihood of response to tamoxifen, as 0 out of 8 patients benefited. Nicholson *et al.* (1993) reported that c-erbB-2 expression did not effect response to tamoxifen in an c-erbB-1 negative group of patients, while a significant loss of hormone sensitivity was found in the c-erbB-1 positive group. Archer *et al.* (1995) found no correlation between c-erbB-2 overexpression and response to tamoxifen therapy.

Table 1.6 – Summary of Effect of C-erbB-2 Overexpression on Response to Therapy

Author	**Therapy**	**Outcome**
Baselga *et al.*, 1997	Taxol	Predicted favourable response to taxol
Kim *et al.*, 2001	Taxol	Predicted favourable response to taxol
Van Poznak *et al.*, 2002	Taxane	No association with favourable response to therapy
Formenti *et al.*, 2002	Taxol & Radiation	Predicted lack of response to therapy
Seidman *et al.*, 2001	Taxol & Herceptin	Predicted favourable response to therapy
Fountzilas *et al.*, 2001	Taxol & Herceptin	Predicted favourable response to therapy
Dieras *et al.*, 2001	Taxol & Herceptin; Taxotere & Herceptin	Predicted favourable response to therapy
Esteva *et al.*, 2002	Taxotere & Herceptin	Predicted favourable response to therapy
Paik *et al.*, 2000	AC, CMF, or AC & CMF	AC superior to CMF in c-erbB-2 overexpressors only
Paik *et al.*, 1998	PF versus PAF	PAF superior to PF in c-erbB-2 overexpressors only
Jarvinen *et al.*, 1998	Epirubicin	Predicted lack of response to therapy
Petit *et al.*, 2001	FEC (dose escalation of E)	C-erbB-2 overexpressors benefited from dose escalation of epirubcin in FEC therapy
Vincent-Salomon *et al.*, 2000	Adriamycin dose escalation	No prediction of response to therapy
Sjostrom *et al.*, 2002	MF	No prediction of response to therapy
Slamon *et al.*, 2001	AC/EC +/- Herceptin; Taxol +/- Herceptin	Addition of herceptin resulted in increased response to therapy
Vargas-Roig *et al.*, 1999	EF or AC	Predicted poor response to therapy
Bottini *et al.*, 1996	CMF	No prediction of response to therapy
Carlomagno *et al.*, 1996	Tamoxifen	Predicted poor response to therapy
Elledge *et al.*, 1998	Tamoxifen	No prediction of response to therapy
Borg *et al.*, 1994	Tamoxifen	Predicted poor response to therapy
Giai *et al.*, 1994	Tamoxifen	Predicted poor response to therapy
Wright *et al.*, 1992	Tamoxifen	Predicted poor response to therapy
Nicholson *et al.*, 1993	Tamoxifen	No prediction of response to therapy
Archer *et al.*, 1995	Tamoxifen	No prediction of response to therapy

1.6 The Metastatic Process

Metastasis is defined as the escape of tumour cells from their primary site and their re-establishment at distant secondary locations. The metastatic spread of solid tumours is responsible directly or indirectly for most cancer-related deaths. Cancer metastasis occurs as a result of a complex series of interactions between the cancer cell and its surroundings, known as the metastatic cascade, as depicted in Table 1.6.1.

Table 1.6.1
The Metastatic Cascade

Initial transforming event
↓
Growth of neoplastic cells
↓
Neovascularisation/angiogenesis of the tumour
↓
Detachment of neoplastic cells from primary tumour
↓
Local invasion of extracellular matrix by tumour cells
↓
Intravasation of tumour cells into lymphatics or vasculature
↓
Survival of tumour cells in circulation and avoidance of immunological attack
↓
Extravasation of tumour cells from vasculature into secondary organ tissue
↓
Survival and proliferation within organ parenchyma

Following the initial transforming event, neoplastic cells proliferate to form the primary tumour mass, from which cells can detach. There is increasing evidence that in epithelial malignancies, loss or down-regulation of expression of the structures responsible for the maintenance of tissue integrity correlates with an increasing tendency for metastatic spread. Such de-adhesion acts as a prelude to the cells invading the extracellular matrix (Ahmad *et al.*, 1997).

The most common cancers in humans are derived from the epithelial cells. In order to metastasise these cells must break contact with their neighbouring cells, traverse the basement membrane and migrate through the stroma, in order to reach either blood capillaries or lymphatic vessels. Next these cells have to penetrate the vessels (intravasation), travel thorough the blood stream or lymph system and then exit the vessels at the new site (extravasation), and proliferate. It is worth noting that while metastasis is an efficient process in that many primary cancers will generate secondary site of metastasis, it is an inefficient process in that the majority of cancer cells do not survive this process. Breast tumours can shed up to 1 million cells a day, but only less than 0.1% are detected in the bloodstream, the rest having destroyed by a combination of mechanical stresses, proteolytic degradation and surveillance by the immune system.

1.6.1 The Seven Steps of Metastasis

1.6.1.1 Local Invasion

This refers to the penetration of the host tissue surrounding the neoplasm. This usually takes place in the extracellular space, but some carcinomas are thought to be capable of intracellular invasion through the cytoplasm of striated muscle fibres, an example of emperipolesis. The extent of local invasion is thought to be mainly a result of growth, motility and tissue destruction, but differentiation may also play a role (Evans, 1991).

1.6.1.2 Detachment From Primary Site

Only rarely can normal cells achieve growth away from their primary site. Apart from pregnancy the only common example is endometriosis. One of the first steps involves the breaking of cell-cell recognition. Breaking of homotypic recognition and changes in heterotypic recognition are characteristic of invasive and metastatic cancers. A reduction in the expression of proteins such as E-cadherin is often seen in epithelial cancers and results in the ability of cancer cell to break apart. E-cadherin expression is lost early on in breast carcinogenesis. Cell-ECM interactions are also altered in cancer cells. This involves changes in the patterns of integrin expression. Integrins provide a major mechanism whereby cells recognise proteins of the extracellular matrix and basement membrane. Ligands of the integrins include collagen type I, collagen type IV,

laminin and fibronectin. In general integrins involved in tissue organisation are decreased while those involved in migration are not. Some examples of changes in integrin expression include the upregulation of $\alpha_v\beta_3$ in melanoma cells, which has a broad range specificity. This means that cells expressing this integrin can migrate over a broad range of matrices. In contrast $\alpha_2\beta_1$ which recognises laminin and collagen is decreased in colon and breast cancers. Integrins $\alpha_3\beta_1$ and $\alpha_6\beta_1$ (laminin receptors) are frequently upregulated in breast and endometrial cancers. An increase in the secretion of proteases also facilitates detachment of cells from the primary through the degradation of the ECM (Evans, 1991).

1.6.1.3 Intravasation

Cancer cells attach to the stromal face of the blood vessel basement membrane, digest the membrane with proteases (discussed below) and migrate between the endothelial cells into the bloodstream (Evans, 1991).

1.6.1.4 Transport

Cancer cells commonly use three routes of transport. Firstly, body cavities such as the peritoneum facilitates the spread of cancers such as ovary or colon. Cancers invading out from the primary site detach from the surface and then are transported by the peritoneal fluid to other sites. A similar process occurs in the lungs, whereby lung cancers or other cancers invading can colonise the space between the pleural membranes surrounding the lungs. This generates a cancer-containing, growth-supporting fluid, which must be removed to maintain lung function. Secondly, blood vessels such as capillaries which consist of a layer of endotheilial cells plus an external basement membrane of glycoproteins. They provide the least difficult barrier to entry and exit of cancer cells. Arteries provide a much more difficult barrier in the form of a smooth muscle layer, and therefore are rarely ever invaded. Thirdly, lymphatic vessels provide even less of a barrier than capillaries as they are not surrounded by a basement membrane. They drain into the subclavian veins and thence into the superior vena cava, hence reaching the blood stream (Evans, 1991).

Once the tumour cells have gained access to the blood system they may be swept away to distant site which they can colonise. Within the bloodstream the tumour cells may

interact with host components such as lymphocytes, monocytes and platelets, through heterotypic adhesion. This may lead to larger clumps incorporating the tumour cells lending them protection from mechanical stress and immune attack.

1.6.1.5 Lodgement at a Distant Site

The next step in the metastatic process involves the attachment of the cancer cell to the endothelial lining. Most tumour cells appear to be arrested in the first capillary bed they encounter, but this does not guarantee growth of a secondary tumour. Tumour cells are seen to lodge in capillaries, arterioles, and occasionally venules, but rarely in arteries (shear may be too high). It is thought that the walls of arterioles may present effective barriers to extravasation, perhaps explaining the low degree of metastasis to tissue such as the skeletal muscle. During the process of lodgement within a blood vessel it is thought that the tumour cell interacts with either the basement membrane or the endothelium. It is thought that there are four possible outcomes from these interactions. Firstly, the cells lodge and go on to form metastasis. This lodgement can occur either by mechanical means, where the cell literally gets "stuck" as it gets jammed in a vessel whose diameter is less than the cell or clump or cells, by specific adhesion in which the tumour cell "recognises" the wall of the blood vessel, due to the molecular content of the surfaces involved, or lastly by selective adhesion. The second outcome is where cells lodge and become dormant. The cells then exist in a dormant state to become active at a later date. The third outcome is the cells lodge but do not survive and the fourth outcome involves the cells failing to lodge and thus pass through the first organ they meet (Evans, 1991).

1.6.1.6 Extravasation

Extravasation is thought to occur due to the retraction of endothelial cells, exposing the glycoproteins of the basement membrane. The tumour cell then attaches to the basement membrane and digests it with protease and glycosidases, allowing the tumour cell to pass through. Different tumours express different integrins, which recognise different glycoproteins. Thus it follows that the basement membrane composition plays a large role in determining whether tumours are successful at extravasation (Evans, 1991).

Extravasation may occur in a number of ways:

(a) The cells may divide and pile up within the lumen of the blood vessel and invade en masse by the destruction of the blood vessel.

(b) Single cells may migrate between endothelial cells either destructively or non-destructively.

(c) Single cells may leave by passing through the endothelial cells rather than between them.

1.6.1.7 Growth

Proliferation of the cancer cells at their new site is initially confined to within 1mm of the vessel, until the tumour can form new blood vessels (angiogenesis) to supply essential nutrients and oxygen. Tumour growth is dependant on a number of factors including the nature of the environment it finds itself in and the nature of the tumour itself. These factors include resistance to host defence mechanisms of humoral and cellular nature, and response to or requirement for specific growth factors (Evans, 1991).

1.6.2 Proteases Involved in Metastasis

Matrix degrading proteases play a role in metastasis, as invasive cancer cells must degrade the surrounding extracellular matrix, which consists of interstitisal stroma and basement membrane. The secretion of such proteases achieves this. Matrix degrading proteases can be classified into four major classes,

1. Matrix metalloproteinases (MMPs)
2. Serine proteinases
3. Cysteine proteinases
4. Aspartyl proteinases

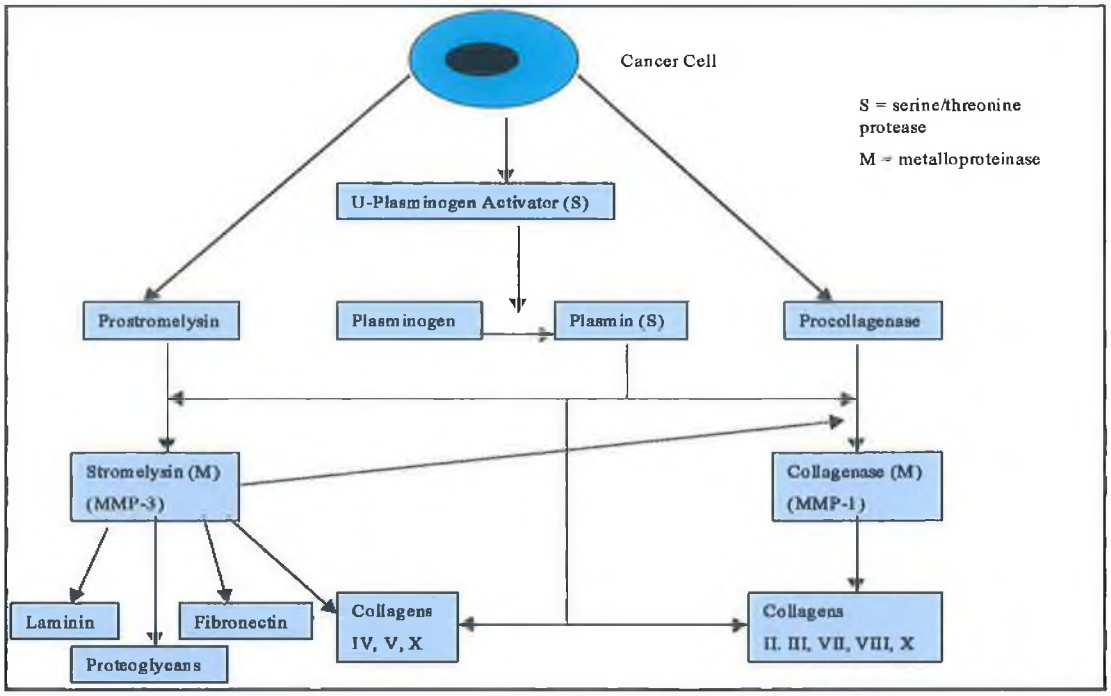

Figure 1.6.2 Interplay of Proteases

1.6.2.1 Matrix Metalloproteases

Matrix metalloproteases (MMPs) are a diverse family of secreted, transmembrane proteases. There are 16 known members, which are characterised by a zinc-binding domain at their catalytic site. MMPs are secreted as zymogens and activated through proteolytic cleavage. Tissue inhibitors of metalloproteases (TIMPs) can inhibit active MMPs. In cancer, MMPs contribute to all invasive steps of the metastatic cascade. They result in the breakdown of basement membrane and stromal matrices. MMPs are not solely produced by the invading cancer cells, but also by host fibroblasts, leukocytes and myofibroblasts, and then bind to their specific receptor at the surface of the cancer cell. Their association with TIMPs completes the tripartite, establishing a well regulated proteolytic complex. During normal physiological events the activity of these enzymes is tightly regulated. However in the case of cancer this regulation is disrupted, leading to increased invasion. Cancer cells release chemoattractants for leukocytes that are recruited to the tumour and contribute to the breakdown of the extracellular matrix. MMPs also promote the invasion of endothelial cells, thus promoting tumour growth, by aiding tumour angiogenesis (Lauwaet *et al.*, 2000).

Table 1.6.2.1

Main members of the MMP family

Group	Enzyme Name	Substrate
Type IV collagenases	MMP-2 (Gelatinase A, 72kDA)	Type IV collagen
		Gelatin
		Collagen types V, VIII, X
		Laminin
	MMP-9 (Gelatinase B, 92kDA)	Type IV collagen
		Gelatin
		Elastin
		Collagen types I, II, IV
Interstitial collagenases	MMP-1	Collagen types I, II, III, VII, X
		Gelatins
	MMP-8	Collagen types I, II, III
Stromelysins	MMP-3 (Stromelysin-1)	Proteoglycan, fibronectin, laminin, collagen type III, IV, V, IX
	MMP-10 (Stromelysin-2)	Proteoglycan, fibronectin, collagen type III, IV, V
	MMP-11 (Stromelysin-3)	α1-proteinase inhibitor
	MMP-7 (Matrilysin) (Pump-1)	Gelatin, proteoglycan, fibronectin
		Activates procollagenase
Other	MMP-14 (MT-MMP)	Activates pro-gelatinase A

MMP-2 and MMP-9 expression has been found to be increased in several tumour types when compared to levels in adjacent tissue (Meyer and Hart, 1998). MMP-2 expression is associated with breast, colorectal and gastric carcinomas. MMP-11 has been found to be expressed specifically in stromal fibroblasts at the tumour-stroma interface, in all epithelial carcinomas to date. Levels of MMP-11 have been shown to be an independent prognostic marker for relapse-free survival in node-positive breast cancer (Ahmad and Hart, 1997). The evidence suggests that tumours can induce the production of MMPs in neighbouring stromal fibroblasts, e.g. by secretion of EGF or TNFα. The co-culture of MCF-7 with human fibroblasts leads to the induction of MMP 1, 2 and 3 in the fibroblasts (Ito *et al.*, 1995), whilst co-culture of rat embryo fibroblasts results in increased MMP-9 levels (Himelstein *et al.*, 1994). The recently discovered MMP-14 is expressed on the cell surface of some tumour cells, where it serves an activator of MMP-2 (Curran *et al.*, 2000).

TIMPs inhibit MMPs by forming tight stoichiometric, non-covalent complexes with either the pro-enzyme or the activated MMP, or by controlling their autocatalytic activation (Woesner, 1991). Their expression is also influenced by local cytokines and growth factors. There are three members of the TIMP family and all have broad range activity on all classes of MMPs. TIMP-1 and 2 have been shown to be able to inhibit the degradation of the extracellular matrix and invasion of cancer cell lines *in vitro*.

1.6.2.2 Serine Proteinases

Serine proteases are characterised by a serine residue at their active site and are produced in an inactive pro-form. Important members of this family are trypsin, thrombin, plasmin, cathepsin G and urokinase type plasminogen activator (uPA). uPA converts inactive plasminogen to plasmin, a highly active protease capable of degrading a wide variety of ECM components. Plasmin can also activate other proteases including several MMPs. uPA is held on the cell surface by a uPA receptor which is also the receptor for vitronectin. uPA is expressed selectively at the invasive tumour-stromal interface in many experimental and human carcinomas and high levels correlate with poor prognosis for breast cancer (Ahmad and Hart, 1997).

1.6.2.3 Cysteine Proteinases

Cathepsin B and cathepsin L are the two cysteine proteases most implicated in cancer metastasis (Sloane, 1990). They are characterised by a cysteine residue at their active site and are lysosomal proteases that are capable of degrading the ECM. Cathepsin B is also capable of activating certain MMPs and receptor bound uPA (Ahmad and Hart, 1997).

1.6.2.4 Aspartyl Proteinases

Cathepsin D degrades a large variety of endocytosed proteins and has been implicated in breast cancer invasion and metastasis, where relapse and metastatic disease correlate with high levels of cathepsin D (Ahmad and Hart, 1997).

1.7 The Role of C-erbB-2 in Cancer Metastasis

1.7.1 Clinical Data Linking C-erbB-2 Overexpression to Metastatic Breast Cancer

C-erbB-2 overexpression is known to be associated with invasion and metastasis in human breast cancer. In a study of 163 breast tumours from patients with different stages of breast cancer, 33% of invasive ductal carcinomas were positive for c-erbB-2. C-erbB-2 protein expression was slightly more common in lymph-node positive (37%) than lymph-node negative cancer (30%). However, 50% of patients with three or more positive lymph-nodes were c-erbB-2 positive (Marx *et al.*, 1990). In another study Quénel *et al.* (1995) found that 24% of 942 invasive ductal carcinomas had positive membrane staining. In this study, multivariate analysis showed that c-erbB-2 was an independent prognostic factor, associated with earlier relapse or metastasis in node-negative patients. In another study, c-erbB-2 plasma levels in 33 patients being treated for advanced breast cancer, were determined. 30.3% of the metastatic breast cancer were found to be c-erbB-2 positive (Revillion *et al.*, 1996). Therefore, c-erbB-2 gene amplification is associated with poor prognosis in non-inflammatory breast carcinoma, mainly where axillary nodes are invaded and are associated with increased risk of multiple metastases developing simultaneously. In patients with inflammatory breast carcinoma, c-erbB-2 overexpression was not found to be associated with a higher risk of death, suggesting that c-erbB-2 plays different roles in these two cancers (Prost *et al.*, 1994). In contrast, a study of 122 primary breast tumours and 62 metastases found that the frequency of amplification of c-erbB-2 was less in metastases, although not enough to be statistically significant (Driouch *et al.*, 1997).

Breast carcinoma *in situ* (CIS) is considered to be the earliest form of breast cancer. Although 90% of patients with CIS are cured by surgery, the hypothesis that CIS lesions are precursors of invasive breast cancer is supported by the reports of a significant rate of local reccurrence in patients who are not treated with mastectomy. Liu *et al.* (1992) assessed the amplification and overexpression of c-erbB-2 in paraffin-embedded specimens from 27 *in situ* carcinomas of the breast and 122 stage II breast cancers. Gene amplification was detected in 48% of *in situ* carcinomas and in 21% of stage II lesions. C-erbB-2 protein levels corresponded with amplification levels. These results suggest that the amplification of c-erbB-2 is an early event in human breast cancer.

P95, a NH_2 terminally truncated c-erbB-2 product correlates with its extracellular domain and both are shed from the cells under varied conditions. Of 161 breast cancers studied, 22.4% expressed p95, 21.7% expressed p185 and 14.3% expressed both. A higher proportion of node positive (23/78) than node negative (9/63) expressed p95. In the group that expressed p185, those that also expressed p95 were associated with node positive patients. The authors claim that P95 may distinguish tumours that have metastasised to the lymph nodes (Christianson *et al.*, 1998).

O-charoenrat *et al.* (2002) studied the profile of ErbB receptors in head and neck squamous cell carcinomas (HNSCC) to determine whether their expression was associated with clinicopathological features and key molecules involved in angiogenesis and metastasis. They also assessed the impact of expression on survival. This study included 54 cases of primary HNSCC, of which 27 cases showed lymph node metastasis. Expression was analysed in the same tissue homogenates by semi-quantitative RT-PCR. HNSCC frequently co-expressed multiple ErbB receptors and showed significant correlation amongst their levels. High expression of c-erbB-1, c-erbB-2 or c-erbB-3 was associated with an infiltrating mode of invasion, nodal metastases and advanced pathological stages. C-erbB-1 and c-erbB-2 levels were strongly correlated (P=0.0004-0.029) with the expression of MMP-2, MMP-7, MMP-9, MMP-10, MMP-11, MMP-13, VEGF-A and VEGF-C whereas the levels of c-erbB-3 and c-erbB-4 showed a weaker correlation (P=0.049-0.01) with some MMPs and VEGF-C. Only nodal metastasis and c-erbB-1 levels were significantly associated with poor outcome in uni- and multi-variate analysis.

Expression of the calcium-dependent cell-cell adhesion molecule E-cadherin was examined in 187 primary breast carcinomas. A marked difference in expression of E-cadherin was observed between infiltrating lobular carcinomas (ILC) and infiltrating ductal carcinomas (IDC), the former showing complete loss of membrane staining, whereas 93% of IDC retained some level of expression. In IDC, reactivity was not related to tumour grade but there was a significant association between reduced membrane levels of E-cadherin and the presence of lymph node metastasis, and a highly significant correlation between the presence of cytoplasmic E-cadherin and metastasis. A significant relationship was also demonstrated between reduced E-cadherin reactivity and expression of EGFR (Jones *et al.*, 1996).

1.7.2 C-erbB-2 Transfection Studies Looking at the Role of C-erbB-2 in Metastasis.

Various groups have transfected both transformed and cancer cell lines with c-erbB-2 to investigate its effect on their metastatic potential.

MCF-10A was transfected with c-erbB-2 and Ha-ras, both separately (MCF-10A-H and MCF-10A-E) and in combination (MCF-10A-HE). In soft agar assays MCF-10A do not grow on agar. MCF-10A-H and MCF-10A-E gave rise to a limited number of colonies, while MCF-10A-HE showed a 10-fold increase in colony formation. Chemotaxis was examined in Boyden chambers. MCF-10A parent cells displayed only weak migratory activity. MCF-10A-H, MCF-10A-E and MCF-10A-HE were found to migrate in response to F-CM (fibroblast conditioned media). They also examined degradation of Matrigel as an indicator for the cells' ability to grow and invade the extracellular matrix. All transfectants invaded Matrigel with MCF-10A-H, MCF-10A-E and MCF-10A-HE having Invasive Indices of 3-, 4- and 5-fold higher respectively than MCF-10A. The MCF10A-HE cells also adopted an invasive stellate growth pattern when plated or embedded in Matrigel, in contrast to the spherical colonies formed by the single transformants MCF10A-H, MCF10A-E, and the parental cells. Expression of MMP-2 was found to be as follows MCF-10A-HE > MCF-10A-E > MCF-10A-H > MCF-10A. TIMP-2 levels were lower in the transfectants. CD44 isoforms were altered in MCF-10A-HE, and expressed more of the lower molecular weight forms. These results indicate that c-erbB-2 and Ha-ras co-expression can induce a more aggressive phenotype *in vitro*, representative of the malignancy of mammary carcinomas (Giunciuglio *et al.*, 1995).

Since basement membrane degradation is a prerequisite for tumour progression Gum *et al.* (1995) investigated whether urokinase, a protease which degrades key components of the basement membrane/extracellular matrix, was regulated by c-erbB-2. H460 lung cancer cells were transfected with c-erbB-2. The transfected cells were found to secrete increased amounts of urokinase protein and have enhanced the promoter activity of the urokinase gene. Levels of urokinase mRNA were also found to be elevated while growth rates were not altered. Urokinase converts inert zymogen plasminogen into the widely acting serine protease plasmin, which cleaves a variety of proteins including

laminin and fibronectin as well as activating type IV collagenase. C-erbB-2-induced expression of urokinase may contribute to tumour progression.

Another group transfected MDA-MB-435 with c-erbB-2. Three transfectants, 435.eB1, 435.eB2 and 435.eB4, were selected expressing 258-, 149- and 165-fold higher levels of c-erbB-2 respectively, as compared to the parent cell line. Single cell suspensions of MDA-MB-435, MDA-MB-435/neo control cells and 435.eB1, 435.eB2 and 435.eB4 were injected into the lateral tail veins of 8-week old female ICR-SCID mice. The size of the metastatic nodule found after 90 days were found to be the same, however numbers increased significantly in the 435.eB1, 435.eB2 and 435.eB4 injected mice. They then created an extravasation model that consisted of Matrigel invasion chambers. Significantly higher rates of invasion were observed in the 435.eB transfectants. No increase in motility was seen using chemoattractants. Similar adhesion ability to the extracellular matrix molecules laminin, fibronectin, collagen IV, vitronectin and Matrigel was observed. They observed higher expression of MMP-2 and MMP-9 in the cultured media of the transfectants, with the greatest expression of both in the highest expression transfectant. C-erbB-2 was not found to effect *in vitro* growth rate, or *in vitro* transforming ability, as measured in soft agar assays (Tan *et al.*, 1997).

A study by Roetger *et al.* (1998) analysed disaggregated cells and cell clusters from freshly dissected breast cancer tissues. They looked to see whether their capability of extravasation is correlated with their expression of c-erbB-2. They found that invasive, predominantly clustered cells from 14/23 tumors were positively stained for c-erbB-2 by immunocytochemistry. In four control breast cancer cell lines (SK-BR-3, MCF-7, MDA-MB-468 and MDA-MB-468, the latter transfected with a full-length c-erbB-2 cDNA vector) producing different levels of the c-erbB-2 receptor, the expression level correlated positively with the invasiveness of the cells. They also showed that the invasive cell populations express the metastasis-associated proteins, matrix metalloproteinase MMP-2, CD44, and integrins $\alpha v\beta 3$ and $\alpha 6$. Zhang *et al.* (1998) was able to show that c-erbB-2 expression may have a direct effect on the expression of gelatinase, Type IV collagenases MMP-2 and MMP-9. NIH 3T3 cells were transfected with point mutation activated neu, a mutant analogue of neu, the rat homologue of c-erbB-2. These cells were then treated with emodin and DK-V-47 (a derivative of emodin) which repress the tyrosine kinase activity of c-erbB-2. A consequence of this repression of kinase activity was an inhibition of anchorage and independent growth

dependant (by 55% and 83% respectively), and a decrease in the expression of MMP-2 and MMP-9. Both compounds virtually abolished the ability of the cells to perform in *in vitro* invasion assays.

Several transgenic mice carrying the activated rat c-erbB-2 gene under the transcriptional control of MMTV have been created. In several strains of MMTV/activated c-erbB-2 mice, early onset of transgene expression in the mammary epithelium of female mice was associated with the synchronous development of tumors involving the entire mammary epithelium. This suggests that c-erbB-2 requires few additional genetic events to transform the mammary epithelial cell. This suggests that activated c-erbB-2 can act as a potent oncogene in the mammary epithelium. It is thought that unactivated c-erbB-2 is the primary mechanism contributing to human breast cancer as biopsies have failed to find evidence of activating mutations. Guy *et al.* (1992) derived six MMTV/unactivated c-erbB-2 transgenic mice lines. Overexpression of normal c-erbB-2 in the mammary epithelium of 5 of these 6 lines resulted in the appearance of focal mammary tumours that metastasised with high frequency. Histological examination revealed focal mammary adenocarcinomas surrounded by hyperplastic mammary epithelium. These tumours were composed of solid nests of pale intermediate cells that were morphologically identical to tumours associated with activated c-erbB-2. Transplantation of the tumour cells into the mammary fat pads of syngenic recipients resulted in the appearance of tumours, confirming their neoplastic potential. Male MMTV/c-erbB-2 carriers did not exhibit any phenotypic abnormalities. The tumours were found to express increased levels of c-erbB-2 when compared to surrounding normal mammary epithelium. A high percentage of tumours bearing MMTV/c-erbB-2 animals developed metastases to the lungs.

Over-expression of c-erbB-2 in MDA-MB-435 cells resulted in increases in mRNA and protein levels of the actin bundling protein fascin. Heightened fascin expression has been observed in other systems to result in greatly increased cell motility. MDA-MB-435 cells over-expressing c-erbB-2 exhibit significantly heightened cellular dynamics and locomotion, while visualisation of bundled microfilaments within fixed cells revealed enhanced formation of dendritic-like processes, microspikes and other dynamic actin based structures (Grothey *et al.*, 2000).

NRG and type I receptor tyrosine kinase (RTK) expression was investigated in the highly invasive and metastatic LM3 breast cancer cell line. Although LM3 cells do not express NRG, they exhibit high levels of c-rbB-2 and c-erbB-3 as well as moderate expression of c-erbB-4. Addition of exogenous NRGβ1 resulted in inhibition of both proliferation and migration of LM3 cells. NRGβ1 was also able to decrease the activity of urokinase-type plasminogen activator (uPA) and matrix metalloproteinase 9 (MMP-9), 2 key enzymes in the invasion and metastatic cascade. NRGβ1 treatment of LM3 cells induced tyrosine phosphorylation of c-erbB-2, c-erbB-3 and c-erbB-4 as well as the formation of c-erbB-2/c-erbB-3 and c-erbB-2/c-erbB-4 heterodimers. Assessment of the signalling pathways involved in NRGβ1 action indicated that the addition of NRGβ1 to LM3 cells resulted in activation of phosphatidylinositol 3- kinase (PI-3K) and in strong induction of the association of the p85 subunit of PI-3K with c-erbB-3. NRGβ1 also caused the rapid activation of ERK1/ERK2 and Stat3 and Stat5 (signal transducers and activators of transcription [STAT]). This is the first demonstration of the ability of NRGβ1 to activate STATs in mammary tumour cells. Blockage of PI-3K activity with its chemical inhibitor wortmannin, or of MEK1/ERKs activity with PD98059, resulted in suppression of the ability of NRGβ1 to inhibit LM3 cell growth. Notwithstanding the suppression of these 2 signalling pathways, NRGβ1 still proved capable of inhibiting uPA activity (Puricelli *et al.*, 2002).

O-charoenrat *et al.* (1999) examined the effects of ligands with different ErbB receptor specificities in terms of their stimulation of HNSCC proliferation, expression of matrix metalloproteinases (MMPs) and invasion. NRG-β1 (NRG-β1; selective c-erbB-3/B-4 ligand) was found to stimulate proliferation in the majority of cell lines, whereas epidermal growth factor (EGF; c-erbB-1 ligand) and betacellulin (BTC; c-erbB-1/B-4 ligand) induced variable responses. All three ligands up-regulated multiple MMPs including collagenases, stromelysins, matrilysin and gelatinase B (MMP-9) but had minimal or no effects on gelatinase A (MMP-2), MT1-MMP and tissue inhibitors of MMPs (TIMPs). NRG-β1 was less active than EGF and BTC at the optimal concentration (relative potency of EGF:BTC:NRG = 3:4:1). *In vitro* invasion through Matrigel was also increased by all three ligands in proportion to their MMP up-regulation. A specific anti-EGFR monoclonal antibody (mAb ICR62) inhibited MMP up-regulation, migration and invasion induced by all three ligands, whereas an anti-c-erbB-2 mAb ICR12 inhibited mitogenic and motogenic responses following ligand

stimulation but had no effect on MMP expression. These results suggest that ErbB ligands may differentially potentiate the invasive phenotype of HNSCC via co-operative induction of cell proliferation, migration and proteolysis. The c-erbB-1 signalling pathway appears to be the dominant component controlling the proteolytic and invasive phenotype in HNSCC, whereas the c-erbB-2 signalling pathway is responsible, in part, for the mitogenic and motogenic effects of ligands.

Studies have shown that tumour cells with metastatic propensity secrete more of the laminin α2 chain than non-metastatic tumour cells do, and that laminin-2, which contains the α2 chain, promotes cell adhesion better than laminin-1. Han *et al.* (1999) examined whether a correlation existed between the expression of the laminin-2 isoform and the metastatic phenotype in melanoma cells. They found that expression of the laminin-2 isoform was upregulated in the metastatic melanoma cell lines tested. Cell attachment studies showed that metastatic melanoma cells attached more efficiently to laminin-2 substrates. Studies on integrin expression revealed that the presence of $\alpha_2\beta_1$ integrin correlated with expression of the laminin-2 isoform in metastatic melanoma cells; anti-integrin α_2 antibody prevented cell attachment to laminin-2 substrates. This interaction, mediated by the $\alpha_2\beta_1$ integrin, stimulated secretion of the 72 kD type IV collagenase and induced a specific 185 kD protein tyrosine phosphorylation, identified as the c-erbB-2 by immunoprecipitation. These studies suggest that upregulation of expression of the laminin-2 chain correlates with the metastatic phenotype of melanoma cells and provides evidence that specific c-erbB-2 tyrosine phosphorylation may be involved in integrin-mediated signalling during tumour cell invasion and metastasis.

C-erbB-2 overexpression in human mammary epithelial cells resulted in acquisition of anchorage-independent growth and invasion capabilities. C-erbB-2 induced invasion was dependent on fibronectin and correlates with the down-regulation of cell surface α_4 integrin. In addition c-erbB-2 co-immunoprecipitated with focal adhesion kinase (FAK) in these cells. C-erbB-2-induced invasion is dependent on the PI3'-kinase pathway (Ignatoski *et al.*, 2000).

Flavopiridol is a flavone that inhibits several cyclin-dependent kinases and exhibits potent growth-inhibitory activity against a number of human tumour cell lines, both *in vitro* and when grown as xenografts in mice. Li *et al.* (2000) investigated whether flavopiridol could be an effective agent against a series of isogenic breast-cancer cell

lines having different levels of c-erbB-2 expression and differential invasion and metastatic characteristics. Flavopiridol was found to inhibit the growth of MDA-MB-435 (parental) and 435.eB (stable transfectants) cells that were established by transfecting c-erbB-2 cDNA into MDA-MB-435. Induction of apoptosis was also observed in these cell lines when treated with flavopiridol. They also found modest up-regulation of Bax and down-regulation of Bcl-2, but there was a significant down-regulation of c-erbB-2 in flavopiridol-treated cells. Gelatin zymography showed that flavopiridol inhibits the secretion of MMPs 2 and 9 in the breast cancer cells and that the inhibition of c-erbB-2 and MMPs may be responsible for the inhibition of cell invasion observed in flavopiridol-treated cells. Collectively, these molecular effects of flavopiridol, however, were found to be independent of c-erbB-2 overexpression, suggesting that flavopiridol may be effective in all breast cancer.

Spencer *et al.* (2000) utilised carcinoma cells depleted of c-erbB-2, but not other ErbB receptor members, to specifically examine the role of c-erbB-2 in carcinoma cell migration and invasion. Cells stimulated with EGF-related peptides show increased invasion of the extracellular matrix, whereas cells devoid of functional c-erbB-2 receptors do not. C-erbB-2 facilitated cell invasion through extracellular regulated kinase (ERK) activation and coupling of the adaptor proteins, p130CAS and c-CrkII, which regulate the actin-myosin cytoskeleton of migratory cells.

Li *et al.* (1999) investigated the effects of genistein in the breast cancer cell line MDA-MB-435 and 435.eB cells that were established by transfecting c-erbB-2 cDNA into MDA-MB-435. They also investigated the effect of genistein on matrix metalloproteinase (MMP) secretion previously shown to be effected by c-erbB-2 transfection. Genistein was found to inhibit MDA-MB-435 and 435.eB cell growth. Induction of apoptosis was also observed in these cell lines when treated with genistein. They also found an up-regulation of Bax and $p21^{WAF1}$ expression and down-regulation of Bcl-2 and c-erbB-2 in genistein-treated cells. Gelatin zymography showed that genistein inhibits the secretion of MMP in the breast cancer cells.

Curcumin, a natural compound present in turmeric, possessing both anti-inflammatory and antioxidant effects, has been studied vigorously as a chemopreventative in several cancer models. Curcumin dose-dependently inhibited c-erbB-2 autophosphorylation in breast cancer cell lines and transphosphorylation *in vitro* and depleted c-erbB-2 protein

in vivo. It dissociated the binding of c-erbB-2 with GRP94 (glucose-regulated protein), a molecular chaperone, and enhanced the depletion of c-erbB-2. The amount of c-erbB-2 protein on the cell membrane was drastically decreased after curcumin treatment. The growth of several breast cancer cell lines was inhibited; the IC50 ranged from 7 to 18 microM, which, however, did not correlate with the expression level of p185neu. Colony formation in the soft agar assay, a hallmark of the transformation phenotype, was preferentially suppressed in c-erbB-2 overexpressing cell lines by 5 μM curcumin (% of control, basal level versus overexpression: 59.3 versus 16.7%; $P < 0.001$ by Student's t test) (Hong etl, 1999).

Overexpression of c-erbB-2 in the prostatic epithelial cell line NbE, resulted in increased cellular spreading and the expression of integrin $\alpha_6\beta_1$. C-erbB-2 transfected clones attached significantly better to specific substrates and spread significantly better on both specific and non-specific substrates as compared to the control clones. Additionally, the expression of integrin $\alpha_6\beta_1$, a key receptor enabling attachment and spreading on laminin, is upregulated on the metastatic clones NbE-neuT-9 and 10 (Vafa *et al.*, 1998). Laminin receptors (integrins $\alpha_6\beta_1$ and $\alpha_6\beta_4$) were found to associate directly with c-erbB-2 in carcinoma cell lines and NIH 3T3 transfected with c-erbB-2. Carcinoma cells treated with a monoclonal antibody to the α_6 integrin subunit showed a ligand-dependent increase of c-erbB-2 phosphorylated molecules coprecipitated with integrins and increased DNA synthesis. The interaction between growth factor receptors and integrins was also studied in NIH3T3 cells overexpressing $\alpha_6\beta_4$ receptors and c-erbB-2 protein. Cells overexpressing both receptors, showed enhanced proliferation rates and invasiveness, further suggesting that $\alpha_6\beta_4$ integrin and ErbB-2 receptor interaction might contribute to generate a more malignant phenotype in carcinoma cells (Falcioni *et al.*, 1997).

CD44 is a transmembrane glycoprotein that binds hyaluronic acid (HA). CD44 cell surface expression was 4.5 times higher in c-erbB-2 overexpressing mouse fibroblasts, than in the parental cell line. Overexpression of surface CD44s in c-erbB-2 transfected cells results in a dramatic enhancement of HA-mediated cell adhesion. Scatchard plot analysis indicates that CD44s in c-erbB-2 transfected cells binds directly and specifically to ankyrin. The binding affinity between CD44s and ankyrin in c-erbB-2 transfected cells was higher than that found in the untransfected cells. Double immunofluorescence staining and confocal microscopic analyses indicate that HA

induces the CD44s to form adhesion plaque-like structures, and causes an accumulation of intracellular ankyrin directly underneath CD44s-adhesion plaque-like structures in c-erbB-2 transfected cells (but not in untransfected cells). These findings suggest that overexpression of CD44s and up-regulation of CD44s-ankyrin interaction by c-erbB-2 may be one of the pre-requisite steps in regulating tumour cell behavior (Zhu *et al.*, 1996).

Expression of the activated rat c-erbB-2/neu oncogene in mouse embryo fibroblast 3T3 cells is sufficient to induce experimental metastases in nude mice. C-erbB-2/neu oncogene-transformed 3T3 cells were more adherent to microvessel endothelial cells and had higher gelatinase activities. It had previously been shown that the adenovirus 5 E1A gene product can suppress c-erbB-2/neu-induced transformation of 3T3 cells, and was subsequently found to reduce the formation of experimental metastatic tumours and inhibited metastasis-associated properties, such as adhesion to microvessel endothelial cells, migration through a layer of reconstituted basement membrane (Matrigel) and secretion of basement membrane-degradative enzymes. The results indicated that the c-erbB-2/neu gene induces higher metastatic potential through the promotion of adhesion and invasion steps of the metastatic cascade. The E1A gene, which functions by inhibiting these steps, is thus a suppressor gene for c-erbB-2/neu-induced experimental metastasis (Yu *et al.*, 1992).

Enforced expression of NRG in c-erbB-2 overexpressing SKBr-3 cells induces dramatic morphological changes and pronounced inhibition of anchorage-dependent and -independent growth. Most SKBr-3/NRG-transfected (SK/NRG) cells exhibited about 15-fold increase in size and persisted as multinucleated cells with extended flattened vacuole-filled cytoplasm with reduced cell attachment. The growth suppression of SK/NRG cells was accompanied by a reduction in S phase, the presence of a G2-M cell cycle delay, and an increase in DNA aneuploid components. In addition, DNA fragmentation assays showed that NRG induced apoptosis of SKBr-3 cells. In contrast, while NRG treatment of other erbB-2 overexpressing breast cancer cell lines led to growth arrest and cell detachment, it did not induce apoptotic features. Thus, this study demonstrates that while growth arrest and cell detachment are general effects of NRG towards erbB-2 overexpressing cells, the ability of NRG to induce apoptosis is a phenomenon confined to selective cells including SKBr-3 cells (Guerra-Vladusic *et al.*, 1999).

The effects of NRG and an anti-c-erbB-2 antibody have been compared in six ovarian cancer cell lines. NRG inhibited anchorage-independent growth of SKOv3 cells that overexpress c-erbB-2 but stimulated the growth of OVCA420, OVCA429, OVCA432, OVCA433, and OVCAR-3 cells that expressed lower levels of the receptor. Thus, cell lines with a high level of c-erbB-2 relative to c-erbB-3 or c-erbB-4 were growth inhibited, whereas cell lines with lower levels of c-erbB-2 were growth stimulated by NRG. Anti- c-erbB-2 antibodies inhibited the growth of SKOv3 cells but failed to affect the growth of the other cell lines. In OVCAR-3 cells that had been transfected with c-erbB-2 cDNA, NRG inhibited rather than stimulated growth. Conversely, when c-erbB-2 expression by SKOv3 cells was downregulated by transfection of the viral E1A gene, NRG stimulated rather than inhibited growth (Xu *et al.*, 1999). C-erbB-2 activation by NRG in the c-erbB-2 overexpressing cell line SKBr3, inhibited anchorage-independent growth while enhancing tyrosine phosphorylation of c-erbB-2. NRG treatment also increased adhesion of SKBr3 cells to plastic and increased invasiveness of tumour cells into Matrigel membranes while increasing expression of the CD44 (HCAM) and CD54 (ICAM-1) adhesion molecules. Tumour cell invasion of Matrigel membranes was partially blocked by either anti-CD44 or anti-CD54 antibodies, indicating a role for these adhesion molecules in the invasion process. Compatible with the increased invasiveness, NRG increased expression of the matrix metalloproteinase 9. In contrast, the agonistic anti-c-erbB-2 antibody ID5 induced only a subset of the responses induced by NRG. ID5 induced tyrosine phosphorylation c-erbB-2, increased invasiveness, and increased expression of CD44. The ID5 antibody failed to increase adhesion to plastic, expression of CD54, or production of matrix metalloproteinase 9 (Xu *et al.*, 1997).

Tan *et al.* (1999) reported that NRG-β1 enhanced aggregation of MCF-7 and SKBR3 human breast cancer cells. NRG-β1 induced tyrosine phosphorylation of c-erbB-2 and c-erbB-3 receptor heterodimers and increased the association of the dimerised receptors with the 85-kDa subunit of phosphatidylinositol 3-kinase (PI3K). NRG-β1 also increased the kinase activities of extracellular signal-regulated protein kinase (ERK) and PI3K in these cells. By using the mitogen-activated protein kinase/ERK 1 (MEK1) inhibitor PD98059 and PI3K inhibitors wortmannin and LY294002, they found that blocking the MEK1-ERK pathway had no effect on NRG-β1 enhanced cell aggregation;

however, blocking the PI3K pathway greatly inhibited NRG-β1 mediated cell aggregation.

A ligand for the c-erbB-2 receptor has not yet been identified but it can be activated by heterodimerization with NRG (NRG)-stimulated erbB3 and erbB4 receptors. The NRGs are a family of polypeptide growth factors that have been shown to play a role in embryogenesis, tumour formation, growth and differentiation of breast cancer cells. The erbB3 and erbB4 receptors are involved in transregulation of erbB2 signalling. The work presented here suggests biological roles for NRG including regulation of the actin cytoskeleton and induction of motility and invasion in breast cancer cells. NRG-expressing breast cancer cell lines are characterised by low erbB receptor levels and a high invasive and metastatic index, while those which overexpress erbB2 demonstrate minimal invasive potential *in vitro* and are non-tumorigenic *in vivo*. Treatment of the highly tumorigenic and metastatic NRG-expressing breast cancer cell line MDA-MB-231 with an NRG-neutralizing antibody significantly inhibited proliferation in culture and motility in the Boyden chamber assay. Addition of exogenous NRG to non-invasive erbB2 overexpressing cells (SKBr-3) at low concentrations induced formation of pseudopodia, enhanced phagocytic activity and increased chemomigration and invasion in the Boyden chamber assay. The specificity of the chemomigration response to NRG is demonstrated by inhibition with the anti-NRG neutralising antibody. These results suggest that either NRG can act as an autocrine or paracrine ligand to promote the invasive behaviour of breast cancer cells *in vitro* or thus may enhance the metastatic process *in vivo* (Hijazi *et al.*, 2000).

Additional evidence exists which show that c-erbB-2 affects the expression of metastatic associated proteins such as E-cadherin and β-catenin. The cadherins are a family of transmembrane glycoproteins that mediate cell-cell adhesion. Several subclasses of cadherins have been described, E-(epithelial), N-(neural) and P-(placental) cadherins. Cadherins appear to function by connecting cells to each other by homophilic interactions, in which they bind selectively to identical cadherin types (Liang, 1999). The E-cadherin molecule plays a central role in maintaining epithelial cell morphology through homotypic Ca^{2+}-dependent interactions. A reduction in E-cadherin expression is found in many breast cancers and is associated with increased invasiveness (D'Souza and Taylor-Papadimitriou, 1994). Three cytoplasmic proteins, α–, β–, γ– catenin have been found to associate with E-cadherin. Disruption of E-

cadherin-mediated intercellular adhesion promotes cell dissociation from the primary cancer nest and the E-cadherin-catenin complex functions as an invasion suppresser system in cancers (Shibata *et al.*, 1996). Overexpression of c-erbB-2 in the human mammary epithelial cell line, MTSV1-7, is associated with reduced ability to undergo morphogenesis *in vitro* and with a decreased level of expression of the E-cadherin and α_2 integrin genes. Signalling from the c-erbB-2 receptor was blocked using the 4D5 antibody to c-erbB-2. Transfectants regained the ability to form three-dimensional structures in collagen gels and the rates of transcription of E-cadherin and α_2 integrin genes were returned to normal (D'Souza and Taylor-Papadimitriou, 1994; D'Souza *et al.*, 1993). C-erbB-2 phosphorylates β-catenin. In human gastric cancer TMK-1 cells expressing a N-terminally truncated β-catenin, which binds c-erbB-2 but not E-cadherin, the association between endogenous β-catenin and c-erbB-2 protein was inhibited, suppressing the phosphorylation of β-catenin. These cells exhibited markedly reduced invasiveness *in vitro* and peritoneal metastasis *in vivo* and developed an epithelial morphology (Shibata *et al.*, 1996).

C-erbB-2 was found to associate with the cadherin-catenin complex through β-catenin and plakoglobin, resulting in the phosphorylation of β-catenin causing disruption of the cadherin-mediated cell adhesion system in cancer cells (Ochiai *et al.*, 1994).

The human papillomavirus type 16 (HPV-16), the type most often associated with cervical cancer, immortalises primary keratinocytes and inhibits serum/calcium-stimulated differentiation in culture. An immortalised keratinocyte cell line generated by cotransfection with HPV-16 E6 and E7 showed decreased membrane E-cadherin expression and redistribution of α-, β-, and γ-catenin from the undercoat membrane to the cytoplasm. Selection of the immortalised keratinocyte cell line for resistance to differentiation generated a more transformed cell line with an invasive phenotype, down-regulated E-cadherin and α-catenin, and up-regulated c-erbB-1. Transfection of an E-cadherin expression construct into the differentiation-resistant cell line restored membrane-bound E-cadherin and catenin expression, down-regulated c-erbB-1, and reversed the invasive phenotype. These results indicated that overexpression of the c-erbB-1 correlates with perturbation of the E-cadherin/catenin complex seen in the HPV-16 E6- and E7-transfected keratinocytes (Wilding *et al.*, 1996).

Geldanamycin depleted c-erbB-2 expression in melanoma cells, resulting in a loss of its association with β-catenin without perturbing either LAR receptor or β-catenin levels or LAR/β-catenin association. Geldanamycin also stimulated tyrosine dephosphorylation of β-catenin and increased β-catenin/E-cadherin association, resulting in substantially decreased cell motility. Geldanamycin also decreased the nuclear β-catenin level and inhibited β-catenin-driven transcription, as assessed using two different β-catenin-sensitive reporters and the endogenous cyclin D1 gene (Bonvini *et al.*, 2001).

1.8 Chemotherapeutic Agents

1.8.1 Adriamycin

Adriamycin is an anthracycline isolated from *Streptomyces*. It has a characteristic four-ring structure that is linked via a glycosidic bond to daunosamine, an amino sugar. Adriamycin is used to treat a broad range of solid tumours.

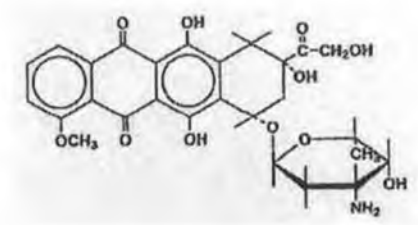

Figure 1.8.1 Structure of adriamycin.

Adriamycin binds tightly to DNA by intercalation, resulting in local uncoiling of the double helix as a result of the separation of the stacked bases by the intercalated moiety. As a result of this the super-coiled double helix is greatly changed by the cumulative effects of these local uncoiling events. Adriamycin induces protein-linked double stranded DNA breaks, which are introduced by topoisomerase II. The drug somehow interferes with the DNA strand breakage reunion of topoisomerase II. There is a direct correlation between decreased topoisomerase II activity and adriamycin resistance. Another mechanism of action of adriamycin is the formation of active oxygen species that form single strand breaks (Pratt *et al.,* 1994).

Adriamycin has a broad range of activity and is used in the treatment of breast, bladder, endometrium, lung, ovarian, stomach and thyroid carcinomas. It is also effective against sarcomas of the bone and soft tissue, paediatric solid tumours, and lymphoid and myelogenous tumours (Hortobagyi, 1997).

Common methods of resistance to adriamycin involve increased drug efflux, due to overexpression of P-glycoprotein, MRP family members and LRP (Clynes *et al.*, 1998; Borst *et al.*, 1999; Cui *et al.*, 1999; Young *et al.*, 1999). Cells selected for resistance to

adriamycin are usually cross resistant to vinca alkaloids and other antibiotics such as actinomycin D. Other cell lines have been found to have altered levels of glutathione peroxidase, glutathione or glutathione S-transferase (Cole *et al.*, 1990). Topoisomerase II-mediated adriamycin-resistance can be divided into 2 categories. The first involves quantitative changes, and usually involves decreased cellular expression of the enzyme. The second mechanism involves decreased drug-induced DNA cleavage, differential expression of topoisomerase isoforms, altered subcellular distribution of topoisomerase II and changes in extrinsic factors modulating topoisomase II activity (Skovsgaard *et al.*, 1994).

1.8.2 The Taxanes

Taxol is a natural product isolated from the bark of the Pacefic yew tree, *Taxus brevifolia*. The anti-tumour activity of the yew bark extract was discovered through a plant screening program in the 1960s. Taxotere is a semi-synthetic product derived from the needles of the European yew, *Taxus baccata*. Both share the tricyclic taxane skeleton but have different substituents at the c-10 and the c-13 side chains. Taxol and taxotere share a unique mechanism of cytotoxic action. Both agents promote assembly of tubulin into microtubules, and render them resistant to depolymerisation. Treated cells are blocked in the G2/M phase of the cell cycle giving rise to mitotic arrest (Francis *et al.*, 1995). Both taxoids bind to the β-subunit of tubulin, but the microtubules produced by taxotere are larger than those produced by taxol. This may explain why taxotere appears to be two to four times more potent than taxol (Vaishampayan *et al.*, 1999).

Taxol →

Taxotere →

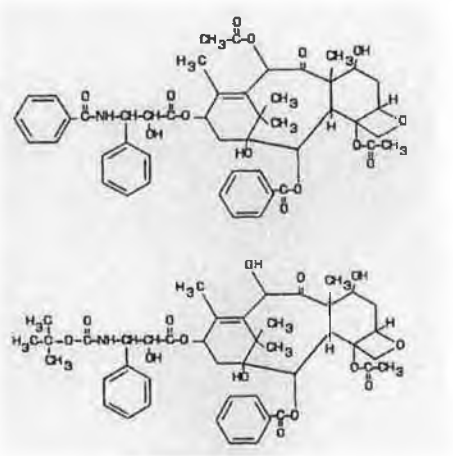

Figure 1.8.2 The taxanes, taxol and taxotere

Resistance to taxanes arises through two major mechanisms. Increased expression of p-glycoprotein (Bradley and Ling, 1994; Gottesman and Pastan, 1993) and alterations in its microtubule binding activity (Cabral and Barlow; 1989; Dumonter *et al.*, 1996; Haber *et al.*, 1995).

1.8.3 Carboplatin

Carboplatin (cis-diammine- 1,1'-cyclobutane dicarboxylate platinum II, CBDCA, JM-8) was developed by Bristol-Myers Squibb in collaboration with the Institute of Cancer Research, Sutton, UK and the Johnson-Matthey Company, Reading, UK. It is the only cisplatin derivative currently available world-wide for cancer treatment (Lebwohl and Canetta, 1998).

Carboplatin is converted to alkylating species in the body forming adducts at the N-7 position of guanine and adenine. These adducts can interact with adjacent bases on the same strand of DNA (intrastrand adducts) or on separate strands (interstrand adducts). The order of preference for adduct formation is G:G > A:G > others. Intrastrand adducts distort the DNA helix whilst interstrand adducts prevent strand separation so that replication is inhibited or abnormal. Carboplatin is effective against ovarian and testicular cancer and has minimal effects on the bone marrow. It also has the advantage of having greatly reduced side effects in comparison to its analogue (King, 2000).

Resistance to carboplatin can occur by altered cellular transport, enhanced DNA repair, increased expression of glutathione and glutathione-S-transferase, and decreased apoptosis, in particular increased bcl-2 expression (King, 2000).

1.8.4 Vincristine

Vincristine is a naturally occurring alkaloid. It is found in minute quantities in the leaves of the periwinkle plant *Catharanthus roseus*. It medicinal value has been known since the 17th century. Extracts of the plant have been used to stop haemorrhage, heal scurvy, relieve toothaches, heal wounds and diabetic ulcers, and to lower blood sugar levels. Svoboda showed anti-leukaemic activity against P-1534 lymphocytic leukaemia

in DBA/2 mice using certain extracts of the plant. Indeed vincristine cured P-1534 leukemia in mice with an acceptable range of side effects (Gidding *et al.*, 1999).

The molecular structure of vincristine is asymmetrical and dimeric, composed of a dihyrdoindole nucleus, vindoline, linked by a carbon-carbon bond to an indole nucleus, catharanthine. Vincristine sulphate in the 1:1 sulphate salt from *Catharanthus roseus*. Vincristine is more frequently used in paediatric oncology, than adult oncology. Paediatric tumours appear to be more sensitive to vincristine and children are able to tolerate higher doses of the drug. It is a key drug in the treatment of acute lymhoblastic leukaemia and non-Hodgkin's lymphoma. In adults response rates are greater in malignancies of haematological origin, than in solid malignancies, with the exception perhaps of AIDS-associated Kaposi's sarcoma (Gidding *et al.*, 1999).

Vincristine inhibits tumour growth by its interference with the mitotic spindle microtubules resulting in the inhibition of mitosis. *In vitro* vincristine induces apoptosis in tumour cells, while in animal models it induces tumour necrosis. Vincristine binds to tubulin or microtubules, which damages the spindle structure in a concentration-dependant manner resulting in microtubule disruption. The concentration of vincristine used determines the effect it has on the microtubules. Low concentrations of vincristine stabilise the spindle apparatus resulting in the failure of chromosomes to segregate, leading to metaphase arrest and inhibition of mitosis. Higher concentrations result in disruption and total depolymerisation of microtubules (Gidding *et al.*, 1999).

Mechanisms of vincristine resistance include p-glycoprotein, mrp1 and lung resistance protein (lrp). Verapamil and cyclosporin A may modulate p-glycoprotein-mediated vincristine resistance. Decreased binding affinity of tubulin for vincristine also plays a role in vincristine resistance. This may be due to changes in tubulin isoforms expressed or different tubulin levels. Also altered stability of microtubules may result in changes in the equilibrium between free and polymerised tubulin in cells (Gidding *et al.*, 1999).

1.8.5 Etoposide (VP-16)

VP-16 is a semi-synthetic derivative of podophyllotoxin, a microtubule inhibitor found in extracts of the mandrake plant (Hande, 1998). Podophyllotoxins have been used as medications by various cultures for over a 1000 years. In the 19th century podophyllin

was found to be topically effective in the treatment of skin cancer. In the 1950s researchers at Sandoz Pharmaceuticals began synthesising a number of derivatives in the hope of identifying agents with increased anti-neoplastic activity and reduced toxicity. Several derivatives were found to have antitumour activity against L1210 leukaemia, the most effective being 4'-demethylepipodophyllin benzylidene glucoside (DEPBG). Two analogues of DEPBG were subsequently synthesised and named VP-16 (1966) and teniposide (1967).

VP-16 went into clinical trials before its mechanism of action (inhibition of topoisomerase II) was understood. This is in part due to the fact that this enzyme was been investigated at the same time and was not understood until 1979. At concentrations achieved *in vivo*, VP-16 causes dose-dependant single strand and double strand DNA breaks. Upon its removal, this DNA breakage is swiftly repaired. Incubation of VP-16 with purified DNA does not result in DNA breaks, however when VP-16 was incubated with isolated nuclei, again DNA breakage was observed. It was subsequently discovered that the missing link was topoisomerase II. Topoisomerase II enzymes, the target for VP-16, require ATP for overall activity and modulate DNA topology by passing an intact helix through the transient double stranded break created in the DNA back bone. They therefore regulate over- and under-winding of the double helix and resolve nucleic acid knots and tangles. VP-16 poisons topoisomerase II by increasing the steady state concentration of their covalent DNA cleavage complexes. This action converts the topoisomerases into physiological toxins that introduce high levels of transient protein-associated breaks in the genome of the treated cells. Replication machinery or helicases attempting to traverse the covalently bound topoisomerase roadblock encounter difficulties leading to the disruption of the cleavage complex and converts transient DNA breakage into permanent double stranded fractures which are no longer held together by the proteinaceous bridges. These breaks then become targets for recombination, sister chromatid exchange, the generation of large deletions or insertions and the production of chromosomal aberrations ultimately leading to apoptosis and cell death (Hande, 1998).

Development of resistance to VP-16 can be due to reduced levels of topoisomerase II within the target cells. Increased expression of MDR-1 also confers resistance to VP-16. Finally mutations or alterations in drug binding sites on topoisomerase II are associated with resistance. VP-16 has demonstrated activity against acute myeloid

leukaemia, Hodgkin's disease, non-Hodgkin's lymphoma, lung cancer, gastric cancer, breast cancer, testicular cancer, Kaposi's sarcoma and ovarian cancer. The major toxicities seen with VP-16 are bone marrow depression, nausea, diarrhoea, mucositis and hypotension (Hande, 1998).

1.8.6 5-Fluorouracil (5-FU)

5-FU was first synthesised in 1957 and is a member of the antimetabolite group of drugs. Its major action is through inhibition of nucleotide synthesis and through incorporation into nucleic acids (Pratt *et al.*, 1994). 5-Fluorouracil was one of the first rationally designed anti-metabolites. Its activation occurs via the physiologic pyrimidine pathway and salvage pathways. 5-FU is activated in analogy to thymine via the physiological pyrimidine pathway before incorporation into DNA. 5-FU also competes with uracil for uptake into RNA. Thymidylate synthase is responsible for the *de novo* syntheisis of deoxythymidine monophosphatase, which is subsequently phosphorylated twice before its incorporation into DNA. This central role of thymidylate synthase makes rapidly proliferating cells vulnerable to the biochemical modulation of 5-FU by tetrahydrofolates. Activated 5-FU builds a stable complex with thymidine synthase abolishing enzyme activity. Elevated levels of thymidylate synthase contribute to resistance to 5-FU (Mader *et al.*, 1998).

1.8.7 Methotrexate

Methotrexate is a folate antagonist first developed for the treatment of malignancies and subsequently used in non-neoplastic diseases as an anti-inflammatory and/or immunosuppressive drug. The transmembrane transport of folate and antifolate analogs that share structural similarity with the folate compounds occurs by at least two different mechanisms, the low affinity reduced folate transmembrane carrier and a membrane associated folate-binding protein. Resistance to methotrexate can be via a number of mechanisms. These include decreased uptake, alteration in of its target enzyme dihydrofolate reductase (DHFR), overproduction of DHFR, decreased ability of cells to convert methotrexate to polyglutamates (Genestier *et al.*, 2000).

1.8.8 Tamoxifen Hormonal Therapy

Estrogens can both promote and inhibit the growth of breast cancer cells. Adenocarcinoma of the breast was the first tumour to be treated by manipulation steroid hormone levels. The initial report by Beatson in 1896 describes the clinical courses of three breast cancer patients who had their ovaries removed (ablative therapy). Lacassagne, who induced the development of breast tumours in male mice by injecting them with estrogen, established the first association between estrogens and mammary tumourigenesis in 1932. Haddow *et al.* demonstrated in 1944, that high doses of estrogen benefited some breast cancer patients. Subsequently this was shown to be true of postmenopausal patients, but not premenopausal patients.

Tamoxifen, the most commonly used drug in breast cancer hormonal therapy, has direct anti-estrogenic effects on the tumour cell. It is used in both adjuvant therapy and in treatment of metastatic disease. It is structurally similar to estrogen and binds in its place. However, it fails to activate the receptor, with the result that estrogen response target genes are not activated, thus inhibiting cell proliferation (Pratt *et al.*, 1994).

Aims of Thesis

The aim of the thesis was to investigate the role of c-erbB-2 in breast cancer, with respect to its effects on:-

- chemotherapeutic drug resistance
- tamoxifen resistance
- expression of estrogen receptors and expression of other members of the ErbB receptor family
- cell growth rate
- adhesion to extracellular matrix proteins
- cell motility
- cell invasiveness

An important goal of this thesis was to establish two cell models with altered levels of c-erbB-2. BT474A, a c-erbB-2 overexpressing cell line, was transfected with a c-erbB-2-targeted ribozyme to reduce levels of c-erbB-2. MCF-7 H3, a c-erbB-2 low-expressing cell line, was transfected with c-erbB-2 cDNA to increase levels of c-erbB-2.

To further investigate the possible role of c-erbB-2 in the emergence of chemotherapeutic drug resistance in breast cancer, two chemotherapeutic drugs, taxol and adriamycin, were chosen to establish resistant variants of the breast cell line MDA-MB-435S-F, which exhibits very low levels of c-erbB-2 expression. Patterns of cross resistance to various chemotherapeutic drugs, ErbB receptor family expression, cell growth rate, adhesion to extracellular matrix, motility and invasion properties, and expression of resistance-related genes in the drug-resistant variants were examined.

2.0 Materials & Methods

2.1 Ultrapure water

Ultrapure water (UHP), was used in the preparation of all media and solutions. This water was purified to a standard of 12-18 MΩ/cm resistance by a reverse osmosis system (Millipore MilII-RO 10 Plus, Elgastat UHP).

2.2 Glassware

The solutions used in the various stages of cell culture were stored in sterile glass bottles. All sterile bottles and other glassware required for cell culture related applications were prepared as follows: glassware and lids were soaked in a 2% RBS-25 (AGB Scientific) for 1 hour. After this time, they were cleansed and washed in an industrial dishwasher, using Neodisher detergent and rinsed twice with UHP. The resulting materials were sterilised by autoclaving as described in Section 2.3.

2.3 Sterilisation Procedures

All thermostable solutions, water and glassware were sterilised by autoclaving at 121°C for 20 minutes at 15 p.s.i.. Thermolabile solutions were filtered through 0.22 μm sterile filters (Millipore, Millex-GV SLGV025BS). Larger volumes (up to 10 litres) of thermolabile solutions were filter sterilised through a micro-culture bell filter (Gelman, 12158).

2.4 Preparation of cell culture media

Basal media used during cell culture was prepared as follows: 10X media was added to sterile UHP water, buffered with HEPES (N-(2-Hydroxyethyl) piperazine-N-(2-ethanesulfonic acid) and $NaHCO_3$ as required and adjusted to pH 7.5 using sterile 1.5 N NaOH or 1.5 N HCl. The media was then filtered through sterile 0.22μm bell filters (Gelman, 12158) and stored in sterile 500ml bottles at 4°C. Sterility checks were performed on all bottles of media by inoculation of media samples on to Colombia

blood agar (Oxoid, CM217), Sabauraud dextrose (Oxoid, CM217) and Thioglycolate broths (Oxoid, CM 173). All sterility checks were then incubated at both 25°C and 37°C. These tests facilitated the detection of bacterial, yeast and fungal contamination.

Basal media were stored at 4°C for up to three months. The HEPES buffer was prepared by dissolving 23.8g of HEPES in 80ml UHP water and this solution was then sterilised by autoclaving. Then 5ml sterile 5N NaOH was added to give a final volume of 100ml. $NaHCO_3$ was prepared by dissolving 7.5g in 100ml UHP water followed by autoclaving. Complete media was then prepared as follows: supplements of 2mM L-glutamine (Gibco, 11140-0350) for all basal media and 1ml 100X non-essential amino acids (Gibco, 11140-035) and 100mM sodium pyruvate (Gibco, 11360-035) were added to MEM. Other components were added as described in Table 2.4.1. Complete media was stored at 4°C for a maximum of one week.

Table 2.4.1 Additional components in media.

Cell Line	**Basal Media**	**Fetal Calf Serum (%)**	**Additional L-Glutamine**	**Bovine Insulin (0.01 mg/mL)**
BT474A and its variants	RPMI 1640	10	2mM	+
MDA-MB-435S-F and its variants	RPMI 1640	10	N/A	-
MCF-7 H3 and its variants	ATCC	5	N/A	-
RPMI 2650 and its variants	MEM	5	N/A	-

2.5 Cells and Cell Culture

All cell culture work was carried out in a class II laminar air-flow cabinet (Nuaire Biological Laminar Air-Flow Cabinet). All experiments involving cytotoxic compounds were conducted in a cytogard laminar air-flow cabinet (Gelman Sciences, CG series). Before and after use the laminar air-flow cabinet was cleaned with 70% industrial

methylated spirits (IMS). Any items brought into the cabinet were also cleaned with IMS. At any time, only one cell line was used in the laminar air-flow cabinet and upon completion of work with any given cell line the laminar air-flow cabinet was allowed to clear for at least 15 minutes so as to eliminate any possibilities of cross-contamination between the various cell lines. The cabinet was cleaned weekly with industrial disinfectants (Virkon or TEGO) and these disinfectants were alternated every month. Details pertaining to the cell lines used for the experiments detailed in this thesis are provided in Table 2.5.1. All cells were incubated at 37°C and where required, in an atmosphere of 5% CO_2. Cells were fed with fresh media or subcultured (see Section 2.5.1) every 2-3 days in order to maintain active cell growth. All of the cell lines listed in Table 2.5.1 are anchorage-dependent cell lines.

2.5.1 Subculturing of cell lines

The waste cell culture medium was removed from the tissue culture flask and discarded into a sterile bottle. The flask was then rinsed out with 1ml of trypsin/EDTA solution (0.25% trypsin (Gibco, 043-05090), 0.01% EDTA (Sigma, E9884) solution in PBS (Oxoid, BRI4a)) to ensure the removal of any residual media. 5ml of trypsin was then added to the flask, which was then incubated at 37°C, for approximately 5 minutes, until all of the cells detached from the inside surface of the flask. The trypsin was deactivated by adding an equal volume of complete media to the flask. The cell suspension was removed from the flask and placed in a sterile universal container (Sterilin, 128a) and centrifuged at 1000rpm for 5 minutes. The supernatant was then discarded from the universal and the pellet was suspended in complete medium. A cell count was performed and an aliquot of cells was used to re-seed a flask at the required density.

Cell line	Basal Medium*	Cell type	Source**
BT474	RPMI 1640	Ductal carcinoma of the breast	ATCC
BT474A	RPMI 1640	Clonal subpopulation of BT474	NCTCC
BT474A/ErbB2-Rz pool	RPMI 1640	C-erbB-2 ribozyme transfected BT474A	NCTCC
BT474A/ErbB2-Rz1	RPMI 1640	Clonal subpopulation of BT474A/ErbB2-Rz pool	NCTCC
BT474A/ErbB2-Rz3	RPMI 1640	Clonal subpopulation of BT474A/ErbB2-Rz pool	NCTCC
BT474A/ErbB2-Rz4	RPMI 1640	Clonal subpopulation of BT474A/ErbB2-Rz pool	NCTCC
BT474A/ErbB2-Rz5	RPMI 1640	Clonal subpopulation of BT474A/ErbB2-Rz pool	NCTCC
MCF-7 H3	ATCC	Breast Adenocarcinoma Clonal subpopulation of MCF-7	NCTCC
MCF-7 H3/ErbB2 pool	ATCC	C-erbB-2 cDNA transfected MCF-7 H3	NCTCC
MCF-7 H3/ErbB2-A	ATCC	Clonal subpopulation of MCF-7 H3/ErbB2 pool	NCTCC
MCF-7 H3/ErbB2-B	ATCC	Clonal subpopulation of MCF-7 H3/ErbB2 pool	NCTCC
MCF-7 H3/ErbB2-C	ATCC	Clonal subpopulation of MCF-7 H3/ErbB2 pool	NCTCC
MDA-MB-435S	RPMI 1640	Breast Ductal Carcinoma	Quintiles[1]
MDA-MB-435S-F	RPMI 1640	Clonal subpopulation of MDA-MB-435S	NCTCC
MDA-MB-435S-F/Taxol-10p	RPMI 1640	Taxol resistant variant of MDA-MB-435S-F	NCTCC
MDA-MB-435S-F/Taxol-10p4p	RPMI 1640	Taxol resistant variant of MDA-MB-435S-F	NCTCC
MDA-MB-435S-F/Adr-10p	RPMI 1640	Adriamycin resistant variant of MDA-MB-435S-F	NCTCC
MDA-MB-435S-F/Adr-10p10p	RPMI 1640	Adriamycin resistant variant of MDA-MB-435S-F	NCTCC

Table 2.5.1 Source description and media requirements of cell lines used in experiments described in this thesis

* ATCC basal media consists of a 1:1 mixture of DMEM and Hams F12.

** ATCC = American Tissue Culture Collection.

*** NCTCC = National Cell and Tissue Culture Centre.

2.5.2 Assessment of cell number and viability

Cells were trypsinised, pelleted and resuspended in media. An aliquot of the cell suspension was then added to trypan blue (Gibco, 525) at a ratio of 5:1. The mixture was incubated for 3 minutes at room temperature. A 10µl aliquot of the mixture was then applied to the chamber of a glass coverslip enclosed haemocytometer. Cells in the 16 squares of the four grids of the chamber were counted. The average cell numbers per 16 squares were multiplied by a factor of 10^4 and the relevant dilution factor to determine the number of cells per ml in the original cell suspension. Non-viable cells stained blue, while viable cells excluded the trypan blue dye as their membrane remained intact, and remained unstained. On this basis, % viability could be calculated.

2.5.3 Cryopreservation of cells

Cells for cryopreservation were harvested in the log phase of growth and counted as described in Section 2.5.2. Cell pellets were resuspended in a suitable volume of serum. An equal volume of a 10 % DMSO/serum solution was added dropwise to the cell suspension. A total volume of 1ml of this suspension (which should contain approximately $7x10^6$ cells) was then placed in cryovials (Greiner, 122278). These vials were then placed in the vapour phase of a liquid nitrogen container, which was equivalent to a temperature of –80°C. After a period of four hours, vials were removed from the vapour phase and transferred to the liquid phase for storage (- 196°C).

2.5.4 Thawing of cryopreserved cells

A volume of 5ml of fresh growth medium was added to a sterile universal. The cryopreserved cells were removed from the liquid nitrogen and thawed at 37°C. The cells were removed from the vials and transferred to the aliquoted media. The resulting cell suspension was centrifuged at 1,000 rpm for 5 minutes. The supernatant was removed and the pellet resuspended in fresh culture medium. An assessment of cell viability on thawing was then carried out (Section 2.5.2). Thawed cells were then added to an appropriately sized tissue culture flask with a suitable volume of growth medium and allowed to attach overnight. The following day, flasks were refed with fresh media to remove any non-viable cells.

2.5.5 Monitoring of sterility of cell culture solutions

Sterility testing was performed in the case of all cell culture media and cell culture related solutions. Samples of prepared basal media were inoculated on to Colombia blood agar plates (Oxoid, CM331), Thioglycollate broths (Oxoid, CM173) and Sabauraud dextrose (Oxoid, CM217) and incubating the plates at 37°C and 25°C. These tests facilitated the detection of bacteria, fungus and yeast contamination. Complete cell culture media were sterility tested at least four days prior to use, using Columbia blood agar.

2.5.6 Serum Batch Testing

One of the main problems associated with the use of FCS in cell culture is its batch to batch variation. In extreme cases this variation may result in a lack of cell growth, whereas in more moderate cases growth may be retarded. To avoid the effects of the above variation, a range of FCS batches were screened for growth of each cell line. A suitable FCS was then purchased in bulk for a block of work with each particular cell line in use. Screening involved growing cells in 96 well plates and growth was recorded as a percentage of growth of a serum with known acceptable growth rate.

Logarithmically growing cells were seeded into a 96 well plate (Costar; 3599) from a single cell suspension at a density of 10^3 cells/well in 100µl of medium without FCS. 100µl volumes of medium containing 10% or 20% FCS was added to respective wells on the 96 well plate, resulting in final dilutions of the FCS to 5% or 10%, respectively. The first column of each plate was maintained as a control where FCS resulting in a known acceptable growth rate was used. Plates were placed at 37°C in 5% CO_2, for 5 days, after which growth was assessed by acid phosphatase method, see section 2.7.4.

2.5.7 Isolation of Clonal Populations by Clonal Dilution

Clonal populations were isolated by plating cells in 96-well plates at a concentration of 1 cell per 3 wells. After 2 days, the 96-well plates were monitored for single cells in wells. Single cell wells were marked and then allowed to grow until they reached levels that would allow them to be subcultured into 24-well plates.

2.6 *Mycoplasma* analysis of cell lines

Cell lines were tested for possible mycoplasma contamination by Dr. Mary Heenan and Mr. Michael Henry at the National Cell and Tissue Culture Centre, Glasnevin, Dublin 9. The protocol used is detailed in the following Sections 2.6.1 and 2.6.2.

2.6.1 Indirect staining procedure for *Mycoplasma* analysis

Mycoplasma negative NRK (Normal rat kidney fibroblast) cells were used as an indicator cells for this analysis. The cells were incubated with a sample volume of supernatant from the cell lines in question and then examined for *Mycoplasma* contamination. A fluorescent Hoechst stain was used in this analysis. The stain binds specifically to DNA and so stains the nucleus of the cell in addition to any *Mycoplasma* present. *Mycoplasma* infection was indicated by fluorescent bodies in the cytoplasm of the NRK cells.

2.6.2 Direct staining procedure for *Mycoplasma* analysis

Direct staining for *Mycoplasma* analysis involved inoculating samples on to a *Mycoplasma* culture broth (Oxoid, CM403). This was supplemented with 16% serum, 0.002% DNA (BDH, 42026), 2μg/ml fungizone (Gibco, 042 05920), $2x10^3$ units penicillin (Sigma, Pen-3) and 10ml of a 25% yeast extract solution. Incubation was carried out at 37°C for a period of 48 hours. Samples of this broth were then streaked onto plates of *Mycoplasma* agar base (Oxoid, CM401) which had been supplemented as described above. The plates were incubated for three weeks at 37°C while exposed to $C0_2$. The plates were examined microscopically every 7 days. The appearance of small oval shaped colonies indicated the presence of *Mycoplasma* infection.

2.7 Miniaturised *in vitro* toxicity assays

2.7.1 "Long–term" *in vitro* toxicity assay

Cells in the exponential phase of growth were harvested by trypsinisation as described in section 2.5.1. Cell suspensions containing $1x10^4$ cells/ml were prepared in cell

culture medium. Volumes of 100µl/well of these cell suspensions were added to 96-well plates (Costar, 3599) using a multichannel pipette. Plates were agitated gently in order to ensure even dispersion of cells over a given well. Cells were then incubated overnight at 37°C in an atmosphere containing 5% CO_2. Cytotoxic drug dilutions were prepared at 2X their final concentration in cell culture medium. Volumes of the drug dilutions (100µl) were then added to each well using a multichannel pipette. Plates were then mixed gently as above. Cells were incubated for a further 6-7 days at 37°C and 5% CO_2 until the control wells had reached approximately 80-90% confluency. Assessment of cell survival in the presence of drug was determined by the acid phosphatase assay (section 2.7.3). The concentration of drug which caused 50% cell kill (IC_{50} of the drug) was determined from a plot of the % survival (relative to the control cells) versus cytotoxic drug concentration.

2.7.2 "Short-term" *in vitro* toxicity assay

Cells in the exponential phase of growth were harvested by trypsinisation as described in section 2.5.1. Cell suspensions containing $2x10^4$ cells/ml were prepared in cell culture medium and the 96-well plates were set up and incubated overnight as described in 2.7.1. Cytotoxic drug dilutions were prepared at 2X their final concentration in cell culture medium. Volumes of the drug dilutions (100µl) were then added to each well using a multichannel pipette. Plates were then mixed gently as above and allowed to incubate at 37°C and 5% CO_2 for 4 hours. After this incubation period the plates were removed from the incubator, the drug was removed from the wells and the plates were washed out with fresh serum-free media. After washing, the wells were re-fed with fresh serum-containing media. Cells were incubated for a further 6-7 days at 37°C and 5% CO_2, until the control wells had reached approximately 80-90% confluency. Assessment of cell survival in the presence of drug was determined by the acid phosphatase assay (section 2.7.3). The concentration of drug which caused 50% cell kill (IC_{50} of the drug) was determined from a plot of the % survival (relative to the control cells) versus cytotoxic drug concentration.

2.7.3 Sulindac and Verapamil-mediated drug toxicity enhancement assays (Long-term assays)

Cells were trypsinised from the flask in the exponential phase of growth as described in section 2.5.1. Cell suspensions containing $1x10^4$ cells/ml were prepared in cell culture medium. Volumes of 100µl/well of this cell suspension were added into 96-well plates (Costar, 3599) using a multichannel pipette. Plates were agitated gently in order to ensure even dispersion of cells over a given well. Cells were then incubated overnight at 37°C in an atmosphere containing 5% CO_2. Cytotoxic drug dilutions and NSAID dilutions were prepared at 4X their final concentration in media. Volumes of 50µl of the drug dilution and 50µl of the NSAID dilution were then added to each relevant well so that a total final volume of 200µl was present in each well. All potential toxicity-enhancing agents were dissolved in DMSO, ethanol or media. Stock solutions were prepared at approximately 15mg/10ml media, filter sterilised with a 0.22µm filter (Millex-GV, SLGV025BS) and then used to prepare all subsequent dilutions. Solvent control experiments showed that no toxicity enhancement effects were due to the presence of DMSO or ethanol. Cells were incubated for a further 6 days at 37°C in an atmosphere containing 5% CO_2. At this point the control wells would have reached approximately 80-90% confluency. Cell number was assessed using the acid phosphatase assay (section 2.7.4).

2.7.4 Assessment of cell number - Acid Phosphatase assay

Following the incubation period of 6-7 days, media was removed from the plates. Each well on the plate was washed twice with 100µl PBS. This was then removed and 100µl of freshly prepared phosphatase substrate (10mM *p*-nitrophenol phosphate (Sigma 104-0) in 0.1M sodium acetate (Sigma, S8625), 0.1% triton X-100 (BDH, 30632), pH 5.5) was added to each well. The plates were then incubated in the dark at 37°C for 2 hours. The enzymatic reaction was stopped by the addition of 50µl of 1N NaOH. The plate was read in a dual beam plate reader at 405nm with a reference wavelength of 620nm.

2.8 Safe handling of cytotoxic drugs

Cytotoxic drugs were handled with extreme caution at all times in the laboratory, due to the potential risks in handling these drugs. Disposable nitrile gloves (Medical Supply Company Ltd) were worn at all times and all work was carried out in cytotoxic cabinets (Gelman Sciences, CG series). All drugs were stored in a safety cabinet at room temperature or in designated areas at 4°C or -20°C. The storage and means of disposal of the cytotoxic drugs used in this work are outlined in Table 2.8.

Cytotoxic Agent	Storage	Disposal
Adriamycin	4°C in dark	Incineration
Taxol	Room temperature in dark	Incineration
Carboplatin	Room temperature in dark	Incineration
Vincristine	4°C in dark	Incineration
Taxotere	4°C in dark	Incineration
VP-16	Room temperature in dark	Incineration
Methotrexate	Room temperature in dark	Incineration
5-fluorouracil	Room temperature in dark	Incineration
Tamoxifen	4°C in dark	Incineration

Table 2.8 Storage and disposal details for chemotherapeutic agents.

2.9 Adaption of MDA-MB-435S-F MDR variants

A number of MDR variants were developed by selecting the sensitive parent cell lines, MDA-MB-435S-F with taxol and adriamycin. Clonal populations were chosen to ensure that subsequent resistant cells were due to drug exposure and not in fact arising from a resistant sub-population already present in the cell line.

2.9.1 IC_{90} Assay to determine drug concentration for pulse selection

Cells were seeded into twelve 25cm^2 flasks at 1.5×10^5 cells per flask and allowed to attach overnight at 37°C. The following day media was removed from the flask and a range of concentrations of appropriate drug was added to the flasks in duplicate.

Complete media was added to two flasks as a 100% survival control. Flasks were returned to the 37°C incubator for a 4 hour incubation. Drug was then removed and the flasks fed with fresh complete media. The flasks were then incubated for 5-7 days until the cells in the control flasks had reached approximately 80% confluency.

Media was then removed from the flasks and cells were rinsed twice with PBS. Cells were then fixed for 10 minutes in 10% formalin. Formalin was then removed and the flasks allowed to air dry overnight at room temperature. Flasks were then stained for 10 minutes with 3ml of crystal violet and then rinsed with water and allowed to air dry. Crystal violet stains were then eluted with 3 ml of 33% acetic acid, diluted 1:10 with UHP and pipetted into a 96-well plate, and then read in a dual beam ELISA plate reader at a wavelength of 570nm (reference wavelength 620nm). The first lane was used as a blank. The concentration of drug which caused 90% cell kill (IC_{90} of the drug) was determined from a plot of the % survival (relative to the control cells) versus cytotoxic drug concentration.

2.9.2 Pulse selection

MDA-MB-435S-F cells were grown to 70-80% confluency in 75cm^2 flasks. The cells were then exposed to the IC_{90} concentration of adriamycin, or taxol for 4 hours, after which the drug was removed and the flasks re-fed with fresh complete media. The cells were then grown in drug-free media for 6 days, refeeding every 2-3 days. This was repeated for 10 "pulses". Invasive potential (see section 2.14) and sensitivity to the selecting drug and a variety of cytotoxic drugs was the determined using miniaturised toxicity assays (see section 2.7.1 and 2.7.2).

2.10 Western blotting

2.10.1 Whole cell extract preparation

Cells were grown to 80-90% confluency in 75cm^2 flasks for western blotting or 175cm^2 flask for immunoprecipitation. Media was removed and cells were trypsinised as described in section 2.5.1. Cells were washed twice with ice cold PBS. All procedures

from this point forward were performed on ice. Cells were resuspended in 100-200µl of NP-40 lysis buffer and incubated on ice for 30 minutes.

Table 2.10.1.1 below provides the details of the lysis buffer. Immediately before use, 10µl of the 100X stocks listed in table 2.10.2 were added to 1ml of lysis buffer.

Addition required per 500ml stock	Final concentration
425ml UHP water	-
25ml 1M Tris-HCl (pH 7.5)	50mM Tris-HCl (pH 7.5)
15ml 5M NaCl	150 mM NaCl
2.5ml NP-40	0.5% NP-40

Table 2.10.1.1: NP-40 lysis buffer

100X stock	Preparation instructions
100mM Na_3 VO_4	1.83g Na_3 VO_4 in 100ml UHP
100mM DTT	154mg in 10ml UHP
100mM PMSF	174mg in 10ml 100% ethanol
100X Protease inhibitors	2.5 mg/ml leupeptin, 2.5 mg/ml aprotinin, 15 mg/ml benzamidine and 1mg/ml trypsin inhibitor in UHP water

Table 2.10.1.2: NP-40 lysis buffer 100X stocks

Cells were sonicated with 9 pulses lasting 0.9 seconds at 50% power. Lysed cells were transferred to an eppendorf and pelleted at 13,000 r.p.m for 10 minutes. Supernatant was removed and protein concentration quantified as detailed in section 2.10.2. Samples were then stored in aliquots at -80°C.

2.10.2 Protein Quantification

Protein levels were determined using the Bio-Rad protein assay kit (Bio-Rad, 5000006) as follows. A 2mg/ml bovine serum albumin (BSA) solution (Sigma, A9543) was prepared freshly in lysis buffer. A protein standard curve (0, 0.2, 0.4, 0.6, 0.8 and

1.0mg/ml) was prepared from the BSA stock with dilutions made in lysis buffer. The Bio-Rad reagent was diluted 1:5 in UHP water and filtered through Whatman paper before use. A 20µl volume of protein standard dilution or sample (diluted 1:20) was added to 0.98ml of diluted dye reagent and the mixture vortexed. After 5 minutes incubation, absorbance was assessed at 570nm. The concentration of the protein samples was determined from the plot of the absorbance at 570nm versus concentration of the protein standard.

2.10.3 Immunoprecipitation

Immunoprecipitations were carried out using 1mg extracted protein (detailed in section 2.10.1) as estimated using the BioRad assay in section 2.10.2. All steps were performed on ice. For biotinylated immunoprecipitations, a cellular labelling and immunoprecipitation kit was purchased (Roche, 1647652). 25 µl of biotin-7-NHS stock solution was added to 1mg of protein extract in 1ml of lysis buffer for 15 minutes at 4°C. The biotinylation reaction was stopped by adding 50 µl of stop solution (1M NH_4Cl) for 15 minutes at 4°C. 50 µl of protein A-agarose or protein G-agarose beads were added to biotinylated or non-biotinylated samples and rocked gently for 3 hours at 4°C to remove any proteins that non-specifically bind to the beads. Beads were pelleted at 12,000rpm for 20s, and supernatant removed to a fresh eppendorf. Antibody was then added to the supernatant (5 µl EGFR Ab-15 (Neomarkers, MS-665-P), 5 µl c-erbB-2 Ab-11 (Neomarkers, MS-432-P), 5 µl c-erbB-3 Ab-4 (Neomarkers, MS-262-P), 4 µl c-erbB-4 Ab-1 (Neomarkers, MS-270-P) and rocked gently at 4°C for 6 hours. Controls used were an irrelevant antibody and the lysis buffer dilutent. 50 µl of protein A-agarose or protein G-agarose beads were added and rocked gently for overnight at 4°C to immunoprecipitate the protein of interest. Beads were pelleted at 12,000rpm for 20s, and supernatant discarded. Beads were washed 2X for 20mins with wash buffer A (50mM Tris, pH7.5, 150mM NaCl, 0.1% Nonidet P-40), 2X for 20mins with wash buffer B (50mM Tris, pH7.5, 500mM NaCl, 0.1% Nonidet P-40) and 1X for 20mins with wash buffer C (10mM Tris, pH7.5). All traces of wash buffer were removed from beads. Beads were resuspended in a total volume of 15 µl of lysis buffer and 10X loading buffer and boiled for three minutes. Samples including beads were loaded onto polyacrylamide gels and western blotting carried out as described in section 2.10.4 and 2.10.5.

2.10.4 Gel electrophoresis

Proteins for analysis by Western blotting were resolved using SDS-polyacrylamide gel electrophoresis (SDS-PAGE). The stacking and resolving gels were prepared as illustrated in table 2.10.4.1. The gels were set in clean 10cm x 8cm gel cassettes, which consisted of a glass plate and an aluminium plate. 0.75cm plastic spacers separated these plates. The resolving gel was added to the gel cassette and allowed to set while covered with 0.1% SDS. Once set, the 0.1% SDS was removed and the stacking gel was then added. A comb was placed into the stacking gel after pouring, in order to create wells for sample loading (maximum sample loading volume of 15-20µl).

Components	**7.5% Resolving Gel**	**12% Resolving Gel**	**5%Stacking Gel**
Acrylamide stock	3.8ml	6.0ml	0.8ml
UHP water	8.0ml	6.0ml	3.6ml
1.875 M Tris-HCl pH 8.8	3.0ml	3.0ml	-
1.25 M Tris-HCl pH 6.8	-	-	0.5ml
10% SDS	150µL	150µL	50µL
10% NH_4-persulfate	60µL	50µL	17µL
TEMED	9µL	7.5µL	9µL

Table 2.10.4.1: Preparation protocol for SDS-PAGE gels (2 x 0.75mm gels).

The acrylamide stock in Table 2.10.4.1 consists of a 30% (29:1) ratio of acrylamide:bis-acrylamide (Sigma, A2792). In advance of samples being loaded in to the relevant sample wells, 25-100µg of protein was diluted in 10X loading buffer. The molecular weight markers (Sigma, C3437) and protein samples were heated to 95°C for 3 minutes. After heating, equal amounts (25-100µg in 10X loading buffer in a total volume of 10µl) of protein were added in to each well. The gels were run at 250V and

45mA until the bromophenol blue dye front was found to have reached the end of the gel, at which time sufficient resolution of the molecular weight markers was achieved.

2.10.5 Western Blotting

Western Blotting was performed by the method of Towbin et al (1979). Once electrophoresis had been completed, the SDS-PAGE gel was equilibrated in transfer buffer (25mM Tris (Sigma, T8404), 192mM glycine (Sigma, G7126), pH 8.3-8.5) for approximately 30 minutes. Six sheets of Whatman 3mm filter paper were soaked in freshly prepared transfer buffer. These were then placed on the cathode plate of a semi-dry blotting apparatus (Bio-rad). Air pockets were then removed from between the filter paper. PVDF membrane (Boehringer Mannheim 1722026) or nitrocellulose membrane (Amersham Pharmacia Biotech, RPN 303D), which had been equilibriated in the same transfer buffer, was placed over the filter paper on the cathode plate. Air pockets were once again removed. The gels were then aligned on to the membrane. Six additional sheets of transfer buffer soaked filter paper were placed on top of the gel and all air pockets removed. The proteins were transferred from the gel to the membrane at a current of 34mA at 15V for 30-40 minutes, until all colour markers had transferred.

Following protein transfer, the membranes were blocked overnight using 5% milk powder (Cadburys; Marvel skimmed milk) in PBS at 4°C. The PVDF membranes were washed with PBS prior to addition of the primary antibody. Membranes were treated with primary antibody for 2-3 hours at room temperature and a negative control where the membrane was exposed to antibody diluent was also performed. Primary antibody was removed after this period and the membranes rinsed 3 times with PBS containing 0.5% Tween 20 (Sigma P1379) for a total of 30 minutes. Secondary antibody (1 in 1,000 dilution of anti-mouse IgG peroxidase conjugate (Sigma, A4914) in PBS, 1 in 2,000 dilution of anti-rabbit IgG (Sigma, A4914) in PBS or, 1 in 1,000 dilution of anti-rat IgG (Dako, P0450) in PBS) was added for 1.5 hour at room temperature. The membranes were washed thoroughly in PBS containing 0.5% Tween for 15 minutes.

Primary Antibody	Dilution
EGFR Ab-12 (Neomarkers, MS-400-P)	1:200
C-erbB-2 Ab-10 (Neomarkers, MS-327-P)	1:400
C-erbB-3 Ab-7 (Neomarkers, MS-313-P)	1:500
C-erbB-4 Ab-2 (Neomarkers, RB-284-P)	1:200
B-actin (Sigma, A5441)	1:10,000
Mdr-1 (Alexis, 801-002-c100)	1:1,000
Mrp-2 (Alexis, MRPr1)	1:100
Anti-phosphotyrosine PY-20 (Affiniti Research Products, PY2000)	1:10,000
Estrogen receptor Ab-1 (Oncogene Reasearch Products, GR17)	1:100
Estrogen receptor Ab-1 beta (Oncogene Reasearch Products, GR39)	1:1000
Anti-biotin HRP (A0185)	1:10,000

Table 2.10.5 List of Primary antibodies and dilutions.

2.10.6 Enhanced chemiluminescence (ECL) detection

Immunoblots were developed using an Enhanced Chemiluminescence kit (Amersham, RPN2109) which facilitated the detection of bound peroxidase-conjugated secondary antibody.

Following the final washing PVDF membranes were subjected to ECL. A layer of parafilm was flattened over a glass plate and the PVDF membrane placed gently upon the plate. A volume of 3ml of a 50:50 mixture of ECL reagents was used to cover the membrane. The ECL reagent mixture was completely removed after a period of one minute and the membrane wrapped in clingfilm. All excess air bubbles were removed. The membrane was then exposed to autoradiographic film (Kodak, X-OMATS) for various times (from 10 seconds to 30 minutes depending on the signal). The exposed autoradiographic film was developed for 3 minutes in developer (Kodak, LX-24). The film was then washed in water for 15 seconds and transferred to a fixative (Kodak, FX-40)

for 5 minutes. The film was then washed with water for 5-10 minutes and left to dry at room temperature.

2.11 Quantification of adriamycin accumulation in MDA-MB-435S-F MDR variants

Cells were seeded into 75cm^2 flasks (Costar, 3375) at 0.5x10^6 cells per flask (six flasks per cell line). Cells were incubated for 48 hours, after which time medium was removed and fresh medium containing adriamycin (10μM) was added. Flasks were incubated at 37°C for a period of two hours. After this two-hour incubation, the media was removed from all flasks, and half the flasks were replaced with fresh media and returned to the 37°C incubator. The remaining flasks were then trypsinised as described in section 2.5.1 and counted as described in section 2.5.2. Pellets were then washed with PBS and frozen at -20°C. After a four-hour incubation, the media was removed from the remaining flasks and the flasks were washed twice with PBS. Cells were then trypsinised as described in section 2.5.1 and counted as described in section 2.5.2. Pellets were then washed with PBS and frozen at -20°C.

When required for HPLC analysis, the frozen pellets were thawed, resuspended in 100μl UHP and added to glass tubes (test samples). Untreated cells were resuspended in 800μl UHP and 100μl aliquots of this were placed in to 8 glass tubes. These were the adriamycin control tubes and were labelled as follows: 50μg/ml, 10μg/ml, 5μg/ml, 2μg/ml, 1μg/ml, 0.5μg/ml, 0.25μg/ml, 0μg/ml adriamycin. 1ml of appropriate concentration of adriamycin was then added to the adriamycin control tubes. A volume of 100μl 33% aqueous silver nitrate (Sigma, S6506) was then added to the pellets (all tubes from 4 and 5), followed by mixing for 5 minutes. A quantity of 300μl of the internal standard (6μg/ml in 50ml methanol) was then added to all tubes.

1.3ml HPLC grade acetonitrile (Labscan) was added to the test sample tubes only. 300μl HPLC grade acetonitrile was added to the adriamycin control tubes. All tubes were maintained at 4°C for 1 hour. This was followed by centrifugation at 4000rpm for 15 minutes. 1.1ml of the supernatant was removed and added to HPLC autosampler

vials. All solvent was then removed under a stream of nitrogen gas. The remaining solids were resuspended in 50µl of HPLC mobile phase The HPLC mobile phase was prepared as follows: 64ml of 0.1M phosphoric acid (Sigma, P6560) was added to 488ml UHP. The pH was then adjusted to 2.3 with 1N potassium hydroxide (Sigma P6310). A volume of 248 ml acetonitrile was added finally and the completed mobile phase allowed to degas at 4°C overnight.

20µl of sample for analysis were automatically injected in to the HPLC system (Beckman System Gold 507 autosampler, 125 pump and 166 detector). Mobile phase flow rate was set at 0.5ml per minute with a total run time of 16 minutes. The column used for HPLC analysis of adriamycin in DLKP was a C18 reversed phase Prodigy 5µm particle size ODS-3 column (Phenomenex, U.K.). Absorbance was monitored at 253nm. A standard curve of adriamycin peak area/daunorubicin internal standard versus adriamycin concentration was used to quantify the levels of adriamycin present in the samples. Results were finally reported as the content of adriamycin per million cells.

2.12 RT-PCR Analysis

2.12.1 Preparation of materials for RNA analysis.

Due to the labile nature of RNA and the high abundance of RNase enzymes in the environment a number of precautionary steps were followed when analysing RNA throughout the course of these studies.

- General laboratory glassware and plasticware are often contaminated by RNases. To reduce this risk, glassware used in these studies were baked at 180°C (autoclaving at 121°C does not destroy RNase enzymes) for at least 8hr. Sterile, disposable plasticware is essentially free of RNases and was therefore used for the preparation and storage of RNA without pre-treatment. Polyallomer ultracentrifuge tubes, eppendorf tubes, pipette tips etc., were all autoclaved before use. All spatulas which came in to contact with any of the solution components were baked, chemicals were weighed out onto baked aluminium-foil and a stock of chemicals for "RNA analysis only" was kept separate from all other laboratory agents.

- All solutions (which could be autoclaved) that came in to contact with RNA were all prepared from sterile ultra-pure water and treated with 0.1% diethyl pyrocarbonate (DEPC) (Sigma, D5758) before autoclaving (autoclaving inactivates DEPC).
- Disposable gloves were worn at all times to protect both the operator and the experiment (hands are an abundant source of RNase enzymes). This prevents the introduction of RNases and foreign RNA/DNA in to the reactions. Gloves were changed frequently.
- All procedures were carried out under sterile conditions when feasible.

2.12.2 Total RNA extraction from cultured cell lines

Adherent cells were grown in 75cm^2 flasks until approximately 80% confluent. Media was then removed and 1ml per 75cm^2 flasks of TRI reagent (Sigma, T-9424) was added to the flask for 5 minutes ensuring that all cells are covered with the solution. TRI reagent is a mixture of guanidine thiocyanate and phenol in a mono-phase solution. It effectively dissolves DNA, RNA, and protein on lysis of cell culture samples. After addition of the reagent, the cell lysate should be passed several times through a pipette to form a homogenous lysate. To ensure complete dissociation of nucleoprotein complexes, the sample was allowed to stand for 5 minutes at room temperature. 0.2ml of chloroform (not containing isoamyl alcohol or any other additive) per ml of TRI reagent was added to the cell lysate. The sample was covered tightly, shaken vigorously for 15 seconds and allowed to stand for 2-15 minutes at room temperature. The resulting mixture was centrifuged at 13,000rpm for 15 minutes at 4°C. Centrifugation separated the mixture into 3 phases: an organic phase (containing protein), an interphase (containing DNA) and a colourless upper aqueous phase (containing RNA). The aqueous phase was then transferred to a fresh tube and 0.5ml of isopropanol per ml of TRI reagent used in sample preparation and mixed. The sample was then allowed to stand for 5-10 minutes at room temperature. The sample was then centrifuged at 13,000rpm for 10 minutes at 4°C. The RNA precipitate formed a pellet on the side and the bottom of the tube. The supernatant was removed and the RNA pellet was washed by adding 1ml (minimum) of 75% ethanol per 1ml of TRI reagent. The sample was vortexed and centrifuged at 8000rpm for 5 minutes at 4°C. Samples can be stored in ethanol at 4°C for at least 1 week and up to one year at -20°C. The RNA pellet was air-

dried briefly. Approximately 50µl DEPC treated H_2O was added to the pellet. The RNA was then stored at -80°C until required for PCR analysis.

2.12.3 RNA quantification

RNA was quantified spectrophotometrically at 260nm and 280nm. An optical density of 1 at 260nm is equivalent to 40mg/ml RNA. An A_{260}/A_{280} ratio is used to indicate the purity of the RNA. Partially solubilised RNA has a ratio of <1.6 (Ausubel *et al.*, 1991). The yield of RNA from most lines of cultured cells is 100-200µg/90mm plate (Sambrook *et al.*, 1989).

2.12.4 Reverse transcription of RNA isolated from cell lines

The following components were used in the reverse transcriptase (RT) reaction for RNA isolated from cell lines. 1µl oligo $(dT)_{12-18}$ primers (1µg/ml) (Promega, C1101), 2µl of total RNA (0.5µg/ml), and 2µl of DEPC-H_2O were mixed together and heated at 70°C for 10 min and then chilled on ice to remove any RNA secondary structure formation and allow oligo (dT) primers to bind to the poly $(A)^+$ tail on the mRNA. 4µl of a 5X buffer (consisting of 250mM Tris-HCL, pH 8.3, 375mM KCl and 15mM $MgCl_2$), 2µl of DTT (100mM), 1µl of dNTPs (10mM each of dATP, dCTP, dGTP and dTTP), 7µl of water and 1µl of Moloney murine leukaemia virus-reverse transcriptase (MMLV-RT) (Sigma, M1302) was then added to the heat-denatured RNA complex and the mixture was incubated at 37°C for 1 hour to allow the MMLV-RT enzyme catalyse the formation of cDNA on the mRNA template. The enzyme was then inactivated and the RNA and cDNA strands separated by heating to 95°C for 2 min. The cDNA was used immediately in the PCR reaction or stored at -20°C until required for analysis.

2.12.5 Polymerase Chain Reaction (PCR) analysis of cDNA formed from mRNA isolated from cell lines

PCR reactions were set up as 50µl volumes using 5 µl of cDNA formed during the RT reaction (see Section 2.12.4). cDNA was amplified for varying cycle numbers but where

possible amplification was carried out in the exponential phase of amplification. The sequences of all primers used for PCR in this thesis are shown in Figure 2.12.5.

Each PCR reaction tube contained 5µl 10Xbuffer (100mM Tris-HCl, pH 9.0, 50mM KCl, 1% Triton X-100), 2 µl 25mM $MgCl_2$, 1µl of first strand target primer* (250ηg/µl), 1µl of second strand target primer* (250ηg/µl), 0.5µl of first strand endogenous β-actin control primer* (250ηg/µl), 0.5µl of second strand endogenous β-actin control primer* (250ηg/µl) and 35.5µl UHP. 5µl of cDNA (pre-heated to 95°C for 3min. to separate strands and remove any secondary structure if the sample had been stored at -20°C) was added to the above. The mixture was heated to 94°C for 5min (reduces non-specific binding of primers to template). 1µl of 10mM dNTP (Sigma, DNTP-100) and 0.5µl of Taq DNA Polymerase enzyme (Sigma; D4545) and water to a total volume of 8.5µl was then added to the above The cDNA was then amplified by PCR (Techne; PHC-3) using the following program:

- 94°C for 3min (denature double stranded DNA)
- 25-35 cycles 94°C for 30sec (denature double stranded DNA);
  X°C for 30sec (anneal primers to cDNA);
  72°C for 30sec (extension);
- 72°C for 7min (extension).
- Storage at 4°C

* All oligonucleotide primers used throughout the course of this thesis were made to order on an "Applied BioSystems 394 DNA/RNA Synthesiser" by Oswel DNA service, Lab 5005, Medical and Biological Services Building, University of Southhampton, Boldrewood, Basset Cresent East, Southhampton, SO16 7PX.

Table 2.12.5 Sequences of primers used for PCR

Gene	Length (bp)	Tm (°C)	Size (bp)	Sequence
c-erbB-1	19 19	49	190	CAG GAC CAA GCC ACA GCA G ATA TTC TTG CTG GAT GCG T
c-erbB-2	20 20	62	332	AGA CGA AGC ATA CGT GAT GG CAT GGT ACT CTG TCT CGT CA
β-actin (large)	29 22	55	383	GAA ATC GTG CGT GAC ATT AAG -GAG AAG CT TCA GGA GGA GCA ATG ATC TTG A
β-actin (small)	23 22	55	142	TGG ACA TCC GCA AAG ACC TGT AC TCA GGA GGA GCA ATG ATC TTG A
c-erbB-3	18 20	47	366	GAA CCT TGA GAT TGT GCT ACA GCT TCT GCC ATT GTC CT
c-erbB-4	21 21	56	141	CGA TTC TCA GTC AGT GTG TGC GTG CTC AAT GCT GGT TAT CTC
mdr-1	20 20	51	157	GTT CAA ACT TCT GCT CCT GA CCC ATC ATT GCA ATA GCA GG
mrp-1	21 21	55	202	GTA CAT TAA CAT GAT CTG GTC CGT TCA TCA GCT TGA TCC GAT
mrp-2	20 19	53	241	CTG CCT CTT CAG AAT CTT AG CCC AAG TTG CAG GCT GGC C
mrp-4	19 18	42	239	CCA TTG AAG ATC TTC CTG G GGT GTT CAA TCT GTG TGC
mrp-5	18 20	49	381	GGA TAA CTT CTC AGT GGG GGA ATG GCA ATG CTC TAA AG
Topo I	30 27	55	180	AGA CGA ATC ATG CCC GAG GAT ATA ATC ATC TCG TGA ACT AGG GTT AAG CAT GAT GTA
Topo IIα	21 26	55	139	ATG CTA GTC CAC CTA AGA CCA TGT GTA GCA GGA GGG CTT GAA GAC AG
Topo IIα	30 28	55	118	TCC TTC ATA TTC TCA GAA GTC AGA AGA TGA ACT TGG AAC TTT ATC TGT CTG TTT CAG A
GSTπ	18 24	55	270	ATG CTG CTG GCA GAT CAG GTA GAT GAG GGA GAT GTA TTT GCA
DHFR	22 20	55	221	GTA GAA GGT AAA CAG AAT CTG G CCA ACT ATC CAG ACC ATG TC
TS	20 21	55	350	TCT GCT GAC AAC CAA ACG TG GAG GAA GAT CTC TTG GAT TCC

A 10μl aliquot of tracking buffer, consisting of 0.25% bromophenol blue (Sigma; B5525) and 30% glycerol in water, was added to each tube of amplified cDNA products. 20μl of cDNA products from each tube were then separated by electrophoresis at 100mV through a 2% agarose (Sigma, A9539) gel containing ethidium bromide (Sigma; E8751), using TBE (22.5mM Tris-HCl, 22.5mM boric acid (Sigma; B7901), 0.5mM EDTA) as running buffer. Molecular weight markers "ϕ-X174" Hae III digest (Sigma, P0672) were run, simultaneously, as size reference. The resulting product bands were visualised as pink bands (due to the intercalation of the cDNA with the ethidium bromide) when the gels were placed on a transilluminator (UVP Transilluminator). The gels were photographed.

2.12.6 Densitometric Analysis

Densitometric analysis was carried out using the MS Windows 3.1 compatible Molecular Analyst software/PC image analysis software available for use on the 670 Imaging Densitometer (Bio-Rad. CA) Version 1.3. Developed negatives of gels were scanned using transmission light and the image transferred to the computer. The amount of light blocked by the DNA band is in direct proportion to the intensity of the DNA present. A standard area was set and scanned and a value was taken for the Optical Density (O.D.) of each individual pixel on the screen. The average value of this O.D. (within a set area, usually cm^2) is normalised for background of an identical set area. The normalised reading is taken as the densitometric value used in analysis. As a result, these O.D. readings were unitless.

2.13 Extracellular Matrix Adherence Assays

2.13.1 Reconstitution of ECM Proteins

Adhesion assays were performed using the method of Torimura *et al.* (1999). Collagen type IV (Sigma C-5533), fibronectin (Sigma F-2006) and laminin (Sigma L-2020) were reconstituted in PBS to a stack concentration of 500 μg/ml. Stocks were aliquoted into sterile eppendorfs. Fibronectin and collagen stocks were stored at -20°C, while laminin stocks were stored at -80°C. Matrigel (Sigma E-1270) was aliquoted and stored at -20°C until use. Matrigel undergoes thermally activated polymerisation when brought to 20-40°C to form a reconstituted basement membrane.

2.13.2 Coating of Plates

Each of the ECM proteins, collagen, fibronectin and laminin, was diluted to 25μg/ml while matrigel was diluted to 1mg/ml with PBS. 250μl aliquots were placed into wells of a 24-well plate. The plates were gently tapped to ensure that the base of each well was completely covered with solution. The plates were then incubated overnight at 4°C. The ECM solutions were then removed from the wells and the wells rinsed twice with sterile PBS. 0.5ml of a sterile 0.1% BSA/PBS solution was dispensed into each well to reduce non-specific binding. The plates were incubated at 37°C for 20 minutes and then rinsed twice again with PBS.

2.13.3 Adhesion Assay

Cells were set up in 75cm^2 flasks and then harvested and resuspended in serum-free DMEM medium. The cells were then plated at a concentration of 2.5×10^4 cells per well in triplicate and incubated at 37°C for 60 minutes. Control wells were those which had been coated but contained no cells. After 60 minutes, the medium was removed from the wells and rinsed gently with PBS. This was then removed and 200μl of freshly prepared phosphatase substrate (10mM *p*-nitrophenol phosphate (Sigma 104-0) in 0.1M sodium acetate (Sigma, S8625), 0.1% triton X-100 (BDH, 30632), pH 5.5) was added to each well. The plates were then incubated in the dark at 37°C for 2 hours. The enzymatic reaction was stopped by the addition of 100μl of 1N NaOH. 100μl aliquots

were transferred to a 96-well plate and read in a dual beam plate reader at 405nm with a reference wavelength of 620nm.

2.14 Invasion Assay

Invasion assay was performed using the method of Albini (1998). Matrigel (Sigma E-1270) (11mg/ml) was diluted to 1mg/ml in serum free DMEM. 100µl of 1mg/ml Matrigel was placed into each insert (Falcon 3097) (8.0µm pore size, 24 well format) which stands on 24-well plate (Costar). The insert and the plate were incubated overnight at 4°C. The following day, cells were harvested and resuspended in DMEM containing 5% FCS at the concentration of 1×10^6 cells/ml. The inserts were washed with serum-free DMEM, then 100µl of the suspension cells were added to each insert and 250µl of DMEM containing 5% FCS was added to the well underneath the insert. Cells were incubated at 37°C for 48 hours. After this time period, the inner side of the insert was wiped with a wet swab while the outer side of the insert was stained with 0.25% crystal violet for 10 minutes and then rinsed and allowed to dry. The inserts were then viewed under the microscope. In some instances crystal violet was eluted with 300µl of 33% glacial acetic acid and 100µl aliquots were transferred to a 96 well plate and the absorbance read on an ELISA reader at 570 and 620nm.

2.15 Motility Assay

Motility assays were carried out in an identical manner to invasion assays, as described in section 2.14, with the exception that the inserts were not coated in Matrigel.

2.16 Zymography

Zymography was used to assess the level of proteolytic activity of different proteases in cell lines. The choice of substrate incorporated into the resolving gel depended on the substrate specificity of the species of enzyme detected. Gelatin is a substrate for matrix metalloproteinases (MMPs), serine and cysteine proteases. In the case of stromelysin 1

and 2 (MMP-3 and MMP-10) and Matrilysin (MMP-7) caesin zymography is more suitable.

The gel was prepared by incorporating gelatin within the polymerised acrylamide matrix. 10% acrylamide gels were used. The amount for one gel was as follows.

Gel component	Resolving Gel (10%)	Stacking Gel
30% Acrylamide/bisacrylamide	3.3ml	0.5ml
3mg/ml Gelatin (Sigma G-8150)	2.5ml	--------
Ultrapure Water	1.7ml	2ml
3M Tris-HCl, PH 8.8	2.5ml	--------
2M Tris-HCl, PH 6.8	--------	0.8ml
10% Ammonium Persulphate	99µl	99µl
TEMED	5µl	5µl

Table 2.16.1 – Zymography gel components.

Cells were grown in petri dishes (Greiner) until they reached 80% confluency. They were then rinsed twice with sterile PBS and then incubated for 4 hours with serum-free media. Media was then replaced with fresh serum-free media and the cells were grown for a further 72 hours. After this time had elapsed, the supernantants were collected and concentrated. Samples were mixed 3:1 with 4X sample buffer (10% glycerol; 0.25 M Tris-HCl, pH 6.8; 0.1% (w/v) bromophenol blue) and loaded onto the gel. The gels were run at 30mA per gel in running buffer (0.025 M Tis; 0.19 M glycine; 0.1% SDS) until the dye front reached the bottom of the gel. Following electrophoresis, the gels were soaked in 2.5% Triton-X-100 with gentle shaking for 30 minutes at room temperature. The gels were rinsed in substrate buffer (50mM Tris-HCl, pH.8.0; 5mM $CaCl_2$) and then incubated for 24 hours in substrate buffer at 37°C. The gels were then stained with Coomassie blue (2.5mg/ml) for 2 hours by shaking and destained in destain water (50ml acetic acid; 150ml isopropanol; 300ml UHP) until clear bands were visible. The gels were then scanned and analysed.

Inhibitors or enhancers of proteinases were added to 2.5% Triton-X-100 and substrate buffer to identify the different classes of proteins (Table 2.16.2).

Inhibitor/Enhancer	Enzyme inhibited/enhanced	Concentration
EDTA (Inhibitor)	MMPs	30mM
PMSF (Inhibitor)	Serine proteases	1mM
Cysteine (Enhancer)	Cysteine proteases	10mM
DTT	Reducing Agent	2mM
Leupeptin (Inhibitor)	Serine and cysteine proteases	100μM

Table 2.16.2

2.17 Transfection of Mammalian Cells with Exogenous DNA

Throughout the course of this thesis it was found necessary to introduce foreign DNA into host cells either to increase the level of expression of a particular gene (by transfecting with an expression plasmid) or decrease the level of expression of a particular gene (by transfecting with a plasmid containing a ribozyme). Sufficient plasmid was produced by transforming JM109 with the plasmid required, growing up a large stock of these cells and isolating the plasmid from them; This isolated plasmid was then transfected into the chosen cell line.

2.17.1 Plasmids and oligonucleotides used

The c-erbB-2 ribozyme was cloned into pHβAPr-1-neo and was a generous gift from Dr. Kevin Scanlon (Suzuki et al, 2000). The c-erbB-2 cDNA constructs were cloned into the $pCMV_4$ expression plasmid and were a generous gift from Dr. Dihua Yu (Yu et al, 1996).

2.17.2 $MgCl_2$ / $CaCl_2$ Transformation of JM109 Cells

10ml of LB broth (Appendix K) was inoculated with a single colony of JM109 bacteria from an agar plate and incubated overnight at 37°C at 200rpm The following day 500μl of this suspension was inoculated into 50ml of LB broth and grown to an OD_{600nm} of

0.3. The cells were then pelleted at 3000rpm for 10min, the supernatant removed and the pellet was resuspended in 10ml of 100mM $MgCl_2$ on ice for 15min. The cells were again precipitated at 3000rpm for 10min and the pellet was resuspended in 10ml of 100mM $CaCl_2$ on ice for a further 15min. The precipitation step was then repeated and the pellet was resuspended in 1-2ml of 100mM $CaCl_2$ and left on ice for at least 15min. The cells were now competent and ready for transformation with the foreign DNA required. 100µl of the competent cell suspension was mixed with 20ng DNA and placed on ice for 40min after which the mixture was heat-shocked at 42°C for 90sec and then placed on ice for 3min. 1ml of LB broth was added to the competent cell suspension and incubated at 37°C for 40min. 400µl of this suspension was spread on a selecting agar plate (Ampicillin/AMP (Roche; 835 269)) and incubated overnight at 37°C. Single colonies which grew on these selecting plates were further colonised on another selecting plate and allowed to grow overnight.

2.17.3 Isolation of Plasmid from JM109 cells

A single colony (from 2.17.2) was inoculated into 10ml of LB AMP 50µg/ml and grown overnight; 2ml of this suspension was added to 200ml of TB AMP 50µg/ml and left to grow overnight at 37°C for large scale isolation of plasmid from JM109 cells. The following day the cells were pelleted and pZ523 spin columns (5 Prime → 3 Prime Inc.; 5-523523) were used to isolate the plasmid according to the manufacturer's instructions. This procedure involved lysing the pellet in 20ml of an ice-cold solution containing 50mM glucose, 25mM Tris-Cl, 10mM EDTA, pH8.0 and 5mg/ml lysozyme (Sigma; L6876) at room temperature for 10-15min. 40ml of a 0.2N NaOH and 1.0% SDS solution was gently mixed with the lysate until the suspension became clear and incubated on ice for 10min. 30ml of 3M postassium-acetate, pH5.2 was added to the above and mixed gently until a flocculent precipitate appeared at which stage the mixture was stored on ice for at least 10min. The sample was centrifuged at 35,000rpm. for 1h at 4°C after which the supernatant was recovered and added to 0.6 volume of 100% Isopropanol, mixed gently and left at room temperature for 20-30min. The suspension was then centrifuged at 35,000g. for 30min at 20°C after which the supernatant was discarded and the pellet washed in ice-cold 70% ethanol and resuspended in 5ml of TE-HCl, pH 8.0. To remove any contaminating RNA the plasmid solution was treated with RNase Plus (5 Prime → 3 Prime Inc.; 5-461036) (to a final dilution of 1:250) for 30min at 37°C followed by phenol:chloroform:isoamyl alcohol

extractions. 10M ammonium acetate was added to the aqueous phase to a final concentration of 2.0M and 0.6 volume of 100% Isopropanol was added to the sample, mixed and stored at room temperature for 20-30min. The sample was centrifuged at maximum speed in an microfuge and the DNA pellet was washed in 70% ethanol and resuspended in 3.6ml of 10mM Tris-Cl, 1mM EDTA, and 1.0M NaCl, pH 8.0. 1.8ml of this sample was loaded into one of two pZ523 columns (following the manufacturer's instructions) and the column effluent was precipitated with 0.6 volume 100% Isopropanol, as described previously. The DNA was pelleted at maximum speed in an microfuge, washed in 70% ethanol and resuspended in TE. The DNA concentration was determined by measuring the OD_{260nm}.

2.17.4 $CaPO_4$ Transfection of Mammalian Cells

On the day prior to transfection the cells to be transfected with plasmid DNA were plated from a single cell suspension (Section 2.5.1) and seeded into a $75cm^2$ flask at $5x10^5$ cells per flask. The plasmid DNA was diluted to 1µg/µl in TE and 10µg DNA was stored overnight in 410µl H_2O at 4°C. On the day of the transfection the diluted DNA was incubated at 37°C for 1h 60µl 2M $CaCl_2$ was added dropwise to the DNA with continual mixing. Immediately the DNA-$CaCl_2$ mixture was added dropwise into the 2XHBS (Appendix K) solution with continual mixing and left at room temperature for 30min to form a DNA-$CaPO_4$ mixture. The DNA-$CaPO_4$ mixture was added to the flask of cells (containing media) dropwise, swirling constantly to ensure even mixing. The cells were then incubated for 4h at 37°C after which time the cells were "shocked" with glycerol to aid the entry of the DNA into the cells. Glycerol-shocking was done by removing the media from the cells and adding 5ml of 10% glycerol in 1XHBS to the cells for 3min. The glycerol was then removed, the cells rinsed twice in 5ml serum-free media and then re-fed with 10ml fresh growth media and incubated for 2-3 days at 37°C.

2.17.5 Selection and Isolation of Colonies

In order to study the true effect of transfection studies, single colonies of stably transfected cells were selected and isolated. The selection process was carried out by feeding the "transfected" cells with media containing geneticin (Sigma; G9516) - the plasmids used had a geneticin-resistant gene, therefore, only those cells containing the

plasmid will survive treatment with geneticin. 2 days after transfection the flask of cells was fed with 200μg/ml geneticin in complete media. When the cells grew readily in this concentration of selecting agent, the concentration was increased step-wise to a final concentration of 800μg/ml. At this stage the cells were plated at clonal density and clonal populations were propagated as described in section 2.5.7. Transfected cells were periodically challenged with geneticin to establish stability of transfectants.

2.18 Statistical Analysis

Analysis of the significance of the difference in the mean IC_{50} value calculated from toxicity assays were performed using a paired student t-test, which was run on Sigma Plot.

A p value < 0.05 was deemed not significant
A p value > 0.05 was deemed significant
A p value > 0.005 was deemed highly significant

3.0 Results

3.1 The Effect of Upregulation of C-erbB-2 in the Human Breast Cancer Cell MCF-7 clone H3 on Resistance to Chemotherapy, Tamoxifen Hormonal Therapy, Invasiveness and Expression Patterns of the ErbB Receptor Family and a Panel of Drug Resistance Asssociated Genes.

An important objective of this thesis was to establish a breast cancer cell model for the investigation of the effects of c-erbB-2 expression on resistance to chemotherapeutic drugs and tamoxifen hormonal therapy and if any effect were found to, to investigate the mechanism(s) involved.

Two breast cancer cell lines were chosen, BT474A and MCF-7 H3 (isolated by Dr. Finbar O'Sullivan, NICB). Both are clonal populations isolated from their parental cell lines BT-474 and MCF-7. BT474 was derived from a solid, invasive ductal breast carcinoma and overexpresses c-erbB-2. MCF-7 was derived from the pleural effusion of a metastatic breast adenocarcinoma and express normal levels of c-erbB-2. Both cell lines are estrogen receptor positive. BT474A was transfected with a c-erbB-2-targeting ribozyme to downregulate expression of c-erbB-2, the results of which are presented in section 3.2. MCF-7 H3 was transfected with a c-erbB-2 encoding cDNA plasmid to upregulate expression of c-erbB-2.

3.1.1 Transfection of MCF-7 H3 with a cDNA Encoding C-erbB-2 and Isolation of Clonal Populations

MCF-7 H3 was co-transfected with a c-erbB-2 expression vector pCMV4/c-erbB-2 (section 2.18.4) and the hygromycin selection plasmid pTK, in order to up-regulate expression of c-erbB-2. Three clones were isolated by clonal dilution from a pooled population (section 2.18.5), and were further analysed. This plasmid was a kind gift from Dr. Dihua Yu. The clones were designated MCF-7 H3/ErbB2-A, MCF-7 H3/ErbB2-B and MCF-7 H3/ErbB2-C.

3.1.2 Effect of C-erbB-2 Upregulation on the Cell Morphology of MCF-7 H3

Transfection of MCF-7 H3 with a c-erbB-2 encoding cDNA had no effect on the morphology of MCF-7 H3. All three clonal populations displayed similar morphology to the parental cell line.

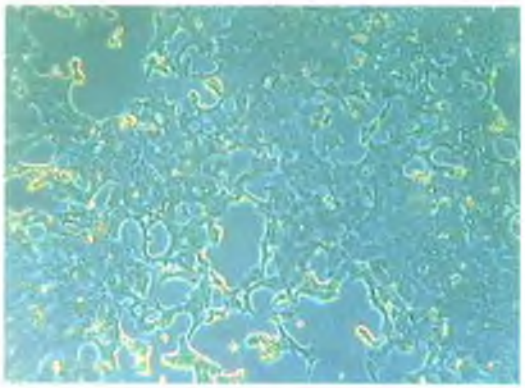

Figure 3.1.2a MCF-7 H3

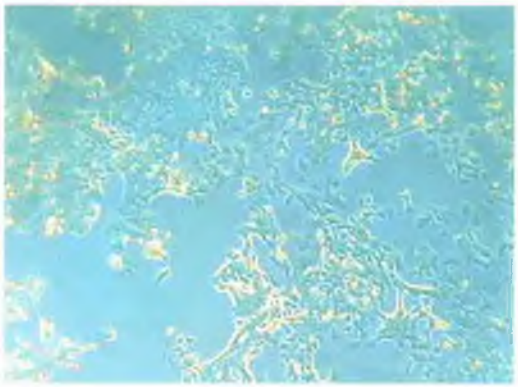

Figure 3.1.2b MCF-7 H3/ErbB2-A

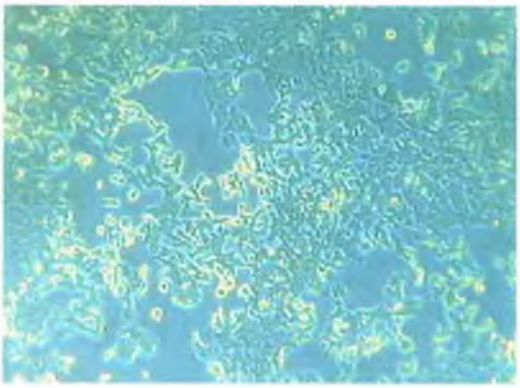

Figure 3.1.2c MCF-7 H3/ErbB2-B

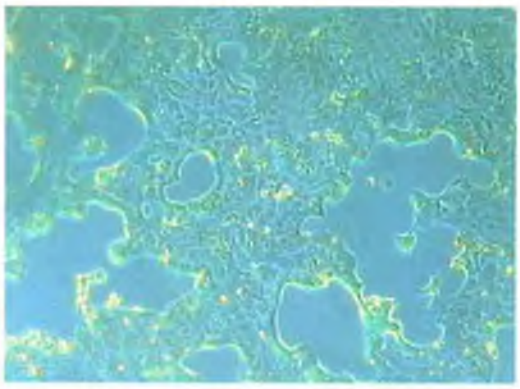

Figure 3.1.2d MCF-7 H3/ErbB2-C

3.1.3 Detection of Upregulation of C-erbB-2 in MCF-7 H3 by C-erbB-2 cDNA Transfection

After transfection of MCF-7 H3 with a c-erbB-2 encoding cDNA, levels of c-erbB-2 were examined at both the mRNA (RT-PCR) and protein (western blotting and immunprecipitation) levels, to determine the success of the transfection.

3.1.3.1 Detection of Levels of C-erbB-2 mRNA in MCF-7 H3 by RT-PCR

Figure 3.1.3.1 shows the expression of c-erbB-2 mRNA by RT_PCR in MCF-7 H3 and its transfectant clonal populations. Densitometry shows an increase in c-erbB-2, as the β-actin levels are low in the clonal populations. It is possible that primer competition is playing a role here and that higher levels of c-erbB-2 mRNA are resulting in reduced amplification of β-actin. Nevertheless, clearer evidence of upregulation in the transfectants would have been hoped for.

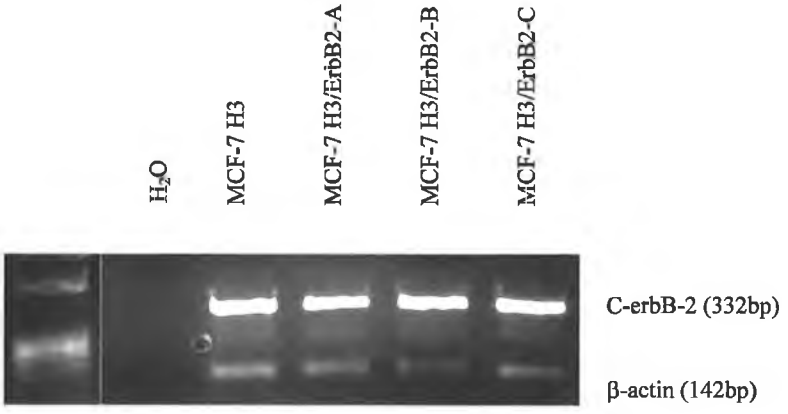

Figure 3.1.3.1 Levels of c-erbB-2 mRNA in MCF-7 H3 c-erbB-2 cDNA transfected clones.

Cell Line	Levels of C-erbB-2 mRNA Expression (%)
MCF-7 H3	100
MCF-7 H3/ErbB2-A	110
MCF-7 H3/ErbB2-B	130
MCF-7 H3/ErbB2-C	142

Table 3.1.3.1 Levels of c-erbB-2 mRNA in MCF-7 H3 c-erbB-2 cDNA transfected clones.

3.1.3.2 Detection of Levels of C-erbB-2 Protein

Expression of c-erbB-2 at the protein level was determined by three separate methods. Figure 3.1.3.2a shows that c-erbB-2 protein levels are elevated in all the clonal populations, as performed by western blotting. Figures 3.1.3.2b (classic immunporecipitation) and 3.1.3.2c (biotinylated immunoprecipitation) also shows elevation of c-erbB-2 protein levels. These results confirm that this transfection was a success.

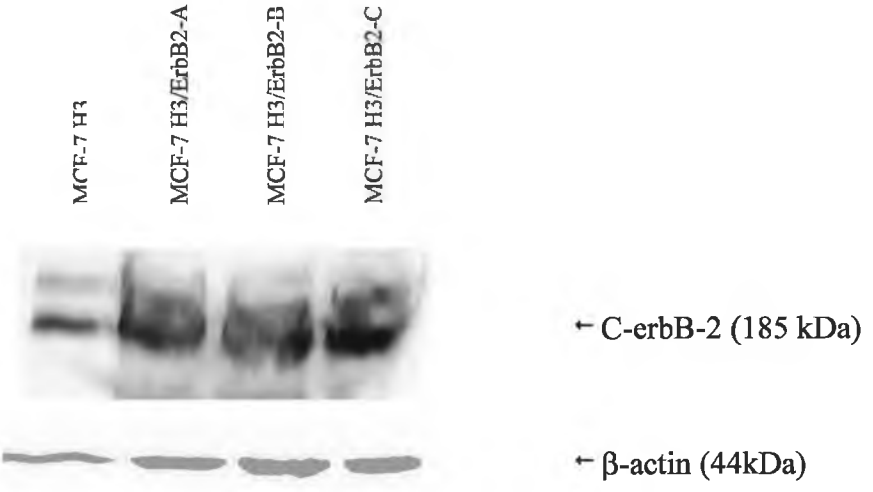

Figure 3.1.3.2a Western Blot of c-erbB-2 protein in MCF-7 H3 c-erbB-2 cDNA transfected clones. C-erbB-2 runs as a doublet with the higher molecular weight form representing its glycosylated form.

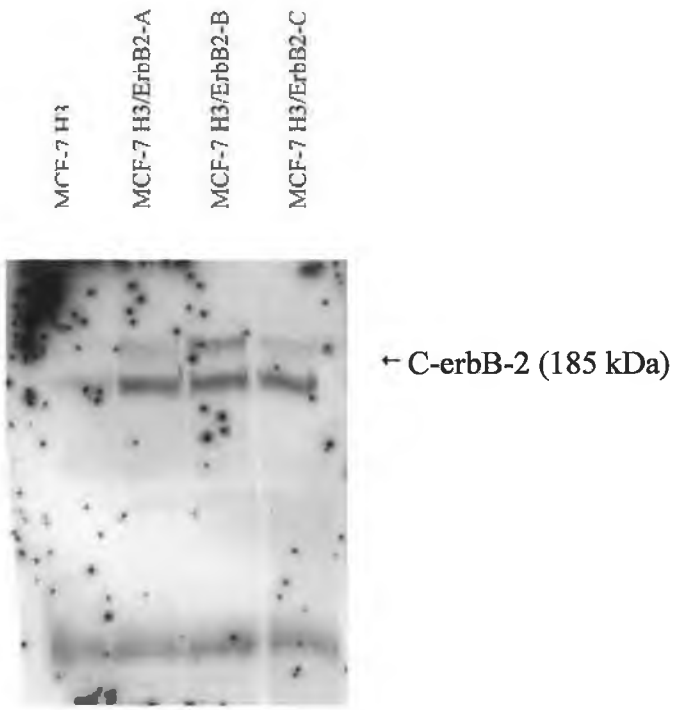

Figure 3.1.3.2b Classic immunoprecipitation of c-erbB-2 protein in MCF-7 H3 c-erbB-2 cDNA transfected clones.

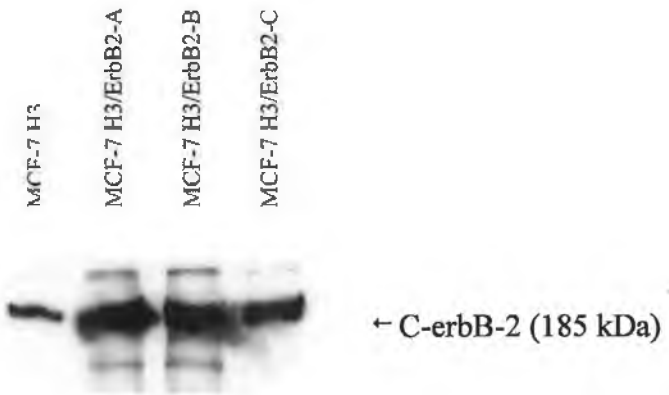

Figure 3.1.3.2c Biotinylated immunoprecipitation of c-erbB-2 protein in MCF-7 H3 c-erbB-2 cDNA transfected clones.

3.1.4 Effect of c-erbB-2 Upregulation In MCF-7 H3 on Chemotherapeutic Drug Resistance

The effect of c-erbB-2 expression on the chemotherapeutic drug resistance of MCF-7 H3 was examined. A panel of chemotherapeutic agents was chosen, including adriamycin, taxol, carboplatin, taxotere, 5-fluorouracil, vincristine and methotrexate. Two methods of toxicity testing were used, entitled long-term and short-term as described in sections 2.7.1 and 2.7.2. The purpose of this was to compare the effect of c-erbB-2 on the sensitivity of MCF-7 H3 to longer drug exposure at lower levels versus shorter exposure at higher levels.

3.1.4.1 Effect of c-erbB-2 Upregulation on Adriamycin Resistance

C-erbB-2 sensitised MCF-7 H3 to adriamycin in two of the clonal populations, MCF-7 H3/ErbB2-A and MCF-7 H3/ErbB2-B. This was observed in both short and long term toxicity assays. There was no significant change in the resistance of MCF-7 H3/ErbB2-C to adriamycin in either long or short term assays compared to the parental cell line MCF-7 H3.

3.1.4.1.1 Long Term Adriamycin IC_{50} Toxicity assay

Cell Line	IC_{50} Adriamycin (ng/ml; n=3)
MCF-7 H3	19.83 ± 2.3*
MCF-7 H3/ErbB2-A	10.30 ± 1.1
MCF-7 H3/ErbB2-B	11.97 ± 0.57
MCF-7 H3/ErbB2-C	27.27 ± 2.6

* ± standard deviation

Table 3.1.4.1.1a Results of long term adriamycin toxicity assay.

Cell Line	Fold Change in Resistance	Significance - Paired Student t-Test
MCF-7 H3	1.00	p = *
MCF-7 H3/ErbB2-A	0.51	0.0415
MCF-7 H3/ErbB2-B	0.60	0.0415
MCF-7 H3/ErbB2-C	1.35	0.1221

*A p level of less than 0.05 is considered significant.

Table 3.1.4.1.1b Fold resistance to adriamycin in long term assays and significance of change.

3.1.4.1.2 Short Term Adriamycin IC_{50} Toxicity assay

Cell Line	IC_{50} Adriamycin (ng/ml; n=3)
MCF-7 H3	348 ± 2.8
MCF-7 H3/ErbB2-A	183 ± 15.0
MCF-7 H3/ErbB2-B	290.3 ± 15.0
MCF-7 H3/ErbB2-C	369 ± 33.8

Table 3.1.4.1.2a Results of short term adriamycin toxicity assay.

Cell Line	Fold Change in Resistance	Significance - Paired Student t-Test
MCF-7 H3	1.00	p =
MCF-7 H3/ErbB2-A	0.52	0.0037
MCF-7 H3/ErbB2-B	0.83	0.0278
MCF-7 H3/ErbB2-C	1.06	0.3837

Table 3.1.4.1.2b Fold resistance to adriamycin in short term assays and significance of change.

3.1.4.2 Effect of c-erbB-2 Upregulation on Taxol Resistance

C-erbB-2 increased the resistance of MCF-7 H3 to taxol in all three clonal populations, MCF-7 H3/ErbB2-A, MCF-7 H3/ErbB2-B and MCF-7 H3/ErbB2-C, in short term toxicity assays. Only MCF-7 H3/ErbB2-C displayed a significant increase ($p < 0.0147$) in resistance to taxol in long term assays, compared to the parental cell line MCF-7 H3.

3.1.4.2.1 Long Term Taxol IC_{50} Toxicity assay

Cell Line	**IC_{50} Taxol (ng/ml; n=3)**
MCF-7 H3	1.09 ± 0.16
MCF-7 H3/ErbB2-A	1.01 ± 0.07
MCF-7 H3/ErbB2-B	1.28 ± 0.09
MCF-7 H3/ErbB2-C	1.62 ± 0.21

Table 3.1.4.2.1a Results of long term taxol toxicity assay.

Cell Line	**Fold Change in Resistance**	**Significance - Paired Student t-Test**
MCF-7 H3	1.00	**p =**
MCF-7 H3/ErbB2-A	0.92	0.3391
MCF-7 H3/ErbB2-B	1.27	0.2818
MCF-7 H3/ErbB2-C	1.48	0.0147

Table 3.1.4.2.1b Fold resistance to taxol in long term assays and significance of change.

3.1.4.2.2 Short Term Taxol IC_{50} Toxicity assay

Cell Line	IC_{50} Taxol (ng/ml; n=3)
MCF-7 H3	9.2 ± 1.0
MCF-7 H3/ErbB2-A	21.7 ± 0.64
MCF-7 H3/ErbB2-B	29.5 ± 4.8
MCF-7 H3/ErbB2-C	28.8 ± 2.4

Table 3.1.4.2.2a Results of short term taxol toxicity assay.

Cell Line	Fold Change in Resistance	Significance - Paired Student t-Test
MCF-7 H3	1.00	p =
MCF-7 H3/ErbB2-A	2.38	0.0018
MCF-7 H3/ErbB2-B	3.20	0.0223
MCF-7 H3/ErbB2-C	3.13	0.0078

Table 3.1.4.2.2b Fold resistance to taxol in short term assays and significance of change.

3.1.4.3 Effect of c-erbB-2 Upregulation on Carboplatin Resistance

Long term toxicity results for carboplatin showed that their was no change in carboplatin resistance, as they showed that c-erbB-2 upregulation decreased resistance to carboplatin in two clonal populations, MCF-7 H3/ErbB2-A and MCF-7 H3/ErbB2-C, while increasing resistance in MCF-7 H3/ErbB2-B. In short term toxicity assays MCF-7 H3/ErbB2-B and MCF-7 H3/ErbB2-C displayed increased resistance to carboplatin, while the sensitivity of MCF-7 H3/ErbB-A to carboplatin was unchanged, compared to the parental cell line.

3.1.4.3.1 Long Term Carboplatin IC_{50} Toxicity assay

Cell Line	**IC_{50} Carboplatin (μg/ml; n=3)**
MCF-7 H3	1.75 ± 0.10
MCF-7 H3/ErbB2-A	1.27 ± 0.03
MCF-7 H3/ErbB2-B	2.10 ± 0.001
MCF-7 H3/ErbB2-C	1.29 ± 0.13

Table 3.1.4.3.1a Results of long term carboplatin toxicity assay.

Cell Line	**Fold Change in Resistance**	**Significance - Paired Student t-Test**
MCF-7 H3	1.00	**p =**
MCF-7 H3/ErbB2-A	0.72	0.0141
MCF-7 H3/ErbB2-B	1.20	0.0298
MCF-7 H3/ErbB2-C	0.73	0.0346

Table 3.1.4.3.1b Fold resistance to carboplatin in long term assays and significance of change.

3.1.4.3.2 Short Term Carboplatin IC_{50} Toxicity assay

Cell Line	IC_{50} Carboplatin (μg/ml)
MCF-7 H3	42.9 ± 3.4
MCF-7 H3/ErbB2-A	40.3 ± 3.8
MCF-7 H3/ErbB2-B	58.8 ± 3.3
MCF-7 H3/ErbB2-C	73.3 ± 4.2

Table 3.1.4.3.2a Results of short term carboplatin toxicity assay.

Cell Line	Fold Change in Resistance	Significance - Paired Student t-Test
MCF-7 H3	1.00	p =
MCF-7 H3/ErbB2-A	0.93	0.1865
MCF-7 H3/ErbB2-B	1.37	0.0010
MCF-7 H3/ErbB2-C	1.70	0.0170

Table 3.1.4.3.2b Fold resistance to carboplatin in short term assays and significance of change.

3.1.4.4 Effect of c-erbB-2 Upregulation on 5-Fluorouracil Resistance

Both long and short term toxicity results for 5-fluorouracil showed that c-erbB-2 upregulation decreased resistance to 5-fluorouracil in two clonal populations, MCF-7 H3/ErbB2-A and MCF-7 H3/ErbB2-C, while increasing resistance in MCF-7 H3/ErbB2-B. This may indicate that c-erbB-2 overexpression in general leads to increased sensitivity to 5-fluorouracil.

3.1.4.4.1 Long Term 5-FU IC_{50} Toxicity assay

Cell Line	**IC_{50} 5-Fluorouracil (μg/ml; n=3)**
MCF-7 H3	0.17 ± 0.005
MCF-7 H3/ErbB2-A	0.12 ± 0.000
MCF-7 H3/ErbB2-B	0.26 ± 0.005
MCF-7 H3/ErbB2-C	0.14 ± 0.005

Table 3.1.4.4.1a Results of long term 5-FU toxicity assay.

Cell Line	**Fold Change in Resistance**	**Significance - Paired Student t-Test**
MCF-7 H3	1.00	**p =**
MCF-7 H3/ErbB2-A	0.70	0.0034
MCF-7 H3/ErbB2-B	1.52	0.0040
MCF-7 H3/ErbB2-C	0.82	0.0040

Table 3.1.4.4.1b Fold resistance to 5-FU in long term assays and significance of change.

3.1.4.4.2 Short Term 5-FU IC_{50} Toxicity assay

Cell Line	IC_{50} 5-Fluorouracil (μg/ml; n=3)
MCF-7 H3	6.06 ± 0.11
MCF-7 H3/ErbB2-A	4.73 ± 0.20
MCF-7 H3/ErbB2-B	7.16 ± 0.28
MCF-7 H3/ErbB2-C	3.30 ± 0.20

Table 3.1.4.4.2a Results of short term 5-FU toxicity assay.

Cell Line	Fold Change in Resistance	Significance - Paired Student t-Test
MCF-7 H3	1.00	**p =**
MCF-7 H3/ErbB2-A	0.78	0.0043
MCF-7 H3/ErbB2-B	1.18	0.0198
MCF-7 H3/ErbB2-C	0.54	0.0018

Table 3.1.4.4.2b Fold resistance to 5-FU in short term assays and significance of change.

3.1.4.5 Effect of c-erbB-2 Upregulation on Vincristine Resistance

C-erbB-2 upregulation decreased the resistance of MCF-7 H3/ErbB2-A and MCF-7 H3/ErbB2-C to vincristine in long term assays. No change was observed in MCF-7 H3/ErbB2-B. Only MCF-7 H3/ErbB2-C displayed decreased resistance in short term assays.

3.1.4.5.1 Long Term Vincristine IC_{50} Toxicity assay

Cell Line	IC_{50} Vincristine (ng/ml; n=3)
MCF-7 H3	2.30 ± 0.17
MCF-7 H3/ErbB2-A	1.36 ± 0.05
MCF-7 H3/ErbB2-B	2.43 ± 0.11
MCF-7 H3/ErbB2-C	1.73 ± 0.05

Table 3.1.4.5.1a Results of long term vincristine toxicity assay.

Cell Line	Fold Change in Resistance	Significance - Paired Student t-Test
MCF-7 H3	1.00	p =
MCF-7 H3/ErbB2-A	0.59	0.0088
MCF-7 H3/ErbB2-B	1.05	0.2697
MCF-7 H3/ErbB2-C	0.75	0.0421

Table 3.1.4.5.1b Fold resistance to vincristine in long term assays and significance of change.

3.1.4.5.2 Short Term Vincristine IC_{50} Toxicity assay

Cell Line	IC_{50} Vincristine (ng/ml; n=3)
MCF-7 H3	73.3 ± 1.52
MCF-7 H3/ErbB2-A	71.3 ± 1.15
MCF-7 H3/ErbB2-B	71.6 ± 2.30
MCF-7 H3/ErbB2-C	53.0 ± 3.46

Table 3.1.4.5.2a Results of short term vincristine toxicity assay.

Cell Line	Fold Change in Resistance	Significance - Paired Student t-Test
MCF-7 H3	1.00	p =
MCF-7 H3/ErbB2-A	0.97	0.3206
MCF-7 H3/ErbB2-B	0.97	0.1993
MCF-7 H3/ErbB2-C	0.72	0.0095

Table 3.1.4.5.2b Fold resistance to vincristine in short term assays and significance of change.

3.1.4.6 Effect of c-erbB-2 Upregulation on Taxotere Resistance

Long term toxicity results for taxotere showed that their was no change in taxotere resistance. C-erbB-2 upregulation resulted in decreased resistance to taxotere in two clonal populations, MCF-7 H3/ErbB2-A and MCF-7 H3/ErbB2-B, while increasing resistance in MCF-7 H3/ErbB2-C. In short term toxicity assays all clones displayed decreased resistance to taxotere, although only MCF-7 H3/ErbB2-B and MCF-7 H3/ErbB2-C were statistically significant.

3.1.4.6.1 Long Term Taxotere IC_{50} Toxicity assay

Cell Line	**IC_{50} Taxotere (ng/ml; n=3)**
MCF-7 H3	0.48 ± 0.03
MCF-7 H3/ErbB2-A	0.37 ± 0.02
MCF-7 H3/ErbB2-B	0.42 ± 0.01
MCF-7 H3/ErbB2-C	0.62 ± 0.02

Table 3.1.4.6.1a Results of long term taxotere toxicity assay.

Cell Line	**Fold Change in Resistance**	**Significance - Paired Student t-Test**
MCF-7 H3	1.00	**p =**
MCF-7 H3/ErbB2-A	0.77	0.0421
MCF-7 H3/ErbB2-B	0.87	0.1037
MCF-7 H3/ErbB2-C	1.29	0.0152

Table 3.1.4.6.1b Fold resistance to taxotere in long term assays and significance of change.

3.1.4.6.2 Short Term Taxotere IC_{50} Toxicity assay

Cell Line	IC_{50} Taxotere (ng/ml; n=3)
MCF-7 H3	6.10 ± 0.17
MCF-7 H3/ErbB2-A	5.36 ± 0.32
MCF-7 H3/ErbB2-B	5.46 ± 0.05
MCF-7 H3/ErbB2-C	5.53 ± 0.05

Table 3.1.4.6.2a Results of short term taxotere toxicity assay.

Cell Line	Fold Change in Resistance	Significance - Paired Student t-Test
MCF-7 H3	1.00	p =
MCF-7 H3/ErbB2-A	0.88	0.0532
MCF-7 H3/ErbB2-B	0.90	0.0188
MCF-7 H3/ErbB2-C	0.91	0.0421

Table 3.1.4.6.2b Fold resistance to taxotere in short term assays and significance of change.

3.1.4.7 Effect of c-erbB-2 Upregulation on Methotrexate Resistance in Long Term assays

C-erbB-2 transfection of MCF-7 H3 resulted in increased resistance to methotrexate in all three clonal populations.

Cell Line	**IC_{50} Methotrexate (ng/ml; n=3)**
MCF-7 H3	5.16 ± 0.47
MCF-7 H3/ErbB2-A	12.36 ± 0.87
MCF-7 H3/ErbB2-B	8.03 ± 0.77
MCF-7 H3/ErbB2-C	10.26 ± 0.70

Table 3.1.4.7a Results of long term methotrexate toxicity assay.

Cell Line	**Fold Change in Resistance**	**Significance - Paired Student t-Test**
MCF-7 H3	1.00	**p =**
MCF-7 H3/ErbB2-A	2.39	0.0100
MCF-7 H3/ErbB2-B	1.55	0.0198
MCF-7 H3/ErbB2-C	1.98	0.0156

Table 3.1.4.7b Fold resistance to methotrexate in long term assays and significance of change.

3.1.4.8 Summary of Changes in resistance To Chemotherapeutic Agents in MCF-7 H3 c-erbB-2 cDNA transfected variants.

The main findings of this section were that c-erbB-2 overexpression conferred resistance to taxol in short term assays but not in long term assays, and resistance to methotrexate in long term assays. Decreased resistance to vincristine, adriamycin and carboplatin was observed in 2 out of 3 clonal populations in long term assays. Interestingly drugs of a similar structure and mechanism of action, taxol and taxotere, did not correspond in their response to c-erbB-2 overexpression.

Type of Toxicity Assay	**MCF-7 H3/ ErbB2-A**	**MCF-7 H3/ ErbB2-B**	**MCF-7 H3/ ErbB2-C**
Adriamycin Long Term	-	-	o
Adriamycin Short Term	-	-	o
Taxol Long Term	o	o	+
Taxol Short Term	+	+	+
Carboplatin Long Term	-	+	-
Carboplatin Short Term	o	+	+
Taxotere Long Term	-	o	+
Taxotere Short Term	o	-	-
Vincristine Long Term	-	o	-
Vincristine Short Term	o	o	-
5-Fluorouracil Long Term	-	+	-
5-Fluorouracil Short Term	-	+	-
Methotrexate Long Term	+	+	+

+ increase in resistance

- decrease in resistance

o no change in resistance

3.1.5 Investigation of Changes in MDR Associated Gene Expression in C-erbB-2 cDNA transfected MCF-7 H3 Breast Cancer Cells.

A panel of genes associated with drug resistance were examined at the mRNA level by RT-PCR to determine whether the changes in drug resistance observed in Section 3.1.4 was due to alterations in classical modes of drug resistance.

3.1.5.1 MDR-1

Figure 3.1.5.1 shows that mdr-1 mRNA was not expressed by MCF-7 H3 or any of its c-erbB-2 transfected clones.

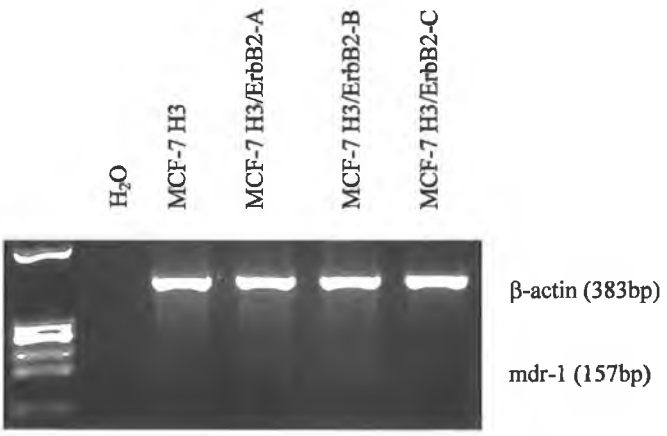

Figure 3.1.5.1 Expression of MDR-1 mRNA in MCF-7 H3 c-erbB-2 cDNA transfected clones. (PCR in Figure 3.3.8.1 was performed with the above at represents a positive control for mdr-1)

3.1.5.2 MRP-1

Figure 3.1.5.2 shows that mrp-1 mRNA expression levels did not change as a results of c-erbB-2 transfection of MCF-7 H3.

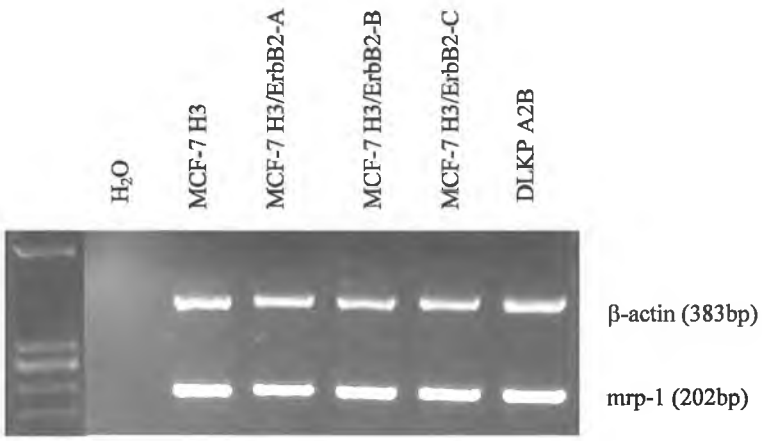

Figure 3.1.5.2 Expression of mrp-1 mRNA in MCF-7 H3 c-erbB-2 cDNA transfected clones.

Cell Line	**Levels of MRP-1 mRNA Expression (%)**
MCF-7 H3	100
MCF-7 H3/ErbB2-A	104.3
MCF-7 H3/ErbB2-B	138.8
MCF-7 H3/ErbB2-C	121.1

Table 3.1.5.2 levels of mrp-1 mRNA in MCF-7 H3 c-erbB-2 cDNA transfected clones.

3.1.5.3 MRP-2

Figure 3.1.5.3 shows that mrp-2 mRNA expression levels did not change as a results of c-erbB-2 transfection of MCF-7 H3.

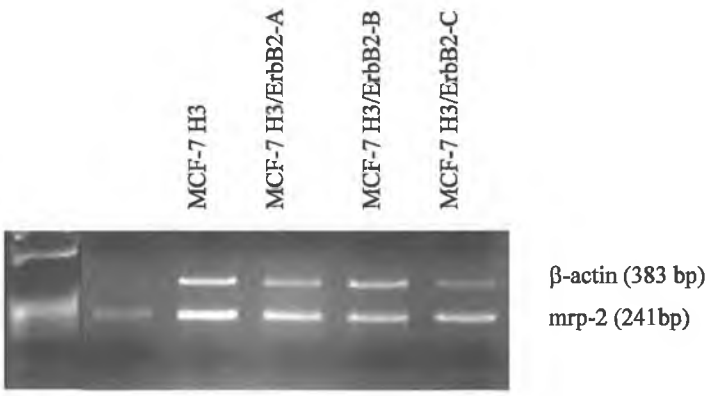

Figure 3.1.5.3 Expression of mrp-2 mRNA in MCF-7 H3 c-erbB-2 cDNA transfected clones.

Cell Line	**Levels of MRP-2 mRNA Expression (%)**
MCF-7 H3	100
MCF-7 H3/ErbB2-A	99
MCF-7 H3/ErbB2-B	87
MCF-7 H3/ErbB2-C	125

Table 3.1.5.3 levels of mrp-2 mRNA in MCF-7 H3 c-erbB-2 cDNA transfected clones.

3.1.5.4 MRP-4

Figure 3.1.5.4 shows that mrp-4 mRNA was not expressed by MCF-7 H3 or any of its c-erbB-2 transfected clones.

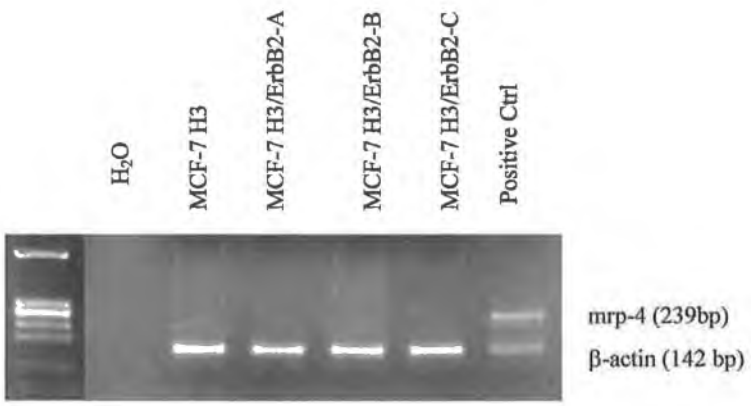

Figure 3.1.5.4 Expression of mrp-4 mRNA in MCF-7 H3 c-erbB-2 cDNA transfected clones.

3.1.5.5 MRP-5

Figure 3.1.5.5 shows that mrp-5 mRNA was not expressed by MCF-7 H3 or any of its c-erbB-2 transfected clones.

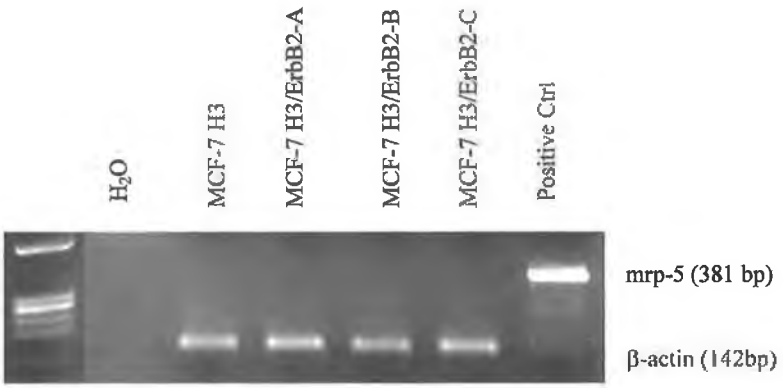

Figure 3.1.5.5 Expression of mrp-5 mRNA in MCF-7 H3 c-erbB-2 cDNA transfected clones.

3.1.5.6 Topoisomerase I

Figure 3.1.5.6 shows that topoisomerase I mRNA levels are unchanged by upregulation of c-erbB-2 in MCF-7 H3.

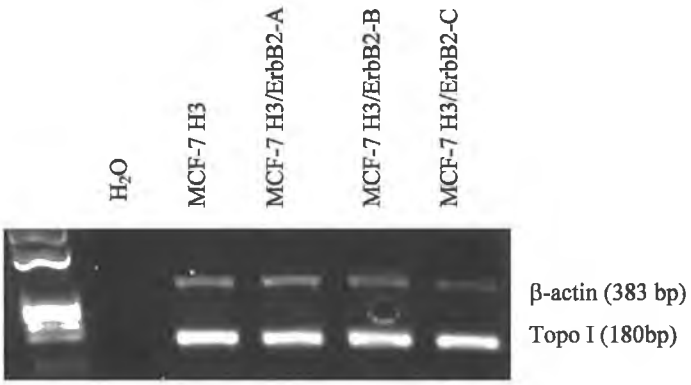

Figure 3.1.5.6 Expression of topoisomerase I mRNA in MCF-7 H3 c-erbB-2 cDNA transfected clones.

Cell Line	Levels of Topo I mRNA Expression (%)
MCF-7 H3	100
MCF-7 H3/ErbB2-A	79
MCF-7 H3/ErbB2-B	100
MCF-7 H3/ErbB2-C	128

Table 3.1.5.6 levels of topoisomerase I mRNA in MCF-7 H3 c-erbB-2 cDNA transfected clones.

3.1.5.7 Topoisomerase IIα

Figure 3.1.5.7 shows that topoisomerase IIα mRNA levels are unchanged by upregulation of c-erbB-2 in MCF-7 H3.

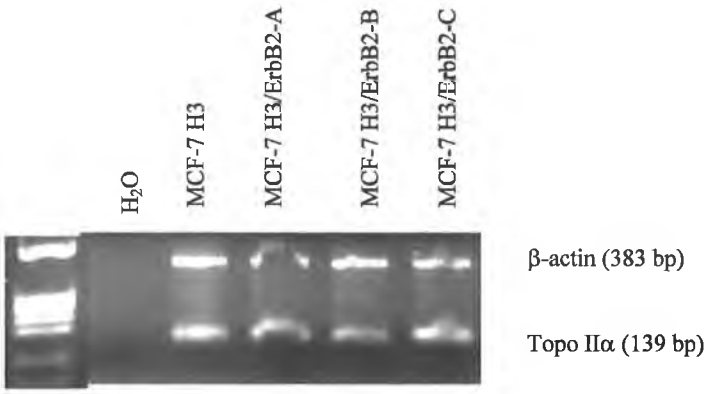

Figure 3.1.5.7 Expression of topoisomerase IIα mRNA in MCF-7 H3 c-erbB-2 cDNA transfected clones.

Cell Line	**Levels of Topo IIα mRNA Expression (%)**
MCF-7 H3	100
MCF-7 H3/ErbB2-A	Band too diffuse for densitometry
MCF-7 H3/ErbB2-B	74
MCF-7 H3/ErbB2-C	128

Table 3.1.5.7 levels of topoisomerase IIα mRNA in MCF-7 H3 c-erbB-2 cDNA transfected clones.

3.1.5.8 Topoisomerase IIβ

Densitometry of figure 3.1.5.8 shows that topoisomerase IIβ mRNA levels were increased by c-erbB-2 transfection of MCF-7 H3 the clonal transfectant population MCF-7 H3/ErbB2-A, but not in the other clonal transfectants.

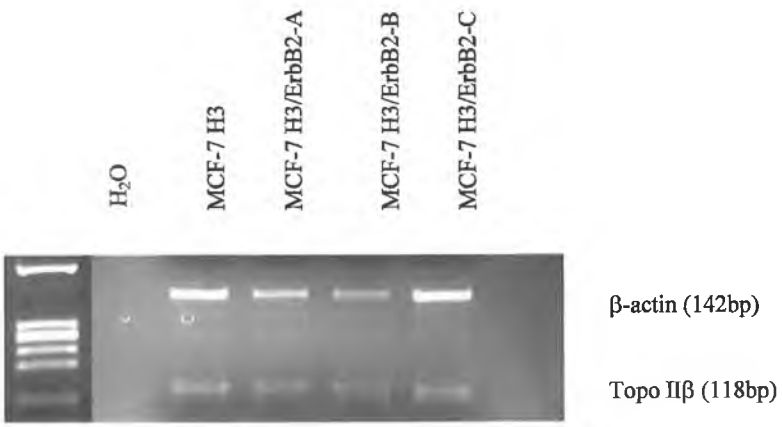

Figure 3.1.5.8 Expression of topoisomerase IIβ mRNA in MCF-7 H3 c-erbB-2 cDNA transfected clones.

Cell Line	**Levels of Topo IIβ mRNA Expression (%)**
MCF-7 H3	100
MCF-7 H3/ErbB2-A	142
MCF-7 H3/ErbB2-B	109
MCF-7 H3/ErbB2-C	83

Table 3.1.5.8 levels of topoisomerase IIβ mRNA in MCF-7 H3 c-erbB-2 cDNA transfected clones.

3.1.5.9 Dihydrofolate reductase

Figure 3.1.5.9 shows that DHFR mRNA was increased by c-erbB-2 transfection of MCF-7 H3.

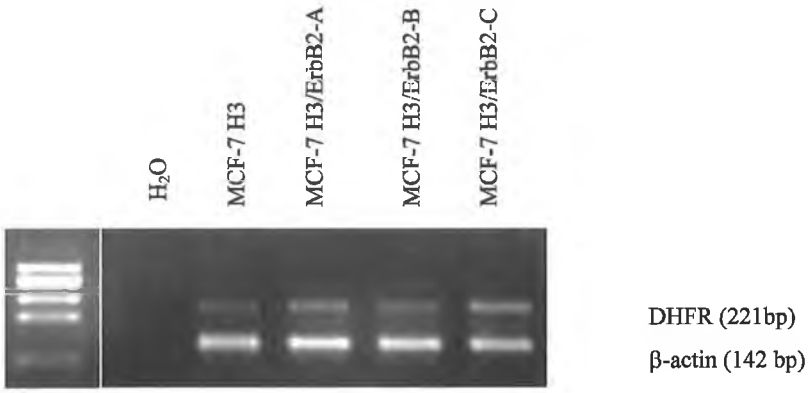

Figure 3.1.5.9 Expression of DHFR mRNA in MCF-7 H3 c-erbB-2 cDNA transfected clones.

Cell Line	**Levels of DHFR mRNA Expression (%)**
MCF-7 H3	100
MCF-7 H3/ErbB2-A	155
MCF-7 H3/ErbB2-B	131
MCF-7 H3/ErbB2-C	220

Table 3.1.5.9 levels of DHFR mRNA in MCF-7 H3 c-erbB-2 cDNA transfected clones.

3.1.5.10 Thymidylate Synthase

Figure 3.1.5.10 shows that thymidylate synthase mRNA increased in only MCF-7 H3/ErbB-C.

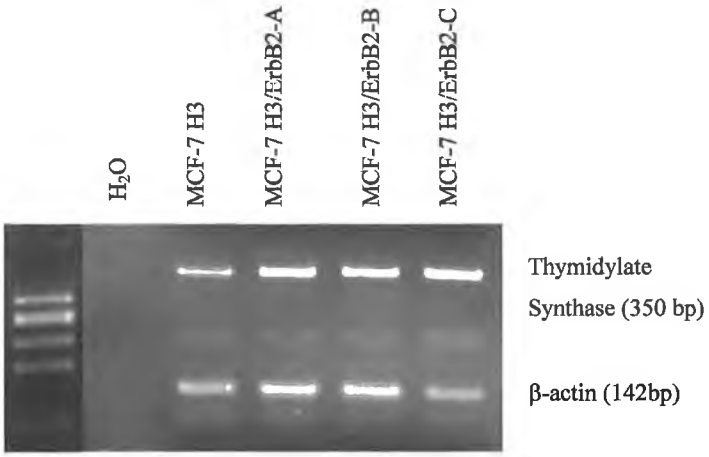

Figure 3.1.5.10 Expression of TS mRNA in MCF-7 H3 c-erbB-2 cDNA transfected clones.

Cell Line	**Levels of Thymidylate Synthase mRNA Expression (%)**
MCF-7 H3	100.0
MCF-7 H3/ErbB2-A	127.2
MCF-7 H3/ErbB2-B	104.4
MCF-7 H3/ErbB2-C	180.5

Table 3.1.5.10 levels of TS mRNA in MCF-7 H3 c-erbB-2 cDNA transfected clones.

3.1.5.11 GSTπ (n=2)

Figure 3.1.5.11 shows that GST π mRNA was not expressed by MCF-7 H3 or any of its c-erbB-2 transfected clones. A non specific band was detected, also detectable in BT474A but not in MDA-MB-435S-F.

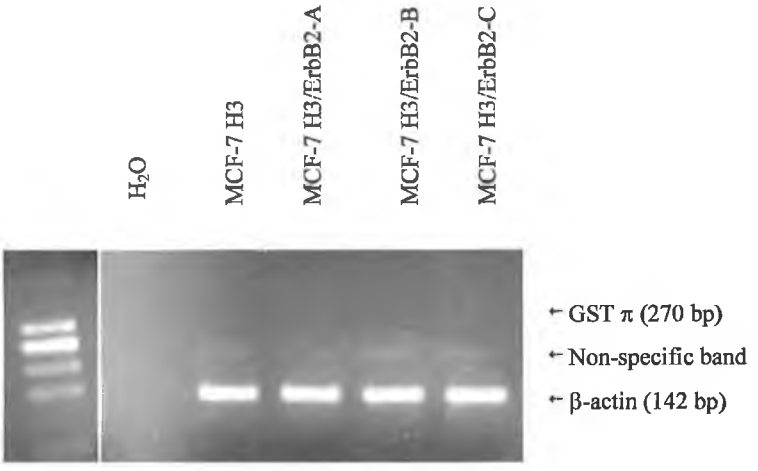

Figure 3.1.5.11 Expression of GST π mRNA in MCF-7 H3 c-erbB-2 cDNA transfected clones. (PCR in Figure 3.3.8.11 was performed with the above and represents a positive control for GSTπ)

3.1.5.12 Summary of Results of Gene Expression Studies in MCF-7 H3 c-erbB-2 cDNA Transfectants

No changes in the expression of drug resistance pumps at the mRNA level, were detected by RT-PCR. This suggested that MDR-1, MRP-1, MRP2, MRP4 and MRP5, do not play a role in c-erbB-2 associated drug resistance. Also, no significant changes in the expression of the different topoisomerase isoforms, thymidylate synthase or GSTπ were detected. The one alteration seen consistent with changes in drug resistance, was an upregulation in the expression of DFHR, which correlated with increased resistance to methotrexate.

RT-PCR	**MCF-7 H3/ ErbB2-A**	**MCF-7 H3/ ErbB2-B**	**MCF-7 H3/ ErbB2-C**
Mdr-1	neg	neg	neg
Mrp-1	o	o	o
Mrp-2	o	o	o
Mrp-4	neg	neg	neg
Mrp-5	neg	neg	neg
Topo I	o	o	o
Topo IIα	o	o	o
Topo IIβ	o	o	o
DHFR	+	+	+
TS	o	o	+
GSTπ	neg	neg	neg
C-erbB-1	+	+	+
C-erbB-4	-	-	-

\+ increase in expression

\- decrease in expression

o no change in expression

neg Not expressed

3.1.6 The Effect of c-erbB-2 Upregulation in MCF-7 H3 on Resistance to Tamoxifen

The effects of c-erbB-2 expression on tamoxifen resistance in MCF-7 H3 were varying. C-erbB-2 upregulation in MCF-7 H3 had no effect on the sensitivity of MCF-7 H3/ErbB2-B to tamoxifen. MCF-7 H3/ErbB2-A showed decreased resistance to tamoxifen when compared to the parental cell line, MCF-7 H3. MCF-7 H3/ErbB2-C was also examined for changes in tamoxifen resistance. Its IC_{50} was greater than 50ng/ml, as no cell kill was achieved in these assays.

Cell Line	**IC_{50} Tamoxifen (ng/ml; n=3;)**
MCF-7 H3	24.33 ± 0.57*
MCF-7 H3/ErbB2-A	16.33 ± 1.15
MCF-7 H3/ErbB2-B	22.23 ± 2.08

* ± standard deviation

Table 3.1.6a Results of long term tamoxifen toxicity assay.

Cell Line	**Fold Change in Resistance**	**Significance - Paired Student t -Test**
MCF-7 H3	1.00	**p =**
MCF-7 H3/ErbB2-A	0.67	0.0051
MCF-7 H3/ErbB2-B	0.91	0.1835

Table 3.1.6b Fold resistance to tamoxifen in long term assays and significance of change.

3.1.7 The Effect of c-erbB-2 Upregulation on Estrogen Receptor Expression

Expression estrogen receptors were examined by western blotting. No changes in the expression of estrogen receptor α expression was detected, while estrogen receptor β was found to be upregulated, particularly isoforms of higher molecular weights. Blots were stripped and reprobed for β-actin

3.1.7.1 Estrogen Receptor α

Figure 3.1.7.1 shows that c-erbB-2 expression in MCF-7 H3 does not affect ERα expression. A non specific band was detected in MCF-7 H3/ErbB2-C, reported often with this antibody, which is not ERβ.

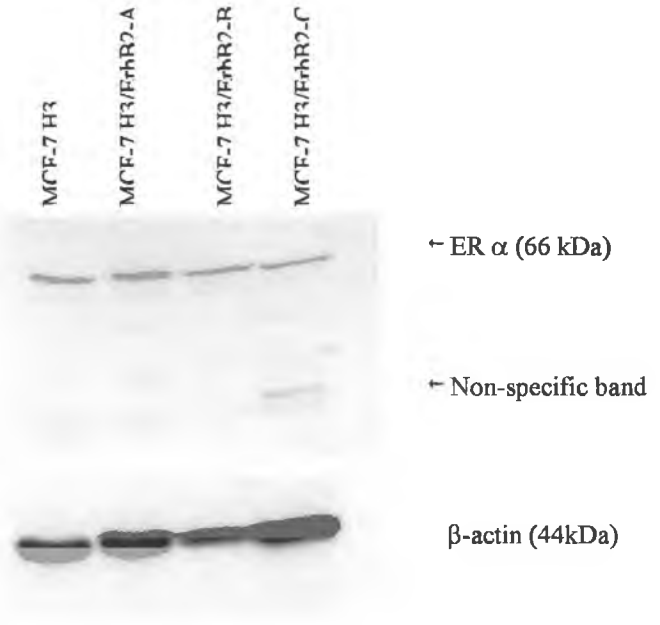

Figure 3.1.7.1 Western blot of estrogen receptor α expression in MCF-7 H3 c-erbB-2 cDNA transfected clones.

3.1.7.2 Estrogen Receptor β

Figure 3.1.7.2 shows that c-erbB-2 upregulation in MCF-7 H3 results in an increase in the expresion of ERβ isoforms.

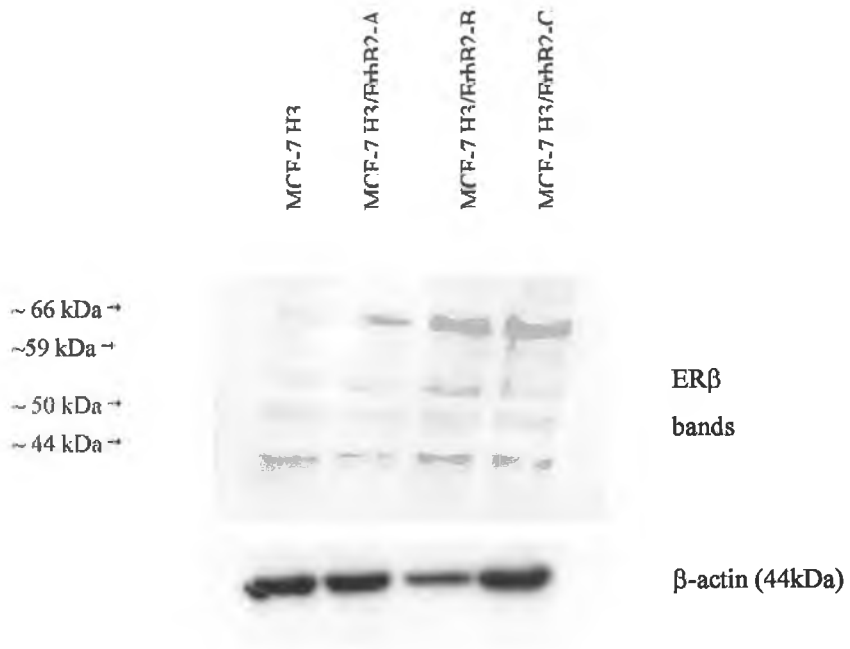

Figure 3.1.7.2 Western blot of estrogen receptor β expression in MCF-7 H3 c-erbB-2 cDNA transfected clones.

3.1.8 The Effect of C-erbB-2 Upregulation on the Levels of mRNA of C-erbB-1 and C-erbB-4 in MCF-7 H3.

In order to determine whether c-erbB-2 had an effect on the expression of other ErbB family members, erbB levels were determined at both mRNA and protein levels (Section 3.1.9). The effect of c-erbB-2 upregulation in MCF-7 H3, on the expression of c-erbB-1 and c-erbB-4 mRNA levels was examined by RT-PCR

3.1.8.1 C-erbB-1

Figure 3.1.8.1 shows that c-erbB-2 upregulation in MCF-7 H3 results in the increase of c-erbB-1 mRNA.

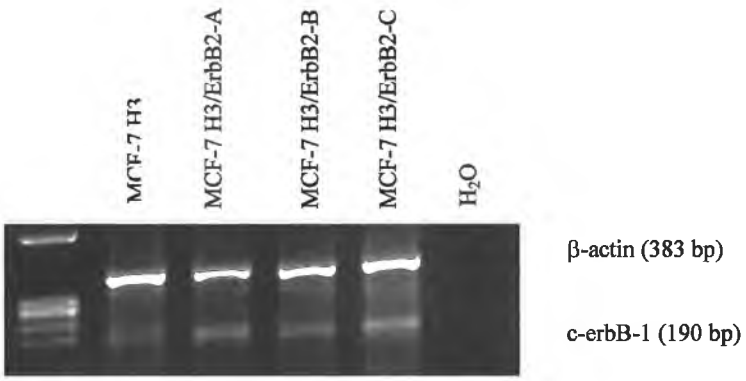

Figure 3.1.8.1 Expression of c-erbB-1 mRNA in MCF-7 H3 c-erbB-2 cDNA transfected clones.

Cell Line	Levels of C-erbB-1 mRNA Expression (%)
MCF-7 H3	100
MCF-7 H3/ErbB2-A	225
MCF-7 H3/ErbB2-B	153
MCF-7 H3/ErbB2-C	209

Table 3.1.8.1 Levels of c-erbB-1 mRNA in MCF-7 H3 c-erbB-2 cDNA transfected clones.

3.1.8.2 C-erbB-4

Figure 3.1.8.2 shows that c-erbB-2 upregulation in MCF-7 H3 results in a decrease of c-erbB-4 mRNA.

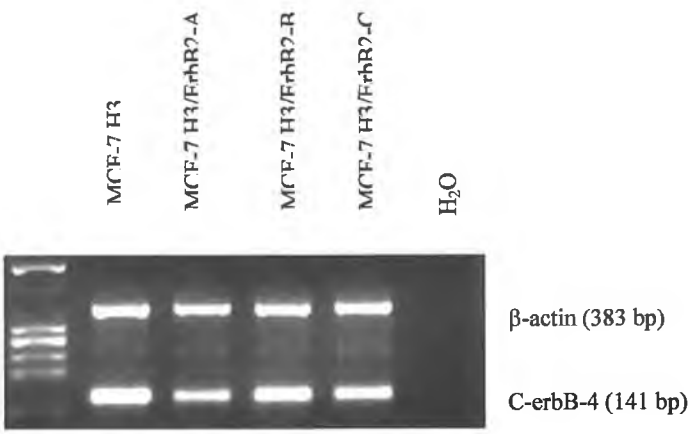

Figure 3.1.8.2 Expression of c-erbB-4mRNA in MCF-7 H3 c-erbB-2 cDNA transfected clones.

Cell Line	Levels of c-erbB-4 mRNA Expression (%)
MCF-7 H3	100
MCF-7 H3/ErbB2-A	52
MCF-7 H3/ErbB2-B	80
MCF-7 H3/ErbB2-C	53

Table 3.1.8.2 Levels of c-erbB-4 mRNA in MCF-7 H3 c-erbB-2 cDNA transfected clones.

3.1.9 Effect of C-erbB-2 Upregulation in MCF-7 H3 on the Expression of Remaining ErbB Receptors at the Protein Level

Changes in the mRNA levels of c-erbB-1 and c-erbB-4 were detected in section 3.1.8. Protein levels of c-erbB-1, c-erbB-3 and c-erbB-4 were examined to determine if these changes were reflected at the protein level.

3.1.9.1 C-erbB-1 western blot

Figure 3.1.9.1 shows that c-erbB-2 upregulation in MCF-7 H3 had no effect on c-erbB-1 protein expression, despite an increase at mRNA level (section 3.1.8.1)

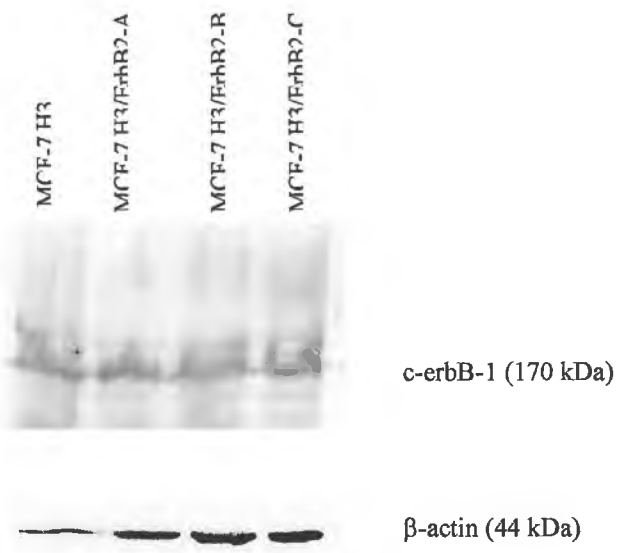

Figure 3.1.9.1a Western blot of c-erbB-1 protein in MCF-7 H3 c-erbB-2 cDNA transfected clones. A control gel was run for detection of β-actin protein, as β-actin was of too low a molecular weight to detect on ErbB gels.

3.1.9.2 C-erbB-3 immunoprecipitation

Figure 3.1.9.2 shows that c-erbB-2 upregulation in MCF-7 H3 results in an increase in c-erbB-3 protein expression, by immunoprecipitation. Immunoprecipiation was performed as levels of c-erbB-3 were too low in this cell line to be detected by western blot.

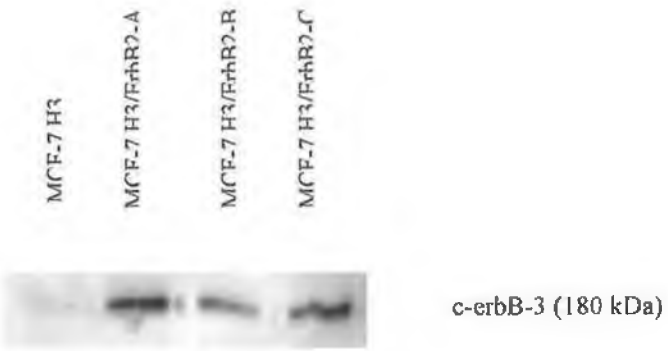

Figure 3.1.9.2 immunoprecipitation of c-erbB-3 protein in MCF-7 H3 c-erbB-2 cDNA transfected clones.

3.1.9.3 C-erbB-4

Figure 3.1.9.3 shows that c-erbB-2 upregulation in MCF-7 H3 results in a decrease in full length c-erbB-4 and intracellular domain truncated protein levels.

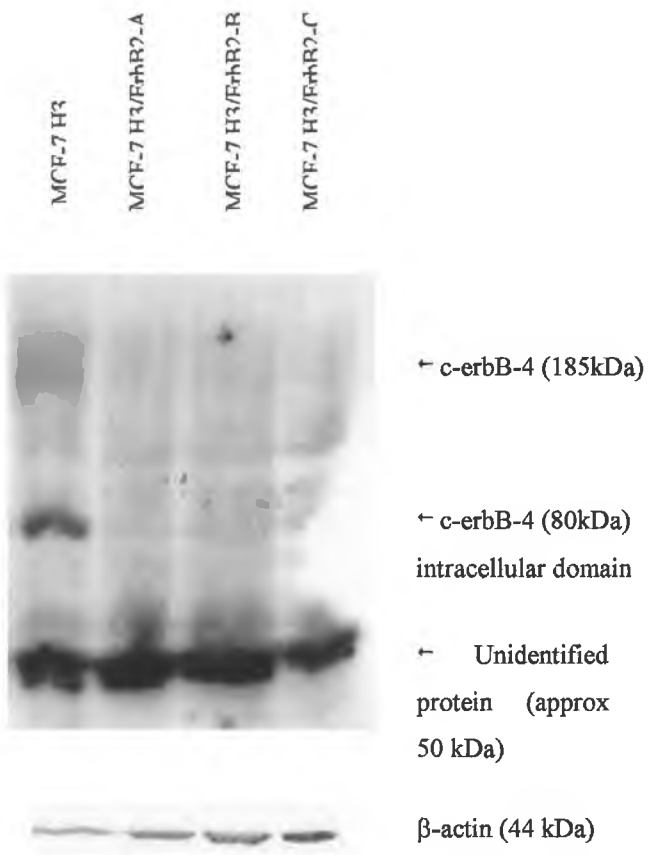

Figure 3.1.9.3a Western blot of c-erbB-4 protein in MCF-7 H3 c-erbB-2 cDNA transfected clones. A control gel was run for detection of β-actin protein, as β-actin was of too low a molecular weight to detect on ErbB gels.

3.1.9.4 Immunoprecipitation of Biotinylated Proteins by ErbB Receptors

The following figure shows biotinylated proteins immunoprecipitated by the ErbB Receptors. The protein extractions were biotinylated and then subjected to immunoprecipitation with the ErbB of interest and then probed with an anti-biotin secondary antibody. The transfectant populations show a distinct increase in the expression of other proteins co-immunoprecipitated with c-erbB-2 or c-erbB-4, suggesting an increase in protein binding to these two receptors, and thus a possible activation of signalling pathways. This also coincides with increases in tyrosine phosphorylated proteins immunoprecipitated by c-erbB-2, 3 and 4, but not 1, as shown in Figure 3.1.9.5

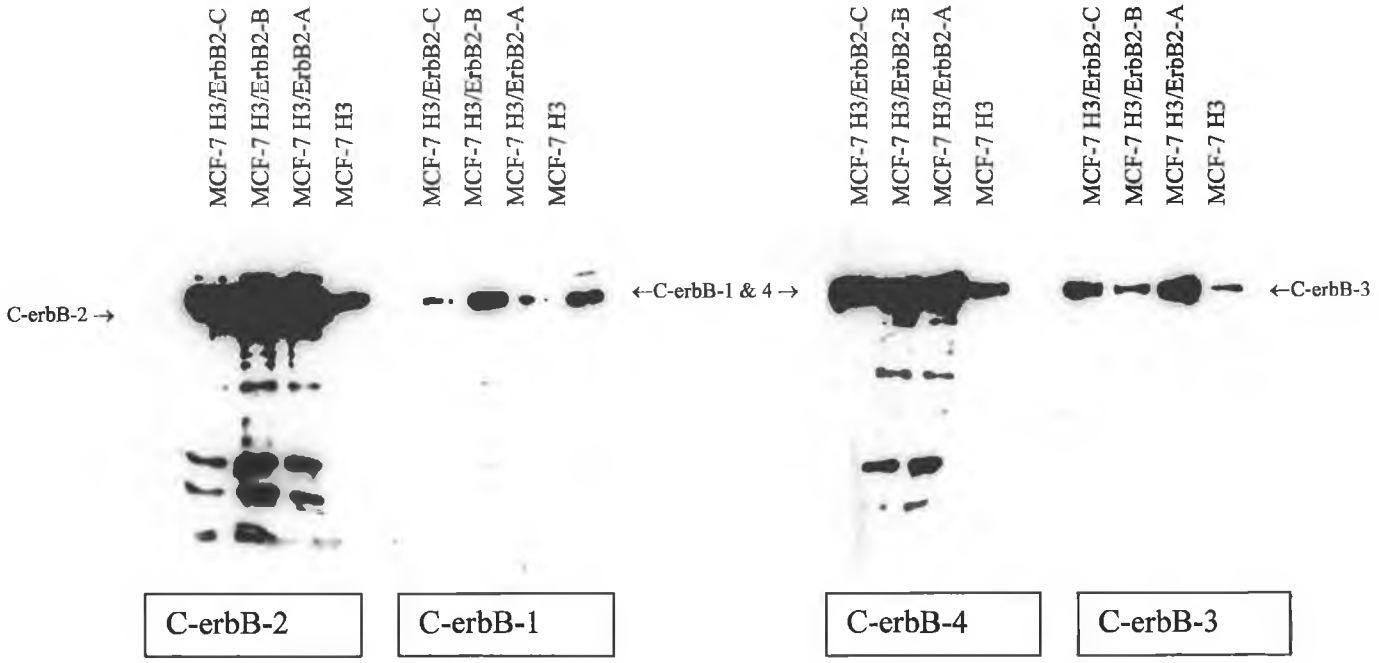

Figure 3.1.9.4 Expression of biotinylated proteins immunoprecipitated by ErbB Receptor Proteins in MCF-7 H3 and its clones A, B and C.

Cell Line	C-erbB-1	C-erbB-2	C-erbB-3	C-erbB-4
MCF-7 H3	1.00	1.00	1.00	1.00
MCF-7 H3/ErbB2-A	0.24	2.57	6.73	2.66
MCF-7 H3/ErbB2-B	1.35	2.75	1.33	2.77
MCF-7 H3/ErbB2-C	0.22	2.25	3.75	2.26

Table 3.1.9.4 Fold Increases In Expression of ErbB Proteins in MCF-7 H3 c-erbB-2 Transfectants.

3.1.9.5 Effect of C-erbB-2 Upregulation on the Phosphorylation of ErbB proteins

The following figure is the previous figure stripped and reprobed with P-tyrosine and shows phosphorylated proteins immunoprecipitated by the ErbB Receptors.

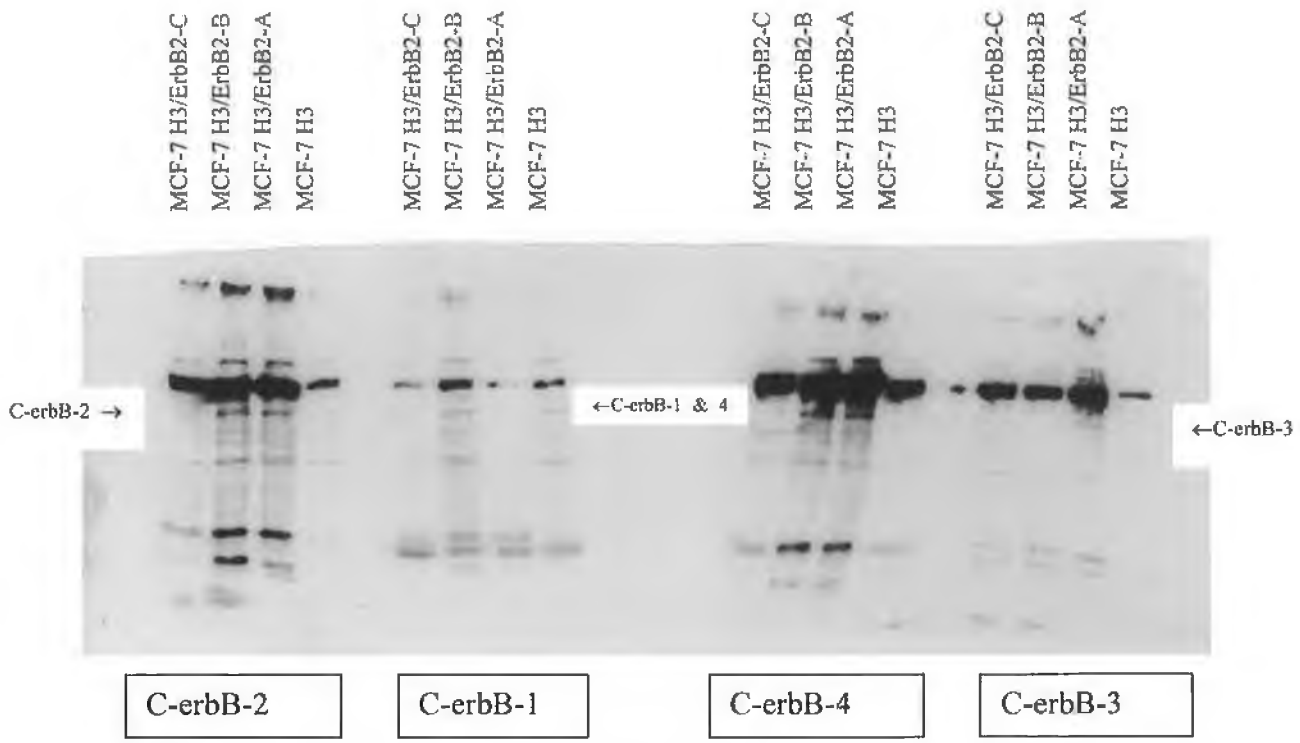

Figure 3.1.9.5 Reprobing of biotinylation blots (figure 3.1.9.4) with P-Tyr antibody post antibody stripping.

Cell Line	C-erbB-1 P-Tyr	C-erbB-2 P-Tyr	C-erbB-3 P-Tyr	C-erbB-4 P-Tyr
MCF-7 H3	1.00	1.00	1.00	1.00
MCF-7 H3/ErbB2-A	0.26	3.08	5.43	0.85
MCF-7 H3/ErbB2-B	1.67	2.78	3.69	1.08
MCF-7 H3/ErbB2-C	0.42	1.99	4.41	1.34

Table 3.1.9.5 - Fold expression of P-Tyr phosphorylation relative to MCF-7 H3

3.1.10 The Effect of C-erbB-2 Upregulation on Growth Rate of MCF-7 H3.

C-erbB-2 transfection of MCF-7 H3 resulted in increased growth rate in two of the clonal populations, MCF-7 H3/ErbB2-B and MCF-7 H3/ErbB2-C, while MCF-7 H3/ErbB2-A displayed a slower growth rate than MCF-7 H3.

Cell Line	Doubling Time (hours)
MCF-7 H3	51
MCF-7 H3/ErbB2-A	55
MCF-7 H3/ErbB2-B	45
MCF-7 H3/ErbB2-C	44

Table 3.1.10 Doubling Times of MCF-7 H3 and it C-erbB-2 Transfected Clones

3.1.11 The Effect of C-erbB-2 Upregulation on Motility of MCF-7 H3

Motility assays were performed as described in section 2.15 to investigate the effects of c-erbB-2 upregulation on the motility of MCF-7 H3. Surprisingly, neither the parental cell line nor the clonal populations were motile in this system. A sample photo of the parental cell line, figure 3.1.11a shows that the membrane contained few or no cells after 48 hours incubation. The clonal populations displayed identical results. The Postive (RPMI 2650- Melphalan) and negative (RPMI 2650) controls Figure 3.1.11b and 3.1.11c show that this assay was operational (RPMI 2650 displays little or no motility, while it Melphalan resistant variants displays high motility (Liang *et al.*, 2001)).

Figure 3.1.11 Motility assay for MCF-7 H3

Figure 3.1.11b RPMI

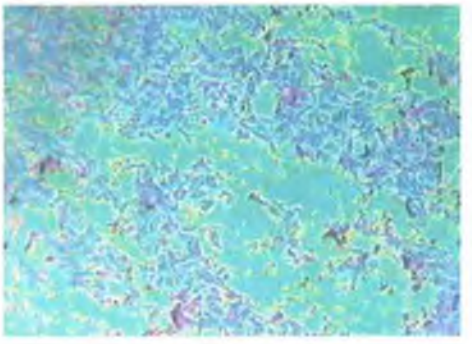

Figure 3.1.11c RPMI Melphalan

3.1.12 The Effect of C-erbB-2 Upregulation on Invasion of Matrigel by MCF-7 H3

Invasion assays were performed as described in section 2.14 to investigate the effects of c-erbB-2 upregulation on the invasiveness of MCF-7 H3. Two of the clonal populations, MCF-7 H3/ErbB2-B and MCF-7 H3/ErbB2-C were found to be more invasive than the parental cell line, MCF-7 H3. Surprisingly MCF-7 H3/ErbB2-A was actually less invasive than MCF-7 H3. Figures 3.1.12.1 to 3.1.12.4 are representative of 3 repeats.

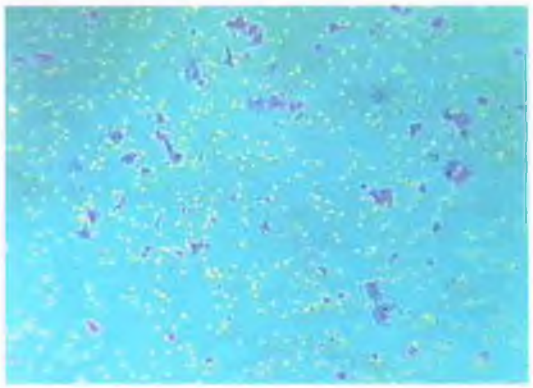

Figure 3.1.12a MCF-7 H3

Figure 3.1.12b MCF-7 H3/ErbB2-A

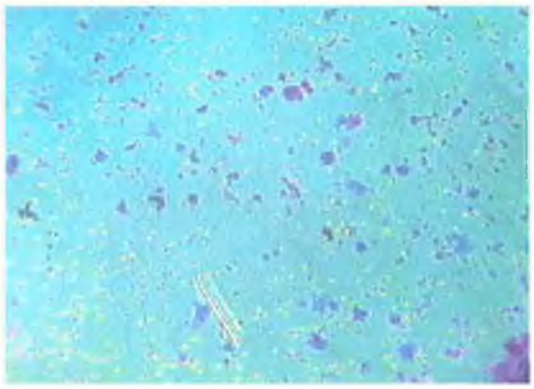

Figure 3.1.12c MCF-7 H3/ErbB2-B

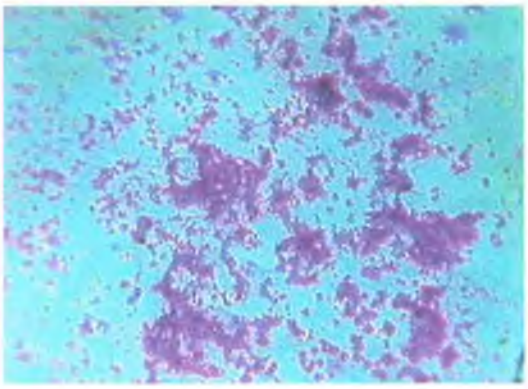

Figure 3.1.12d MCF-7 H3/ErbB2-C

3.1.13 The Effect of C-erbB-2 Upregulation on Adhesive Properties of MCF-7 H3 to Components of the Extracellular Matrix

Cells use various adhesion molecules such as integrins to interact with extracellular matrix components such as collagen type IV, laminin and fibronectin. To detect changes in the adhesive properties of MCF-7 H3 due to upregulation of c-erbB-2, adhesion assay were performed as described in section 2.13.

Figure 3.1.13.1 shows the levels of adhesion of MCF-7 H3 and its c-erbB-2 transfected clones to laminin after 1 hour. The clonal populations MCF-7 H3/ErbB2-A and MCF-7 H3/ErbB2-B show increased adhesion to laminin compared to their parental cell line. MCF-7 H3/ErbB2-C on the other hand displays decreased adhesion to laminin.

Figure 3.1.13.2 shows the levels of adhesion of MCF-7 H3 and its c-erbB-2 transfected clones to collagen type IV after 1 hour. The clonal populations MCF-7 H3/ErbB2-A and MCF-7 H3/ErbB2-B show increased adhesion to collagen type IV compared to their parental cell line. MCF-7 H3/ErbB2-C on the other hand displays decreased adhesion to collagen type IV. This profile is similar to that seen for laminin in section 3.1.13.1.

Figure 3.1.13.3 shows the levels of adhesion of MCF-7 H3 and its c-erbB-2 transfected clones to fibronectin after 1 hour. All three clonal populations, MCF-7 H3/ErbB2-A, MCF-7 H3/ErbB2-B and MCF-7 H3/ErbB2-C show decreased adhesion to fibronectin compared to their parental cell line.

Figure 3.1.13.4 shows the levels of adhesion of MCF-7 H3 and its c-erbB-2 transfected clones to matrigel after 1 hour. Only the clonal populations MCF-7 H3/ErbB2-C show any major change in adhesiveness to matrigel (reduction in adhesion).

3.1.13.1 Adhesion to Laminin.

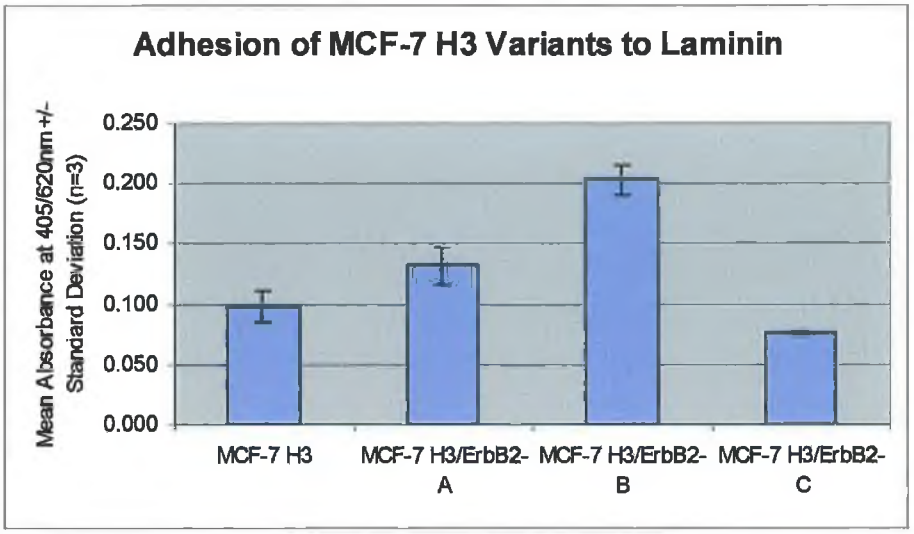

Figure 3.1.13.1 Levels of adhesion of MCF-7 H3 and c-erbB-2 transfected clones to laminin.

Cell Line	Fold Changes in Cells Attached to Laminin After 1 hour
MCF-7 H3	1.00
MCF-7 H3/ErbB2-A	1.35
MCF-7 H3/ErbB2-B	2.07
MCF-7 H3/ErbB2-C	0.77

Table 3.1.13.1 Fold changes in adhesion to laminin relative to the parental cell line MCF-7 H3.

3.1.13.2 Adhesion to Collagen Type IV

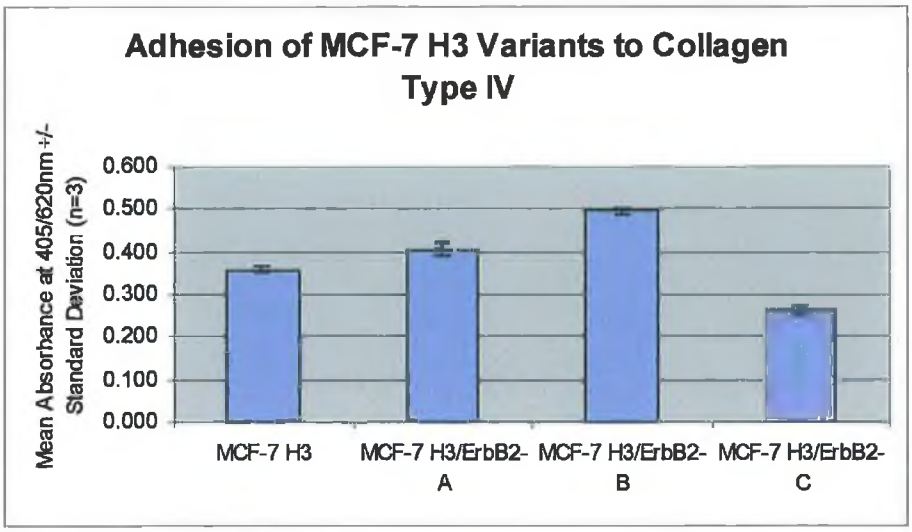

Figure 3.1.13.2 Levels of adhesion of MCF-7 H3 and c-erbB-2 transfected clones to collagen type IV.

Cell Line	Fold Changes in Cells Attached to Collagen Type IV After 1 hour
MCF-7 H3	1.00
MCF-7 H3/ErbB2-A	1.13
MCF-7 H3/ErbB2-B	1.39
MCF-7 H3/ErbB2-C	0.74

Table 3.1.13.2 Fold changes in adhesion to collagen type IV relative to the parental cell line MCF-7 H3.

3.1.13.3 Adhesion to Fibronectin

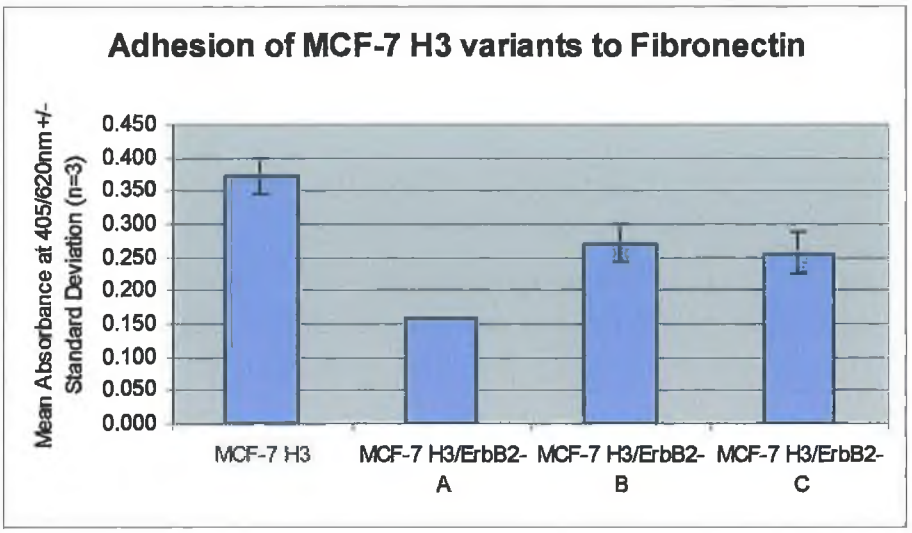

Figure 3.1.13.3 Levels of adhesion of MCF-7 H3 and c-erbB-2 transfected clones to fibronectin.

Cell Line	Fold Changes in Cells Attached to Fibronectin After 1 hour
MCF-7 H3	1.00
MCF-7 H3/ErbB2-A	0.43
MCF-7 H3/ErbB2-B	0.73
MCF-7 H3/ErbB2-C	0.69

Table 3.1.13.3 Fold changes in adhesion to fibronectin relative to the parental cell line MCF-7 H3.

3.1.13.4 Adhesion to Matrigel

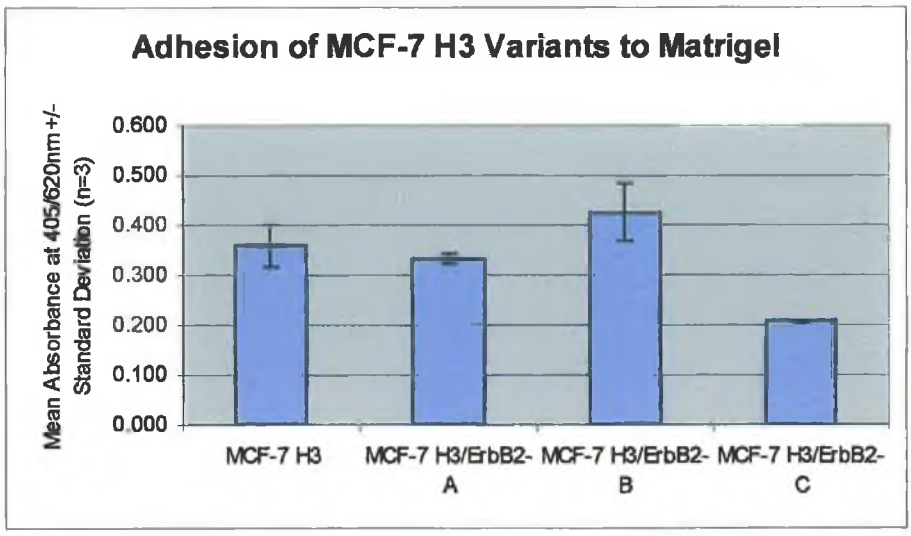

Figure 3.1.13.4 Levels of adhesion of MCF-7 H3 and c-erbB-2 transfected clones to matrigel.

Cell Line	**Fold Changes in Cells Attached to Matrigel After 1 hour**
MCF-7 H3	1.00
MCF-7 H3/ErbB2-A	0.92
MCF-7 H3/ErbB2-B	1.18
MCF-7 H3/ErbB2-C	0.58

Table 3.1.13.4 Fold changes in adhesion to matrigel relative to the parental cell line MCF-7 H3.

3.1.13.5 Summary of Adhesion results

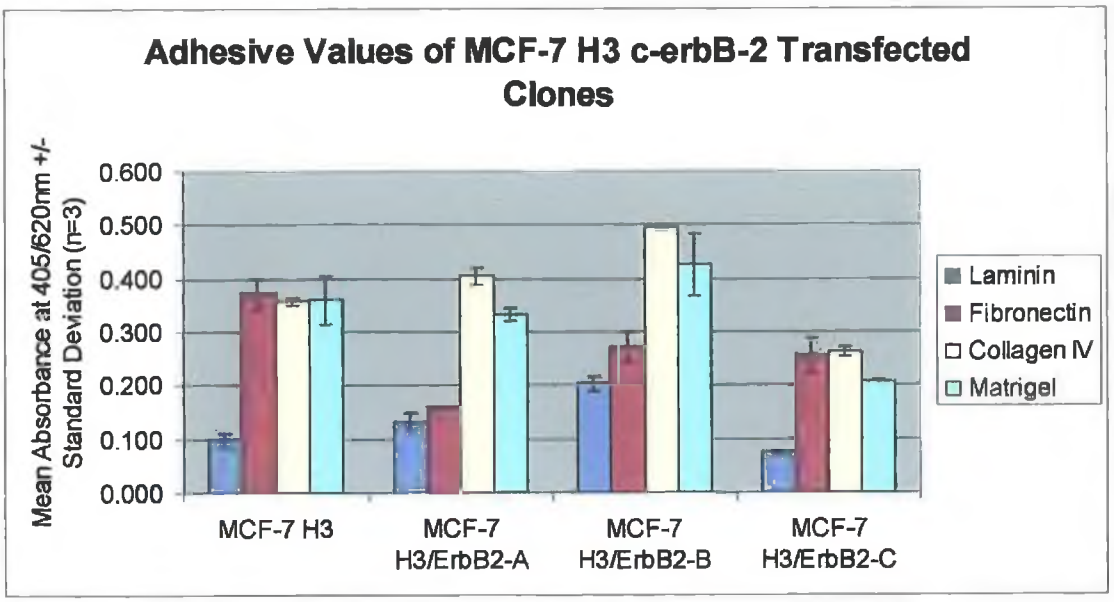

Figure 3.1.13.5 Adhesion of MCF-7 H3 c-erbB-2 transfectants to ECM proteins.

	Laminin	Fibronectin	Collagen Type IV	Matrigel
MCF-7 H3	1.00	1.00	1.00	1.00
MCF-7 H3/ErbB2-A	1.35	0.43	1.13	0.92
MCF-7 H3/ErbB2-B	2.07	0.73	1.39	1.18
MCF-7 H3/ErbB2-C	0.77	0.69	0.74	0.58

Table 3.1.13.5 Fold decrease in adhesion of MCF-7 H3 c-erbB-2 transfected variants to ECM proteins relative to parental cell lines MCF-7 H3.

3.1.14 The Effect of C-erbB-2 Upregulation on Secretion of Proteases by MCF-7 H3

Matrix metalloproteinases (MMPs), cysteine proteases and serine protease, which are secreted by cells, play an important role in degrading the extracellular matrix. To further investigate the mechanisms by which c-erbB-2 exerts an influence of the invasiveness of MCF-7 H3, zymography was performed to detect the secretion of proteases in these cells, as described in section 2.16.

3.1.14.1 Detection of the Expression of Proteases Secreted by MCF-7 H3 and its C-erbB-2 cDNA Transfected Variants

The BHK (baby hamster kidney) cell line, was used as a positive control for the secretion of pro-MMP2 (72 kDa), MMP-2 (66kDa), pro-MMP-9 (92kDa) and MMP9 (86kDa). The MCF-7 H3 parent cell line and its c-erbB-2 cDNA transfected variants display secretion bands corresponding to pro-MMP-2, pro-MMP-9 and MMP-9. There are also many additional bands expressed by MCF-7 H3 and MCF-7 H3/ErbB2-A, which are absent in MCF-7 H3/ErbB2-B and MCF-7 H3/ErbB2-C. These additional bands are stronger in MCF-7 H3/ErbB2-A than in the parental cell line MCF-7 H3. It is also worth noting that MCF-7 H3/ErbB2-A is not invasive while MCF-7 H3 is slightly invasive and both MCF-7 H3/ErbB2-B and MCF-7 H3/ErbB2-C are much more invasive.

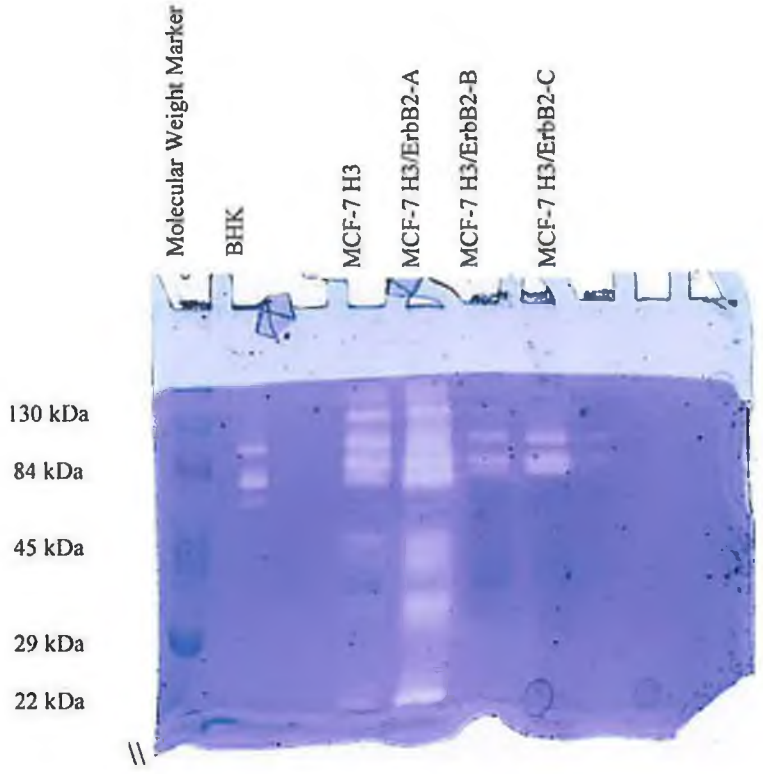

Figure 3.1.14.1 Zymogram of gelatin proteases secreted by MCF-7 H3

3.1.14.2 Identification of the Classes of Proteases Secreted by MCF-7 H3 and its C-erbB-2 cDNA Transfected Variants

To investigate the identity of the gelatin degrading proteases secreted by MCF-7 H3 and its c-erbB-2 transfected variants, protease inhibitors were used.

3.1.14.2.1 The effect of EDTA and PMSF on Protease activity

EDTA is a chelating agent, which can bind zinc and calcium ions, which are needed for the activation of MMPs. PMSF is a serine and cysteine protease inhibitor.

Figure 3.1.14.2.1b shows that the addition of EDTA to the substrate buffer eliminates expression of all protease bands in BHK, and the majority of those in MCF-7 H3/ErbB2-B and MCF-7 H3/ErbB2-C, indicating the gelatin degrading proteases secreted these cell lines are members of the matrix metalloproteinase family. There are still bands present in MCF-7 H3 and MCF-7 H3/ErbB2-A, which are therefore not matrix metalloproteinases.

Figure 3.1.14.2.1b also shows the effects of addition of PMSF to the substrate buffer, which suppresses slightly the expression of protease bands in the BHKs, but does not eliminate them, and has no effect on any of the bands from the four other cell lines, suggesting the proteases are not serine or cysteine proteases.

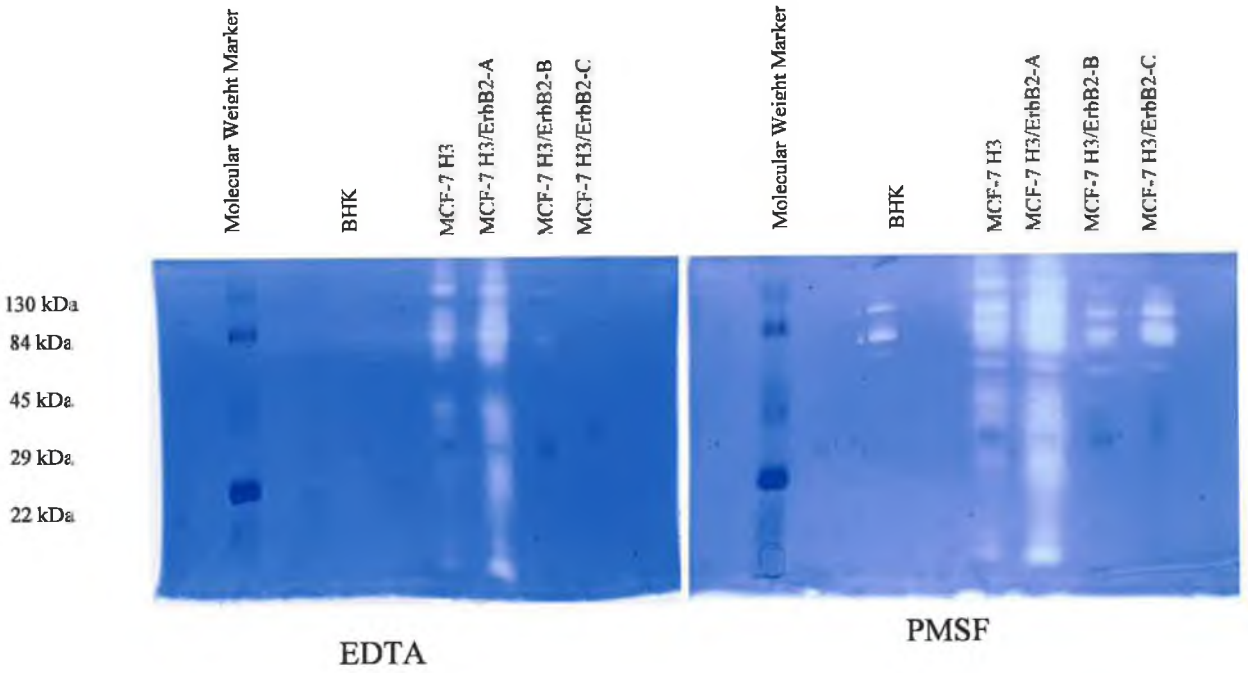

Figure 3.1.14.2.1b Effect of EDTA and PMSF on Protease Activity

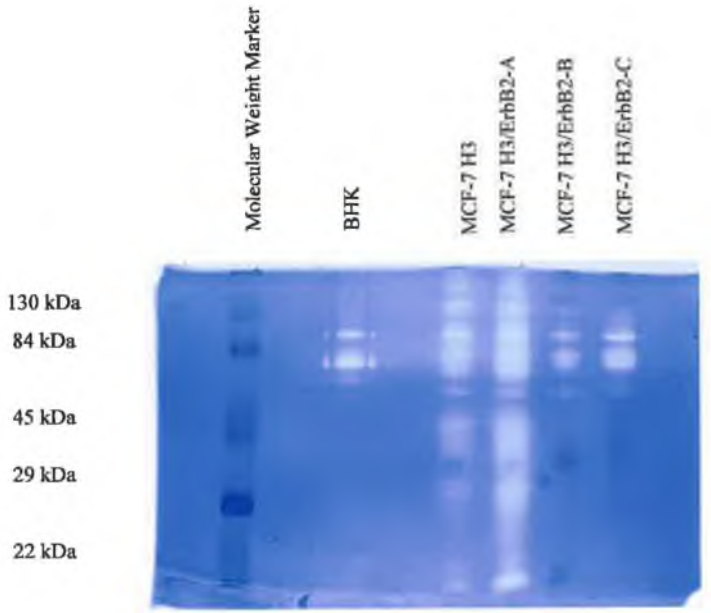

Figure 3.1.14.2.1a Protease secretion by MCF-7 H3 and its Variants

3.1.14.2.2 The effect of L-Cysteine

Cysteine keeps cysteine proteases in their reduced form, thus making them more active. If the extra bands in MCF-7 H3 and MCF-7 H3/ErbB2-A are cysteine proteases then their bands should appear stronger. Figure 3.3.14.2.2b showed that addition of cysteine to the substrate buffer did not enhance any of the bands in MCF-7 H3 or MCF-7 H3/ErbB2-A indicating that these bands are not cysteine proteases. Surprisingly it eliminates the expression of all bands secreted by BHK, MCF-7 H3/ErbB2-B and MCF-7 H3/ErbB2-C. It also eliminates the expression of bands of lower molecular weight in MCF-7 H3 and MCF-7 H3/ErbB2-A. This was repeated twice.

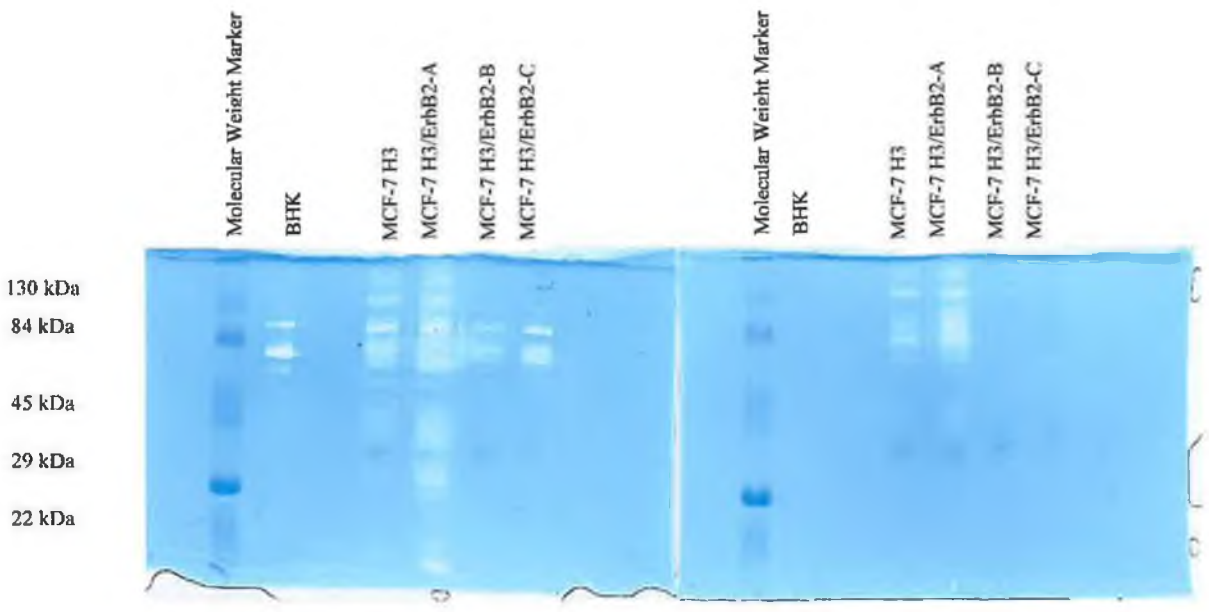

Figure 3.1.14.2.2b Effect of cysteine on Protease secretion. Figure 3.1.14.2.2a Protease secretion by MCF-7 H3 and its Variants

3.1.14.3 Investigation of the Findings of the Effects of the Addition of Cysteine on the Proteases Secreted by MCF-7 H3 and its C-erbB-2 cDNA Transfected Variants

Previously it was determined that the extra bands detected in MCF-7 H3 and MCF-7 H3/ErbB2-A were not MMPs, cysteine proteases or serine proteases. Also cysteine had the surprise effect of inhibiting various bands secreted by MCF-7 H3 and MCF-7 H3/ErbB2-A, and also MMP bands. Cysteine is also a reducing agent, and it was possible that it was having a reducing affect on the proteases secreted. To further clarify this, DTT was chosen, as it is also a reducing agent, to see if this effect could be mimicked. Leupeptin another serine and cysteine protease inhibitor was also chosen as PMSF has a short half life and it was possible that it was being inactivated before it could act on the bands.

Figure 3.1.14.3b demonstrated that the addition DTT to the substrate buffer had the same effect as cysteine. This shows that reducing agents have an inhibitory effect on the activity of MMPs and also on the unidentified bands.

Addition of PMSF previously had little effect of the band activity in these cell lines other than suppressing slightly the activity of the MMPs in the BHKs. Another serine and cysteine protease inhibitor, Leupeptin, was used to see whether these definitely were not either of these types of proteases. Leupeptin is a serine and cysteine protease inhibitor. It inhibits plasmin, trypsin, papain and cathepsin B. It has no effect on pepsin, cathepsin A or cathepsin D. Figure 3.1.14.3c shows that leupeptin suppressed/eliminated the majority of bands secreted by the 5 cell lines, including BHK secreted MMP-2 and MMP-9. It has not inhibited the MMPs in the MCF-7 H3 variants however.

These results suggest that the extra bands secreted by MCF-7 H3 and MCF-7 H3/ErbB2-A are serine proteases as they are not enhanced by cysteine.

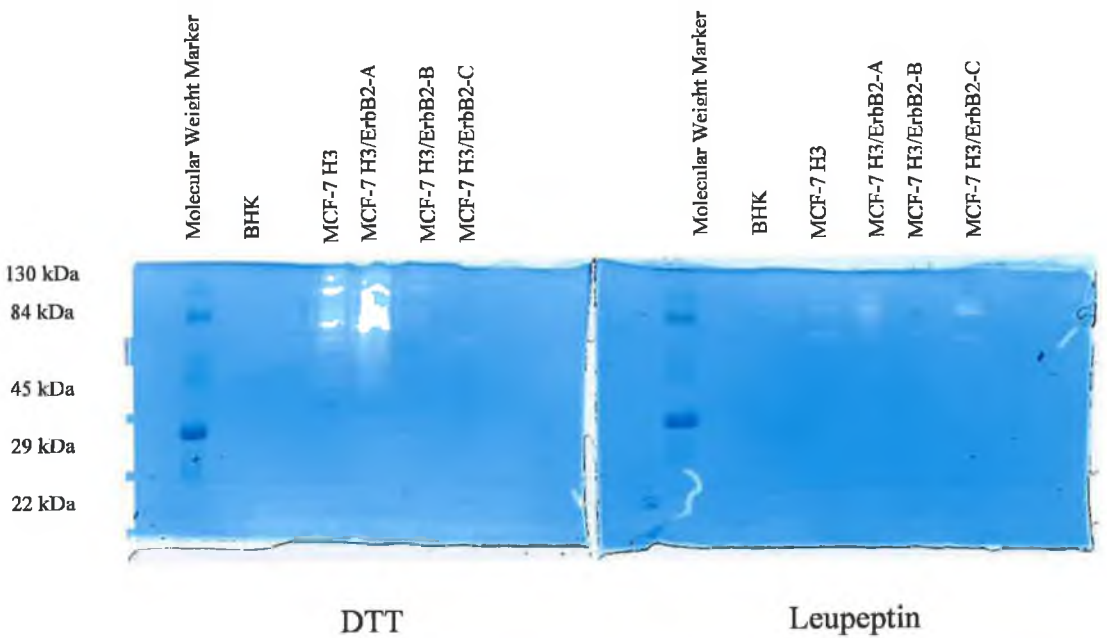

Figure 3.1.14.3b Effect of DTT and Leupeptin on Protease Activity

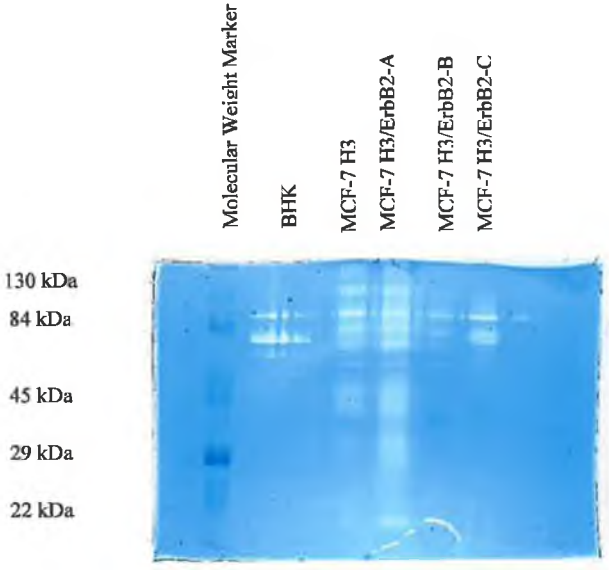

Figure 3.1.14.3a Protease secretion by MCF-7 H3 and its Variants

3.2 The Effect of Downregulation of C-erbB-2 in the Human Breast Cancer Cell BT474A on Resistance to Chemotherapy, Tamoxifen Hormonal Therapy, Invasiveness and Expression Patterns of the ErbB Receptor Family and a Panel of Drug Resistance Asssociated Genes.

As mentioned in section 3.1, the first objective of this thesis was to establish a breast cancer cell model for the investigation of the effects of c-erbB-2 expression on resistance to chemotherapeutic drugs and tamoxifen hormonal therapy. Two breast cancer cell lines were chosen, BT474A and MCF-7 H3. BT474A was transfected with a c-erbB-2 targeting ribozyme to down regulate expression of c-erbB-2, the results of which are presented in section 3.2.

3.2.1 Establishment of BT474A transfected with c-erbB-2 Ribozyme.

BT474A was transfected with a hammerhead ribozyme targeting c-erbB-2 (section 2.18.4), a generous gift from Dr. Kevin Scanlon. The transfected cell line was then selected with G418 (section 2.18.5). Attempts to isolate clones in 96-well plates by dilution cloning failed for this cell line, most likely due to their dislike of low cell density. 6-well plates were seeded with 5ml of a 20 cells/ml solution, and allowed to form colonies. Colonies were then upscaled to 12.5 cm^2 hybridoma flasks using cloning rings. Four clones were isolated, designated BT474A/ErbB2-Rz1, BT474A/ErbB2-Rz3, BT474A/ ErbB2-Rz4 and BT474A/ ErbB2-Rz5.

3.2.2 Effect of C-erbB-2 Downregulation on the Cell Morphology of BT474A

Transfection of BT474A with a c-erbB-2-targeted ribozyme had no effect on the morphology of BT474A/ErbB2-Rz pool, BT474A/ErbB2-Rz3 or BT474A/ErbB2-Rz5. BT474A/ErbB2 Rz1 and BT474A/ErbB2 Rz4 cell morphology appeared to be more spread out than the parental cell line BT474A.

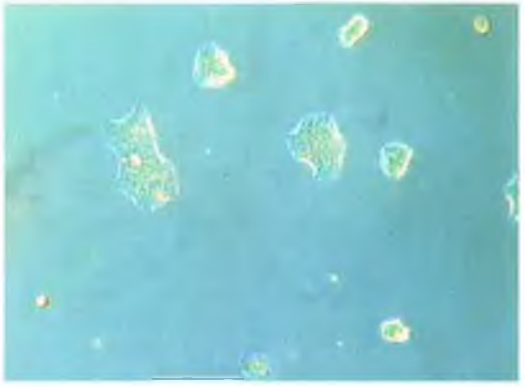

Figure 3.2.2a BT474A

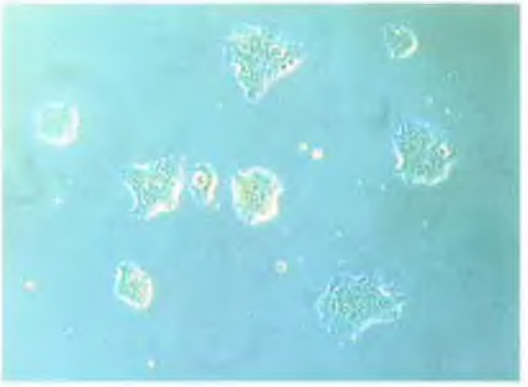

Figure 3.2.2b BT474A/ErbB2-Rz pool

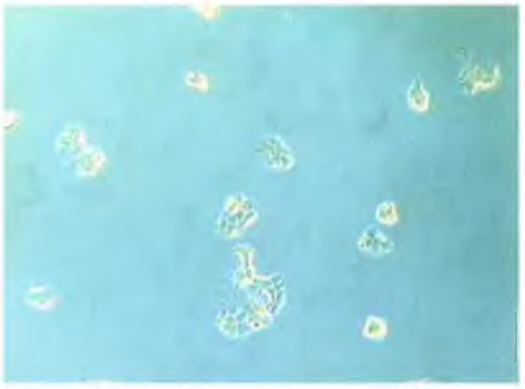

Figure 3.2.2c BT474A/ErbB2-Rz1

Figure 3.2.2d BT474A/ErbB2-Rz3

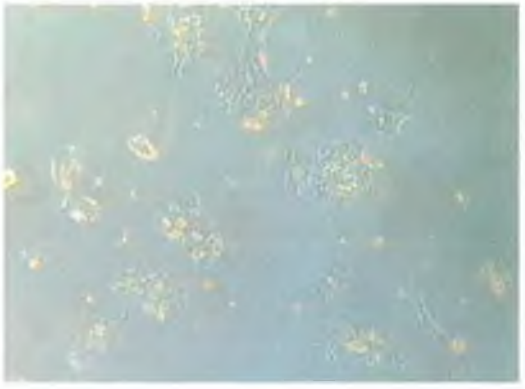

Figure 3.2.2e BT474A/ErbB2-Rz4

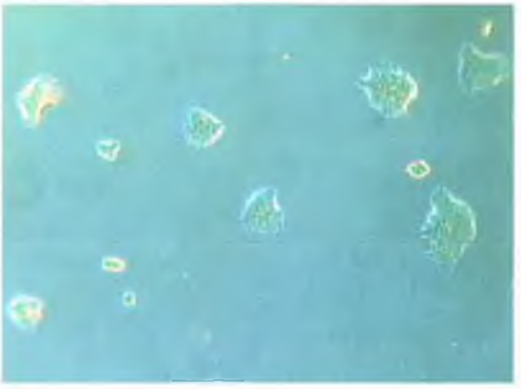

Figure 3.2.2f BT474A/ErbB2-Rz5

3.2.3 Detection of c-erbB-2 Downregulation by C-erbB-2 Targeting Ribozyme Transfection

The effect of the c-erbB-2 targeting ribozyme on the expression of c-erbB-2 in BT474A was examined at the mRNA and protein level. Figure 3.2.3.1 shows that c-erbB-2 mRNA levels were reduced in the clonal populations BT474A/ErbB2-Rz3, BT474A/ErbB2-Rz4 and BT474A/ErbB2-Rz5. A reduction was not seen in the pooled population or in BT474A/ErbB2-Rz1. It should be noted that while this PCR was performed at 25 cycles, the c-erbB-2 bands were still becoming saturated, and the β-actin bands were faint as a result of primer competition. It is therefore possible that no reduction in c-erbB-2 was seen in the pooled population or in BT474A/ErbB2-Rz1 because of c-erbB-2 saturation. Figures 3.2.3.2a and 3.2.3.2b show the level of c-erbB-2 protein expression by western blotting. All the clonal ribozyme transfectant populations displayed decreased c-erbB-2 expression when β-actin was taken into account. The pooled population did not show a decrease in c-erbB-2 in this western blot. Figure 3.2.3.2b also includes the mutant ribozyme contol transfectant pooled population. While the blot is somewhat saturated, it clearly shows that c-erbB-2 levels are unchanged in the contol.

3.2.3.1 Detection of Levels of C-erbB-2 mRNA

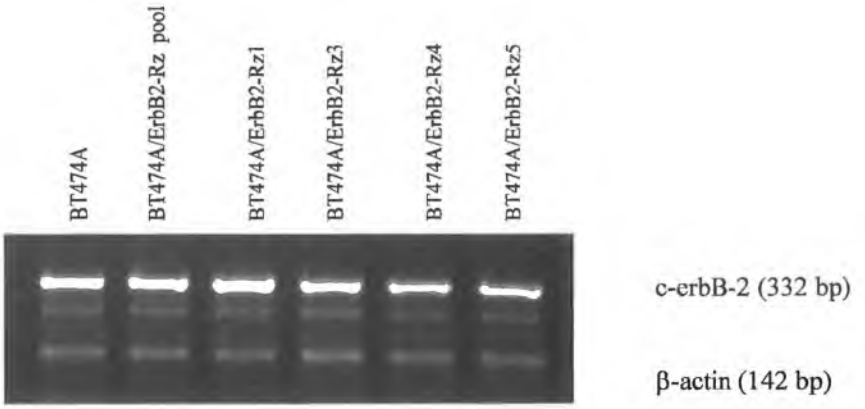

Figure 3.2.3.1 Levels of c-erbB-2 expression in BT474A c-erbB-2 ribozyme transfected pool and clonal populations.

Cell Line	Levels of C-erbB-2 mRNA Expression (%)
BT474A	100.0
BT474A/ErbB2-Rz pool	100
BT474A/ErbB2-Rz1	123
BT474A/ErbB2-Rz3	71
BT474A/ErbB2-Rz4	68
BT474A/ErbB2-Rz5	77

Table 3.2.3.1 Levels of c-erbB-2 expression.

3.2.4 Effect of c-erbB-2 Downregulation in BT474A on Chemotherapeutic Drug Resistance

The effect of c-erbB-2 expression on the chemotherapeutic drug resistance of BT474A was examined. A panel of chemotherapeutic agents was chosen, including adriamycin, taxol, carboplatin, taxotere, 5-fluorouracil, and methotrexate. As with the MCF-7 H3 c-erbB-2 transfection, as reported in section 3.1.4, two methods of toxicity testing were used, entitled long-term and short-term as described in sections 2.7.1 and 2.7.2. The purpose of this was to compare the effect of c-erbB-2 on the sensitivity of BT474A to longer drug exposure at lower levels versus shorter exposure at higher levels. An additional purpose of this section was to see if the opposite of what happened in MCF-7 H3, would happen in BT474A.

3.2.4.1 Effect of c-erbB-2 Downregulation on Adriamycin Resistance

Long term toxicity assays for adriamycin showed that all four clonal populations and the pool population decreased resistance to adriamycin in long term assays. In contrast, all four clonal populations and the pool population displayed increased resistance to adriamycin in short term assays.

3.2.4.1.1 Long Term Adriamycin IC_{50} Toxicity assay

Cell Line	IC_{50} Adriamycin (ng/ml; n=3)
BT474A	40.3 +/- 4.04 *
BT474A/ErbB2-Rz pool	16.1 +/- 1.41
BT474A/ErbB2-Rz1	13.8 +/- 0.11
BT474A/ErbB2-Rz3	11.0 +/- 0.76
BT474A/ErbB2-Rz4	17.3 +/- 0.28
BT474A/ErbB2-Rz5	14.3 +/- 0.75

* +/- standard deviation

Table 3.2.4.1.1a Results of long term toxicity assays

Cell Line	Fold Change in Resistance	Significance – Paired Student t-Test
BT474A	1.00	p =
BT474A/ErbB2-Rz pool	0.40	0.0167
BT474A/ErbB2-Rz1	0.34	0.0079
BT474A/ErbB2-Rz3	0.27	0.0047
BT474A/ErbB2-Rz4	0.43	0.0094
BT474A/ErbB2-Rz5	0.35	0.0053

Table 3.2.4.1.1b Fold resistance to adriamycin in long term assays and significance of change.

3.2.4.1.2 Short Term Adriamycin IC_{50} Toxicity assay

Cell Line	IC_{50} Adriamycin (ng/ml; n=3)
BT474A	104 +/- 4.58
BT474A/ErbB2-Rz pool	212 +/- 15.94
BT474A/ErbB2-Rz1	156 +/- 15.27
BT474A/ErbB2-Rz3	179 +/- 13.79
BT474A/ErbB2-Rz4	276 +/- 25.10
BT474A/ErbB2-Rz5	225 +/- 21 (n=2)

Table 3.2.4.1.2a Results of short term toxicity assays

Cell Line	Fold Change in Resistance	Significance – Paired Student t-Test
BT474A	1.00	p =
BT474A/ErbB2-Rz pool	2.03	0.0113
BT474A/ErbB2-Rz1	1.50	0.0442
BT474A/ErbB2-Rz3	1.72	0.0190
BT474A/ErbB2-Rz4	2.65	0.0061
BT474A/ErbB2-Rz5	2.16	0.0681

Table 3.2.4.1.2b Fold resistance to adriamycin in short term assays and significance of change.

3.2.4.2 Effect of c-erbB-2 Downregulation on Taxol Resistance

C-erbB-2 ribozyme transfection of BT474A resulted in an increase in resistance to taxol in both long and short term assays. Only BT474A/ErbB2-Rz1 failed to show any increase in resistance in short term assays.

3.2.4.2.1 Long Term Taxol IC_{50} Toxicity assay

Cell Line	IC_{50} Taxol (ng/ml; n=3)
BT474A	1.86 +/- 0.05
BT474A/ErbB2-Rz pool	4.16 +/- 0.20
BT474A/ErbB2-Rz1	4.13 +/- 0.05
BT474A/ErbB2-Rz3	8.8 +/- 0.70
BT474A/ErbB2-Rz4	5.93 +/- 0.32
BT474A/ErbB2-Rz5	7.10 +/- 0.7

Table 3.2.4.2.1a Results of long term toxicity assays

Cell Line	Fold Change in Resistance	Significance – Paired Student t-Test
BT474A	1.00	p =
BT474A/ErbB2-Rz pool	2.24	0.0014
BT474A/ErbB2-Rz1	2.22	0.0000
BT474A/ErbB2-Rz3	4.73	0.0009
BT474A/ErbB2-Rz4	3.19	0.0013
BT474A/ErbB2-Rz5	3.82	0.0058

Table 3.2.4.2.1b Fold resistance to taxol in long term assays and significance of change.

3.2.4.2.2 Short Term Taxol IC_{50} Toxicity assay

Cell Line	IC_{50} Taxol (ng/ml; n=3)
BT474A	15.6 +/- 1.15
BT474A/ErbB2-Rz pool	21.2 +/- 3.21
BT474A/ErbB2-Rz1	14.6 +/- 0.57
BT474A/ErbB2-Rz3	24.3 +/- 2.30
BT474A/ErbB2-Rz4	58.6 +/- 1.52
BT474A/ErbB2-Rz5	35.3 +/- 1.15

Table 3.2.4.2.2a Results of short term toxicity assays

Cell Line	Fold Change in Resistance	Significance – Paired Student t-Test
BT474A	1.00	p =
BT474A/ErbB2-Rz pool	1.35	0.0421
BT474A/ErbB2-Rz1	0.93	0.4226
BT474A/ErbB2-Rz3	1.55	0.0058
BT474A/ErbB2-Rz4	3.75	0.0001
BT474A/ErbB2-Rz5	2.26	0.0045

Table 3.2.4.2.2b Fold resistance to taxol in short term assays and significance of change.

3.2.4.3 Effect of c-erbB-2 Downregulation on Carboplatin Resistance

Long term toxicity assays for carboplatin showed that only BT474A/ErbB2-Rz pool and BT474A/ErbB2-Rz3 had any statistically significant increased sensitivity to carboplatin (figure 3.2.4.3.1a). None of the other clonal populations displayed increased sensitivity in comparison to their parental cell line. In contrast, all four clonal populations and the pool population displayed increased resistance to carboplatin in short term assays, as shown in figure 3.2.4.3.2a.

3.2.4.3.1 Long Term Carboplatin IC_{50} Toxicity assay

Cell Line	**IC_{50} Carboplatin (μg/ml; n=3)**
BT474A	2.43+/- 0.20
BT474A/ErbB2-Rz pool	1.38 +/- 0.10
BT474A/ErbB2-Rz1	2.20 +/- 0.05
BT474A/ErbB2-Rz3	1.93 +/- 0.35
BT474A/ErbB2-Rz4	2.13 +/- 0.25
BT474A/ErbB2-Rz5	2.53 +/- 0.15

Table 3.2.4.3.1a Results of long term toxicity assays

Cell Line	**Fold Change in Resistance**	**Significance – Paired Student t-Test**
BT474A	1.00	**p =**
BT474A/ErbB2-Rz pool	0.56	0.0268
BT474A/ErbB2-Rz1	0.90	0.1283
BT474A/ErbB2-Rz3	0.79	0.0377
BT474A/ErbB2-Rz4	0.87	0.1884
BT474A/ErbB2-Rz5	1.04	0.5779

Table 3.2.4.3.1b Fold resistance to carboplatin in long term assays and significance of change.

3.2.4.3.2 Short Term Carboplatin IC_{50} Toxicity assay

Cell Line	IC_{50} Carboplatin (μg/ml; n=3)
BT474A	33.0 +/- 3.00
BT474A/ErbB2-Rz pool	78 +/- 4.35
BT474A/ErbB2-Rz1	34.6 +/- 0.57
BT474A/ErbB2-Rz3	58.3 +/- 3.51
BT474A/ErbB2-Rz4	80.0 +/- 5.03
BT474A/ErbB2-Rz5	70 +/- 6.24

Table 3.2.4.3.2a Results of short term toxicity assays

Cell Line	Fold Change in Resistance	Significance – Paired Student t-Test
BT474A	1.00	p =
BT474A/ErbB2-Rz pool	2.36	0.0050
BT474A/ErbB2-Rz1	1.05	0.4444
BT474A/ErbB2-Rz3	1.77	0.0212
BT474A/ErbB2-Rz4	2.42	0.0075
BT474A/ErbB2-Rz5	2.12	0.0175

Table 3.2.4.3.2b Fold resistance to carboplatin in short term assays and significance of change.

3.2.4.4 Effect of c-erbB-2 Downregulation on 5-Fluorouracil Resistance

Long term toxicity assays for 5-fluorouracil showed that BT474A/ErbB2-Rz pool, BT474A/ErbB2-Rz1 and BT474A/ErbB2-Rz3 were more resistant to 5-fluororacil in long term toxicity assays. In short term toxicity assays for 5-fluorouracil, while BT474A/ErbB2-Rz pool and BT474A/ErbB2-Rz1 were less resistant to 5-fluorouracil, BT474A/ErbB2-Rz3 and BT474A/ErbB2-Rz4 were more resistant. BT474A/ErbB2-Rz5 was sensitised to 5-FU in short term assays.

3.2.4.4.1 Long Term 5-FU IC_{50} Toxicity assay

Cell Line	**IC_{50} 5-Fluorouracil (μg/ml; n=3)**
BT474A	0.091+/- 0.012
BT474A/ErbB2-Rz pool	0.123 +/- 0.005
BT474A/ErbB2-Rz1	0.196 +/- 0.020
BT474A/ErbB2-Rz3	0.366 +/- 0.007
BT474A/ErbB2-Rz4	0.108 +/- 0.005
BT474A/ErbB2-Rz5	0.091 +/- 0.007

Table 3.2.4.4.1a Results of long term toxicity assays

Cell Line	**Fold Change in Resistance**	**Significance – Paired Student t-Test**
BT474A	1.00	**p =**
BT474A/ErbB2-Rz pool	1.35	0.0188
BT474A/ErbB2-Rz1	2.15	0.0052
BT474A/ErbB2-Rz3	4.02	0.0001
BT474A/ErbB2-Rz4	1.19	0.0634
BT474A/ErbB2-Rz5	1.00	1.0000

Table 3.2.4.4.1b Fold resistance to 5-fluorouracil in long term assays and significance of change.

3.2.4.4.2 Short Term 5-FU IC_{50} Toxicity assay

Cell Line	IC_{50} 5-Fluorouracil (μg/ml; n=3)
BT474A	4.86+/- 0.63
BT474A/ErbB2-Rz pool	4.13 +/- 0.63
BT474A/ErbB2-Rz1	4.50 +/- 0.20 (n=2)
BT474A/ErbB2-Rz3	7.86 +/- 1.05
BT474A/ErbB2-Rz4	5.6 +/- 0.43
BT474A/ErbB2-Rz5	2.06 +/- 0.32

Table 3.2.4.4.1a Results of short term toxicity assays

Cell Line	Fold Change in Resistance	Significance – Paired Student t-Test
BT474A	1.00	p =
BT474A/ErbB2-Rz pool	0.84	0.1823
BT474A/ErbB2-Rz1	0.92	0.3607
BT474A/ErbB2-Rz3	1.61	0.0102
BT474A/ErbB2-Rz4	1.15	0.0258
BT474A/ErbB2-Rz5	0.42	0.0365

Table 3.2.4.4.1b Fold resistance to 5-fluorouracil in short term assays and significance of change.

3.2.4.5 Effect of c-erbB-2 Downregulation on Methotrexate Resistance in Long Term Toxicity Assay

Cell Line	IC_{50} Methotrexate (ng/ml; n=3)
BT474A	9.66 +/- 1.76
BT474A/ErbB2-Rz pool	> 20 (Not fully determined)
BT474A/ErbB2-Rz4	16.8 +/- 1.15
BT474A/ErbB2-Rz5	> 20 (Not fully determined)

Table 3.2.4.5a Results of long term toxicity assays

3.2.4.6 Summary of Changes in resistance To Chemotherapeutic Agents in BT474A c-erbB-2 Ribozyme transfected variants.

The main findings of this section were that c-erbB-2 downregulation in BT474A increased resistance to taxol in both short and long term assays. Resistance to carboplatin was increased in short term assays only, while adriamycin resistance was increased in short term assays, but oppositely decreased in long term assays.

Type of Toxicity Assay	BT474A/ Rz pool	BT474A/ Rz1	BT474A/ Rz3	BT474A/ Rz4	BT474A/ Rz5
Adriamycin Long Term	-	-	-	-	-
Adriamycin Short Term	+	+	+	+	+
Taxol Long Term	+	+	+	+	+
Taxol Short Term	+	o	+	+	+
Carboplatin Long Term	-	o	-	o	o
Carboplatin Short Term	+	o	+	+	+
5-Fluorouracil Long Term	+	+	+	o	o
5-Fluorouracil Short Term	o	o	+	+	-
Methotrexate Long Term	+	npf	npf	+	+

+ increase in resistance
- decrease in resistance
o no change in resistance
npf not performed

3.2.5 Investigation of Changes in MDR Associated Gene Expression in C-erbB-2 Ribozyme Transfected BT474A Breast Cancer Cells.

A panel of genes associated with drug resistance were examined at the mRNA level by RT-PCR to determine whether the changes in drug resistance observed in Section 3.2.4 was due to alterations in classical modes of drug resistance.

3.2.5.1 MDR-1

Figure 3.2.5.1 shows that mdr-1 mRNA is not expressed in BT474A or any of its variants.

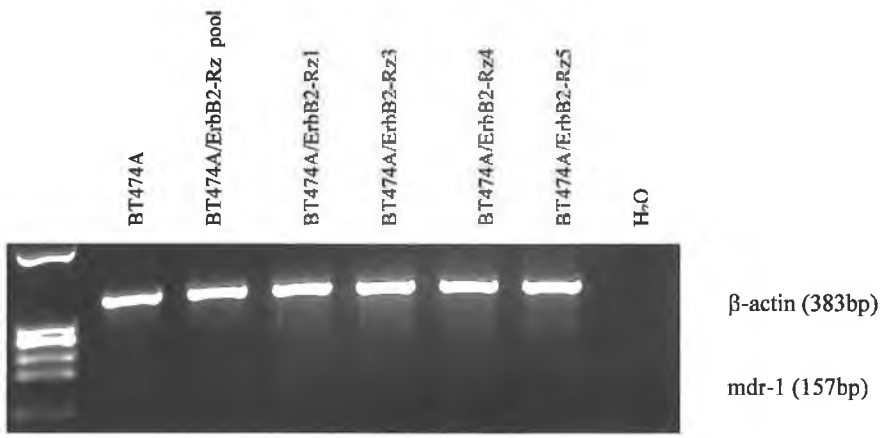

Figure 3.2.5.1 Levels of mdr-1 mRNA expression in BT474A c-erbB-2 ribozyme transfected pool and clonal populations. (PCR in Figure 3.3.8.1 was performed with the above at represents a positive control for mdr-1)

3.2.5.2 MRP-1

Figure 3.2.5.2 shows that mrp-1 mRNA levels were not affected by c-erbB-2 expression in BT474A.

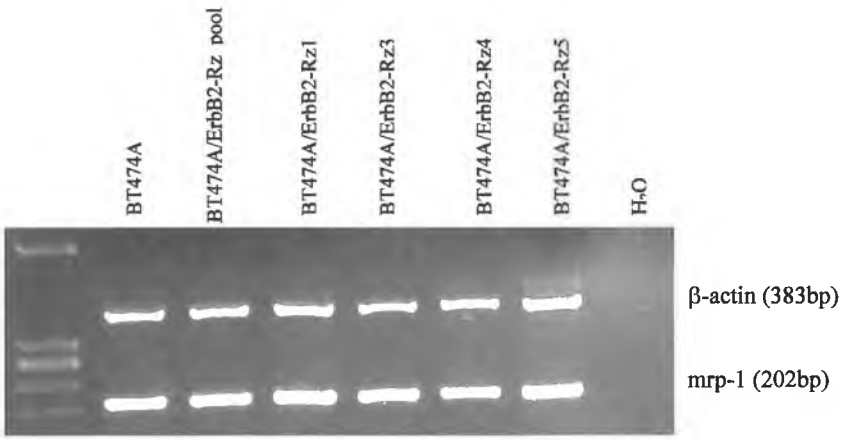

Figure 3.2.5.2 Levels of mrp1 mRNA expression in BT474A c-erbB-2 ribozyme transfected pool and clonal populations.

Cell Line	Levels of MRP-1 mRNA Expression (%)
BT474A	100
BT474A/ErbB2-Rz pool	94.8
BT474A/ErbB2-Rz1	113.0
BT474A/ErbB2-Rz3	111.5
BT474A/ErbB2-Rz4	84.7
BT474A/ErbB2-Rz5	99.9

Table 3.2.5.2 Levels of mrp-1 mRNA expression.

3.2.5.3 MRP-2

Figure 3.2.5.3 shows that mrp-2 mRNA levels increased in response to a reduction in c-erbB-2 expression in BT474A.

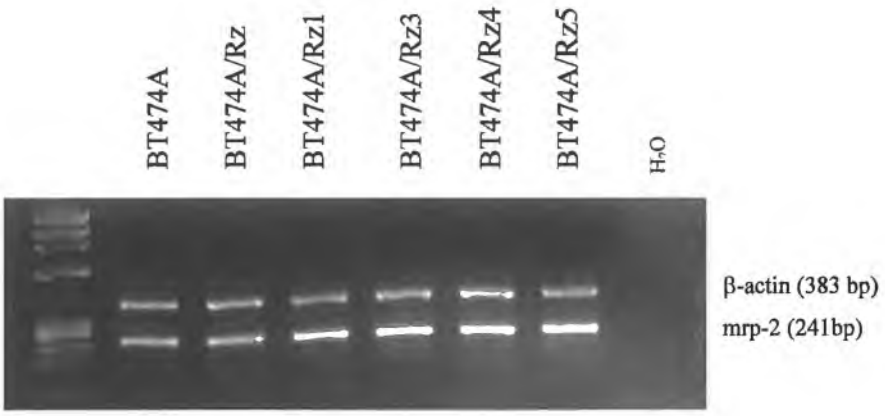

Figure 3.2.5.3 Levels of mrp-2 mRNA expression in BT474A c-erbB-2 ribozyme transfected pool and clonal populations.

Cell Line	Levels of MRP-2 mRNA Expression (%)
BT474A	100
BT474A/ErbB2-Rz pool	91.9
BT474A/ErbB2-Rz1	141.1
BT474A/ErbB2-Rz3	135.5
BT474A/ErbB2-Rz4	107.7
BT474A/ErbB2-Rz5	162.5

Table 3.2.5.3 Levels of mrp-2 mRNA expression.

3.2.5.4 MRP-4

Figure 3.2.5.4 shows that mrp-4 mRNA is not expressed in BT474A or any of its variants.

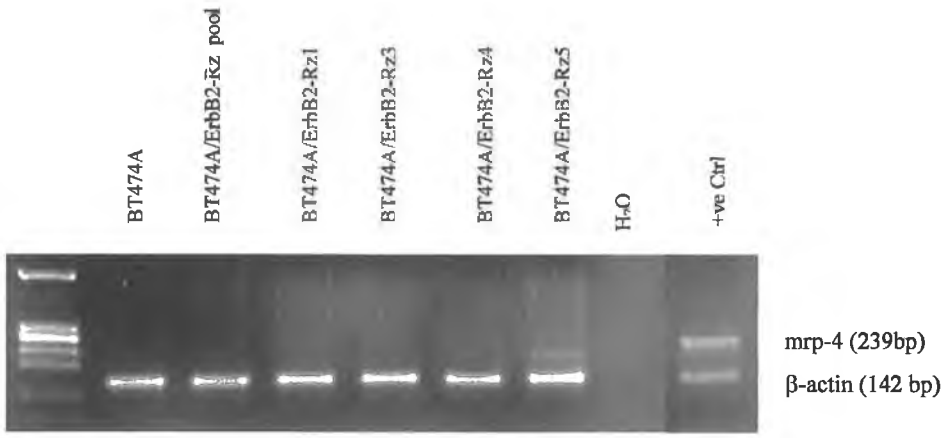

Figure 3.2.5.4 Levels of mrp-4 mRNA expression in BT474A c-erbB-2 ribozyme transfected pool and clonal populations.

3.2.5.5 MRP-5

Figure 3.2.5.5 shows that mrp-5 mRNA is expressed at very low levels in and was not affected by c-erbB-2 expression in BT474A.

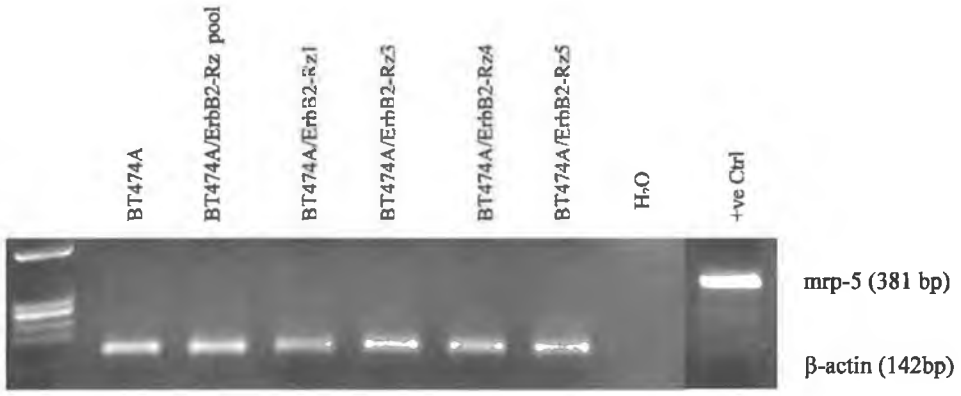

Figure 3.2.5.5 Levels of mrp-5 mRNA expression in BT474A c-erbB-2 ribozyme transfected pool and clonal populations.

3.2.5.6 Topoisomerase I

Densitometry of figure 3.2.5.6 shows that topoisomerase I mRNA levels increased in BT474A/ErbB2-Rz1, BT474A/ErbB2-Rz4 and BT474A/ErbB2-Rz5.

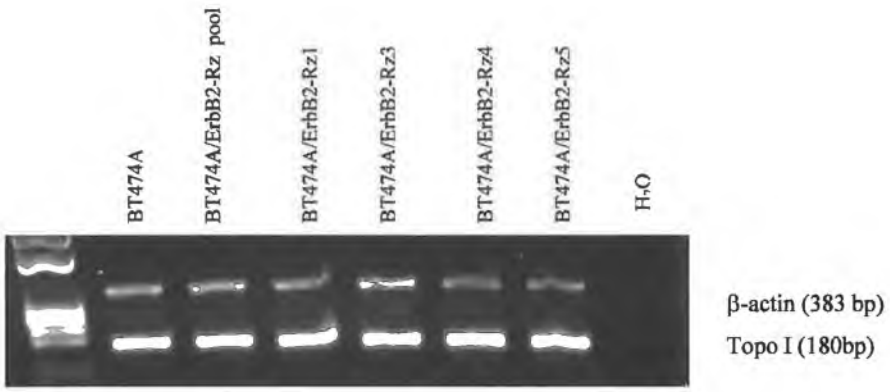

Figure 3.2.5.6 Levels of topisomerase I mRNA expression in BT474A c-erbB-2 ribozyme transfected pool and clonal populations.

Cell Line	Levels of Topoisomerase I mRNA Expression (%)
BT474A	100
BT474A/ErbB2-Rz pool	96
BT474A/ErbB2-Rz1	131
BT474A/ErbB2-Rz3	85
BT474A/ErbB2-Rz4	160
BT474A/ErbB2-Rz5	171

Table 3.2.5.6 Levels of topoisomerase I mRNA expression.

3.2.5.7 Topoisomerase IIα

Figure 3.2.5.7 shows that topoisomerase IIα mRNA levels were reduced in BT474A/ErbB2-Rz pooled population and in BT474A/ErbB2-Rz4 and BT474A/ErbB2-Rz5.

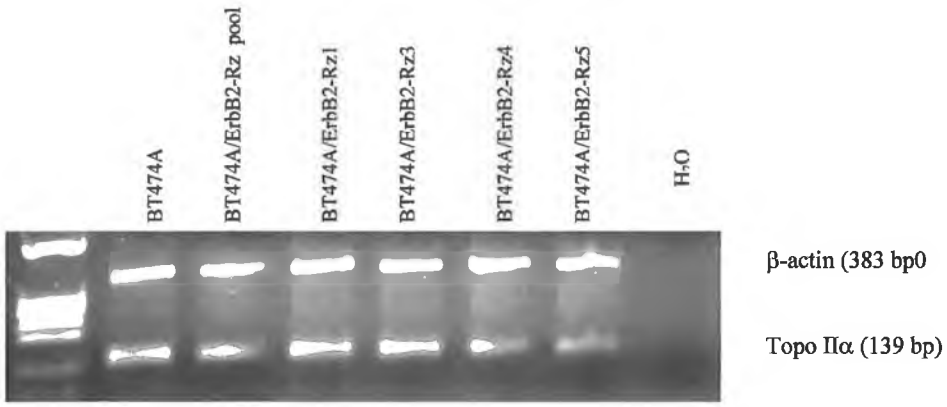

Figure 3.2.5.7 Levels of topoisomerase IIα mRNA expression in BT474A c-erbB-2 ribozyme transfected pool and clonal populations.

Cell Line	Levels of Topoisomerase IIα mRNA Expression (%)
BT474A	100
BT474A/ErbB2-Rz pool	86
BT474A/ErbB2-Rz1	121
BT474A/ErbB2-Rz3	121
BT474A/ErbB2-Rz4	76
BT474A/ErbB2-Rz5	70

Table 3.2.5.7 Levels of topoisomerase IIα mRNA expression.

3.2.5.8 Topoisomerase IIβ

Figure 3.2.5.8 shows that topoisomerase IIβ mRNA levels were increased in BT474A/ErbB2-Rz pooled population, and in BT474A/ErbB2-Rz1 and BT474A/ErbB2-Rz5.

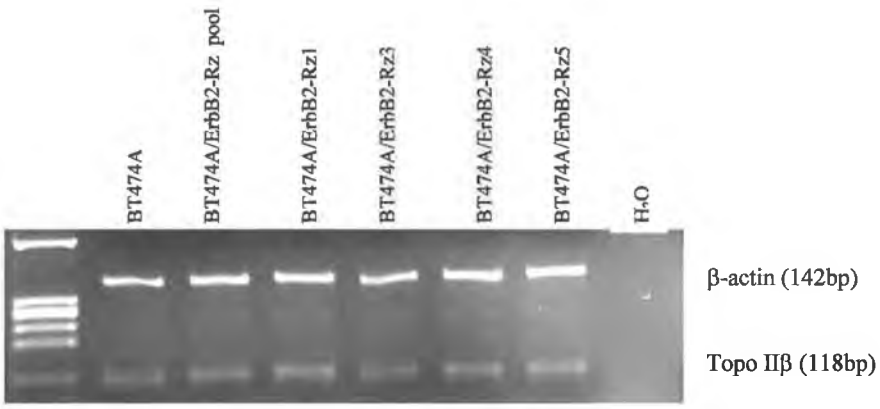

Figure 3.2.5.8 Levels of topoisomerase IIβ mRNA expression in BT474A c-erbB-2 ribozyme transfected pool and clonal populations.

Cell Line	Levels of Topoisomerase IIβ mRNA Expression (%)
BT474A	100
BT474A/ErbB2-Rz pool	138
BT474A/ErbB2-Rz1	131
BT474A/ErbB2-Rz3	85
BT474A/ErbB2-Rz4	107
BT474A/ErbB2-Rz5	139

Table 3.2.5.8 Levels of topoisomerase IIβ mRNA expression.

3.2.5.9 Dihydrofolate reductase (DHFR)

Figure 3.2.5.9 shows that DHFR mRNA levels increased in response to a reduction in c-erbB-2 expression in BT474A in BT474A/ErbB2-Rz pool, BT474A/ErbB2-Rz3 and BT474A/ErbB2-Rz5. Levels were not increased in the two remaining clonal populations.

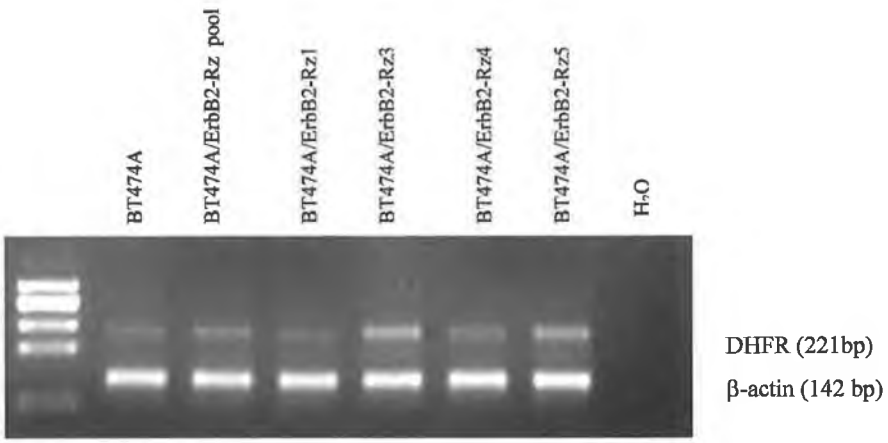

Figure 3.2.5.9 Levels of DHFR mRNA expression in BT474A c-erbB-2 ribozyme transfected pool and clonal populations.

Cell Line	Levels of DHFR mRNA Expression (%)
BT474A	100
BT474A/ErbB2-Rz pool	116
BT474A/ErbB2-Rz1	88
BT474A/ErbB2-Rz3	160
BT474A/ErbB2-Rz4	109
BT474A/ErbB2-Rz5	157

Table 3.2.5.9 Levels of DHFR mRNA expression.

3.2.5.10 Thymidylate Synthase (TS)

Taking into consideration β-actin level, figure 3.2.5.10 showed that TS mRNA levels increased in response to a reduction in c-erbB-2 expression in BT474A.

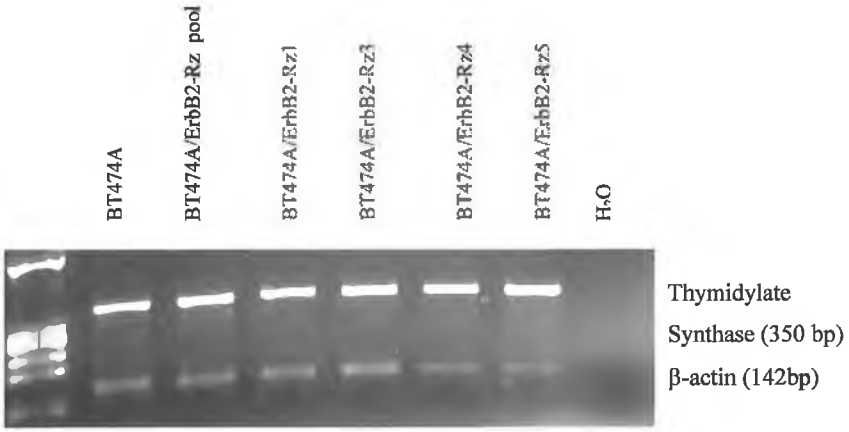

Figure 3.2.5.10 Levels of TS mRNA expression in BT474A c-erbB-2 ribozyme transfected pool and clonal populations.

Cell Line	Levels of TS mRNA Expression (%)
BT474A	++
BT474A/ErbB2-Rz pool	+++
BT474A/ErbB2-Rz1	+++
BT474A/ErbB2-Rz3	+++
BT474A/ErbB2-Rz4	+++
BT474A/ErbB2-Rz5	+++

Table 3.2.5.10 Levels of TS mRNA expression.

3.2.5.11 GSTπ

Figure 3.2.5.11 shows that GSTπ mRNA levels increased in response to a reduction in c-erbB-2 expression in BT474A.

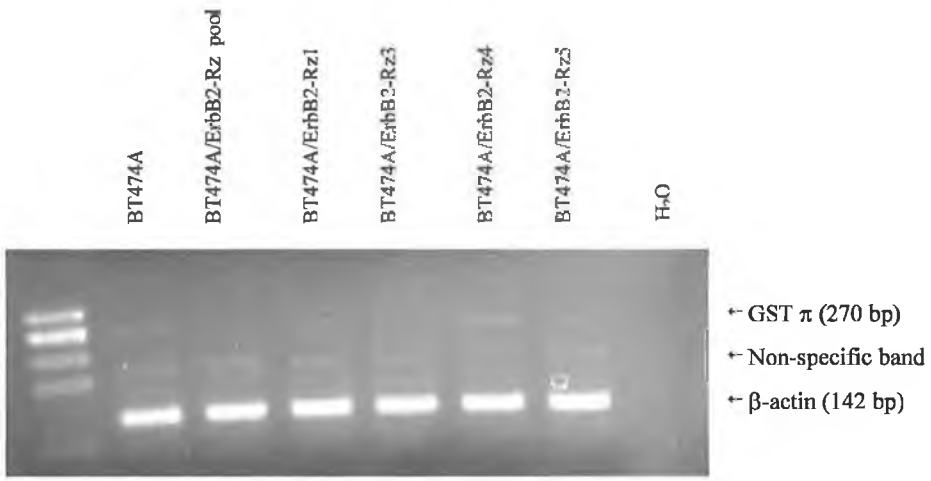

Figure 3.2.5.11 Levels of GSTπ mRNA expression in BT474A c-erbB-2 ribozyme transfected pool and clonal populations.

Cell Line	Levels of GST π mRNA Expression (%)	Levels of Extra Band Expression (%)
BT474A	+	+
BT474A/ErbB2-Rz pool	++	+
BT474A/ErbB2-Rz1	++	+++
BT474A/ErbB2-Rz3	++	++
BT474A/ErbB2-Rz4	+	+++
BT474A/ErbB2-Rz5	++	++

Table 3.2.5.11 Levels of GSTπ mRNA expression.

3.1.5.12 Summary of Results of Gene Expression Studies in BT474A c-erbB-2 Ribozyme Transfectants

No changes in the expression of drug resistance pumps at the mRNA level, were detected by RT-PCR, with the exception of mrp2 mRNA which was increased. This suggested that MDR-1, MRP-1, MRP4 and MRP5, do not play a role in c-erbB-2 associated drug resistance of BT474A, while MRP2 may. The mRNA for topoisomerase isoforms I and IIb were in general increased in the BT474A c-erbB-2 ribozyme transfected variants. Thymidylate synthase, GSTπ and DHFR were also increased at the mRNA in response to c-erbB-2 downregulation.

RT-PCR	BT474A/ Rz pool	BT474A/ Rz1	BT474A/ Rz3	BT474A/ Rz4	BT474A/ Rz5
Mdr-1	neg	neg	neg	neg	neg
Mrp-1	o	o	o	o	o
Mrp-2	o	+	+	o	+
Mrp-4	neg	neg	neg	neg	neg
Mrp-5	o	o	o	o	o
Topo I	o	+	-	+	+
Topo IIα	-	+	+	-	-
Topo IIβ	+	+	-	o	+
DHFR	+	o	+	o	+
TS	+	+	+	+	+
GSTπ	+	+	+	o	+
C-erbB-1	o	o	o	+	o
C-erbB-4	o	o	-	o	o

+ increase in expression

- decrease in expression

o no change in expression

neg Not expressed

3.2.6 The Effect of c-erbB-2 Downregulation in BT474A on Resistance to Tamoxifen

C-erbB-2 downregulation in BT474A does not effect any major changes in resistance to tamoxifen.

Cell Line	IC_{50} Tamoxifen (ng/ml; n=3)
BT474A	498 +/- 7.63
BT474A/ErbB2-Rz pool	433 +/- 20.2
BT474A/ErbB2-Rz1	471 +/- 10.4
BT474A/ErbB2-Rz3	656 +/- 30.5
BT474A/ErbB2-Rz4	455 +/- 8.6
BT474A/ErbB2-Rz5	523 +/- 20.8

Table 3.2.6 Results of tamoxifen toxicity assays

Cell Line	Fold Change in Resistance	Significance – Paired Student T-Test
BT474A	1.00	P =
BT474A/ErbB2-Rz pool	0.87	0.0246
BT474A/ErbB2-Rz1	0.95	0.0038
BT474A/ErbB2-Rz3	1.32	0.0073
BT474A/ErbB2-Rz4	0.91	0.0058
BT474A/ErbB2-Rz5	1.05	0.0820

Table 3.2.6 Fold resistance to tamoxifen in long term assays and significance of change.

3.2.7 The Effect of c-erbB-2 Downregulation on Estrogen Receptor Expression

Expression estrogen receptors were examined by western blotting. No changes in the expression of estrogen receptor α expression was detected, while estrogen receptor β was found to be downregulated. Blots were stripped and reprobed for β-actin.

3.2.7.1 Estrogen Receptor α

Estrogen receptor α expression is unaffected by c-erbB-2 expression in BT474A.

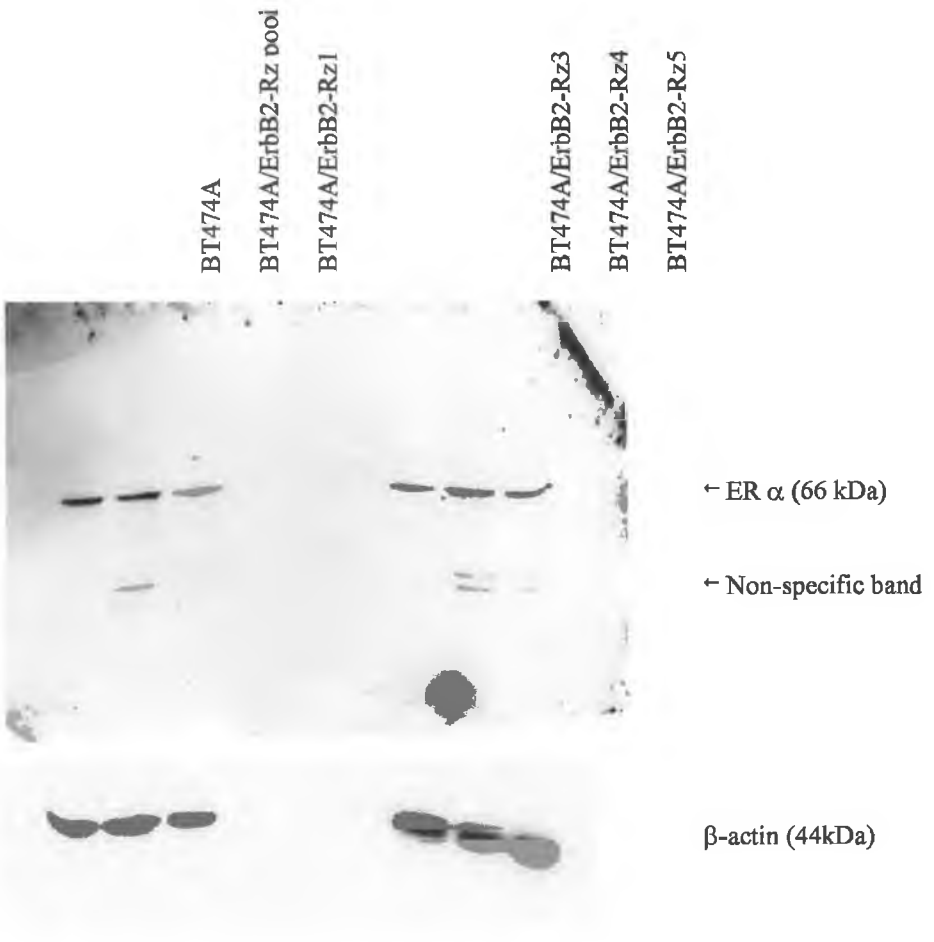

Figure 3.2.7.1a Estrogen Receptor α expression in BT474A

3.2.7.2 Estrogen Receptor β

Estrogen receptor β expression is decreased with decreasing c-erbB-2 expression in BT474A. this is very similar to the observations in Section 3.1.7.2 where estrogen receptor β expression increased with increasing c-erbB-2 levels. It should also be noted that estrogen receptor β levels in the mutant ribozyme population are unaltered, indicating that the changes observed in the other populations are specific to the active ribozyme.

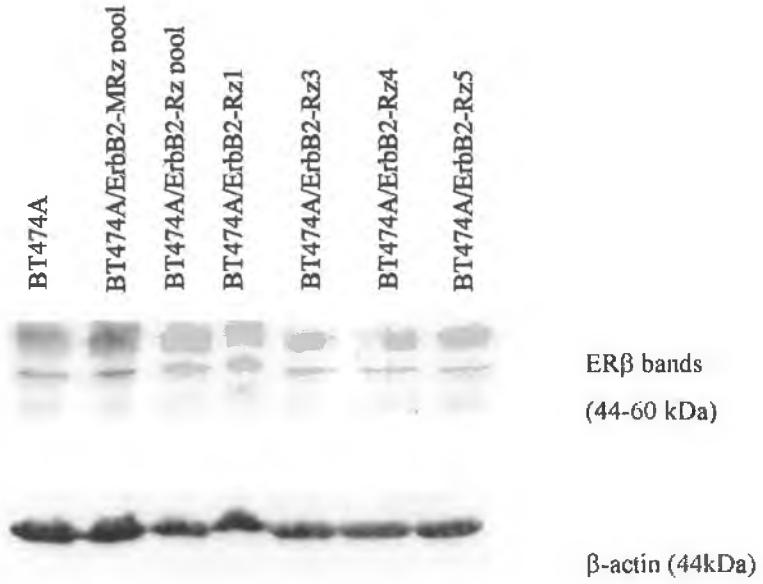

Figure 3.2.7.2 Estrogen Receptor β expression in BT474A

3.2.8 The Effect of C-erbB-2 Downregulation on the mRNA Expression c-erbB-1 and c-erbB-4 in BT474A

In order to determine whether c-erbB-2 had an effect on the expression of other ErbB family members, erbB levels were determined at both mRNA and protein levels (Section 3.2.9). The effect of c-erbB-2 upregulation in BT474A, on the expression of c-erbB-1 and c-erbB-4 mRNA levels was examined by RT-PCR

3.2.8.1 C-erbB-1 mRNA

Figure 3.2.8.1 shows that c-erbB-1 mRNA levels were unaffected by c-erbB-2 levels in BT474A.

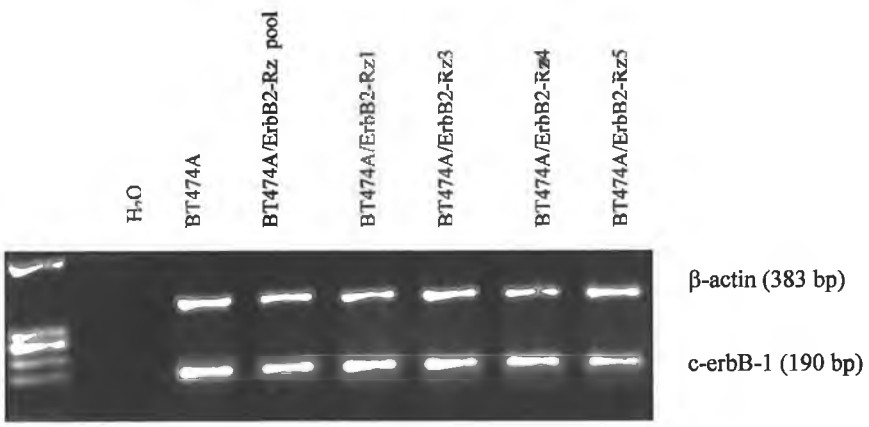

Figure 3.2.8.1 Levels of c-erbB-1 mRNA expression in BT474A c-erbB-2 ribozyme transfected pool and clonal populations.

Cell Line	Levels of C-erbB-1 mRNA Expression (%)
BT474A	100.0
BT474A/ErbB2-Rz pool	106.2
BT474A/ErbB2-Rz1	117.3
BT474A/ErbB2-Rz3	96.8
BT474A/ErbB2-Rz4	125.3
BT474A/ErbB2-Rz5	88.8

Table 3.2.8.1 Levels of c-erbB-1 mRNA expression.

3.2.8.2 C-erbB-4 mRNA

Figure 3.2.8.2 shows that c-erbB-4 mRNA levels were unaffected by c-erbB-2 levels in BT474A.

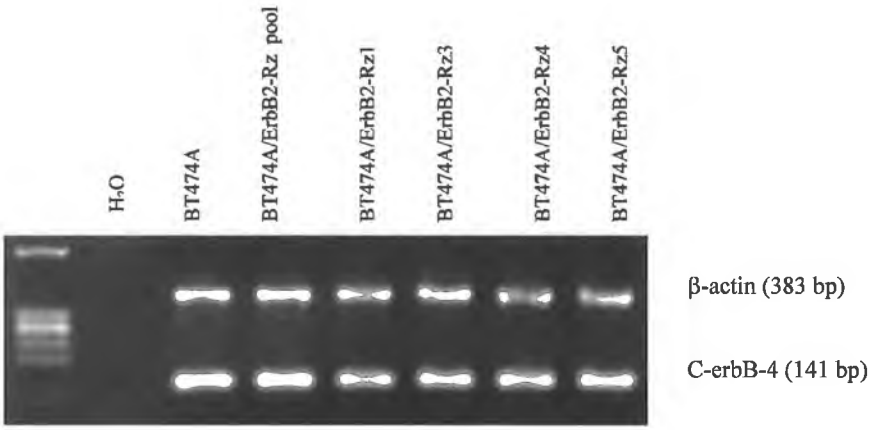

Figure 3.2.8.2 Levels of c-erbB-4 mRNA expression in BT474A c-erbB-2 ribozyme transfected pool and clonal populations.

Cell Line	**Levels of C-erbB-4mRNA Expression (%)**
BT474A	100
BT474A/ErbB2-Rz pool	94.5
BT474A/ErbB2-Rz1	86.2
BT474A/ErbB2-Rz3	76.6
BT474A/ErbB2-Rz4	109.7
BT474A/ErbB2-Rz5	106.9

Table 3.2.8.2 Levels of c-erbB-4 mRNA expression.

3.2.9 Effect of C-erbB-2 Downregulation in BT474A on the Expression of Remaining ErbB Receptors at the Protein level.

No changes in the mRNA levels of c-erbB-1 or c-erbB-4 were detected in section 3.2.8. Protein levels of c-erbB-1, c-erbB-3 and c-erbB-4 were examined to determine whether ErbB protein levels had also remained unchanged.

3.2.9.1 C-erbB-1 protein

Figure 3.2.9.1 shows that c-erbB-1 protein expression is unaffected by c-erbB-2 expression in BT474A. It should also be noted that c-erbB-1 protein levels in the mutant ribozyme population are unaltered.

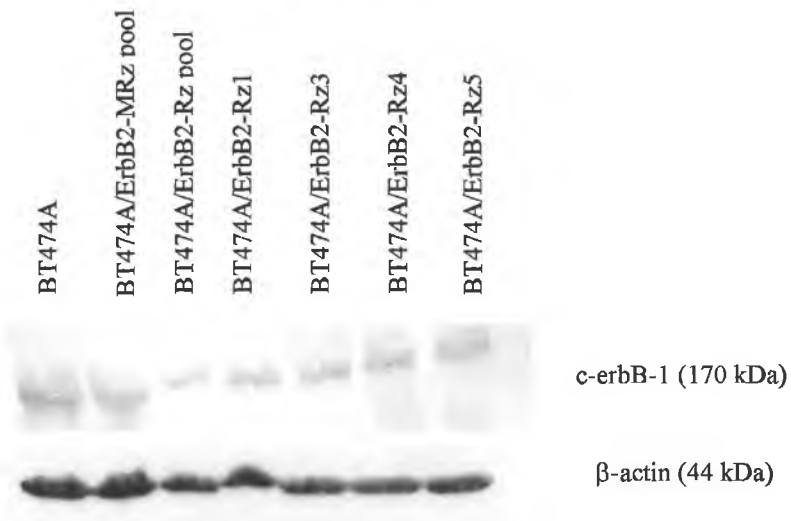

Figure 3.2.9.1 C-erbB-1 protein expression in BT474A A control gel was run for detection of β-actin protein, as β-actin was of too low a molecular weight to detect on ErbB gels. This is also the case in section 3.2.9.2

3.2.9.2 C-erbB-3 protein

Figure 3.2.9.2 shows that c-erbB-3 protein expression decreased in BT474A/ErbB2-Rz1, BT474A/ErbB2-Rz4 and BT474A/ErbB2-Rz5 in response to decreasing c-erbB-2 expression in BT474A. It should also be noted that c-erbB-3 protein levels in the mutant ribozyme population are unaltered.

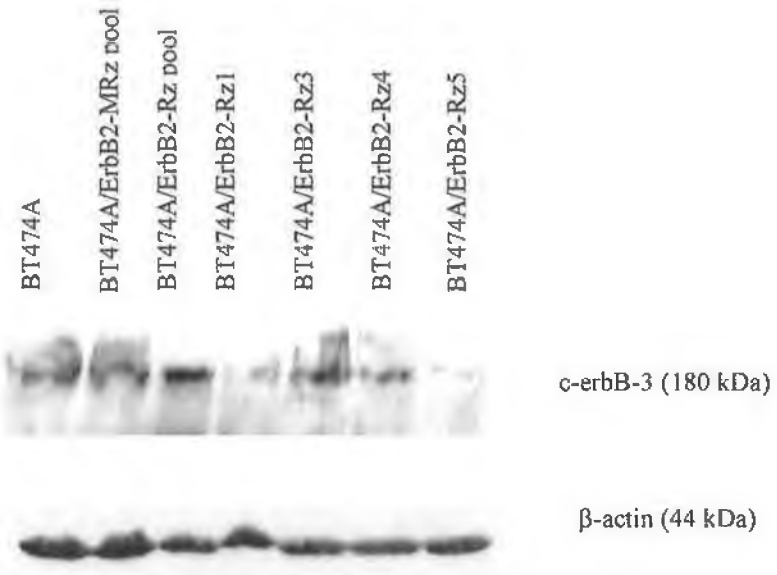

Figure 3.2.9.2 C-erbB-3 protein expression in BT474A

3.2.10 The Effect of C-erbB-2 Downregulation on Motility of BT474A

Motility assays were performed as described in section 2.15 to investigate the effects of c-erbB-2 downregulation on the motility of BT474A. Surprisingly, similar to results for MCF-7 H3, neither the parental cell line nor the clonal populations were motile in this system. A sample photo of the parental cell line, figure 3.2.10a shows that the membrane contained little or no cells after 48 hours incubation. The clonal populations displayed identical results. The Positive (RPMI 2650- Melphalan) and negative (RPMI 2650) controls Figure 3.2.10b and 3.2.10c show that this assay was operational.

Figure 3.2.10a Motility assay for BT474A

Figure 3.2.10b RPMI

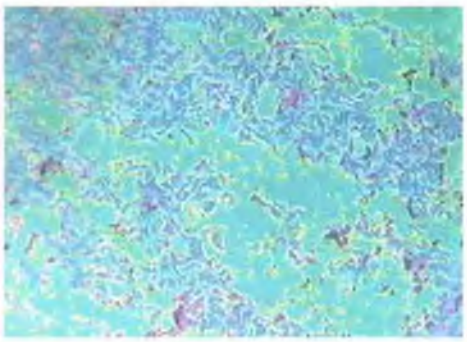

Figure 3.2.10c RPMI Melphalan

3.2.11 The Effect of C-erbB-2 Downregulation on Invasion of Matrigel by BT474A

Invasion assays were performed as described in section 2.14 to investigate the effects of c-erbB-2 downregulation on the invasiveness of BT474A. C-erbB-2 downregulation was found to decrease the invasiveness of BT474A, with this reduction in invasiveness greatest in the four clonal populations. Figures 3.2.11.1 to 3.2.11.6 are representative of 3 repeats.

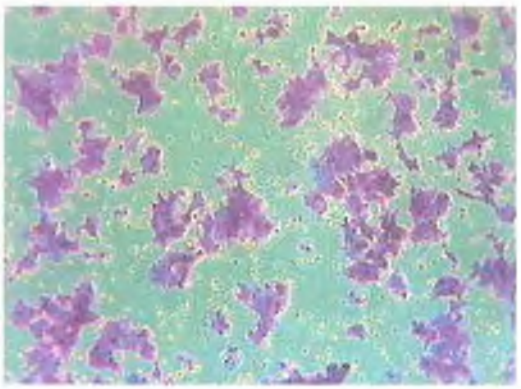

Figure 3.2.11a BT474A

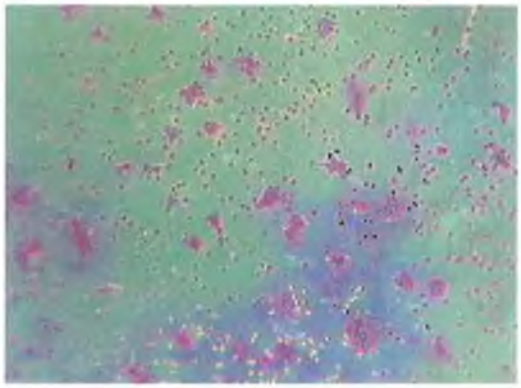

Figure 3.2.11b BT474A/ErbB2-Rz pool

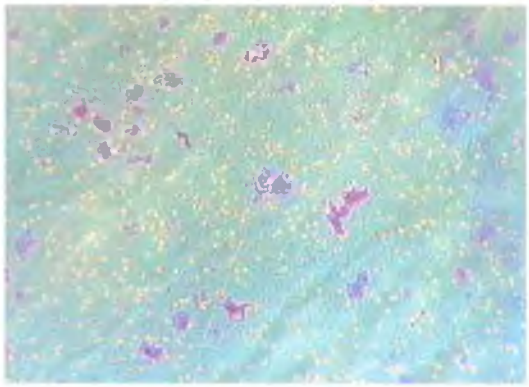

Figure 3.2.11c BT474A/ErbB2-Rz1

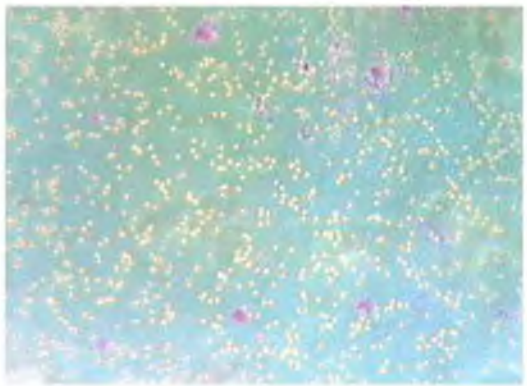

Figure 3.2.11d BT474A/ErbB2-Rz3

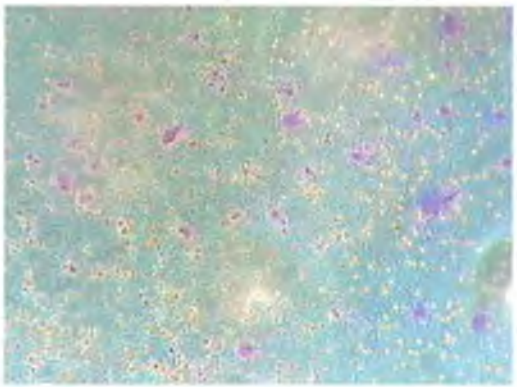

Figure 3.2.11e BT474A/ErbB2-Rz4

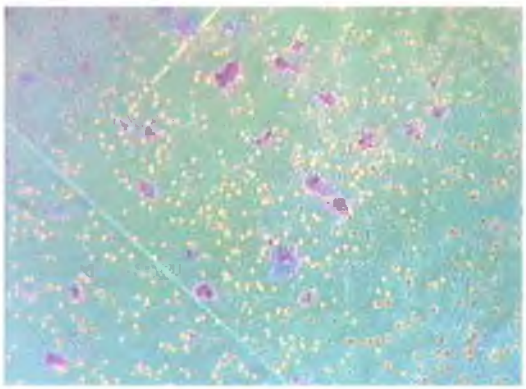

Figure 3.2.11f BT474A/ErbB2-Rz5

3.2.12 The Effect of C-erbB-2 Downregulation on Adhesive Properties of BT474A to Components of the Extracellular Matrix

Cells use various adhesion molecules such as integrins to interact with extracellular matrix components such as collagen type IV, laminin and fibronectin. To detect changes in the adhesive properties of BT474A due to downregulation of c-erbB-2, adhesion assay were performed as described in section 2.13.

Figure 3.2.12.1 shows the levels of adhesion of BT474A and its c-erbB-2 ribozyme transfected clones to laminin after 1 hour. All the clonal populations displayed reduced adhesion to laminin in comparison to the parental cell line.

Figure 3.2.12.2 shows the levels of adhesion of BT474A and its c-erbB-2 ribozyme transfected clones to collagen type IV after 1 hour. All the clonal populations and the pool population displayed decreased adhesion to collagen type IV compared to their parental cell line.

Figure 3.2.12.3 shows the levels of adhesion of BT474A and its c-erbB-2 ribozyme transfected clones to fibronectin after 1 hour. The pool population and all the clonal populations, with the exception of BT474A/ErbB2-Rz4 showed decreased adhesion to fibronectin compared to their parental cell line.

Figure 3.2.12.4 shows the levels of adhesion of BT474A and its c-erbB-2 ribozyme transfected clones to matrigel after 1 hour. All the clonal populations displayed reduced adhesion to matrigel in comparison to the parental cell line.

3.2.12.1 Adhesion to Laminin.

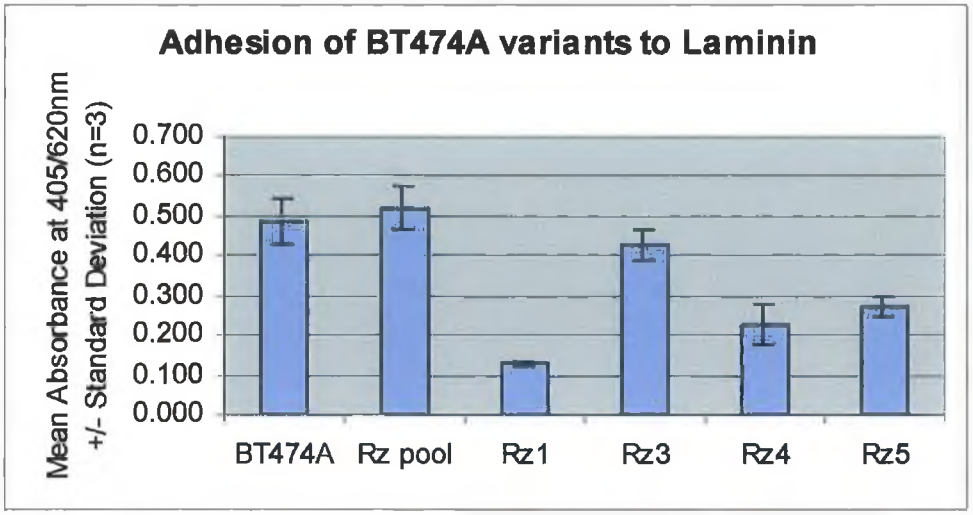

Figure 3.2.12.1 Levels of adhesion of BT474A and c-erbB-2 ribozyme transfected clones to laminin.

Cell Line	Fold Changes in Cells Attached to Laminin After 1 hour
BT474A	1.00
BT474A/ErbB2-Rz pool	1.07
BT474A/ErbB2-Rz1	0.27
BT474A/ErbB2-Rz3	0.88
BT474A/ErbB2-Rz4	0.46
BT474A/ErbB2-Rz5	0.55

Table 3.2.12.1 Fold changes in adhesion to laminin relative to the parental cell line BT474A.

3.2.12.2 Adhesion to Collagen Type IV

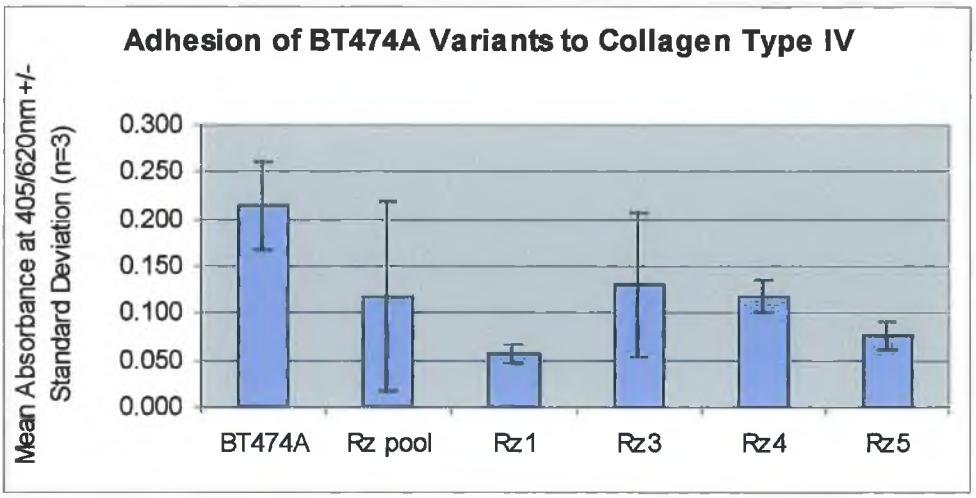

Figure 3.2.12.2 Levels of adhesion of BT474A and c-erbB-2 ribozyme transfected clones to collagen type IV.

Cell Line	Fold Changes in Cells Attached to Collagen Type IV After 1 hour
BT474A	1.00
BT474A/ErbB2-Rz pool	0.55
BT474A/ErbB2-Rz1	0.26
BT474A/ErbB2-Rz3	0.61
BT474A/ErbB2-Rz4	0.55
BT474A/ErbB2-Rz5	0.35

Table 3.2.12.2 Fold changes in adhesion to collagen type IV relative to the parental cell line BT474A.

3.2.12.3 Adhesion to Fibronectin

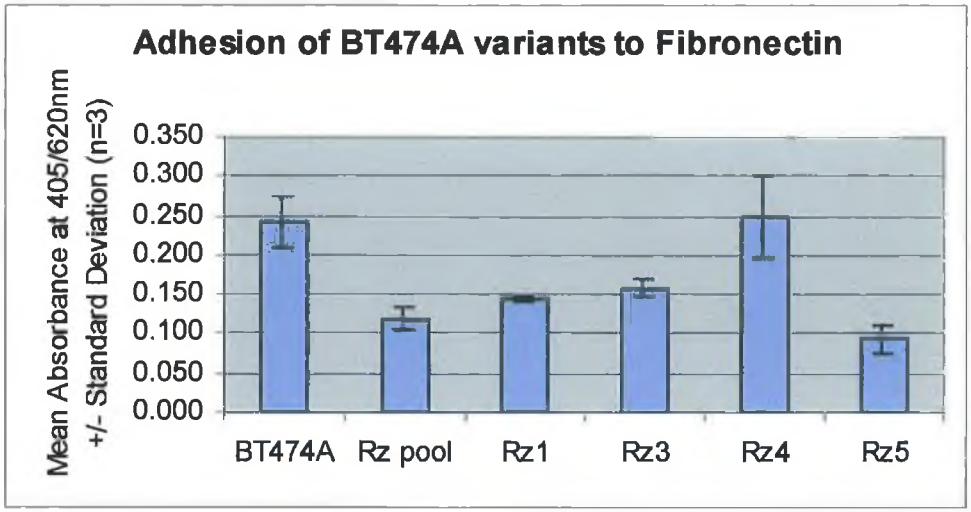

Figure 3.2.12.3 Levels of adhesion of BT474A and c-erbB-2 ribozyme transfected clones to fibronectin.

Cell Line	Fold Changes in Cells Attached to Fibronectin After 1 hour
BT474A	1.00
BT474A/ErbB2-Rz pool	0.49
BT474A/ErbB2-Rz1	0.59
BT474A/ErbB2-Rz3	0.65
BT474A/ErbB2-Rz4	1.03
BT474A/ErbB2-Rz5	0.39

Table 3.2.12.3 Fold changes in adhesion to fibronectin relative to the parental cell line BT474A.

3.2.12.4 Adhesion to Matrigel

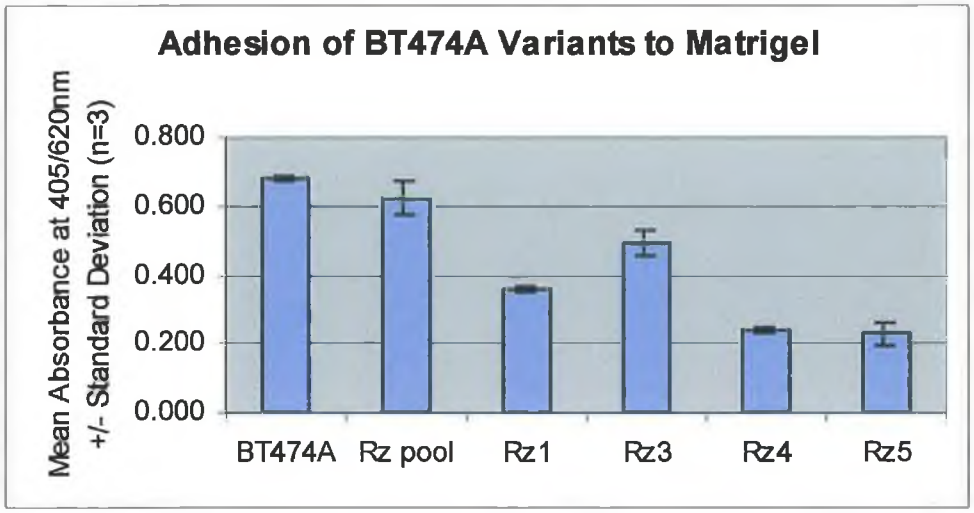

Figure 3.2.12.4 Levels of adhesion of BT474A and c-erbB-2 ribozyme transfected clones to matrigel.

Cell Line	Fold Changes in Cells Attached to Matrigel After 1 hour
BT474A	1.00
BT474A/ErbB2-Rz pool	0.92
BT474A/ErbB2-Rz1	0.53
BT474A/ErbB2-Rz3	0.73
BT474A/ErbB2-Rz4	0.35
BT474A/ErbB2-Rz5	0.34

Table 3.2.12.4 Fold changes in adhesion to matrigel relative to the parental cell line BT474A.

3.2.12.5 Summary of Adhesion results

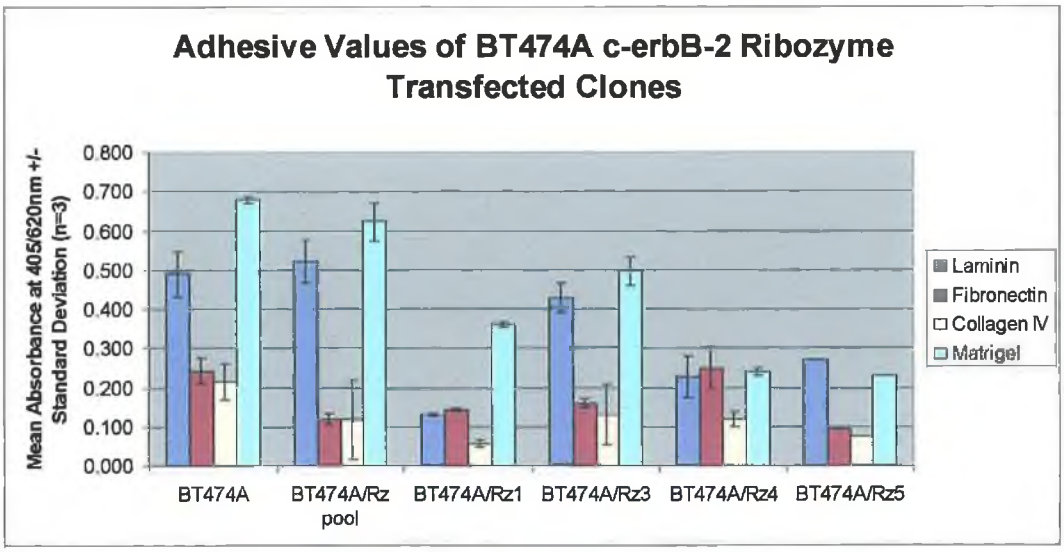

Figure 3.2.12.5 Adhesion of BT474A c-erbB-2 ribozyme transfectants to ECM proteins.

	Laminin	Fibronectin	Collagen Type IV	Matrigel
BT474A	1.00	1.00	1.00	1.00
BT474A/ErbB2-Rz pool	1.07	0.49	0.55	0.92
BT474A/ErbB2-Rz1	0.27	0.59	0.26	0.53
BT474A/ErbB2-Rz3	0.88	0.65	0.61	0.73
BT474A/ErbB2-Rz4	0.46	1.03	0.55	0.35
BT474A/ErbB2-Rz5	0.55	0.39	0.35	0.34

Table 3.1.13.5 Fold decrease in adhesion of BT474A c-erbB-2 ribozyme transfected variants to ECM proteins relative to parental cell lines BT474A.

3.2.13 The Effect of C-erbB-2 Downregulation on Secretion of Proteases by BT474A

Matrix metalloproteinases (MMPs), cysteine proteases and serine protease, which are secreted by cells, play an important role in degrading the extracellular matrix. To further investigate the mechanisms by which c-erbB-2 exerts an influence of the invasiveness of BT474A, zymography was performed to detect the secretion of proteases in these cells, as described in section 2.16.

3.2.13.1 Detection of the Expression of Proteases Secreted by BT474A and its C-erbB-2 Ribozyme Transfected Variants

BHK (baby hamster kidney) cell line, which secretes MMP-2 and MMP-9, was used as the positive control in these studies.

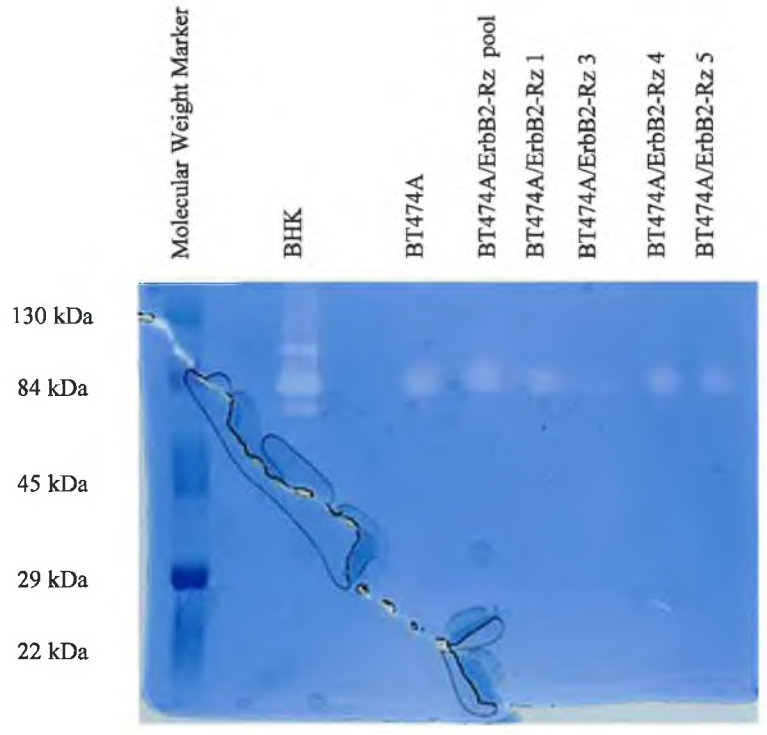

Figure 3.2.13.1 Zymogram of gelatin proteases secreted by BT474A with BHK as a positive control for the secretion of pro-MMP2 (72 kDa), MMP-2 (66kDa), pro-MMP-9 (92kDa) and MMP9 (86kDa). The BT474A parent cell line and its c-erbB-2 ribozyme transfected variants display secretion bands corresponding to pro-MMP-2,

pro-MMP-9 and MMP-9. There is also an additional band expressed appearing just above MMP-9.

3.2.13.2 Identification of the Classes of Proteases Secreted by BT474A and its C-erbB-2 Ribozyme Transfected Variants

To investigate the identity of the gelatin degrading proteases secreted by BT474A and its c-erbB-2 ribozyme transfected variants, protease inhibitors were used. EDTA is a chelating agent, which can bind zinc and calcium ions, which are needed for the activation of MMPs. PMSF is a serine and cysteine protease inhibitor.

Figure 3.2.13.2b shows that addition of EDTA to the substrate buffer eliminates expression of all protease bands, indicating the gelatin degrading proteases secreted by BT474A parent and c-erbB-2 ribozyme transfected variants are members of the matrixmetalloproteinase family.

Figure 3.2.13.2b also shows that addition of PMSF to the substrate buffer suppresses slightly the expression of all protease bands, but does not eliminate them, suggesting the proteases are not serine proteases. Perhaps though there are serine proteases secreted by the cells that are involved in MMP action/stabilisation.

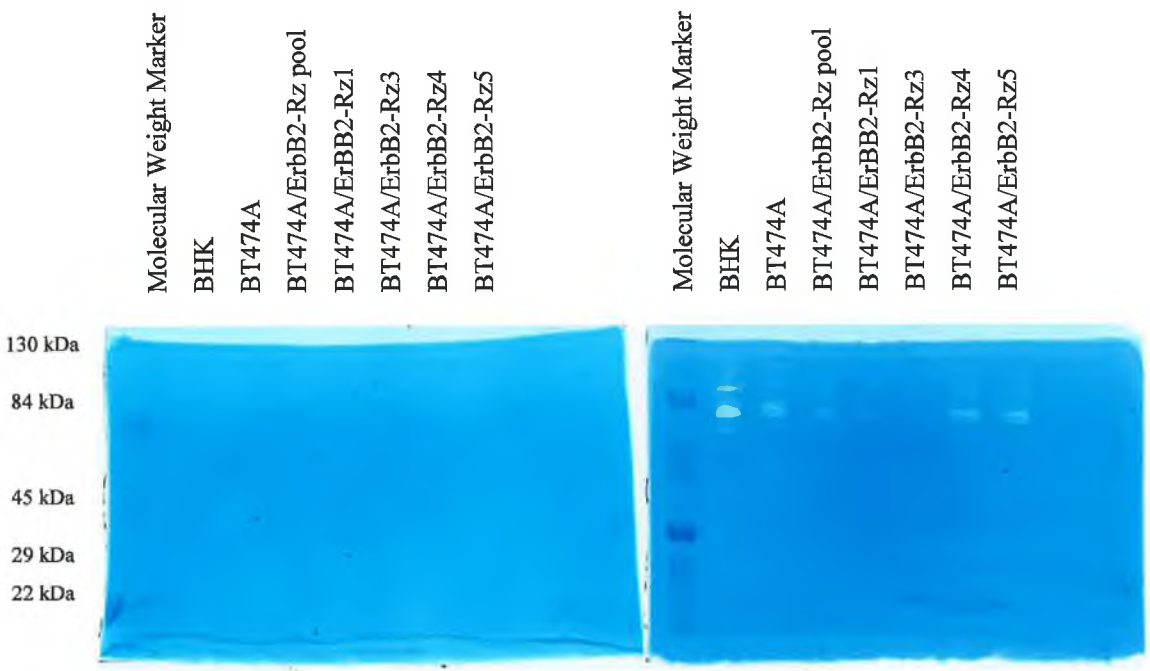

Figure 3.2.13.2b The effect of EDTA and PMSF on Protease Activity

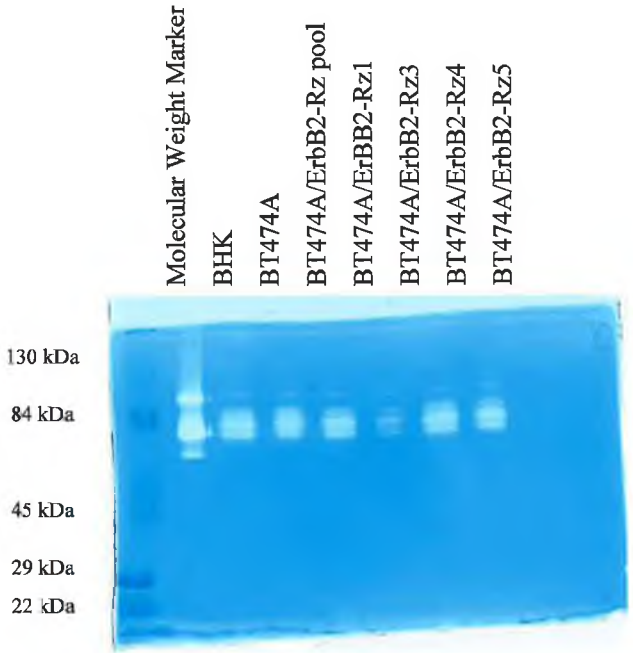

Figure 3.2.13.2a Protease secretion by BT474A and its Variants.

3.3 Establishment of novel MDR variants of the MDA-MB-435S-F cell line

MDA-MB-435S is a spindle shaped strain which evolved from the parent line MDA-MB-435 isolated by Cailleau et al (1976), from the pleural effusion of a 31 year old female with metastatic, ductal adenocarcinoma of the breast. Clonal populations were established by clonal dilution, entitled MDA-MB-435S-A, MDA-MB-435S-B, MDA-MB-435S-C, MDA-MB-435S-D, MDA-MB-435S-E and MDA-MB-435S-F. It was desired to select with a clonal population so that any emergence of drug resistance would be due to adaptation of the cells to the selecting drug and not due to selection of a resistant subpopulation already present within the cell line. The clonal population MDA-MB-435S-F was chosen to establish MDR-variants, due to its low-level c-erbB-2 mRNA expression (figure 3.3). This would allow us to examine whether c-erbB-2 induction would play a role in taxol or adriamycin resistance. An attempt was also made to transfect MDA-MB-435S-F with c-erbB-2, but was not successful. Hs578T is also a breast cancer cell line, and was included in an initial screen of breast cell lines for levels of c-erbB-2 expression.

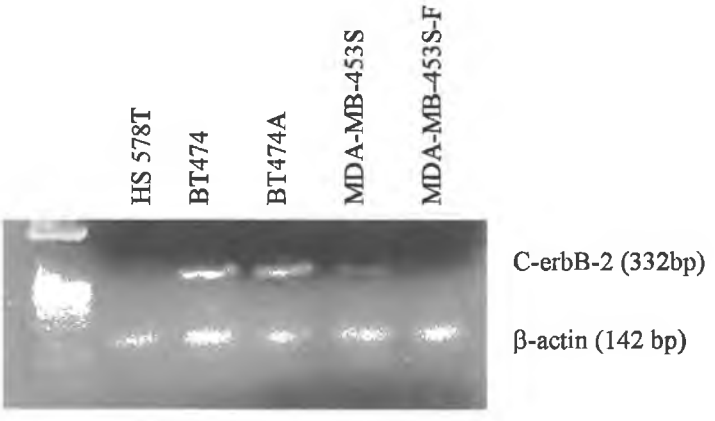

Figure 3.3 Expression of c-erbB-2 mRNA in Hs578T, BT474, BT474A, MDA-MB-435S and MDA-MB-435S-F.

3.3.1 Establishment of MDA-MB-435S-F taxol resistant variants

The MDA-MB-435S-F cells were exposed to the IC_{90} value of 15ng/ml taxol for four hours, once a week for 10 weeks. The cell line resulting from this exposure was designated MDA-MB-435S-F/Taxol-10p. This cell line displayed a 9.15-fold increase in resistance to taxol.

It was decided to attempt to further increase the resistance of this cell line to taxol. An IC_{90} assay was carried out to establish the IC_{90} value of MDA-MB-435S-F/Taxol-10p. This value was found to be 125ng/ml. MDA-MB-435S-F/Taxol-10p cells were then exposed to 125ng/ml taxol for four hours, once a week for 4 weeks. The cell line resulting from this exposure was designated MDA-MB-435S-F/Taxol-10p4p. This cell line displayed a 31.85-fold increase in resistance to taxol.

3.3.2 Establishment of MDA-MB-435S-F adriamycin resistant variants

The MDA-MB-435S-F cells were exposed to the IC_{90} value of 120ng/ml adriamycin for four hours, once a week for 10 weeks. The cell line resulting from this exposure was designated MDA-MB-435S-F/Adr-10p. This cell line displayed a 1.16-fold increase in resistance to adriamycin.

It was decided to attempt to further increase the resistance of this cell line to adriamycin. An IC_{90} assay was carried out to establish the IC_{90} value of MDA-MB-435S-F/Adr-10p, which was 200ng/ml. One flask of MDA-MB-435S-F/Adr-10p cells was then exposed to 200ng/ml adriamycin for four hours, once a week for 10 weeks. The cell line resulting from this exposure was designated MDA-MB-435S-F/Adr-10p10p. This cell line displayed a 1.40-fold increase in resistance to adriamycin.

3.3.3 Morphology of MDR variants of the MDA-MB-435S-F

The morphology of MDA-MB-435S-F was found not to have changed dramatically during the selection procedure with either adriamycin or taxol. The one observation made was that the adriamycin and taxol selected variants appeared not to observe cell-cell contact inhibition to the same extent as MDA-MB-435S-F. The cells in all four variants appeared to have gained the ability to overcome monolayer growth, to grow on top of each other. Also if cells floating in the media were removed, and placed in a new flask, they would reattach and grow.

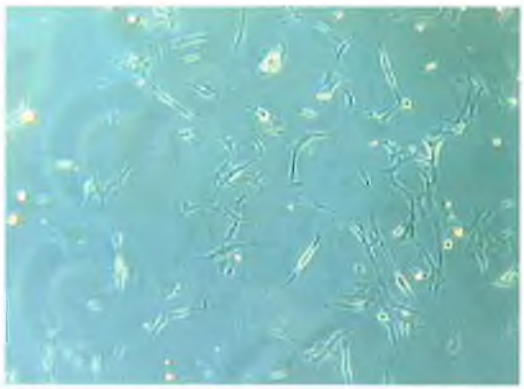

Figure 3.3.3a MDA-MB-435S-F

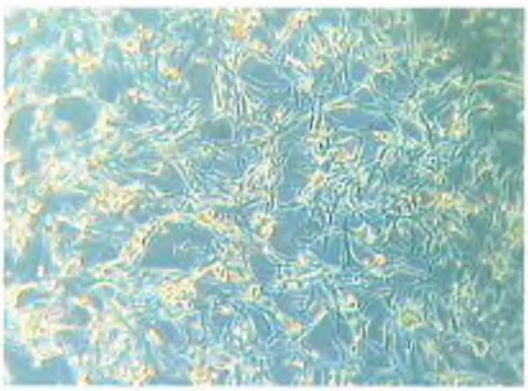

Figure 3.3.3b MDA-F/Taxol-10p

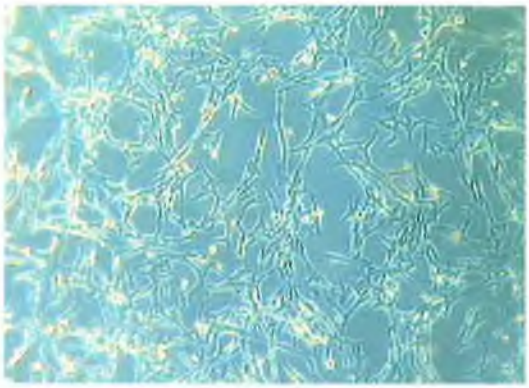

Figure 3.3.3c MDA-F/Taxol-10p4p

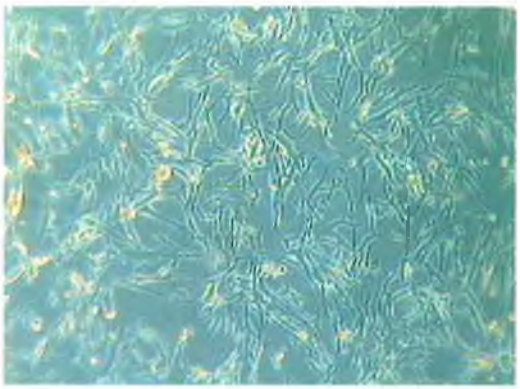

Figure 3.3.3d MDA-F/Adr-10p

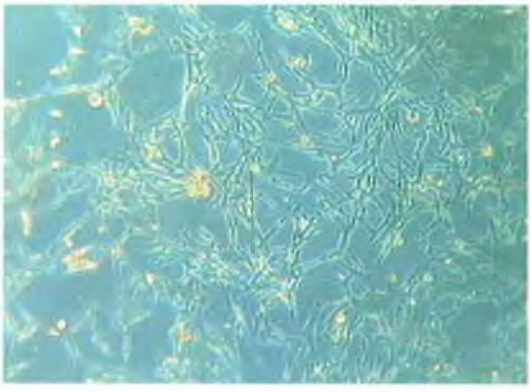

Figure 3.3.3e MDA-F/Adr-10p10p

3.3.4 Cross resistance profiles of MDA-MB-435S-F MDR variants

When cell lines are repeatedly exposed to chemotherapeutic drug, not only do the cells develop resistance to the drug in question, but they also can develop a cross-resistance to a variety of other chemotherapeutic drugs.

To investigate this phenomenon, the resistance profiles to a variety of drugs were tested in the MDA-MB-435S-F MDR variants, by short term toxicity assay. These drugs included taxol, adriamycin, carboplatin, VP-16, taxotere, vincristine and 5 –fluorouracil. Long term toxicity assays were also performed for adriamycin and taxol.

Table 3.3.4.1a represents the IC_{50} values of each of the chemotherapeutic agents for the parental MDA-MB-435S-F cell line and its taxol selected variant MDA-MB-435S-F/Taxol-10p. MDA-MB-435S-F/Taxol-10p was generated from MDA-MB-435S-F, by ten pulses with 15ng/ml taxol. The results demonstrate that the taxol-resistant variant exhibited cross resistance to taxol, taxotere, vincristine and carboplatin. Adriamycin and VP-16 resistance were unchanged in MDA-MB-435S-F/Taxol-10p, while the cell line was sensitised to 5-Fluorouracil.

Table 3.3.4.2a represents the IC_{50} values of each of the chemotherapeutic agents for the parental MDA-MB-435S-F cell line and its taxol selected variant MDA-MB-435S-F/Taxol-10p4p. MDA-MB-435S-F/Taxol-10p4p was generated from MDA-MB-435S-F/Taxol-10p, by an additional four pulses with 125ng/ml taxol. The results demonstrate that MDA-MB-435S-F/Taxol-10p4p exhibited cross resistance to taxol, taxotere, and vincristine as was the case with MDA-MB-435S-F/Taxol-10p, but to a greater extent. This pattern of resistance might suggest a microtubule, rather than an efflux pump, associated mechanism of resistance. It was, however, no longer resistant to carboplatin or sensitised to 5-fluorouracil. Again VP-16 resistance was unchanged in MDA-MB-435S-F/Taxol-10p4p, while the cell line was now resistant to adriamycin.

Table 3.3.4.3a represents the IC_{50} values of each of the chemotherapeutic agents for the parental MDA-MB-435S-F cell line and its adriamycin selected variant MDA-MB-435S-F/Adr-10p. MDA-MB-435S-F/Adr-10p was generated from MDA-MB-435S-F, by ten pulses with 120ng/ml adriamycin. The results demonstrate that adriamycin resistance of MDA-MB-435S-F/Adr-10p was not significantly increased in comparison

to the parental cell line, despite the fact that high cell kill was observed during selection with adriamycin. However MDA-MB-435S-F/Adr-10p was resistance to VP-16 and sensitised to 5-fluorouracil, vincristine and taxol. No change in resistance to carboplatin or taxotere was observed.

Table 3.3.4.4a represents the IC_{50} values of each of the chemotherapeutic agents for the parental MDA-MB-435S-F cell line and its adriamycin selected variant MDA-MB-435S-F/Adr-10p10p. MDA-MB-435S-F/Adr-10p10p was generated from MDA-MB-435S-F/Adr-10p, by an additional ten pulses with 200ng/ml adriamycin. This additional ten pulse did generate an adriamycin resistant variant of MDA-MB-435S-F, although the increase was not large. The results demonstrate that MDA-MB-435S-F/Adr-10p10p exhibited cross resistance to taxotere, vincristine and VP-16, was sensitised to taxol, carboplatin and 5-fluorouracil.

3.3.4.1 Cross resistance profile of MDA-MB-435S-F/Taxol-10p in Short Term Toxicity Assays

IC_{50} (n=3)	MDA-MB-435S-F	MDA-MB-435S-F/ Taxol-10p
Adriamycin (ng/ml)	271 ± 3	242 ± 21
Taxol (ng/ml)	28.3 ± 1.52	259 ± 3**
Carboplatin (μg/ml)	41.3 ± 1.5	54.3 ± 5.1*
Taxotere (ng/ml)	3.33 ± 0.37	12.23 ± 0.37 **
VP-16 (ng/ml)	1844 ± 77	2225 ± 152
5-fluorouracil (μg/ml)	7.43 ± 0.68	3.50 ± 0.17**
Vincristine (ng/ml)	12.9 ± 1.3	74.6 ± 0.5**

** $p < 0.005$

* $p < 0.05$

Table 3.3.4.1.a IC_{50} values for MDA-MB-435S-F and MDA-MB-435S-F/Taxol-10p.

Drug	Fold resistance	Student t-test (p =)
Adriamycin	0.89	0.1320
Taxol	9.15	0.00006
Carboplatin	1.31	0.0301
Taxotere	3.67	0.0015
VP-16	1.20	0.0998
5-fluorouracil	0.47	0.0074
Vincristine	5.78	

Table 3.3.4.1.b Fold resistance of MDA-MB-435S-F/Taxol-10p to MDA-MB-435S-F.

3.3.4.2 Cross resistance profile of MDA-MB-435S-F/Taxol-10p4p in Short Term Toxicity Assays

IC_{50} (n=3)	MDA-MB-435S-F	MDA-MB-435S-F/ Taxol-10p4p
Adriamycin (ng/ml)	271 ± 3	456 ± 20**
Taxol (ng/ml)	28.3 ± 1.52	900 ± 40**
Carboplatin (μg/ml)	41.3 ± 1.5	33 ± 3.4
Taxotere (ng/ml)	3.33 ± 0.37	62.4 ± 1.3**
VP-16 (ng/ml)	1844 ± 77	1740 ± 17
5-fluorouracil (μg/ml)	7.43 ± 0.68	6.83 ± 0.60
Vincristine (ng/ml)	12.9 ± 1.3	176 ± 56**

** $p < 0.005$

Table 3.3.4.2.a IC_{50} values for MDA-MB-435S-F and MDA-MB-435S-F/Taxol-10p4p.

Drug	Fold resistance	Student t-test (p =)
Adriamycin	1.68	0.0039
Taxol	31.80	0.0007
Carboplatin	0.79	0.0544
Taxotere	18.73	.0002
VP-16	0.94	0.1827
5-fluorouracil	0.91	0.1884
Vincristine	13.64	

Table 3.3.4.2.b Fold resistance of MDA-MB-435S-F/Taxol-10p4p to MDA-MB-435S-F.

3.3.4.3 Cross resistance profile of MDA-MB-435S-F/Adr-10p in Short Term Toxicity Assays

$IC_{50}0$ (n=3)	MDA-MB-435S-F	MDA-MB-435S-F/ Adr-10p
Adriamycin	271 ± 3	316 ± 15
Taxol	28.3 ± 1.52	20.3 ± 2.1*
Carboplatin	41.3 ± 1.5	37.6 ± 1.15
Taxotere	3.33 ± 0.37	3.76 ± 0.20
VP-16	1844 ± 77	2663 ± 148**
5-fluorouracil	7.43 ± 0.68	3.36 ± 0.40*
Vincristine	12.9 ± 1.3	6.9 ± 0.69**

** $p < 0.005$

* $p < 0.05$

Table 3.3.4.3.a IC_{50} values for MDA-MB-435S-F and MDA-MB-435S-F/Adr-10p.

Drug	Fold resistance	Student t-test (p =)
Adriamycin	1.16	0.0288
Taxol	0.71	0.0056
Carboplatin	0.91	0.0571
Taxotere	1.12	0.1333
VP-16	1.44	0.0031
5-fluorouracil	0.45	0.0226
Vincristine	0.53	

Table 3.3.4.3.b Fold resistance of MDA-MB-435S-F/Adr-10p to MDA-MB-435S-F.

3.3.4.4 Cross resistance profile of MDA-MB-435S-F/Adr-10p10p in Short Term Toxicity Assays

IC_{50} (n=3)	MDA-MB-435S-F	MDA-MB-435S-F/ Adr-10p10p
Adriamycin	271 ± 3	381 ± 11.54**
Taxol	28.3 ± 1.52	17.6 ± 0.2*
Carboplatin	41.3 ± 1.5	24.6 ± 1.52*
Taxotere	3.33 ± 0.37	4.76 ± 0.152*
VP-16	1844 ± 77	3785 ± 79**
5-fluorouracil	7.43 ± 0.68	3.43 ± 0.05*
Vincristine	12.9 ± 1.3	32.1 ± 2.5 (n=2)**

** $p < 0.005$

* $p < 0.05$

Table 3.3.4.4.a IC_{50} values for MDA-MB-435S-F and MDA-MB-435S-F/ Adr-10p10p.

Drug	Fold resistance	Student t-test (p =)
Adriamycin	1.40	0.0038
Taxol	0.62	0.0079
Carboplatin	0.59	0.0098
Taxotere	1.42	0.0269
VP-16	2.05	0.00002
5-fluorouracil	0.46	0.0106
Vincristine	1.61	

Table 3.3.4.4.b Fold resistance of MDA-MB-435S-F/Adr-10p10p to MDA-MB-435S-F.

3.3.4.5 Summary of Short Term Resistance Profiles of MDA-MB-435S-F MDR Variants

Table 3.3.4.5 summarises the results of short term toxicity testing of the MDA-MB-435S-F taxol and adriamycin selected variants.

Cell Line	MDA-MB-435S-F	MDA-MB-435S-F/ Taxol-10p	MDA-MB-435S-F/ Taxol-10p4p	MDA-MB-435S-F/ Adr-10p	MDA-MB-435S-F/ Adr-10p10p
Adriamycin	1.00	0.89	1.68	1.16	1.40
Taxol	1.00	9.15	31.80	0.71	0.62
Carboplatin	1.00	1.31	0.79	0.91	0.59
Taxotere	1.00	3.67	18.73	1.12	1.42
VP-16	1.00	1.20	0.94	1.44	2.05
5-fluorouracil	1.00	0.47	0.91	0.45	0.46
Vincristine	1.00	5.78	13.64	0.53	1.61

Table 3.3.4.5 Summary of fold changes in resistance of MDA-MB-435S-F MDR variants

3.3.4.6 Long Term Toxicity Profiles for Adriamycin and Taxol

Long term toxicity assays also show that MDA-MB-435S-F failed to develop resistance to adriamycin, while developing resistance to taxol in long term assays.

Cell Line	**IC50 Taxol Long Term (ng/ml; n=3)**	**IC50 Adriamycin Long Term (ng/ml; n=3)**
MDA-MB-435S-F	2.12 ± 0.057	26.6 ± 1.95
MDA-MB-435S-F/ Taxol-10p	5.76 ± 0.251	30.6 ± 3.21
MDA-MB-435S-F/ Taxol-10p4p	9.63 ± 0.152	37.0 ± 2.64
MDA-MB-435S-F/ Adr-10p	3.16 ± 0.057	22.6 ± 1.52
MDA-MB-435S-F /Adr-10p10p	2.16 ± 0.208	20.2 ± 0.91

Table 3.3.4.6 IC50 values for MDA-MB-435S-F taxol and adriamycin selected variants in long term toxicity assays.

3.3.5 Adriamycin Accumulation in MDA-MB-435S-F MDR Variants

Adriamycin accumulation and efflux was examined in MDA-MB-435S-F and its taxol and adriamycin selected variants. In brief, as described in Section 2.11, cells were grown for 48 hours, after which time medium was removed and fresh medium containing adriamycin (10μM) was added. After a two-hour incubation, the media was removed from all flasks, and half the flasks were replaced with fresh media and returned to the 37°C incubator. Cells were collected from the remaining flasks by trypsinisation and adriamycin accumulation quantified. After a four-hour incubation, media was removed and cells collected by trypsinisation and adriamycin remaining in cells quantified. Efflux was calculated as the % of adriamycin effluxed during the four hour incubation.

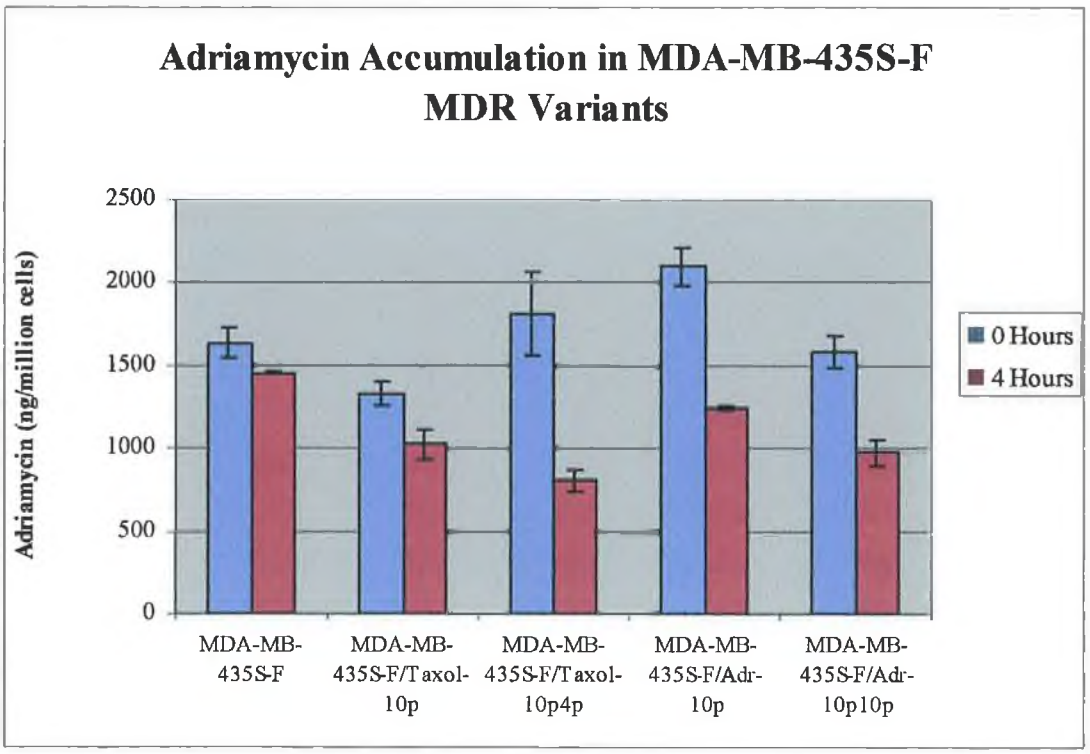

Figure 3.3.5 Adriamycin Accumulation in MDA-MB-435S-F MDR variants.

Table 3.3.5a describes the amount of adriamycin accumulated by MDA-MB-435S-F/Taxol-10p, MDA-MB-435S-F/Taxol-10p4p, MDA-MB-435S-F/Adr-10p and MDA-MB-435S-F/Adr-10p10p, as a % of that accumulated by the parental cell line MDA-MB-435S-F. Adriamycin uptake in MDA-MB-435S-F/Taxol-10p was less than that of the parent, while MDA-MB-435S-F/Taxol-10p4p and MDA-MB-435S-F/Adr-10p

accumulated more adriamycin than MDA-MB-435S-F. MDA-MB-435S-F/Adr-10p10p was similar to the parent.

Cell Line	% Adriamycin Influx relative to Parent
MDA-MB-435S-F	100.00
MDA-MB-435S-F/Taxol-10p	81.45
MDA-MB-435S-F/Taxol-10p4p	110.78
MDA-MB-435S-F/Adr-10p	128.41
MDA-MB-435S-F/Adr-10p10p	97.06

Table 3.3.5a % Adriamycin accumulated after 2 hour adriamycin exposure.

Table 3.3.5b describes the amount of adriamycin effluxed by MDA-MB-435S-F, MDA-MB-435S-F/Taxol-10p, MDA-MB-435S-F/Taxol-10p4p, MDA-MB-435S-F/Adr-10p and MDA-MB-435S-F/Adr-10p10p. All the selected variants exhibited greater efflux than the parent cell line. Adriamycin efflux was greater in MDA-MB-435S-F/Taxol-10p4p than in MDA-MB-435S-F/Taxol-10p, which corresponds to their adriamycin resistance profiles, as described in Section 3.3.4.5. Adriamycin efflux was similar in MDA-MB-435S-F/Adr-10p and MDA-MB-435S-F/Adr-10p10p.

Cell Line	% Adriamycin Effluxed after 4 hours
MDA-MB-435S-F	11.0
MDA-MB-435S-F/Taxol-10p	23.1
MDA-MB-435S-F/Taxol-10p4p	55.4
MDA-MB-435S-F/Adr-10p	40.6
MDA-MB-435S-F/Adr-10p10p	38.6

Table 3.3.5b % Adriamycin effluxed 4 hours post adriamycin removal from media.

Figure 3.3.5 shows that that the final adriamycin content is least in MDA-MB-435S-F/Taxol-10p4p followed by MDA-MB-435S-F/Adr-10p10p, which corresponds somewhat to their adriamycin resistance profiles, as described in Section 3.3.4.5.

3.3.6 Circumvention of Adriamycin Resistance by Verapamil and Sulindac in MDA-MB-435S-F MDR Variants

As described in section 3.3.5 all the MDR variants of MDA-MB-435S-F display increased adriamycin efflux. Despite this increase in adriamycin efflux, which one would assume would confer resistance to adriamycin, Table 3.3.4.5 shows that only MDA-MB-435S-F/Taxol-10p4p and MDA-MB-435S-F/Adr-10p10p display any increase in adriamycin resistance. To further investigate mechanisms of increased adriamycin efflux, combination assays were performed with adriamycin and either sulindac or verapamil. Sulindac circumvents MRP mediated adriamycin drug resistance, while verapamil is a modulator of MDR-1 mediated drug resistance, and to a lesser extent MRP. It was desired to see whether verapamil or sulindac could circumvent adriamycin resistance in MDA-MB-435S-F and its MDR variants.

Verapamil and sulindac were found to enhance adriamycin resistance in MDA-MB-435S-F and all its MDR variants. Sulindac was more potent than verapamil in the parental cell line MDA-MB-435S-F. The reverse was true for MDA-MB-435S-F/Taxol-10p, MDA-MB-435S-F/Taxol-10p4p, MDA-MB-435S-F/Adr-10p and MDA-MB-435S-F/Adr-10p10p. This would suggest that the role of MRP in the adriamycin resistance of MDA-MB-435S-F is declining while MDR-1 is emerging to play a greater role.

3.3.6.1 Adriamycin and Verapamil in MDA-MB-435S-F

	Average % Cell Survival (n=3)	**Standard Deviation**
Control	100.00	0.000
Adriamycin (10ng/ml)	98.49	1.204
Verapamil (10μg/ml)	100.98	0.370
Adriamycin (10ng/ml) + Verapamil (10μg/ml)	45.37	4.769
Verapamil (20μg/ml)	99.86	0.540
Adriamycin (10ng/ml) + Verapamil (20μg/ml)	20.08	3.760
Verapamil (30μg/ml)	99.20	2.875
Adriamycin (10ng/ml) + Verapamil (30μg/ml)	9.45	0.995

Table 3.3.6.1 Adriamycin and verapamil combination assays in MDA-MB-435S-F

3.3.6.2 Adriamycin and Sulindac in MDA-MB-435S-F

	Average % Cell Survival (n=3)	Standard Deviation
Control	100.00	0.000
Adriamycin (10ng/ml)	96.22	4.205
Sulindac (3μg/ml)	99.81	2.110
Adriamycin (10ng/ml) + Sulindac (3μg/ml)	39.87	4.492
Sulindac (6μg/ml)	98.08	2.214
Adriamycin (10ng/ml) + Sulindac (6μg/ml)	7.51	0.685
Sulindac (12μg/ml)	99.59	3.129
Adriamycin (10ng/ml) + Sulindac (12μg/ml)	3.11	0.358

Table 3.3.6.2 Adriamycin and sulindac combination assays in MDA-MB-435S-F

3.3.6.3 Adriamycin and Verapamil in MDA-MB-435S-F/Taxol-10p

	Average % Cell Survival (n=3)	Standard Deviation
Control	100.00	0.000
Adriamycin (10ng/ml)	100.49	2.642
Verapamil (10μg/ml)	99.01	0.416
Adriamycin (10ng/ml) + Verapamil (10μg/ml)	90.50	2.266
Verapamil (20μg/ml)	98.78	2.091
Adriamycin (10ng/ml) + Verapamil (20μg/ml)	61.06	3.258
Verapamil (30μg/ml)	98.01	0.815
Adriamycin (10ng/ml) + Verapamil (30μg/ml)	36.48	3.910

Table 3.3.6.3 Adriamycin and verapamil combination assays in MDA-MB-435S-F/Taxol-10p

3.3.6.4 Adriamycin and Sulindac in MDA-MB-435S-F/Taxol-10p

	Average % Cell Survival (n=3)	Standard Deviation
Control	100.00	0.000
Adriamycin (10ng/ml)	98.27	0.822
Sulindac (3μg/ml)	98.34	1.282
Adriamycin (10ng/ml) + Sulindac (3μg/ml)	98.00	1.367
Sulindac (6μg/ml)	97.44	3.021
Adriamycin (10ng/ml) + Sulindac (6μg/ml)	90.67	2.078
Sulindac (12μg/ml)	98.82	3.233
Adriamycin (10ng/ml) + Sulindac (12μg/ml)	74.35	1.864

Table 3.3.6.4 Adriamycin and sulindac combination assays in MDA-MB-435S-F/Taxol-10p

3.3.6.5 Adriamycin and Verapamil in MDA-MB-435S-F/Taxol-10p4p

	Average % Cell Survival (n=3)	Standard Deviation
Control	100.00	0.000
Adriamycin (10ng/ml)	99.50	2.244
Verapamil (10μg/ml)	99.73	1.846
Adriamycin (10ng/ml) + Verapamil (10μg/ml)	14.35	2.352
Verapamil (20μg/ml)	98.77	4.124
Adriamycin (10ng/ml) + Verapamil (20μg/ml)	4.50	2.313
Verapamil (30μg/ml)	99.98	0.363
Adriamycin (10ng/ml) + Verapamil (30μg/ml)	2.72	2.165

Table 3.3.6.5 Adriamycin and verapamil combination assays in MDA-MB-435S-F/Taxol-10p4p

3.3.6.6 Adriamycin and Sulindac in MDA-MB-435S-F/Taxol-10p4p

	Average % Cell Survival (n=3)	Standard Deviation
Control	100.00	0.000
Adriamycin (10ng/ml)	91.31	3.596
Sulindac (3μg/ml)	98.98	1.842
Adriamycin (10ng/ml) + Sulindac (3μg/ml)	46.30	2.272
Sulindac (6μg/ml)	98.97	1.609
Adriamycin (10ng/ml) + Sulindac (6μg/ml)	18.11	3.310
Sulindac (12μg/ml)	99.93	2.112
Adriamycin (10ng/ml) + Sulindac (12μg/ml)	13.26	1.602

Table 3.3.6.6 Adriamycin and sulindac combination assays in MDA-MB-435S-F/Taxol-10p4p

3.3.6.7 Adriamycin and Verapamil in MDA-MB-435S-F/Adr-10p

	Average % Cell Survival (n=3)	Standard Deviation
Control	100.00	0.000
Adriamycin (10ng/ml)	78.38	4.616
Verapamil (10μg/ml)	102.00	4.668
Adriamycin (10ng/ml) + Verapamil (10μg/ml)	16.54	1.313
Verapamil (20μg/ml)	101.45	5.689
Adriamycin (10ng/ml) + Verapamil (20μg/ml)	6.55	1.273
Verapamil (30μg/ml)	102.51	5.337
Adriamycin (10ng/ml) + Verapamil (30μg/ml)	4.41	0.468

Table 3.3.6.7 Adriamycin and verapamil combination assays in MDA-MB-435S-F/Adr-10p

3.3.6.8 Adriamycin and Sulindac in MDA-MB-435S-F/Adr-10p

	Average % Cell Survival (n=3)	Standard Deviation
Control	100.00	0.000
Adriamycin (10ng/ml)	81.14	7.074
Sulindac (3μg/ml)	96.50	2.731
Adriamycin (10ng/ml) + Sulindac (3μg/ml)	33.59	12.181
Sulindac (6μg/ml)	98.86	2.203
Adriamycin (10ng/ml) + Sulindac (6μg/ml)	13.48	3.816
Sulindac (12μg/ml)	96.89	2.030
Adriamycin (10ng/ml) + Sulindac (12μg/ml)	3.42	1.261

Table 3.3.6.8 Adriamycin and sulindac combination assays in MDA-MB-435S-F/Adr-10p

3.3.6.9 Adriamycin and Verapamil in MDA-MB-435S-F/Adr-10p10p

	Average % Cell Survival (n=3)	Standard Deviation
Control	100.00	0.000
Adriamycin (10ng/ml)	100.63	1.000
Verapamil (10μg/ml)	101.51	2.469
Adriamycin (10ng/ml) + Verapamil (10μg/ml)	82.57	7.926
Verapamil (20μg/ml)	98.07	8.143
Adriamycin (10ng/ml) + Verapamil (20μg/ml)	38.41	8.165
Verapamil (30μg/ml)	100.39	1.822
Adriamycin (10ng/ml) + Verapamil (30μg/ml)	21.16	2.147

Table 3.3.6.9 Adriamycin and verapamil combination assays in MDA-MB-435S-F/Adr-10p10p

3.3.6.10 Adriamycin and Sulindac in MDA-MB-435S-F/Adr-10p10p

	Average % Cell Survival (n=3)	Standard Deviation
Control	100.00	0.000
Adriamycin (10ng/ml)	99.48	2.295
Sulindac (3μg/ml)	98.27	1.413
Adriamycin (10ng/ml) + Sulindac (3μg/ml)	99.10	3.304
Sulindac (6μg/ml)	99.39	1.300
Adriamycin (10ng/ml) + Sulindac (6μg/ml)	82.54	3.857
Sulindac (12μg/ml)	99.89	0.181
Adriamycin (10ng/ml) + Sulindac (12μg/ml)	27.67	4.594

Table 3.3.6.10 Adriamycin and sulindac combination assays in MDA-MB-435S-F/Adr-10p10p

3.3.7 Circumvention of Taxol Resistance by Verapamil and Sulindac in MDA-MB-435S-F MDR Variants

It was reported in section 3.3.6 that verapamil and sulindac were found to enhance adriamycin resistance in MDA-MB-435S-F and all its MDR variants. Sulindac was more potent than verapamil in the parental cell line MDA-MB-435S-F. The reverse was found for MDA-MB-435S-F/Taxol-10p, MDA-MB-435S-F/Taxol-10p4p, MDA-MB-435S-F/Adr-10p and MDA-MB-435S-F/Adr-10p10p. This suggested that the role of mrp in the adriamycin resistance of MDA-MB-435S-F is declining while MDR-1 is emerging to play a greater role.

Sulindac was not found to circumvent taxol resistance, indicating that taxol is not transported by MRP. Interestingly taxol was circumvented by verapamil only in MDA-MB-435S-F/Taxol-10p and MDA-MB-435S-F/Taxol-10p4p. It had no effect on taxol resistance in the parental cell line or either of the adriamycin selected variants. It is possible that the verapamil circumvention of adriamycin observed in section 3.3.6 was as a result of inhibition of MRP transport of adriamycin, and not by MDR-1 transport. However if this were the case then sulindac circumvention would be stronger than verapamil. However a discrepancy remains, if taxol is transported by MDR-1 in MDA-MB-435S-F/Taxol-10p and MDA-MB-435S-F/Taxol-10p4p, why is enhanced circumvention by verapamil of adriamycin resistance or larger increases in adriamycin resistance, not observed in this cell line? Perhaps verapamil is inhibiting the transport of taxol through some novel transporter protein.

3.3.7.1 Taxol and Verapamil in MDA-MB-435S-F

	Average % Cell Survival (n=3)	Standard Deviation
Control	100.00	0.00
Taxol (2ng/ml)	31.75	5.23
Verapamil (10μg/ml)	100.10	1.59
Taxol (2ng/ml) + Verapamil (10μg/ml)	29.91	4.73
Verapamil (20μg/ml)	99.46	2.46
Taxol (2ng/ml)+ Verapamil (20μg/ml)	28.62	7.32
Verapamil (30μg/ml)	99.58	1.82
Taxol (2ng/ml)+ Verapamil (30μg/ml)	28.03	6.00

Table 3.3.7.1 Taxol and verapamil combination assays in MDA-MB-435S-F

3.3.7.2 Taxol and Sulindac in MDA-MB-435S-F

	Average % Cell Survival (n=3)	Standard Deviation
Control	100.00	0.00
Taxol (2ng/ml)	35.67	1.60
Sulindac (3μg/ml)	97.90	2.23
Taxol (2ng/ml)+ Sulindac (3μg/ml)	33.61	1.71
Sulindac (6μg/ml)	97.73	0.89
Taxol (2ng/ml)+ Sulindac (6μg/ml)	32.14	1.56
Sulindac (12μg/ml)	98.28	1.32
Taxol (2ng/ml)+ Sulindac (12μg/ml)	29.25	1.49

Table 3.3.7.2 Taxol and sulindac combination assays in MDA-MB-435S-F

3.3.7.3 Taxol and Verapamil in MDA-MB-435S-F/Taxol-10p

	Average % Cell Survival (n=3)	Standard Deviation
Control	100.00	0.00
Taxol (5ng/ml)	58.16	1.62
Verapamil (10μg/ml)	99.05	1.82
Taxol (5ng/ml) + Verapamil (10μg/ml)	15.58	0.62
Verapamil (20μg/ml)	98.63	0.27
Taxol (5ng/ml)+ Verapamil (20μg/ml)	15.14	0.37
Verapamil (30μg/ml)	97.19	1.92
Taxol (5ng/ml)+ Verapamil (30μg/ml)	16.33	1.05

Table 3.3.7.3 Taxol and verapamil combination assays in MDA-MB-435S-F/Taxol-10p

3.3.7.4 Taxol and Sulindac in MDA-MB-435S-F/Taxol-10p

	Average % Cell Survival (n=3)	Standard Deviation
Control	100.00	0.00
Taxol (5ng/ml)	62.35	1.20
Sulindac (3μg/ml)	99.53	2.06
Taxol (5ng/ml)+ Sulindac (3μg/ml)	60.29	0.41
Sulindac (6μg/ml)	94.78	7.39
Taxol (5ng/ml)+ Sulindac (6μg/ml)	60.21	1.07
Sulindac (12μg/ml)	98.45	3.11
Taxol (5ng/ml)+ Sulindac (12μg/ml)	59.69	3.11

Table 3.3.7.4 Taxol and sulindac combination assays in MDA-MB-435S-F/Taxol-10p

3.3.7.5 Taxol and Verapamil in MDA-MB-435S-F/Taxol-10p4p

	Average % Cell Survival (n=3)	**Standard Deviation**
Control	100.00	0.00
Taxol (10ng/ml)	48.71	2.43
Verapamil (10μg/ml)	100.08	1.62
Taxol (10ng/ml) + Verapamil (10μg/ml)	5.25	4.55
Verapamil (20μg/ml)	98.46	1.30
Taxol (10ng/ml)+ Verapamil (20μg/ml)	8.18	0.86
Verapamil (30μg/ml)	98.04	1.61
Taxol (10ng/ml)+ Verapamil (30μg/ml)	8.02	0.61

Table 3.3.7.5 Taxol and verapamil combination assays in MDA-MB-435S-F/Taxol-10p4p

3.3.7.6 Taxol and Sulindac in MDA-MB-435S-F/Taxol-10p4p

	Average % Cell Survival (n=3)	Standard Deviation
Control	100.00	0.00
Taxol (10ng/ml)	46.71	4.34
Sulindac (3μg/ml)	99.43	3.12
Taxol (10ng/ml)+ Sulindac (3μg/ml)	44.44	4.56
Sulindac (6μg/ml)	99.50	3.08
Taxol (10ng/ml)+ Sulindac (6μg/ml)	43.78	4.55
Sulindac (12μg/ml)	96.61	3.14
Taxol (10ng/ml)+ Sulindac (12μg/ml)	40.63	3.40

Table 3.3.7.6 Taxol and sulindac combination assays in MDA-MB-435S-F/Taxol-10p4p

3.3.7.7 Taxol and Verapamil in MDA-MB-435S-F/Adr-10p

	Average % Cell Survival (n=3)	**Standard Deviation**
Control	100.00	0.00
Taxol (3ng/ml)	22.27	1.76
Verapamil (10μg/ml)	99.90	5.84
Taxol (3ng/ml) + Verapamil (10μg/ml)	21.33	0.54
Verapamil (20μg/ml)	98.71	2.47
Taxol (3ng/ml)+ Verapamil (20μg/ml)	26.39	5.95
Verapamil (30μg/ml)	101.20	8.90
Taxol (3ng/ml)+ Verapamil (30μg/ml)	22.26	0.77

Table 3.3.7.7 Taxol and verapamil combination assays in MDA-MB-435S-F/Adr-10p

3.3.7.8 Taxol and Sulindac in MDA-MB-435S-F/Adr-10p

	Average % Cell Survival (n=3)	Standard Deviation
Control	100.00	0.00
Taxol (3ng/ml)	22.56	2.86
Sulindac (3μg/ml)	98.57	5.61
Taxol (3ng/ml)+ Sulindac (3μg/ml)	23.89	1.23
Sulindac (6μg/ml)	96.89	7.58
Taxol (3ng/ml)+ Sulindac (6μg/ml)	22.06	2.68
Sulindac (12μg/ml)	98.44	6.44
Taxol (3ng/ml)+ Sulindac (12μg/ml)	20.62	1.55

Table 3.3.7.8 Taxol and sulindac combination assays in MDA-MB-435S-F/Adr-10p

3.3.7.9 Taxol and Verapamil in MDA-MB-435S-F/Adr-10p10p

	Average % Cell Survival (n=3)	Standard Deviation
Control	100.00	0.00
Taxol (3ng/ml)	22.46	1.86
Verapamil (10μg/ml)	81.54	8.68
Taxol (3ng/ml) + Verapamil (10μg/ml)	17.72	2.62
Verapamil (20μg/ml)	68.38	7.41
Taxol (3ng/ml)+ Verapamil (20μg/ml)	18.65	1.63
Verapamil (30μg/ml)	65.37	1.33
Taxol (3ng/ml)+ Verapamil (30μg/ml)	16.92	1.57

Table 3.3.7.9 Taxol and verapamil combination assays in MDA-MB-435S-F/Adr-10p10p

3.3.7.10 Taxol and Sulindac in MDA-MB-435S-F/Adr-10p10p

	Average % Cell Survival (n=3)	Standard Deviation
Control	100.00	0.00
Taxol (3ng/ml)	18.76	1.45
Sulindac (3µg/ml)	102.62	2.33
Taxol (3ng/ml)+ Sulindac (3µg/ml)	17.25	1.27
Sulindac (6µg/ml)	103.86	5.60
Taxol (3ng/ml)+ Sulindac (6µg/ml)	16.88	1.85
Sulindac (12µg/ml)	109.86	4.13
Taxol (3ng/ml)+ Sulindac (12µg/ml)	17.82	1.21

Table 3.3.7.10 Taxol and sulindac combination assays in MDA-MB-435S-F/Adr-10p10p

3.3.8 Expression of Drug Resistance Associated Genes in MDA-MB-435S-F MDR variants

A panel of genes associated with drug resistance were examined at the mRNA level by RT-PCR to determine whether their expression was affected by taxol and adriamycin selection.

3.3.8.1 MDR1

Figure 3.3.8.1 shows that MDR-1 mRNA expression was induced by taxol but not adriamycin in MDA-MB-435S-F.

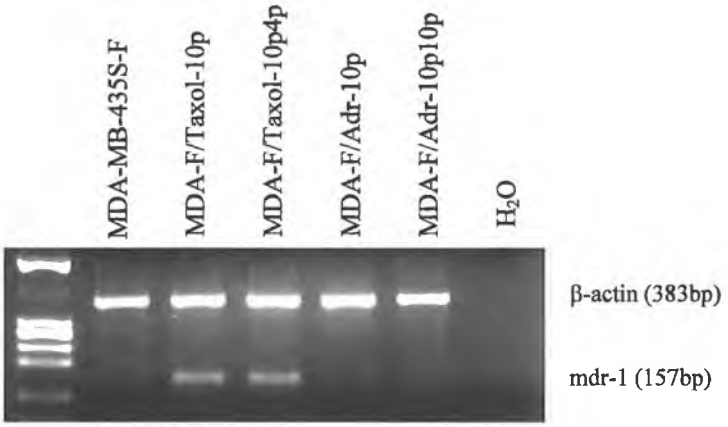

Figure 3.3.8.1 Expression of MDR-1 mRNA in MDA-MB-435S-F MDR variants.

3.3.8.2 MRP-1

Figure 3.3.8.2 shows that mrp-1 mRNA expression was induced slightly by taxol and adriamycin in MDA-MB-435S-F.

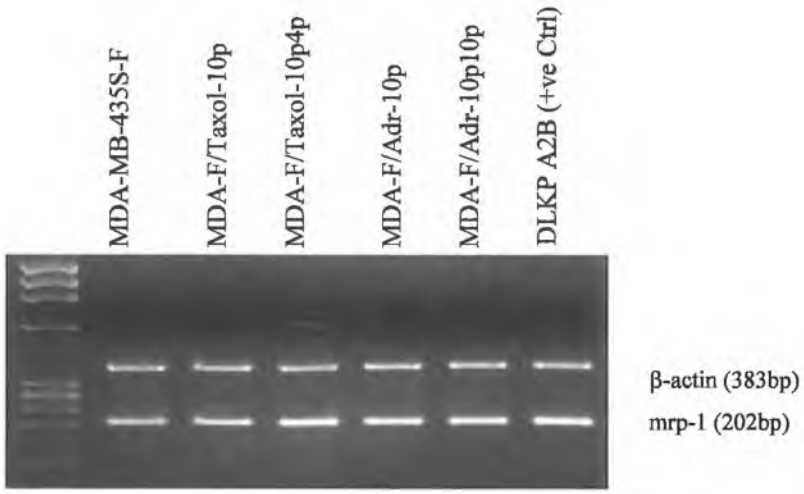

Figure 3.3.8.2 Expression of mrp-1 mRNA in MDA-MB-435S-F MDR variants.

Cell Line	Levels of mrp1 mRNA Expression (%)
MDA-MB-435S-F	100
MDA-MB-435S-F/Taxol-10p	115.1
MDA-MB-435S-F/Taxol-10p4p	141.5
MDA-MB-435S-F/Adr-10p	131.6
MDA-MB-435S-F/Adr-10p10p	117.8

Table 3.3.8.2 Levels of MRP-1 mRNA in MDA-MB-435S-F MDR variants.

3.3.8.3 MRP-2

Figure 3.3.8.3 shows that mrp-2 mRNA expression was reduced by taxol and adriamycin in MDA-MB-435S-F. This result is dependent on β-actin levels, being lower in MDA-MB-435S-F.

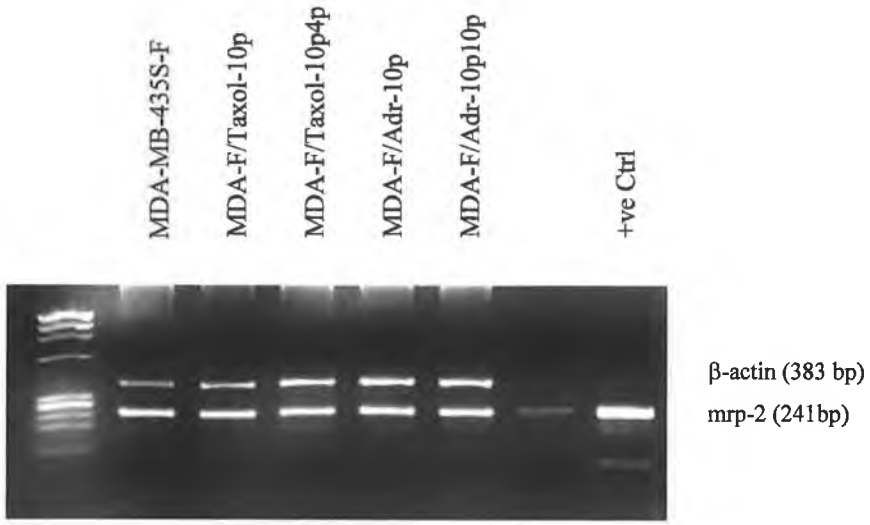

Figure 3.3.8.3 Expression of mrp-2 mRNA in MDA-MB-435S-F MDR variants.

Cell Line	Levels of mrp2 mRNA Expression (%)
MDA-MB-435S-F	100
MDA-MB-435S-F/Taxol-10p	77.8
MDA-MB-435S-F/Taxol-10p4p	47.1
MDA-MB-435S-F/Adr-10p	47.7
MDA-MB-435S-F/Adr-10p10p	56.4

Table 3.3.8.3 Levels of mrp-2 mRNA in MDA-MB-435S-F MDR variants.

3.3.8.4 MRP-4

Figure 3.3.8.4 shows that neither MDA-MB-435S-F nor any of it adriamycin or taxol selected variants expressed mrp-4 mRNA.

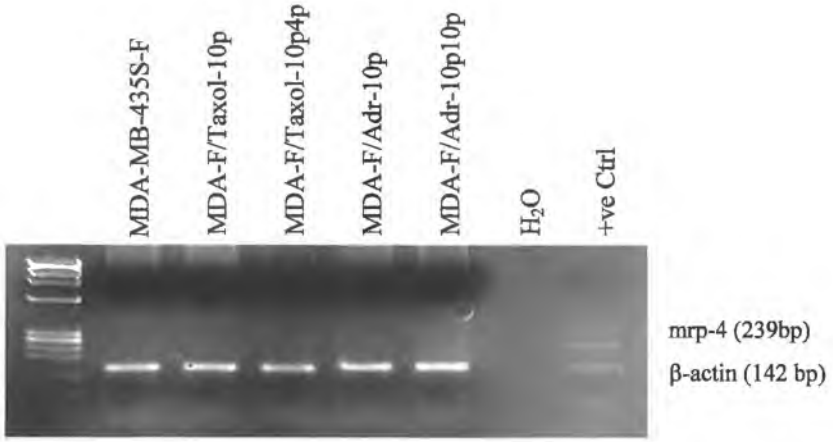

Figure 3.3.8.4 Expression of mrp-4 mRNA in MDA-MB-435S-F MDR variants.

3.3.8.5 MRP-5

Figure 3.3.8.5 shows that neither MDA-MB-435S-F nor any of it adriamycin or taxol selected variants expressed mrp-5 mRNA.

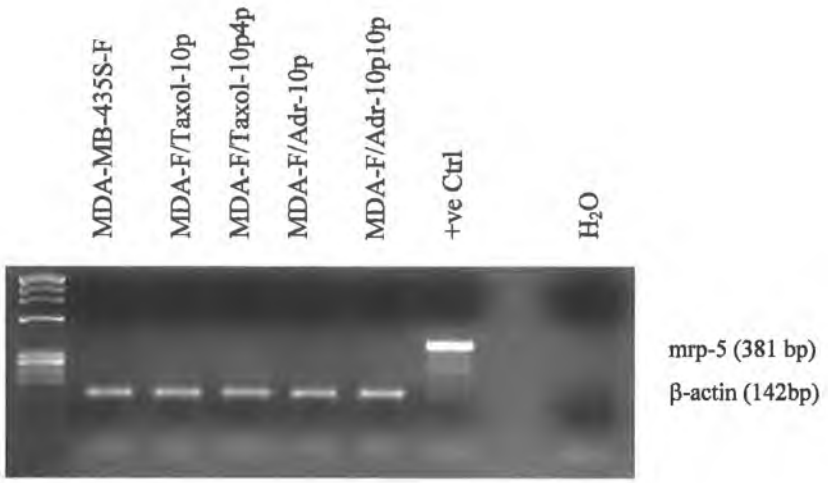

Figure 3.3.8.5 Expression of mrp-5 mRNA in MDA-MB-435S-F MDR variants.

3.3.8.6 Dihydrofolate Reductase (DHFR)

Figure 3.3.8.6 shows no change in the expression of DHFR mRNA in response to adriamycin or taxol selection.

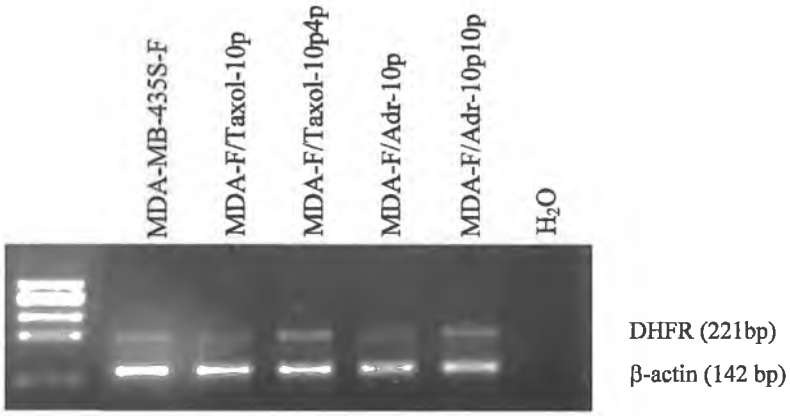

Figure 3.3.8.6 Expression of DHFR mRNA in MDA-MB-435S-F MDR variants.

Cell Line	Levels of DHFR mRNA Expression (%)
MDA-MB-435S-F	100
MDA-MB-435S-F/Taxol-10p	72
MDA-MB-435S-F/Taxol-10p4p	101
MDA-MB-435S-F/Adr-10p	84
MDA-MB-435S-F/Adr-10p10p	128

Table 3.3.8.6 Levels of DHFR mRNA in MDA-MB-435S-F MDR variants.

3.3.8.7 Glutathione-S-Transferase π (GSTπ)

Figure 3.3.8.7 shows reduced expression of GSTπ mRNA in both taxol and adriamycin selected variants of MDA-MB-435S-F. This is dependent on β-actin levels being lower in MDA-MB-435S-F. By eye, there appears to be no change in expression.

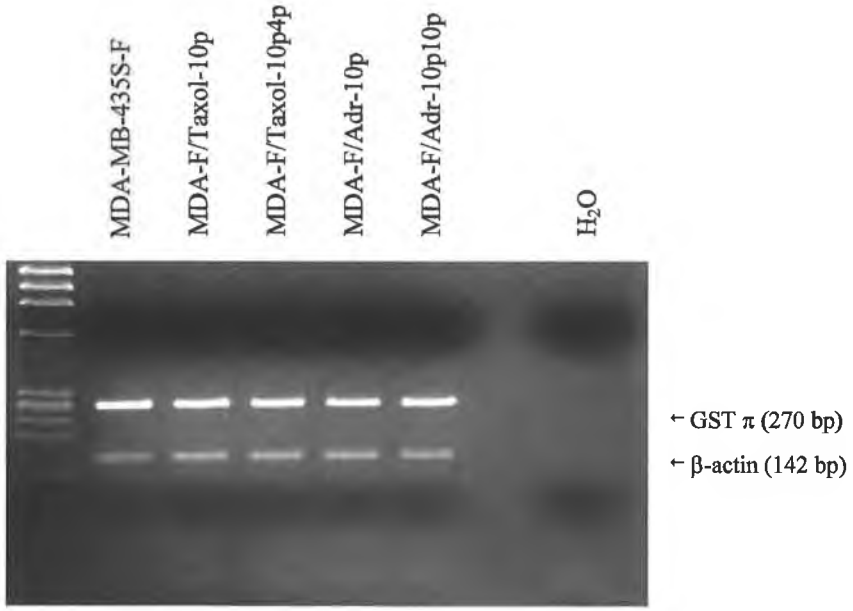

Figure 3.3.8.7 Expression of GSTπ mRNA in MDA-MB-435S-F MDR variants.

Cell Line	Levels of GSTπ mRNA Expression (%)
MDA-MB-435S-F	100
MDA-MB-435S-F/Taxol-10p	62.1
MDA-MB-435S-F/Taxol-10p4p	62.4
MDA-MB-435S-F/Adr-10p	52.0
MDA-MB-435S-F/Adr-10p10p	70.3

Table 3.3.8.7 Levels of GSTπ mRNA in MDA-MB-435S-F MDR variants.

3.8.8.8 Thymidylate Synthase (TS)

Densitometry of figure 3.3.8.8 shows a slight reduction in expression of TS mRNA in MDA-MB-435S-F/Taxol-10p, which increases in MDA-MB-435S-F/Taxol-10p4p after further taxol selection, to levels greater than the parental cell line. Reduced expression of TS mRNA was detected in both MDA-MB-435S-F/Adr-10p and MDA-MB-435S-F/Adr-10p10p.

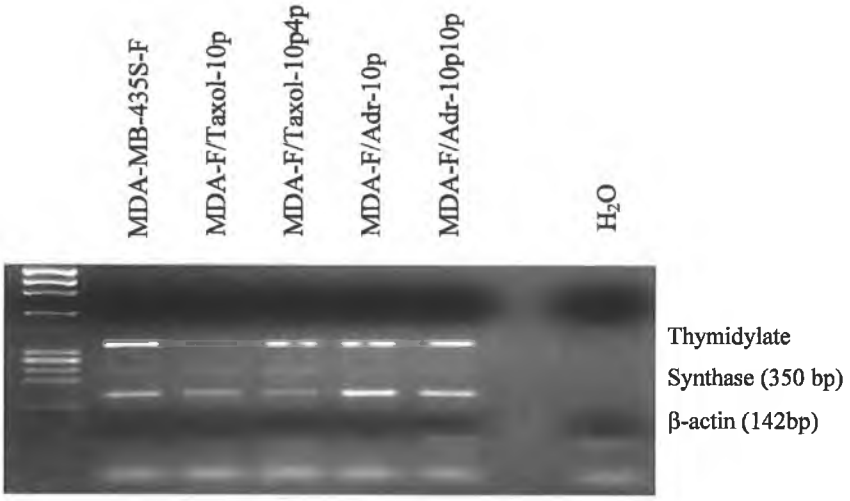

Figure 3.3.8.8 Expression of TS mRNA in MDA-MB-435S-F MDR variants.

Cell Line	Levels of TS mRNA Expression (%)
MDA-MB-435S-F	100
MDA-MB-435S-F/Taxol-10p	79.3
MDA-MB-435S-F/Taxol-10p4p	121.5
MDA-MB-435S-F/Adr-10p	75.9
MDA-MB-435S-F/Adr-10p10p	84.1

Table 3.3.8.8 Levels of TS mRNA in MDA-MB-435S-F MDR variants.

3.3.8.9 Topoisomerase I (Topo I)

Figure 3.3.8.9 shows that expression of Topo I mRNA decreased in later stage Taxol selection, as it is not decreased in MDA-MB-435S-F/Taxol-10p, but does decrease in MDA-MB-435S-F/Taxol-10p4p. Topo I levels decreased with increasing adriamycin resistance as shown in MDA-MB-435S-F/Adr-10p and MDA-MB-435S-F/Adr-10p10p.

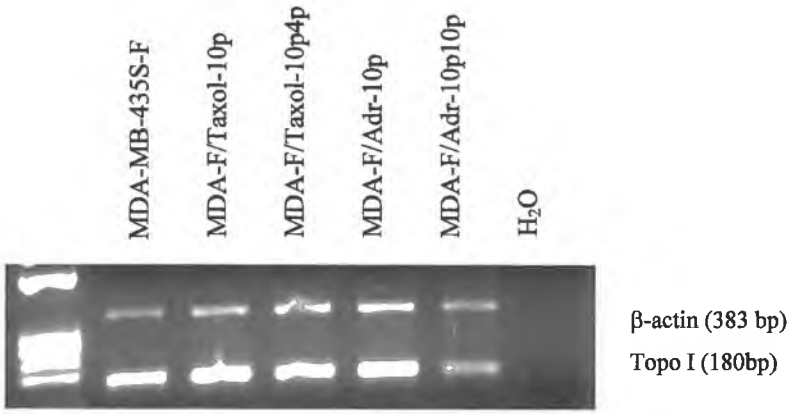

Figure 3.3.8.9 Expression of Topo I mRNA in MDA-MB-435S-F MDR variants.

Cell Line	Levels of Topo I mRNA Expression (%)
MDA-MB-435S-F	100
MDA-MB-435S-F/Taxol-10p	102
MDA-MB-435S-F/Taxol-10p4p	63
MDA-MB-435S-F/Adr-10p	81
MDA-MB-435S-F/Adr-10p10p	52

Table 3.3.8.9 Levels of Topo I mRNA in MDA-MB-435S-F MDR variants.

3.3.8.10 Topoisomerase IIα

Figure 3.3.8.10 shows that expression of Topo IIα mRNA was not detectable in the parental cell line MDA-MB-435S-F. Its expression was induced by taxol and adriamycin selection. Expression was not detectable in MDA-MB-435S-F/Adr-10p10p, but this is most likely a reflection on the low levels of β-actin in this cell line, in this PCR prep. Densitometry could not be performed to compare expression of Topo IIα as it was not detectable in the parental cell line.

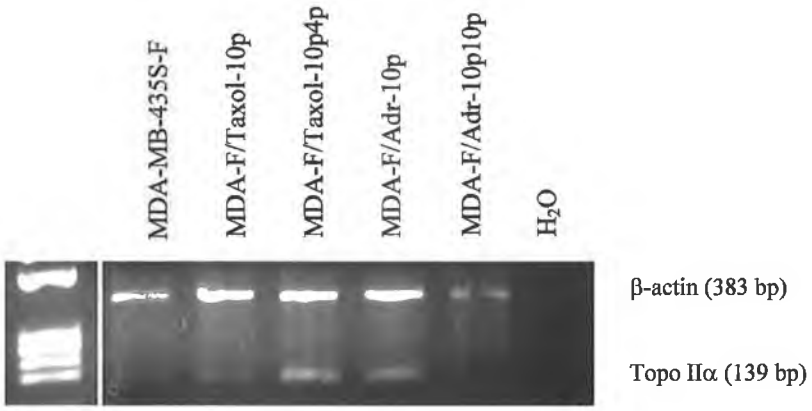

Figure 3.3.8.10 Expression of Topo IIα mRNA in MDA-MB-435S-F MDR variants.

Cell Line	Levels of Topo IIα mRNA Expression (%)
MDA-MB-435S-F	-
MDA-MB-435S-F/Taxol-10p	+
MDA-MB-435S-F/Taxol-10p4p	+++
MDA-MB-435S-F/Adr-10p	++
MDA-MB-435S-F/Adr-10p10p	-

Table 3.3.8.9 Levels of Topo IIα mRNA in MDA-MB-435S-F MDR variants.

3.3.8.11 Topoisomerase IIβ

Densitometry of figure 3.3.8.11 showed that expression of Topo IIβ mRNA is increased by taxol selection. In contrast levels of expression were reduced by adriamycin selection. Visually there appears to be no change in the expression of Topo IIβ mRNA.

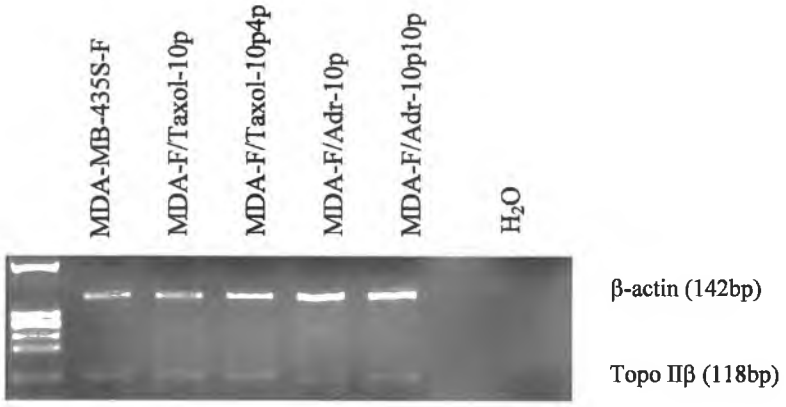

Figure 3.3.8.11 Expression of Topo IIβ mRNA in MDA-MB-435S-F MDR variants.

Cell Line	Levels of Topo IIβ mRNA Expression (%)
MDA-MB-435S-F	100
MDA-MB-435S-F/Taxol-10p	151
MDA-MB-435S-F/Taxol-10p4p	134
MDA-MB-435S-F/Adr-10p	71
MDA-MB-435S-F/Adr-10p10p	90

Table 3.3.8.11 Levels of Topo IIβ mRNA in MDA-MB-435S-F MDR variants.

3.3.8.11 Summary of Changes in Gene Expression

Table 3.3.8.11 give an overview of the changes in drug resistance associated gene expression. Taxol selection of MDA-MB-435S-F resulted in upregulation of MDR-1, mrp-1, topo I and topo IIα mRNA expression and downregulation of mrp-2 mRNA expression. TS mRNA decreased in MDA-MB-435S-F/Taxol-10p, while TS mRNA increased in MDA-MB-435S-F/Taxol-104p. Adriamycin selection of MDA-MB-435S-F resulted in upregulation of mrp-1, topo I and topo IIα mRNA expression, downregulation of mrp-2 and TS mRNA expression. Mrp-4 and mrp-5 mRNA were undetectable in these cell lines.

RT-PCR	MDA-F	MDA-F/ Taxol-10p	MDA-F/ Taxol-10p4p	MDA-F/ Adr-10p	MDA-F/ Adr-10p10p
Mdr-1	neg	+	+	neg	neg
Mrp-1	exp	o	+	+	o
Mrp-2	exp	-	-	-	-
Mrp-4	neg	neg	neg	neg	neg
Mrp-5	neg	neg	neg	neg	neg
Topo I	exp	o	-	-	-
Topo IIα	neg	+	+	+	inconclusive
Topo IIβ	exp	o	-	-	-
DHFR	exp	-	o	-	+
TS	exp	-	-	-	-
GSTπ	exp	-	+	-	-
C-erbB-1	exp	-	-	-	-
C-erbB-2	exp	-	-	-	-
C-erbB-4	exp	-	-	-	-

Table 3.3.8.11 Summary of changes in expression of drug resistance related genes.

+ increase in expression

- decrease in expression

o no change in expression

neg Not expressed

exp expressed by parental cell line

3.3.9 Levels of $p170^{MDR-1}$ and MRP-1 protein expression in MDA-MB-435S-F MDR variants

Western blots were performed to examine the expression of MDR-1 and MRP-1 at the protein level, to determine whether changes in their expression detected at the mRNA level were reflected at the protein level.

Figure 3.3.9.1 shows the expression of MDR-1 protein in MDA-MB-435S-F MDR variants. Taking β-actin into account, there only appears to be a slight increase in MDR-1 expression in the MDA-MB-435S-F MDR variants. Figure 3.3.9.2 shows the expression of MRP-1 protein in MDA-MB-435S-F MDR variants. Taking β-actin into account, MRP-1 expression is increased in all of the MDA-MB-435S-F MDR variants.

3.3.9.1 $p170^{MDR-1}$ protein expression

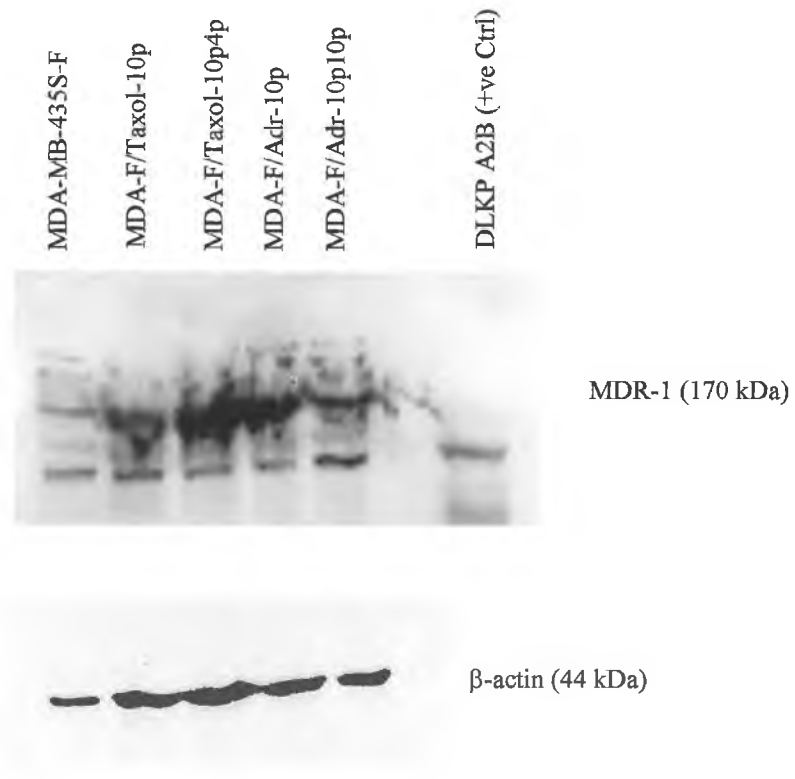

Figure 3.3.9.1 Expression of $p170^{MDR-1}$ protein in MDA-MB-435S-F MDR variants.

3.3.9.2 MRP-1 protein expression

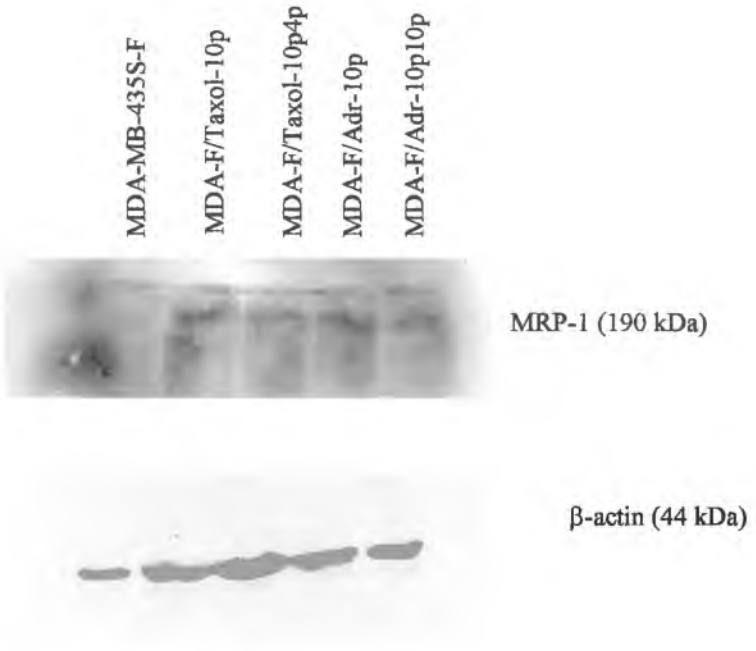

Figure 3.3.9.2 Expression of MRP-1 protein in MDA-MB-435S-F MDR variants.

Note - A control gel was run for the detection of β-actin levels in the protein preps, due to the β-actin being of too low a molecular weight to detect on the same gel as MDR-1 and MRP-1.

3.3.10 Expression of Members of the ErbB Receptor Family in MDA-MB-435S-F MDR variants.

In order to determine the effects of taxol and adriamycin selection on the expression of ErbB receptors, RT-PCR was performed to determine the expression of ErbB receptors at the mRNA level in these drug selected variants. Western blotting and immunoprecipitation were then performed to determine whether any changes were also reflected at the protein level.

3.3.10.1 Expression of ErbB Receptor mRNA

Figure 3.3.10.1.1 shows the expression of c-erbB-1 mRNA in MDA-MB-435S-F Taxol and adriamycin selected variants. C-erbB-1 mRNA levels were unaffected by taxol or adriamycin selection.

Figure 3.3.10.1.2 shows the expression of c-erbB-2 mRNA in MDA-MB-435S-F Taxol and adriamycin selected variants. C-erbB-2 mRNA expression decreased with increasing taxol and adriamycin resistance. This decrease was greater in the adriamycin selected variants than the taxol selected variants.

Figure 3.3.10.1.3 shows the expression of c-erbB-4 mRNA in MDA-MB-435S-F Taxol and adriamycin selected variants. C-erbB-4 mRNA expression was not induced in the initial selection with taxol, which generated the cell line MDA-MB-435S-F/Taxol-10p. It was induced though following four further pulses, generating the cell line MDA-MB-435S-F/Taxol-10p4p. C-erbB-4 mRNA expression was initially induced in the first selection with adriamycin, which generated the cell line MDA-MB-435S-F/Adr-10p. Levels then reverted back similar to the parent in the subsequent additional pulses resulting in MDA-MB-435S-F/Adr-10p10p.

3.3.10.1.1 C-erbB-1 mRNA expression

Figure 3.3.10.1.1 shows the expression of c-erbB-1 mRNA in MDA-MB-435S-F Taxol and adriamycin selected variants. No c-erbB-1 signal difference was apparent between the parental cell line or the taxol or adriamycin selected variants.

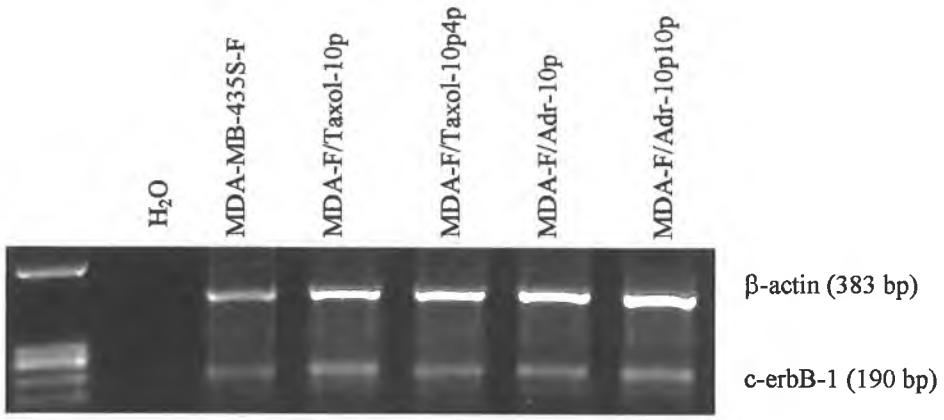

Figure 3.3.10.1.1 Expression of c-erbB-1 mRNA in MDA-MB-435S-F Taxol and adriamycin selected variants.

Cell Line	**Levels of C-erbB-1 mRNA Expression (%)**
MDA-MB-435S-F	100
MDA-MB-435S-F/Taxol-10p	93
MDA-MB-435S-F/Taxol-10p4p	70
MDA-MB-435S-F/Adr-10p	64
MDA-MB-435S-F/Adr-10p10p	60

Table 3.3.10.1.1 Levels of C-erbB-1 mRNA expression in MDA-MB-435S-F variants.

3.3.10.1.2 C-erbB-2 mRNA expression

Figure 3.3.10.1.2 shows the expression of c-erbB-2 mRNA in MDA-MB-435S-F Taxol and adriamycin selected variants. C-erbB-2 mRNA expression decreased with increasing taxol and adriamycin resistance.

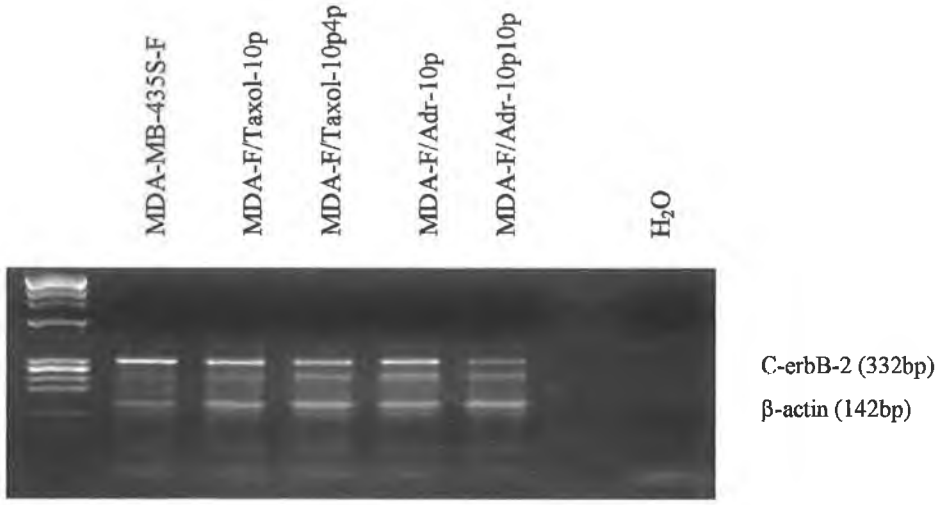

Figure 3.3.10.1.2 Expression of c-erbB-2 mRNA in MDA-MB-435S-F Taxol and adriamycin selected variants (unidentified bands are also present and may be due to primer dimer formation).

Cell Line	Levels of C-erbB-2 mRNA Expression (%)
MDA-MB-435S-F	100
MDA-MB-435S-F/Taxol-10p	66.6
MDA-MB-435S-F/Taxol-10p4p	51.3
MDA-MB-435S-F/Adr-10p	58.4
MDA-MB-435S-F/Adr-10p(200-10p)	29.6

Table 3.3.10.1.2 Levels of C-erbB-2 mRNA expression in MDA-MB-435S-F variants.

3.3.10.1.3 C-erbB-4 mRNA expression

Figure 3.3.10.1.3 shows the expression of c-erbB-4 mRNA in MDA-MB-435S-F Taxol and adriamycin selected variants. C-erbB-4 mRNA expression was unchanged in MDA-MB-435S-F/Taxol-10p, and then increased in MDA-MB-435S-F/Taxol-10p4p. C-erbB-4 mRNA expression increased in MDA-MB-435S-F/Adr-10p, returned to parental levels in MDA-MB-435S-F/Adr-10p10p.

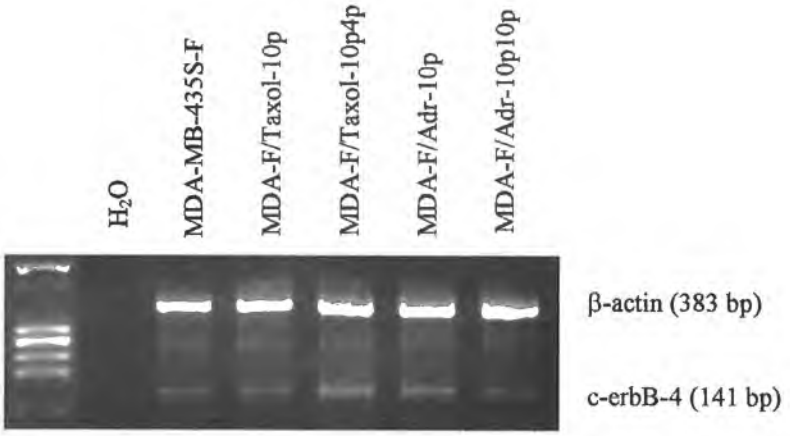

Figure 3.3.10.1.3 Expression of c-erbB-4 mRNA in MDA-MB-435S-F Taxol and adriamycin selected variants.

Cell Line	Levels of C-erbB-4 mRNA Expression (%)
MDA-MB-435S-F	100
MDA-MB-435S-F/Taxol-10p	103
MDA-MB-435S-F/Taxol-10p4p	167
MDA-MB-435S-F/Adr-10p	143
MDA-MB-435S-F/Adr-10p10p	90

Table 3.3.10.1.3 Levels of C-erbB-4 mRNA expression in MDA-MB-435S-F variants.

3.3.10.2 Expression of ErbB Receptor protein

Figure 3.3.10.1.1 showed that the expression of c-erbB-1 mRNA in MDA-MB-435S-F Taxol and adriamycin selected variants was unchanged. C-erbB-1 protein expression was found to have increased with increasing taxol and adriamycin resistance, as shown in figure 3.3.10.2.1.

Figure 3.3.10.1.2 showed that the expression of c-erbB-2 mRNA in MDA-MB-435S-F Taxol and adriamycin selected variants decreased with increasing taxol and adriamycin resistance. This decrease was greater in the adriamycin selected variants than the taxol selected variants. Figure 3.3.10.2.2 showed that the expression of c-erbB-2 protein was in fact unchanged in the MDA-MB-435S-F MDR variants. It should be noted that the lane containing BT474A protein is not evenly loaded and therefore does not reflect the levels of c-erbB-2 expressed compared to MDA-MB-435S-F, but rather was included as a positive control in this immunoprecipitation.

Figure 3.3.10.2.3 showed that c-erbB-3 protein expression decreased with increasing taxol resistance and also with adriamycin selection

Figure 3.3.10.1.3 showed while the expression of c-erbB-4 mRNA in MDA-MB-435S-F was increased in MDA-MB-435S-F/taxol-10p4p and MDA-MB-435S-F/Adr-10p, levels were similar to the parental cell line in the other two variants. C-erbB-4 protein expression was virtually undetectable in any of the MDA-MB-435S-F variants (figure 3.3.10.2.4).

3.3.10.2.1 C-erbB-1 protein expression

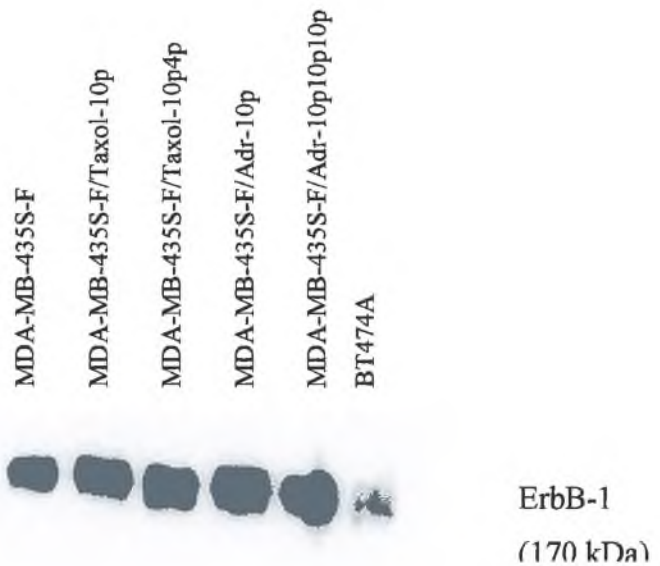

Figure 3.1.10.2.1a Immunoprecipitation of c-erbB-1 protein expression in MDA-MB-435S-F MDR variants

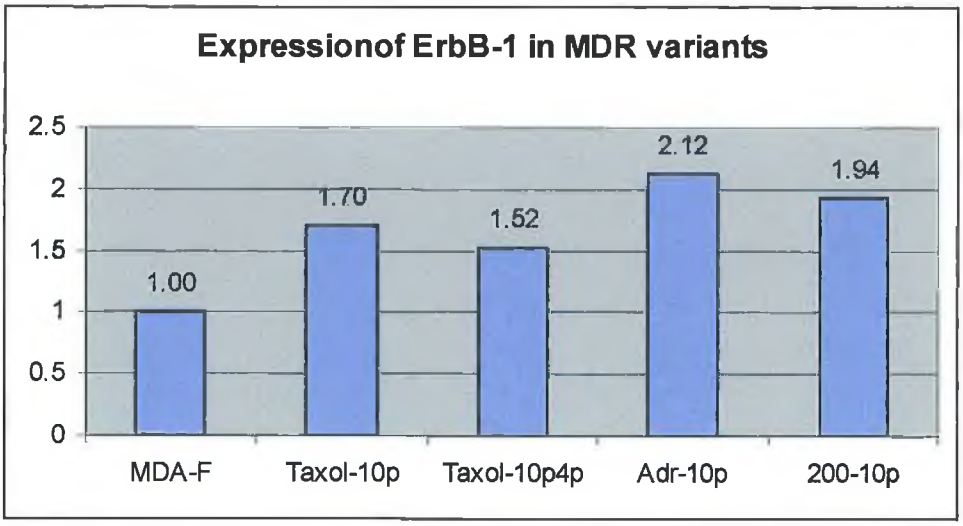

Figure 3.1.10.2.1b C-erbB-1 Expression in MDA-MB-435S-F MDR variants

3.3.10.2.2 C-erbB-2 protein expression

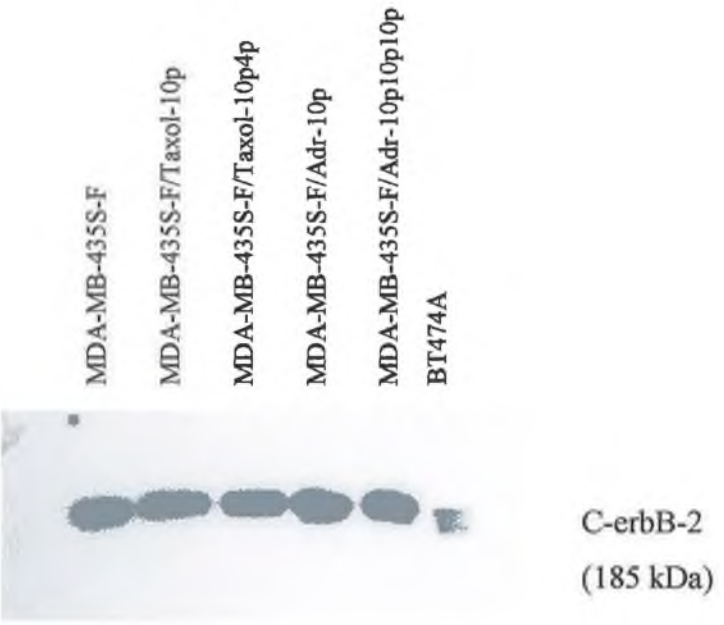

Figure 3.3.10.2.2a Immunoprecipitation of c-erbB-2 protein expression in MDA-MB-435S-F MDR variants

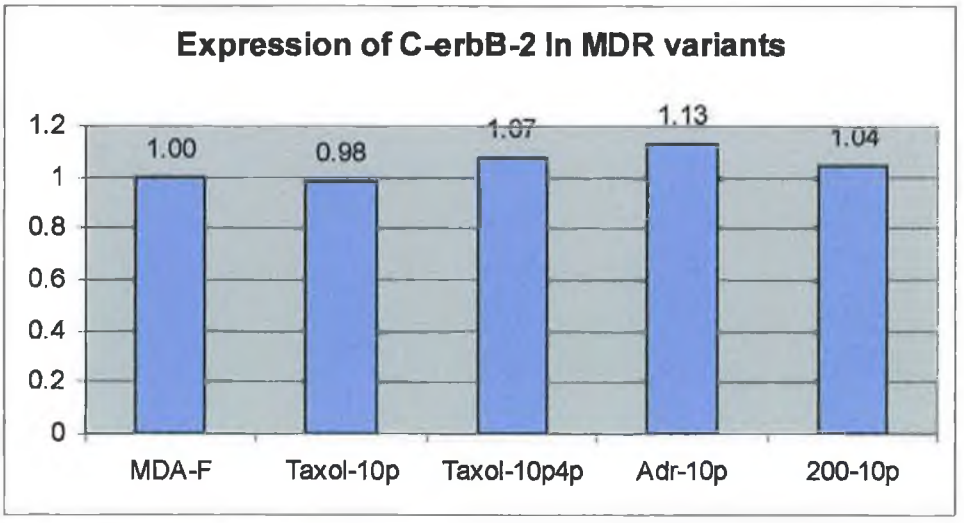

Figure 3.3.10.2.2b C-erbB-2 Expression in MDA-MB-435S-F MDR variants

3.3.10.2.3 C-erbB-3 protein expression

Figure 3.1.10.2.3 shows that c-erbB-3 protein expression is decreased in both taxol and adriamycin selected variants.

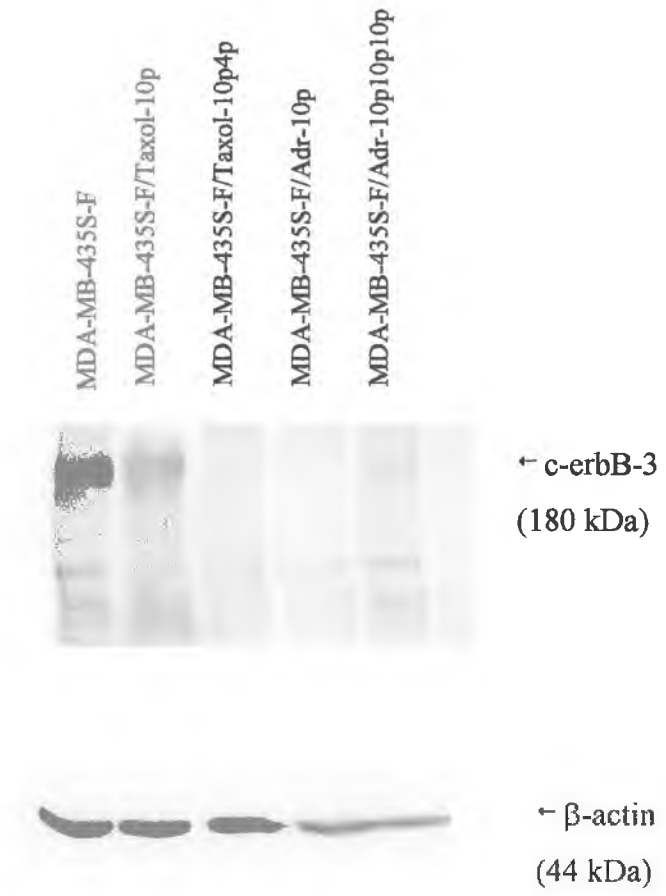

Figure 3.1.10.2.3 C-erbB-3 Expression in MDA-MB-435S-F MDR variants. A control gel was run for the detection of β-actin.

3.3.10.2.4 C-erbB-4 protein expression

Figure 3.1.10.2.4 shows that c-erbB-4 protein expression is virtually undetectable in all variants of MDA-MB-435S-F.

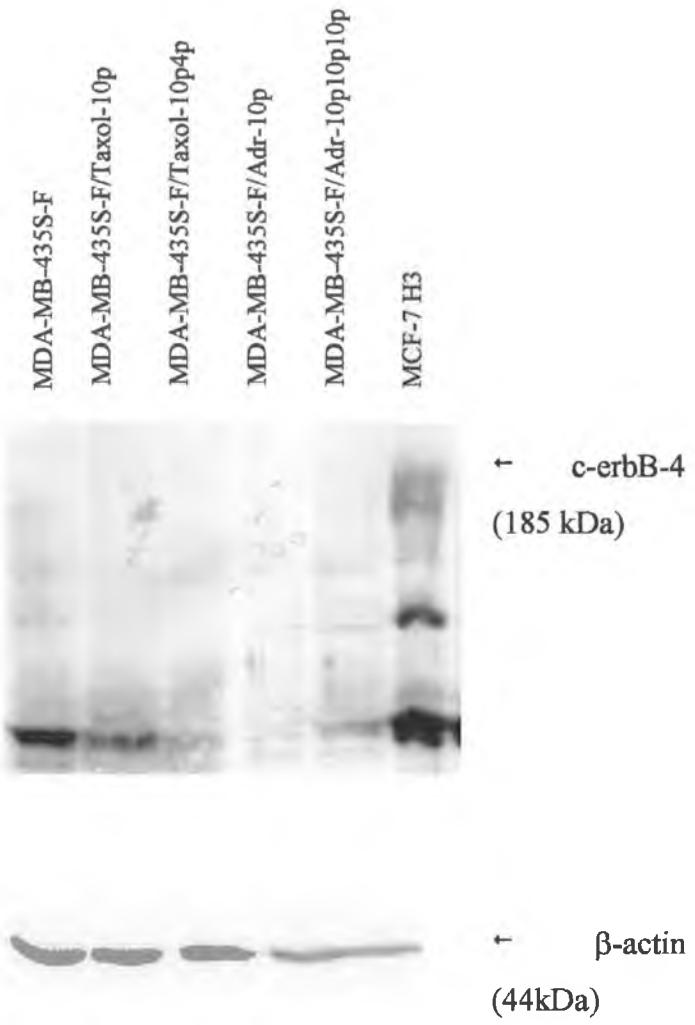

Figure 3.1.10.2.4 C-erbB-4 Expression in MDA-MB-435S-F MDR variants

3.3.11 Doubling Times of MDA-MB-435S-F MDR Variants

Table 3.3.11 shows the doubling times for MDA-MB-435S-F and each of its MDR variants. With increased taxol resistance, decreased growth rate was observed. MDA-MB-435S-F/Adr-10p has a much slower grower than MDA-MB-435S-F, however further selection with adriamycin saw return of growth rate almost to that of MDA-MB-435S-F.

Cell Line	Doubling Time (Hours)
MDA-MB-435S-F	33 ± 2.7
MDA-MB-435S-F/Taxol-10p	35 ± 1.5
MDA-MB-435S-F/Taxol-10p4p	44 ± 3.7
MDA-MB-435S-F/Adr-10p	44 ± 3.4
MDA-MB-435S-F/Adr-10p10p	37 ± 1.2

Table 3.3.11 Doubling Times of MDA-MB-435S-F MDR variants.

3.3.12 Motility Assays

Motility assays were performed, as described in Section 2.15, to access the locomotive ability of MDA-MB-435S-F and its MDR variants. The procedure used to demonstrate cell motility was similar to that used for invasion assays, with exception of the non-inclusion of matrigel prior to the addition of cells.

3.3.12.1 Motility of Taxol selected MDA-MB-435S-F variants.

Figure 3.3.12.1a shows the MDA-MB-435S-F cells which have moved through the membrane in a 48-hour assay. This cell line is highly motile. Figures 3.3.12.1b and 3.3.12.1c show the motility of the taxol slected variants MDA-MB-435S-F/Taxol-10p and MDA-MB-435S-F/Taxol-10p4p in the 48-hour assay. While these cell lines were highly motile, decreased motility was observed with increasing taxol resistance.

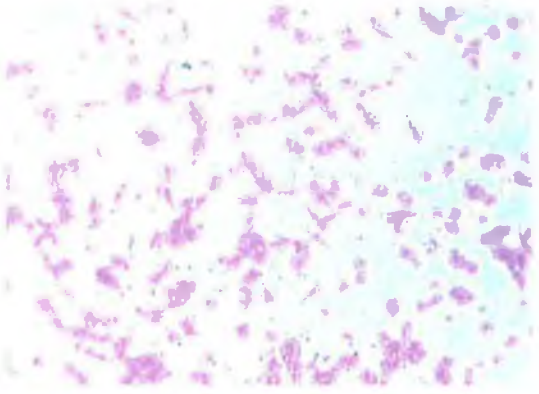

Figure 3.3.12.1a MDA-MB-435S-F

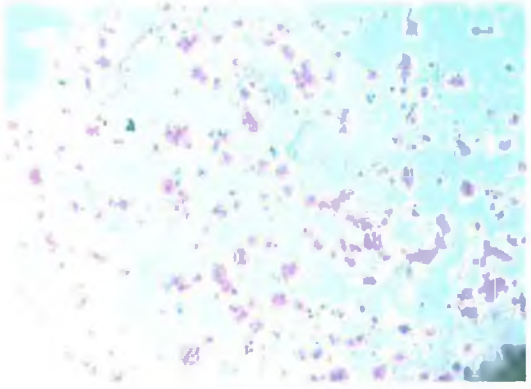

Figure 3.3.12.1b MDA-F/Taxol-10p

Figure 3.3.12.1c MDA-F/Taxol-10p4p

3.3.12.2 Motility of Adriamycin selected MDA-MB-435S-F variants.

Again Figure 3.3.12.2a shows the motility of MDA-MB-435S-F in a 48-hour assay. Figures 3.3.12.2b shows no significant change in the motility of the adriamycin selected variant MDA-MB-435S-F/Adr-10p. Figure 3.3.12.2c show that further selection with adriamycin resulted in a reduction in the motility of MDA-MB-435S-F/Adr-10p10p.

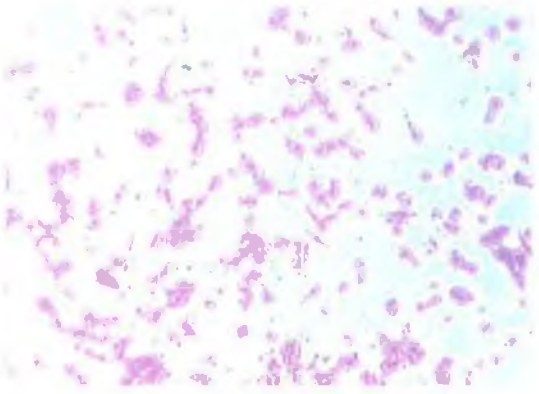

Figure 3.3.12.2a MDA-MB-435S-F

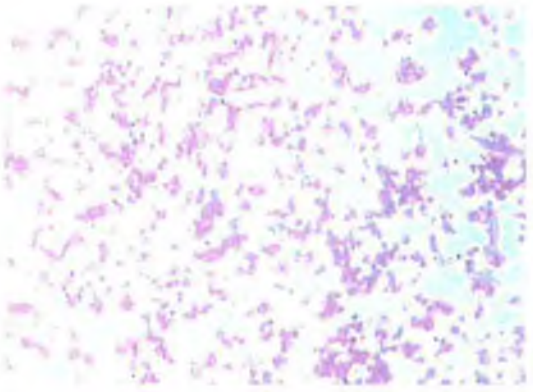

Figure 3.3.12.2b MDA-F/Adr-10p

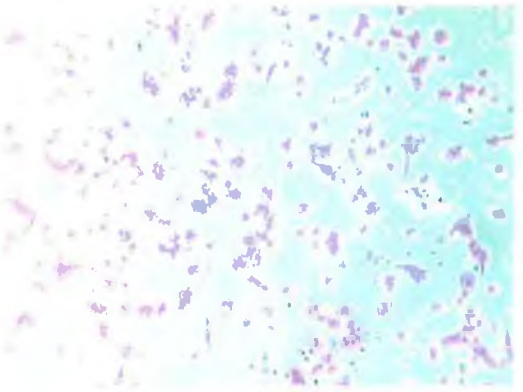

Figure 3.3.12.2c MDA-F/Adr-10p10p

It can be concluded from this that the adriamycin and taxol selection of MDA-MB-435S-F results in reduced motility.

3.3.13 Invasive Properties of MDA-MB-435S-F MDR variants: Discovery of a New *In Vitro* Model for Studying Different Phases of Invasion

Adhesion of cells to the extracellular matrix or basement membrane is the first step of cell invasion. The cell will then utilise various mechanisms to degrade the extracellular matrix, thereby facilitating its movement through it. Invasion assays were performed, as described in Section 2.14, to access the invasiveness of MDA-MB-435S-F and its MDR variants. Cell culture inserts, which stand in medium containing 24-well plates, were coated with matrigel prior to cell addition. Cells were allowed to migrate through the matrigel and subsequently through the 8 μM of the membrane of the insert to the underside of the insert.

3.3.13.1 Invasion of MDA-MB-435S-F MDR variants into matrigel

3.3.13.1.1 Invasion of Taxol selected MDA-MB-435S-F variants.

The ability of MDA-MB-435-F and its taxol-selected variants to invade through matrigel was assessed.

Figure 3.3.13.1.1a displays invasion of matrigel by MDA-MB-435S-F in a 48-hour assay. This cell line is highly invasive. Figure 3.3.13.1.1b displays invasion of matrigel by MDA-MB-435S-F/Taxol-10p. This cell line is highly invasive, although there appears to be very slightly fewer cells attached to the underside of the membrane. Figure 3.3.13.1.1c displays invasion of matrigel by MDA-MB-435S-F/Taxol-10p4p. Again this cell line is also highly invasive. Similar to MDA-MB-4345S-F/Taxol-10p, there are fewer cells attached to the underside of the membrane, compared to the parental cell line. Selection of MDA-MB-435S-F with taxol would appear at first glance to have made the cells less invasive. This is not the case however, as will be described in section 3.3.13.2.

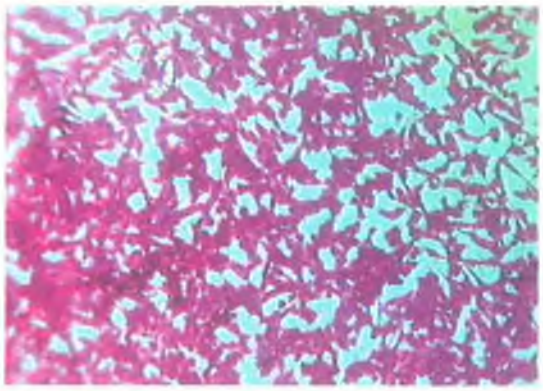

Figure 3.3.13.1.1a MDA-MB-535S-F

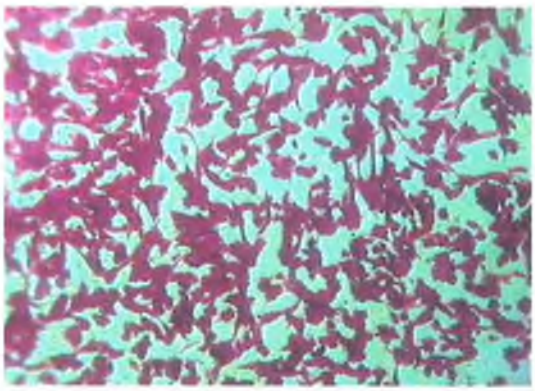

Figure 3.3.13.1.1b MDA-MB-435S-F/Taxol-10p

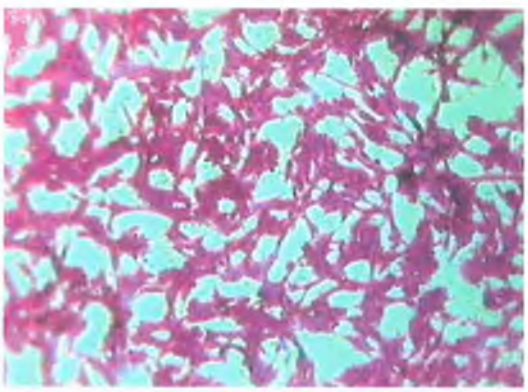

Figure 3.3.13.1.1c MDA-MB-435S-F/Taxol-10p4p

3.3.13.1.2 Invasion of Adriamycin selected MDA-MB-435S-F variants.

The ability of MDA-MB-435-F and its adriamycin-selected variants to invade through matrigel was assessed.

Figure 3.3.13.1.2a displays invasion of matrigel by MDA-MB-435S-F in a 48-hour assay. As noted before, this cell line is highly invasive. Figure 3.3.13.1.2b displays invasion of matrigel by MDA-MB-435S-F/Adr-10p. This cell line is considerably less invasive than the parental cell line MDA-MB-435S-F. Figure 3.3.13.1.2c displays invasion of matrigel by MDA-MB-435S-F/Adr-10p10p. This cell line is considerably less invasive than the parental cell line MDA-MB-435S-F/Adr-10p. These results would initially indicate that increasing adriamycin resistance in Mda-MB-435S-F coincides with decreased invasiveness. This is not the case though as is shown the following section 3.3.13.2.

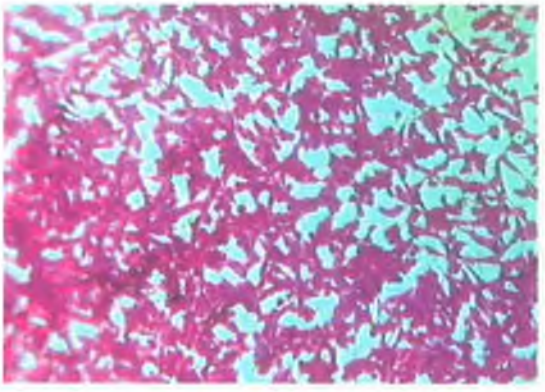

Figure 3.3.13.1.2a MDA-MB-535S-F

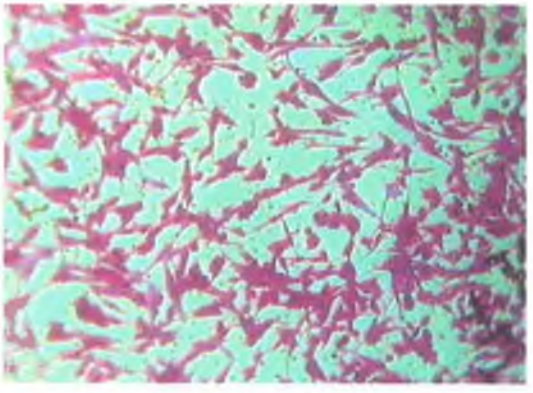

Figure 3.3.13.1.2b MDA-F/Adr-10p

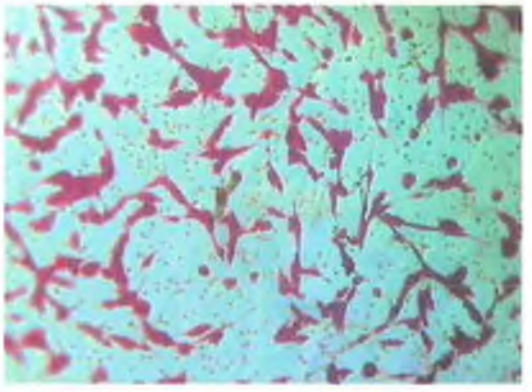

Figure 3.3.13.1.2c MDA-F/Adr-10p10p

3.3.13.2 Discovery of An *In Vitro* Model For Two-Stage Invasiveness

An unexpected observation was made in the invasion assays of MDA-MB-435S-F and its MDR variants. When the invasion inserts removed for crystal violet staining, it was observed that a portion of cells had detached from the bottom of the insert and reattached to the bottom of the 24-well plate, in the adriamycin and taxol selected variants. This did not occur with the parental cell line MDA-MB-435S-F. It is thought that this could indicate a more invasive phenotype, pertaining to the "seed and soil" model of cancer cell invasion as described in the introduction.

Figure 3.3.13.2a shows that no cells were attached to the bottom surface of the 24-well plate in invasion assays of MDA-MB-435S-F. Figures 3.3.13.2b and 3.3.13.2c show that a large number of cells had detached from the bottom of the insert and reattached to the bottom surface of the 24-well plate in invasion assays of MDA-MB-435S-F/Taxol-10p and MDA-MB-435S-F/Taxol-10p4p. This indicates that the taxol selection of MDA-MB-435S-F results in highly aggressive invasive behaviour. Figures 3.3.13.2d and 3.3.13.2e show that a number of cells had detached from the bottom of the insert and reattached to the bottom surface of the 24-well plate in invasion assays of MDA-MB-435S-F/Adr-10p and MDA-MB-435S-F/Adr-10p10p. The aggressive invasive behaviour of the adrimycin selected variants was not as great as that observed in the taxol selected variants. Also the number of cell invading in the adrimaycin selected variants is less than that of the parental cell line. This may however be an indication of a more aggressive phenotype, which could convey a greater chance of the survival of the invasive cell in a foreign environment.

Figure 3.3.13.2a MDA-MB-535S-F.

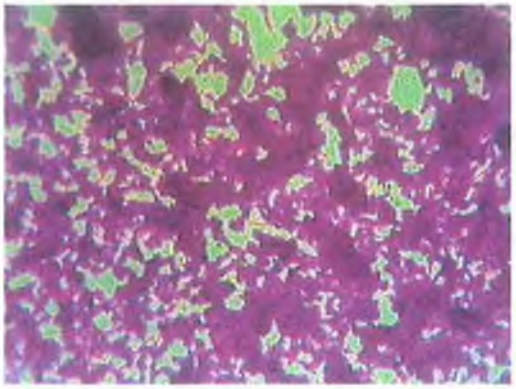

Figure 3.3.13.2b MDA-F/Taxol-10p

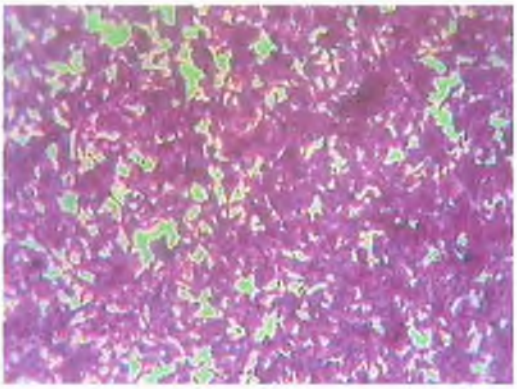

Figure 3.3.13.2c MDA-F/Taxol-10p4p

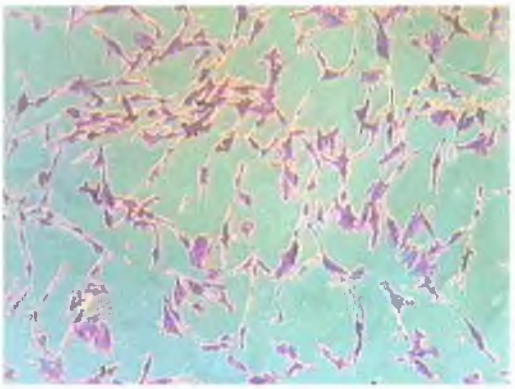

Figure 3.3.13.2d MDA-F/Adr-10p

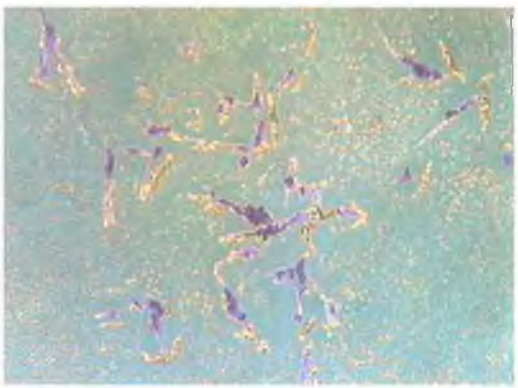

Figure 3.3.13.2e MDA-F/Adr-10p10p

3.3.14 The Adhesive Properties of the MDA-MB-435S-F MDR variants

Cells use various adhesion molecules such as integrins to interact with the extracellular components such as collagen type IV, laminin and fibronectin. To detect the adhesiveness of MDA-MB-435S-F parental cell line and its MDR variants to as collagen type IV, laminin, fibronectin and matrigel, adhesion assays were carried out as described in section 2.13.

Figure 3.3.14.1 shows the levels of adhesion of MDA-MB-435S-F and its MDR variants to laminin after 1 hour. MDA-MB-435S-F is more adhesive to laminin than either the taxol- or the adriamycin-selected variants. Loss of adhesion to laminin is greater in taxol-selected variants than in adriamycin-selected variants.

Figure 3.3.14.2 shows the levels of adhesion of MDA-MB-435S-F and its MDR variants to collagen type IV after 1 hour. MDA-MB-435S-F is more adhesive to collagen type IV than either the taxol or the adriamycin selected variants. Loss of adhesion to collagen type IV is greater in taxol selected variants than in MDA-MB-435S-F/Adr-10p. No great reduction in adhesion to collagen type IV was observed in MDA-MB-435S-F/Adr-10p10p.

Figure 3.3.14.3 shows the levels of adhesion of MDA-MB-435S-F and its MDR variants to fibronectin after 1 hour. MDA-MB-435S-F is more adhesive to fibronectin than either the taxol or the adriamycin selected variants. Loss of adhesion to fibronectin is greater in taxol selected variants than in adriamycin selected variants.

Figure 3.3.14.4 shows the levels of adhesion of MDA-MB-435S-F and its MDR variants to matrigel after 1 hour. MDA-MB-435S-F is more adhesive to matrigel than either the taxol or the adriamycin selected variants. While the loss of adhesion to matrigel was large in the taxol selected variants, it was only slight in the adriamycin selected variants.

3.3.14.1 Adhesion to Laminin.

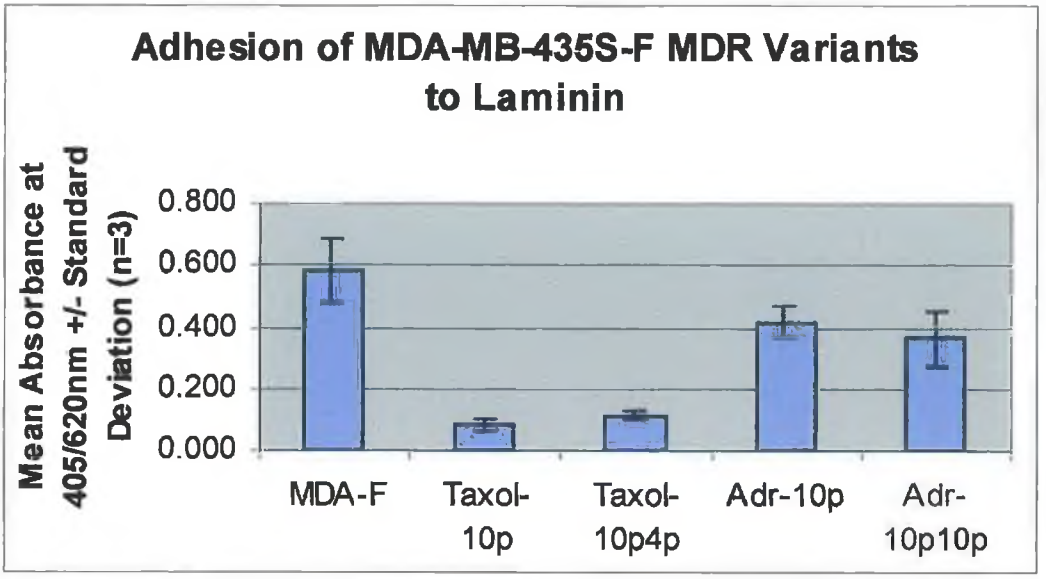

Figure 3.3.14.1 Levels of MDA-MB-435S-F and MDR variant cell adhesion to laminin.

Cell Line	Fold Changes in Cells Attached to Laminin After 1 hour
MDA-MB-435S-F	1.00
MDA-MB-435S-F/Taxol-10p	0.14
MDA-MB-435S-F/Taxol-10p4p	0.20
MDA-MB-435S-F/Adr-10p	0.71
MDA-MB-435S-F/Adr-10p10p	0.62

Table 3.3.14.1 Fold change in adhesion to laminin relative to the parental cell line MDA-MB-435S-F.

3.3.14.2 Adhesion to Collagen Type IV

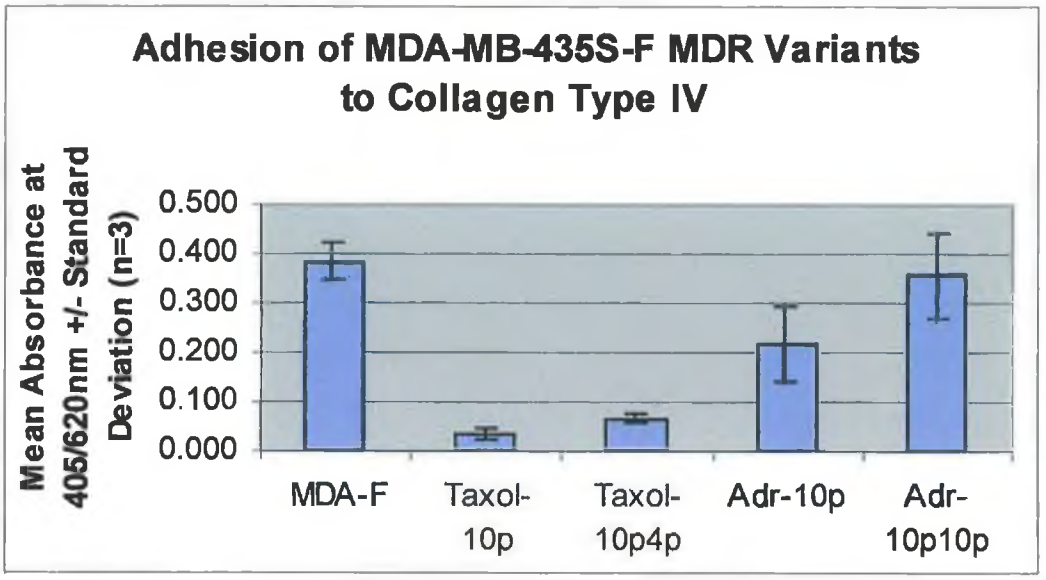

Figure 3.3.14.2 Levels of MDA-MB-435S-F and MDR variant cell adhesion to collagen type IV.

Cell Line	Fold Changes in Cells Attached to Collagen Type IV After 1 hour
MDA-MB-435S-F	1.00
MDA-MB-435S-F/Taxol-10p	0.09
MDA-MB-435S-F/Taxol-10p4p	0.17
MDA-MB-435S-F/Adr-10p	0.56
MDA-MB-435S-F/Adr-10p10p	0.93

Table 3.3.14.2 Fold change in adhesion to collagen type IV relative to the parental cell line MDA-MB-435S-F.

3.3.14.3 Adhesion to Fibronectin

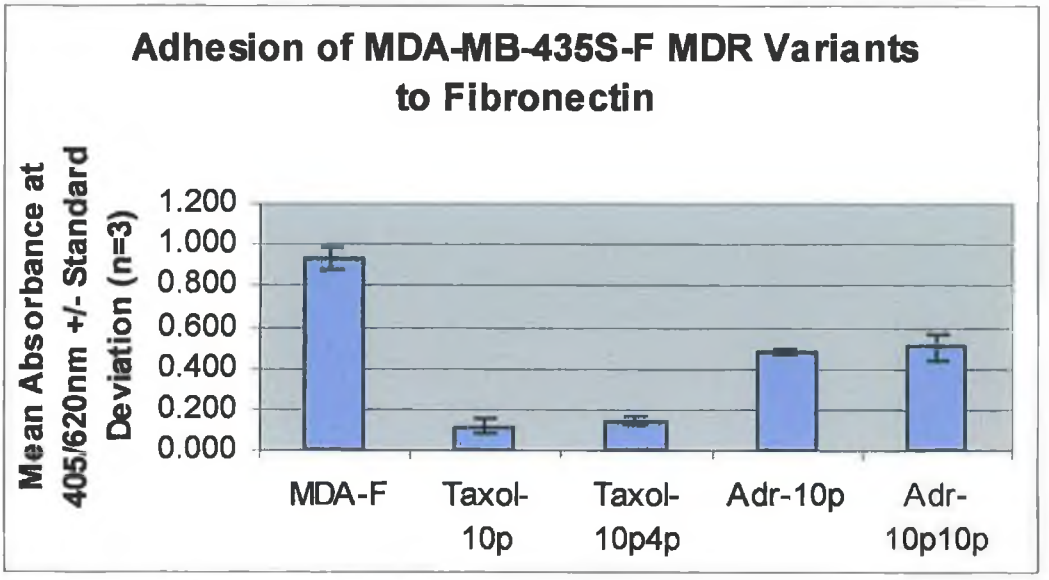

Figure 3.3.14.3 Levels of MDA-MB-435S-F and MDR variant cell adhesion fibronectin.

Cell Line	Fold Changes in Cells Attached to Fibronectin After 1 hour
MDA-MB-435S-F	1.00
MDA-MB-435S-F/Taxol-10p	0.13
MDA-MB-435S-F/Taxol-10p4p	0.15
MDA-MB-435S-F/Adr-10p	0.51
MDA-MB-435S-F/Adr-10p10p	0.54

Table 3.3.14.3 Fold change in adhesion to fibronectin relative to the parental cell line MDA-MB-435S-F.

3.3.14.4 Adhesion to Matrigel

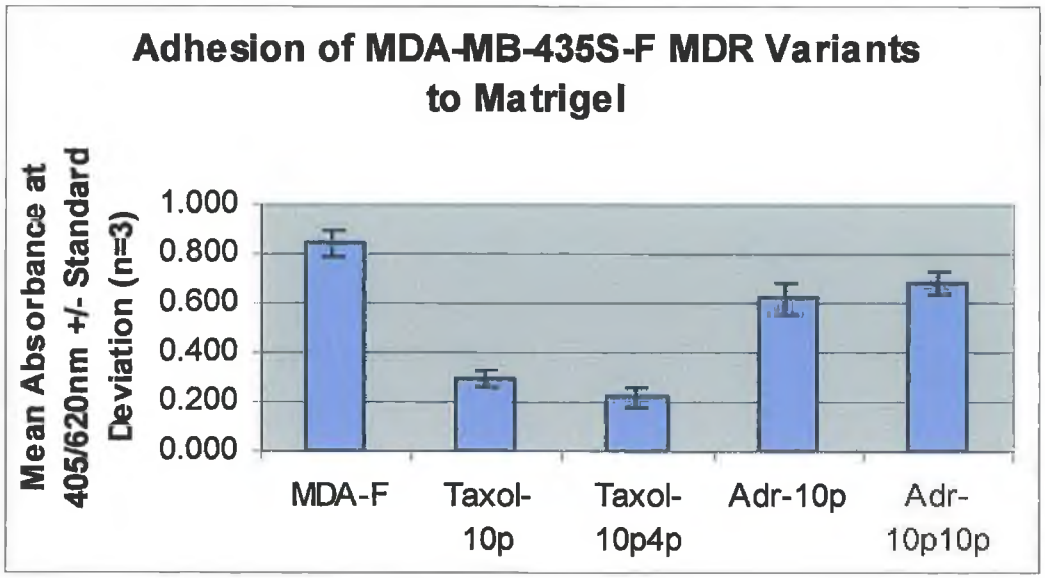

Figure 3.3.14.4 Levels of MDA-MB-435S-F and MDR variant cell adhesion matrigel.

Cell Line	Fold Changes in Cells Attached to Matrigel After 1 hour
MDA-MB-435S-F	1.00
MDA-MB-435S-F/Taxol-10p	0.35
MDA-MB-435S-F/Taxol-10p4p	0.26
MDA-MB-435S-F/Adr-10p	0.73
MDA-MB-435S-F/Adr-10p10p	0.81

Table 3.3.14.4 Fold change in adhesion to matrigel relative to the parental cell line MDA-MB-435S-F.

3.3.14.5 Summary of Adhesion results

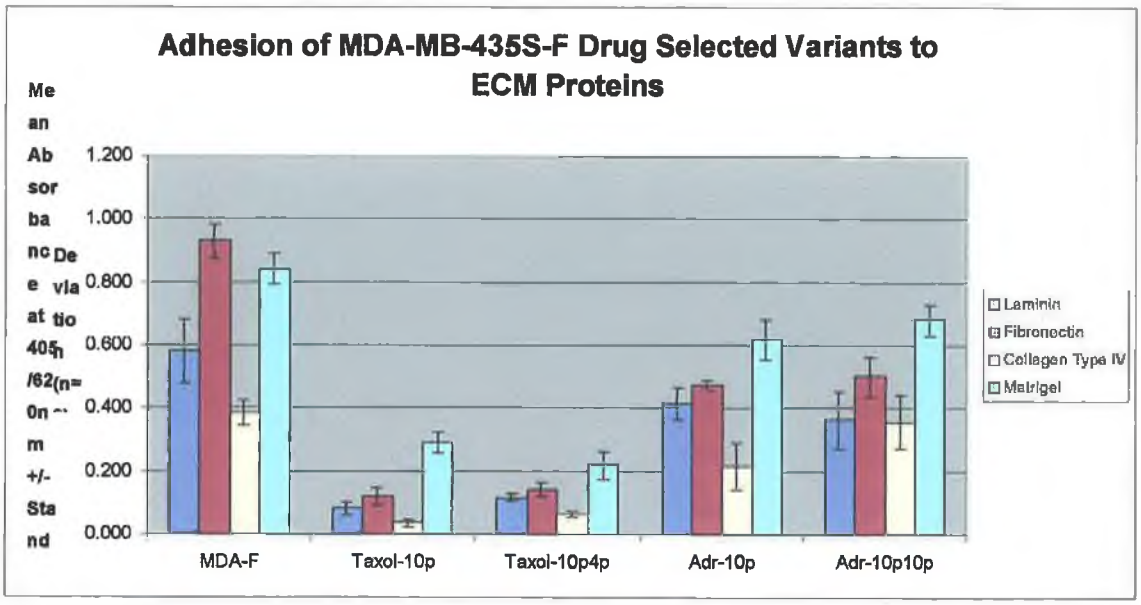

Figure 3.3.14.5.1 Adhesion of MDA-MB-435S-F Drug Selectant Variants to ECM Proteins

	Laminin	Fibronectin	Collagen Type IV	Matrigel
MDA-MB-435S-F	1.00	1.00	1.00	1.00
MDA-MB-435S-F/Taxol-10p	0.14	0.13	0.09	0.35
MDA-MB-435S-F/Taxol-10p4p	0.20	0.15	0.17	0.26
MDA-MB-435S-F/Adr-10p	0.71	0.51	0.56	0.73
MDA-MB-435S-F/Adr-10p10p	0.62	0.54	0.93	0.81

Table 3.3.14.5 Fold decrease in adhesion of MDA-MB-435-S-F MDR variants to ECM proteins relative to parental cell line MDA-MB-435S-F.

The following figures display the results presented in sections 3.3.14.1, 3.3.14.2, 3.3.14.3 and 3.3.14.4 in a different manner. The purpose of this is to show the preference of each cell line for particular ECM substrates, and how this is altered by taxol and adriamycin selection. MDA-MB-435S-F and all its variants are adherent to laminin, fibronectin, collagen type IV and matrigel.

MDA-MB-435S-F is most adhesive to fibronectin, followed by matrigel and laminin and least adhesive to collagen type IV. Figure 3.3.14.5.3 demonstrates the adhesive properties of the taxol selected cell line MDA-MB-435S-F/Taxol-10p. The graph demonstrates that the cell line is now most adhesive to matrigel, followed by fibronectin, laminin and lastly least adhesive to collagen type IV. In comparison to the parent cell line, MDA-MB-435S-F/Taxol-10p shows greatly reduced adhesion properties, with adhesion to laminin at 0.14, fibronectin at 0.13, collagen type IV at 0.09 and matrigel at 0.35 of the parent cell line.

The second taxol selected cell line, MDA-MB-435S-F/Taxol-10p4p also shows changes in adhesive properties. Figure 3.3.14.5.4 shows that the MDA-MB-435S-F/Taxol-10p4p is most adhesive to matrigel, followed by fibronectin, laminin and lastly collagen type IV. Interestingly adhesion to laminin, fibronectin and collagen type IV is slightly greater than for MDA-MB-435S-F/Taxol-10p, with adhesion to laminin at 0.20, fibronectin at 0.15, collagen type IV at 0.17. The cell line is however less adhesive to matrigel at 0.26 of the parent.

The adriamycin selected cell lines also show reduced adhesion, although not to the same extent as the taxol selected cell lines. Again as with the Taxol selected cell lines, MDA-MB-435S-F/Adr-10p and MDA-MB-435S-F/Adr-10p10p are most adhesive to matrigel, followed by fibronectin, laminin and least adhesive to collagen type IV. The loss of adhesion in these cell lines is not as great as in the taxol selected cell lines but is still significant. Adr-10p has adhesive values to laminin at 0.71, fibronectin at 0.51, collagen type IV at 0.56 and matrigel at 0.73 of the parent, while Adr-10p10p has values of adhesion to laminin at 0.62, fibronectin at 0.54, collagen type IV at 0.93 and matrigel at 0.81 of the parent.

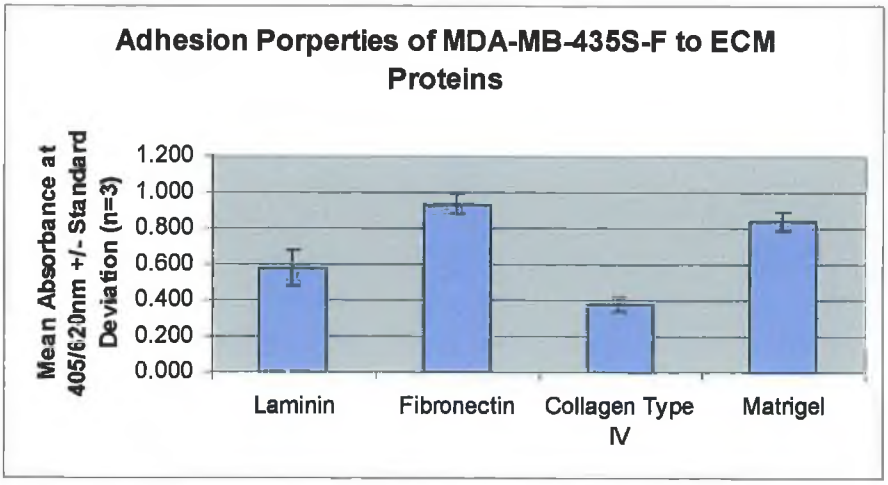

Figure 3.3.14.5.2 – Adhesion properties of parent cell line MDA-MB-435S-F.

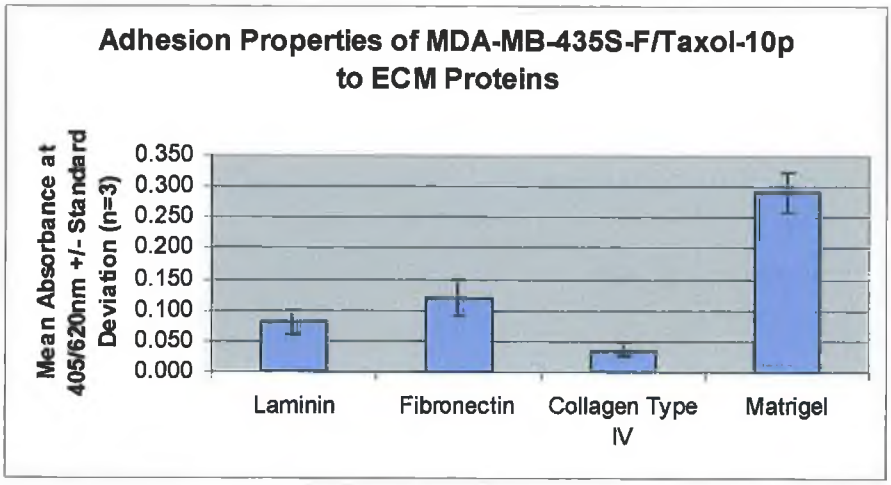

Figure 3.3.14.5.3 - Adhesion properties of taxol selected cell line MDA-MB-435S-F/Taxol-10p.

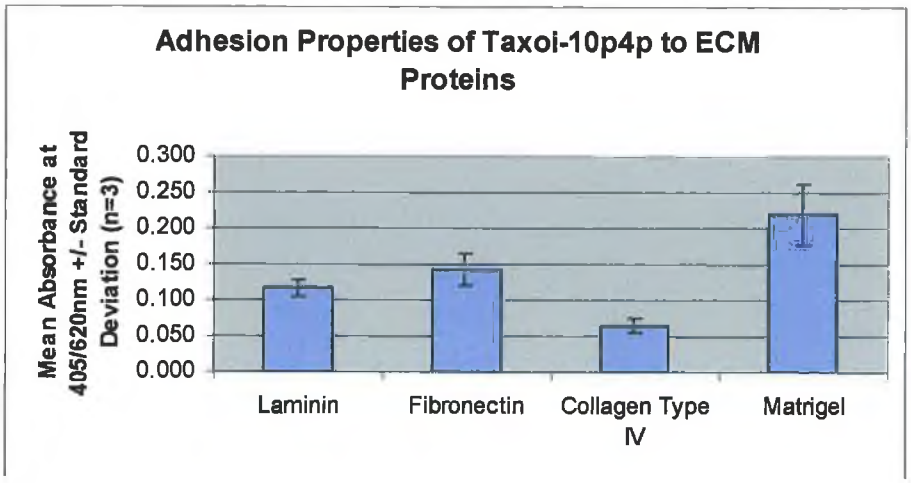

Figure 3.3.14.5.4 - Adhesion properties of taxol selected cell line MDA-MB-435S-F/Taxol-10p4p.

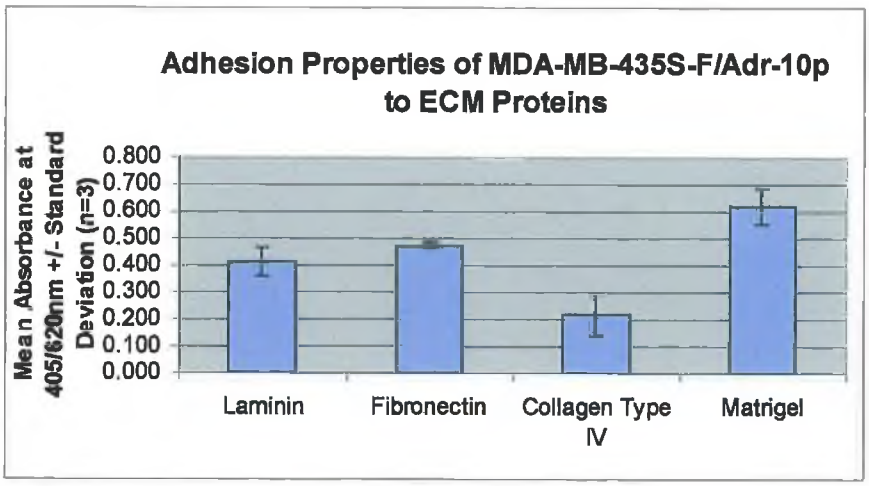

Figure 3.3.14.5.5 - Adhesion properties of adriamycin selected cell line MDA-MB-435S-F/Adr-10p.

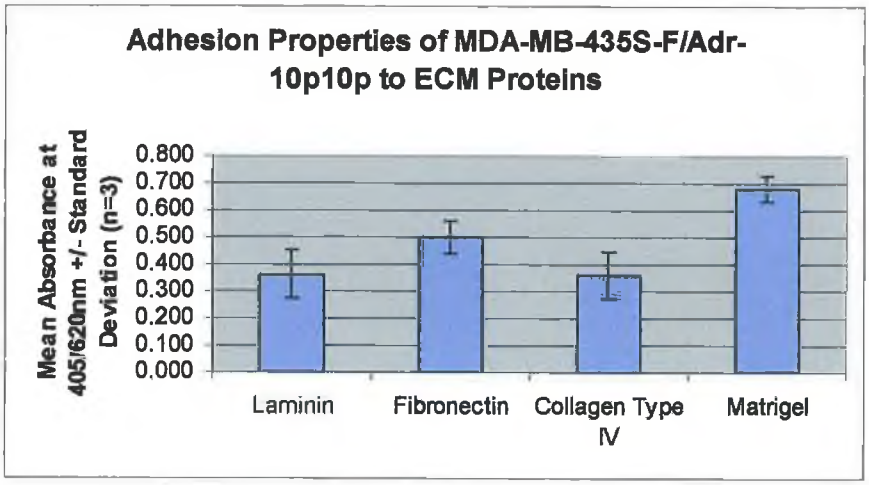

Figure 3.3.14.5.6 - Adhesion properties of adriamycin selected cell line MDA-MB-435S-F/Adr-10p10p

3.3.15 Protease secretion by MDA-MB-435S-F MDR variants.

Matrix metalloproteinases (MMPS), cysteine proteinases and serine proteineases, which are secreted by cells, play an important role in degrading the extracellular matrix. To investigate the mechanism underlying the invasive phenotype of the MDA-MB-435S-F parental cell line and its MDR variants, studies of MMPs were carried out as described in section 2.16.

3.3.15.1 Expression of Gelatin Degrading Proteases by MDA-MB-435S-F and Its MDR variants

BHK (baby hamster kidney) cell line, which secretes MMP-2 and MMP-9, was used as the positive control in these studies.

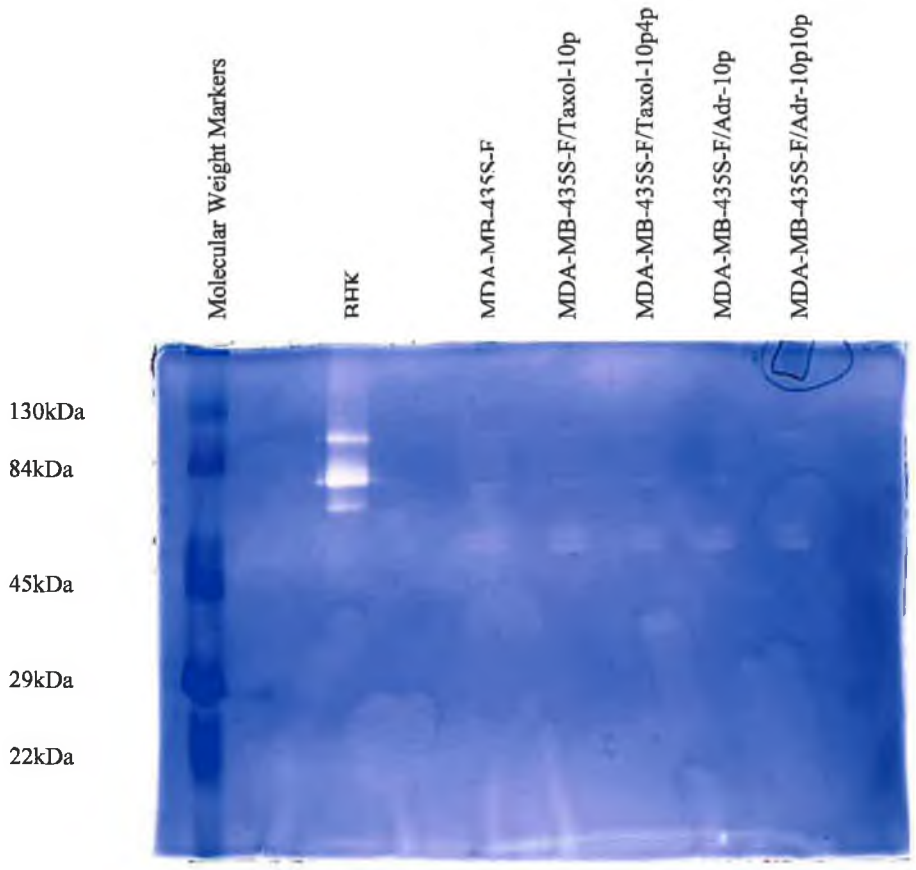

Figure 3.3.15.1 Zymogram of gelatin proteases secreted by MDA-MB-435S-F with BHK as a positive control for the secretion of pro-MMP2 (72 kDa), MMP-2 (66kDa), pro-MMP-9 (92kDa) and MMP9 (86kDa). The MDA-MB-435S-F parent cell line and its MDR variants display secretion bands corresponding to pro-MMP-2 and

pro-MMP-9. There are also double bands expressed at approximately 50-60kDa. A candidate for this is MMP-1, which runs as a doublet at 52 and 57 kDa in their unglycosylated and glycosylated forms of the proenzyme.

3.3.15.2 Invastigation of Type of Class of Gelatin Degrading Proteases by MDA-MB-435S-F and Its MDR variants

To confirm that the bands detected in MDA-MB-435S-F and its MDR variants were MMPs, proteinase inhibitors were added.

3.3.15.2.1 The effect of EDTA

EDTA is a chelating agent which can bind the zinc and calcium which are needed for the activation of MMPs.

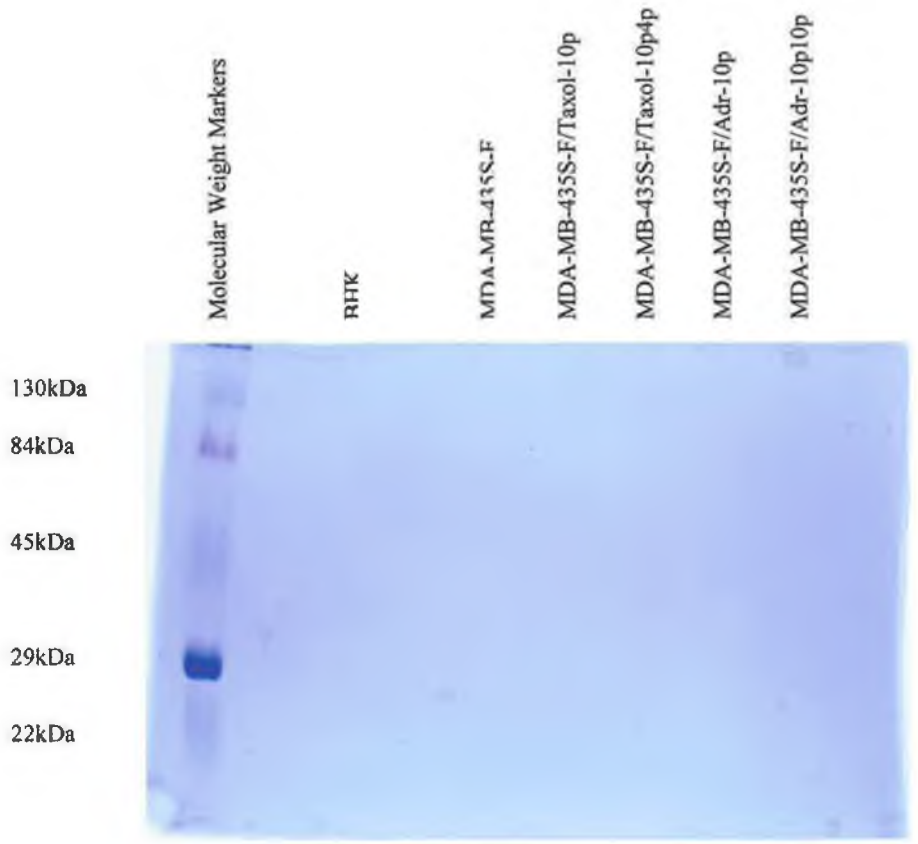

Figure 3.3.15.2.1 Addition of EDTA to the substrate buffer eliminates expression of all protease bands, indicating the gelatin degrading proteases secreted by MDA-MB-435S-F parent and MDR variants are probably members of the matrix metalloproteinase family.

3.3.15.2.2 The effect of PMSF

PMSF is a serine and cysteine proteinase inhibitor.

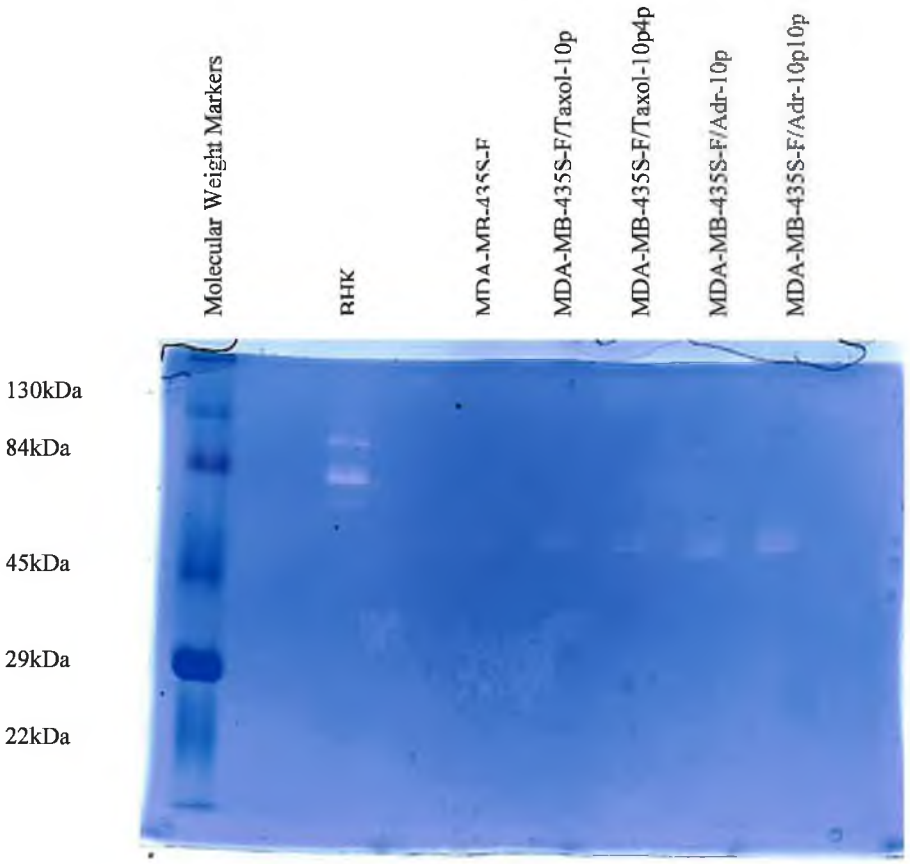

Figure 3.3.15.2.2 Addition of PMSF to the substrate buffer suppresses slightly expression of all protease bands, but does not eliminate them, suggesting the proteases are not serine or cysteine proteases.

3.3.16 Analysis of Populations Isolated from Invasion Assays

Three populations of cells were isolated from MDA-MB-435S-F and its MDR variants. Invasion assays were set up as described in section 2.14. After allowing cells to invade for 48 hours, the three populations were isolated as follows. Firstly cells which had not invaded were isolated from the inside of the invasion chamber (Non-Invasive), by pipetting up remaining cells and transferring to a well containing fresh media. A second population was isolated from the bottom side of the insert by trypsinisation (Invasive) of cells into a well containing fresh media. The third population was isolated from those cells, which had invaded, detached from the bottom of the insert and reattached to the bottom of the 24-well plate (Superinvasive). These populations were allowed to grow until they reached levels for further subculturing.

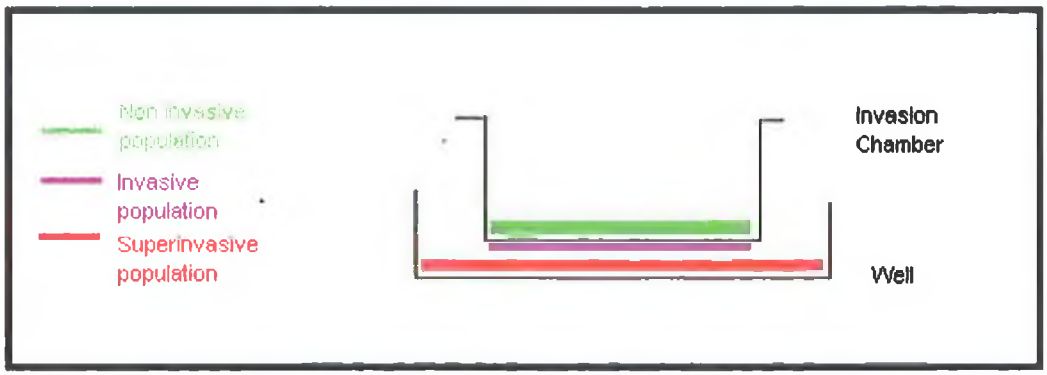

Figure 3.3.16 Diagram of isolation of populations from invasion chamber

3.3.16.1 Morphology of Isolated Populations

No changes were observed in the morphology of the three invasive populations isolated, except for an increased tendency of Invasive and Superinvasive cells to lack of cell contact growth inhibition.

3.3.16.1.1 Morphology of Non-Invasive Populations

Figure 3.3.16.1.1a MDA-MB-535S-F

Figure 3.3.16.1.1b MDA-F/Taxol-10

Figure 3.3.16.1.1c MDA- F/Taxol-10p4p

Figure 3.3.16.1.1d MDA-F/Adr-10p

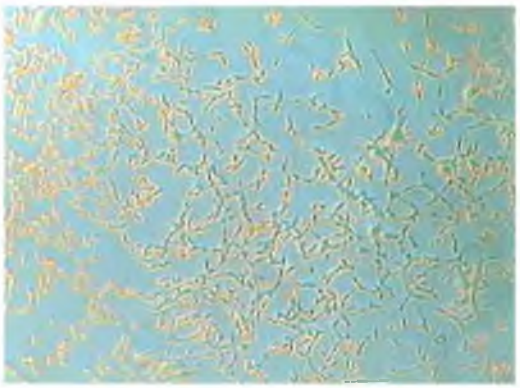

Figure 3.3.16.1.1 e MDA-F/Adr-10p10p

3.3.16.1.2 Morphology of Invasive Populations

Figure 3.3.16.1.2a MDA-MB-535S-F

Figure 3.3.16.1.2b MDA- F/Taxol-10p

Figure 3.3.16.1.2 c MDA- F/Taxol-10p4p

Figure 3.3.16.1.2d MDA-F/Adr-10p

Figure 3.3.16.1.2e MDA-F/Adr-10p10p

3.3.16.1.3 Morphology of Superinvasive Populations

Figure 3.3.16.1.3a MDA-F/Taxol-10p

Figure 3.3.16.1.3b MDA-F/Taxol-10p4p

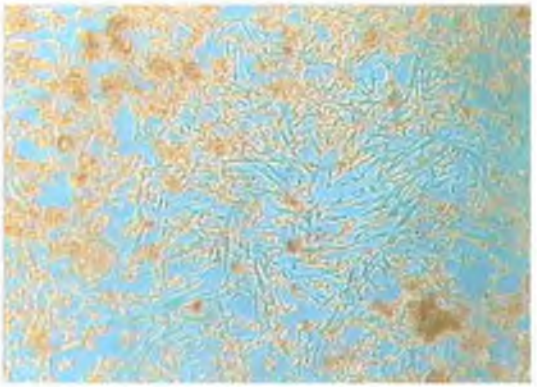

Figure 3.3.16.1.3c MDA-F/Adr-10p

Figure 3.3.16.1.3d MDA-F/Adr-10p10p

3.3.16.2 Motility of Isolated Populations

Motility assays were performed to compare the motility of the three populations isolated from MDA-MB-435S-F and its MDR variants. Motility assays were performed as described in section 2.15. Post-motility assay, the bottom side of the motility chambers and also the bottom of the 24 well plate were stained with crystal violet. The crystal violet was then eluted with 33% acetic acid and transferred to a 96-well plate and the absorbance read at 570nm.

These results show that the superinvasive populations were far more motile than either the non-invasive or invasive populations. Total cell motility showed that the MDA-MB-435S-F/Taxol-10p4p invasive populations were far more motile than the parental cell line. Unexpectedly, within this cell line, the invasive population was more motile than the superinvasive population.

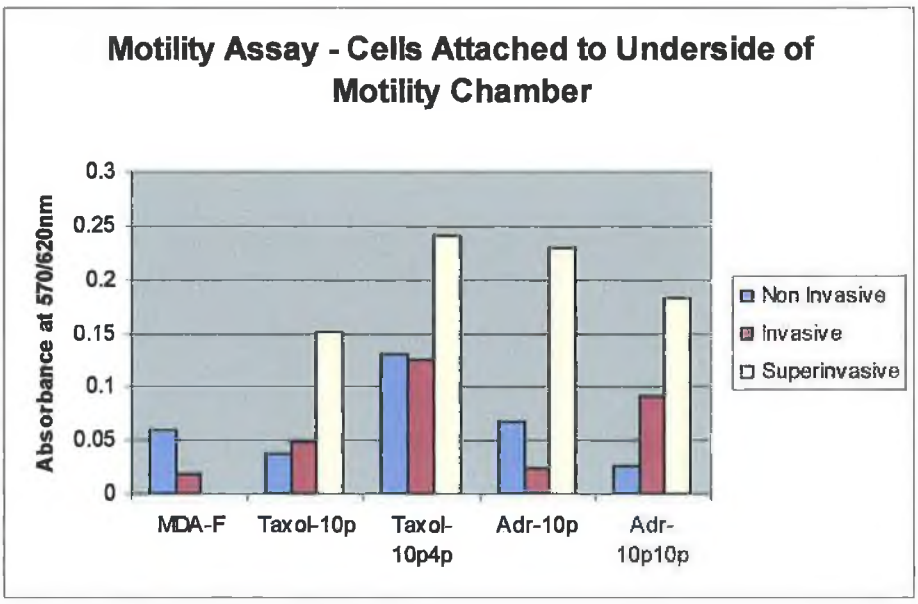

Figure 3.3.16.2a Comparison of levels of locomotion to underside of motility chamber by Non-Invasive, Invasive and Superinvasive populations, isolated from MDA-MB-435S-F and its MDR variants.

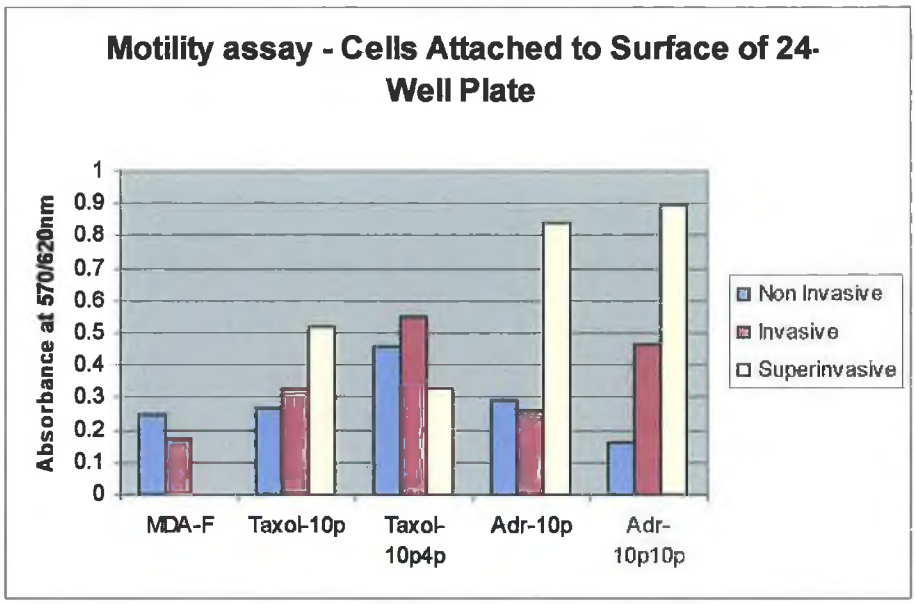

Figure 3.3.16.2b Comparison of levels of cells attached to bottom of 24 well plate after motility assay of Non-Invasive, Invasive and Superinvasive populations, isolated from MDA-MB-435S-F and its MDR variants.

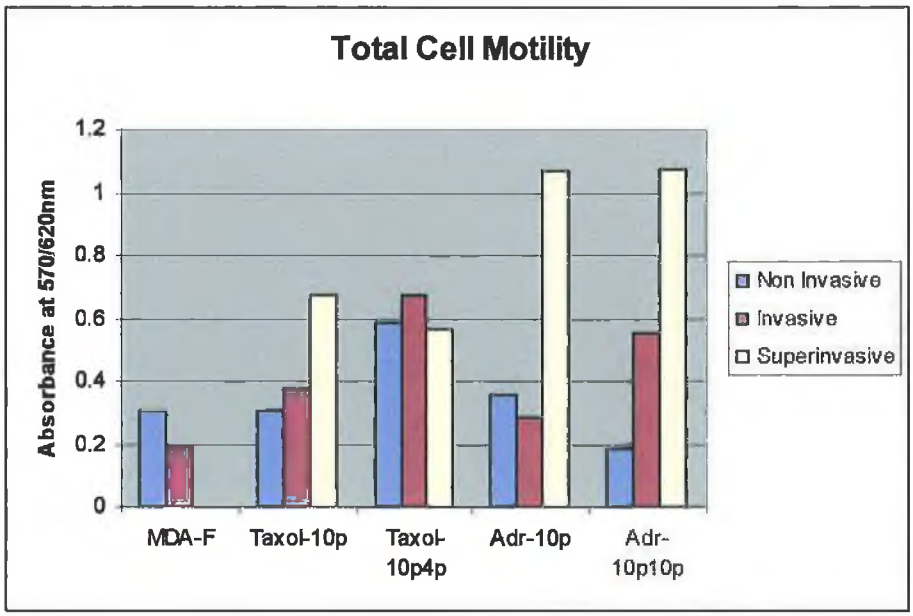

Figure 3.3.16.2c Comparison of total cell motility by Non-Invasive, Invasive and Superinvasive populations, isolated from MDA-MB-435S-F and its MDR variants.

3.3.16.3 Invasiveness of Isolated Populations

Invasion assays were performed to compare the invasiveness of the three populations isolated from MDA-MB-435S-F and its MDR variants. Invasion assays were performed as described in section 2.14. After invasion the bottom side of the invasion chambers and also the bottom of the 24 well plate were stained with crystal violet. The crystal violet was then eluted with 33% acetic acid and transferred to a 96-well plate and the absorbance read at 570nm.

Figure 3.3.16.3.c shows that there was a general trend towards increased invasiveness in the adriamycin and taxol selected variants compared to their parental cell line MDA-MB-435S-F. It was also observed that the superinvasive populations were more invasive than the other supopulations. Again similar to the motility assays in section 3.3.16.2, the invasive subpopulation of MDA-MB-435S-F/Taxol-10p4p was more invasive than its superinvasive subpopulation. All subpopulations were capable of invading regardless of their point of isolation, but they did show different rates of invasion.

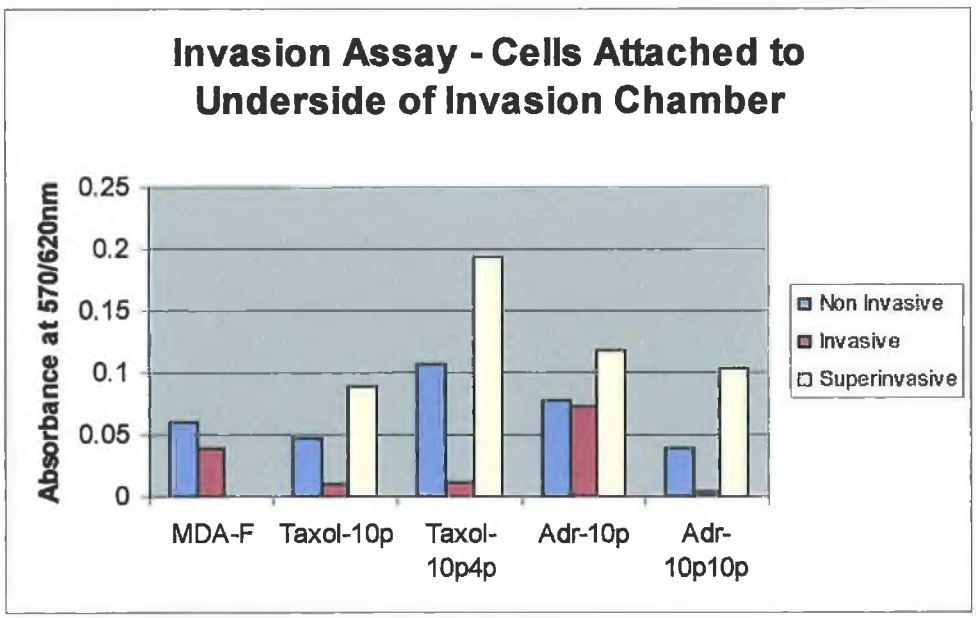

Figure 3.3.16.3a Comparison of levels of invasion to underside of invasion chamber by Non-Invasive, Invasive and Superinvasive populations, isolated from MDA-MB-435S-F and its MDR variants.

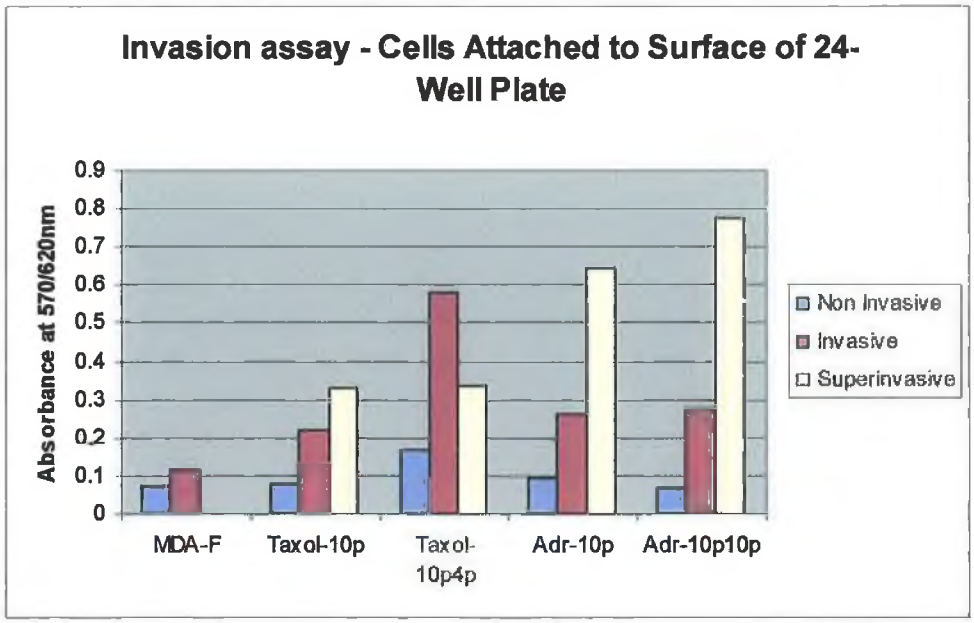

Figure 3.3.16.3b Comparison of levels of cells attached to bottom of 24 well plate after invasion by Non-Invasive, Invasive and Superinvasive populations, isolated from MDA-MB-435S-F and its MDR variants.

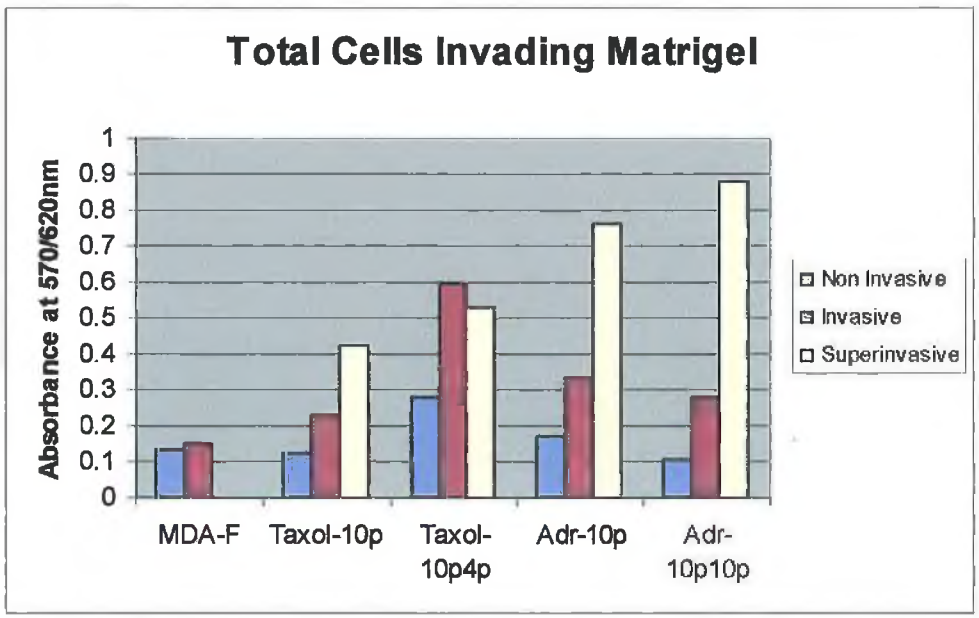

Figure 3.3.16.3c Comparison of total cell by Non-Invasive, Invasive and Superinvasive populations, isolated from MDA-MB-435S-F and its MDR variants.

3.3.16.4 Adhesion of Superinvasive Populations to ECM Components in Comparison to Parental Populations

Adhesion assays were performed as described in section 2.13 to compare the adhesiveness of the superinvasive populations in comparison to the parental populations from which they were isolated.

Results showed that all of the superinvasive populations with the exception of MDA-MB-435S-F/Taxol-10p were more adhesive to laminin, fibronectin, collagen type IV and matrigel. On the other hand MDA-MB-435S-F/Taxol-10p is less adhesive to these ECM proteins.

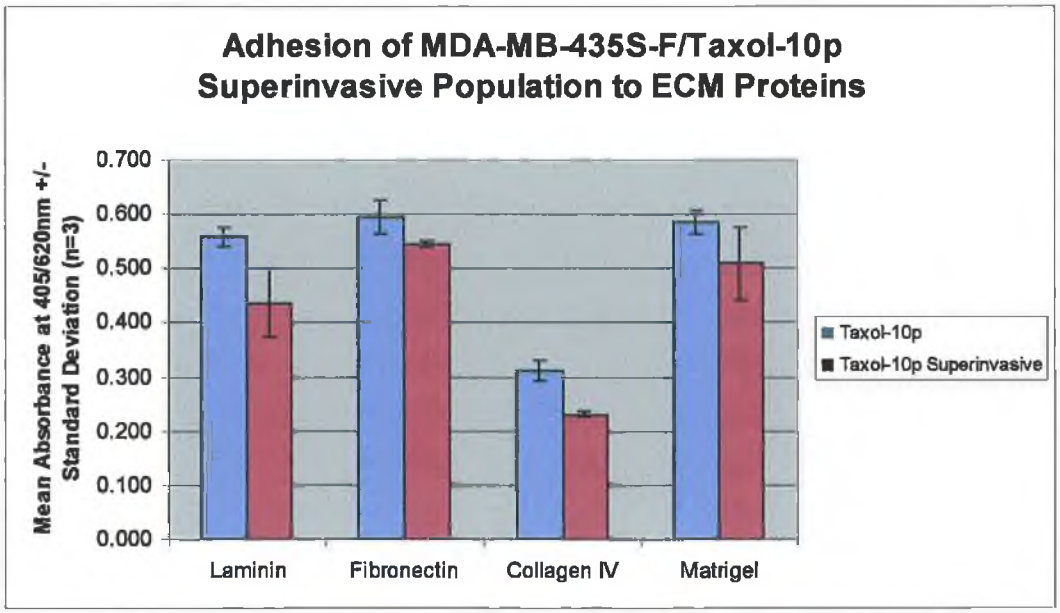

Figure 3.3.16.4.1 Comparison of adhesion of MDA-MB-435S-F/Taxol-10p superinvasive population to ECM proteins compared to its parental cell line MDA-MB-435S-F/Taxol-10p

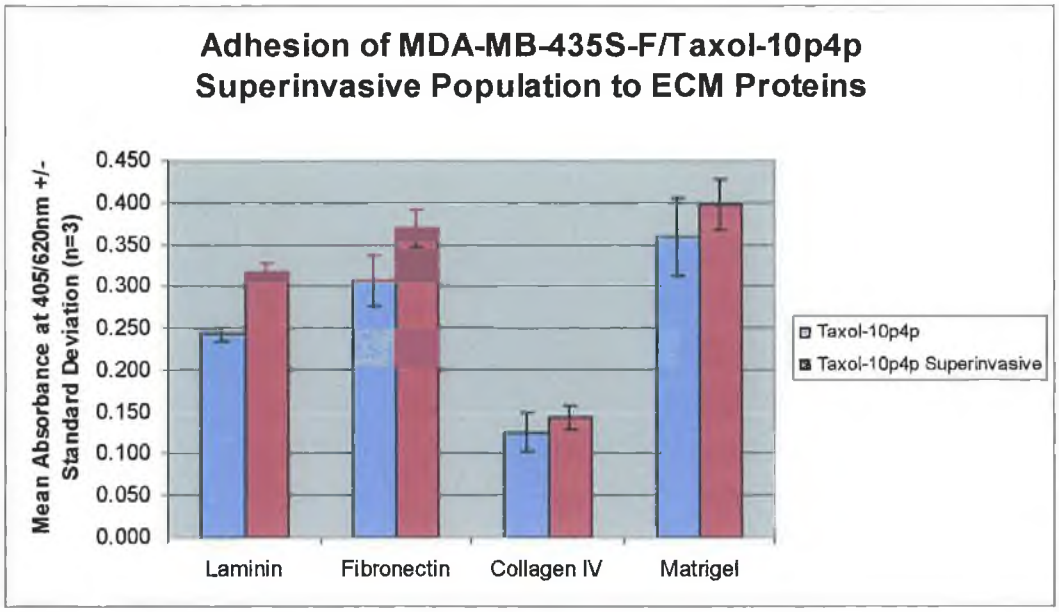

Figure 3.3.16.4.2 Comparison of adhesion of MDA-MB-435S-F/Taxol-10p4p superinvasive population to ECM proteins compared to its parental cell line MDA-MB-435S-F/Taxol-10p4p

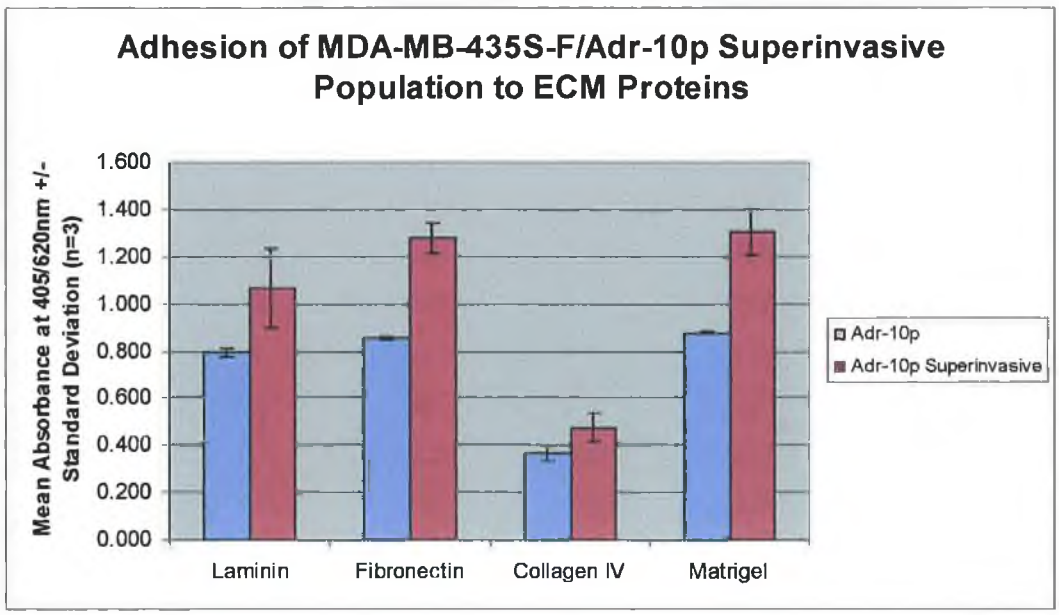

Figure 3.3.16.4.3 Comparison of adhesion of MDA-MB-435S-F/Adr-10p superinvasive population to ECM proteins compared to its parental cell line MDA-MB-435S-F/Adr-10p

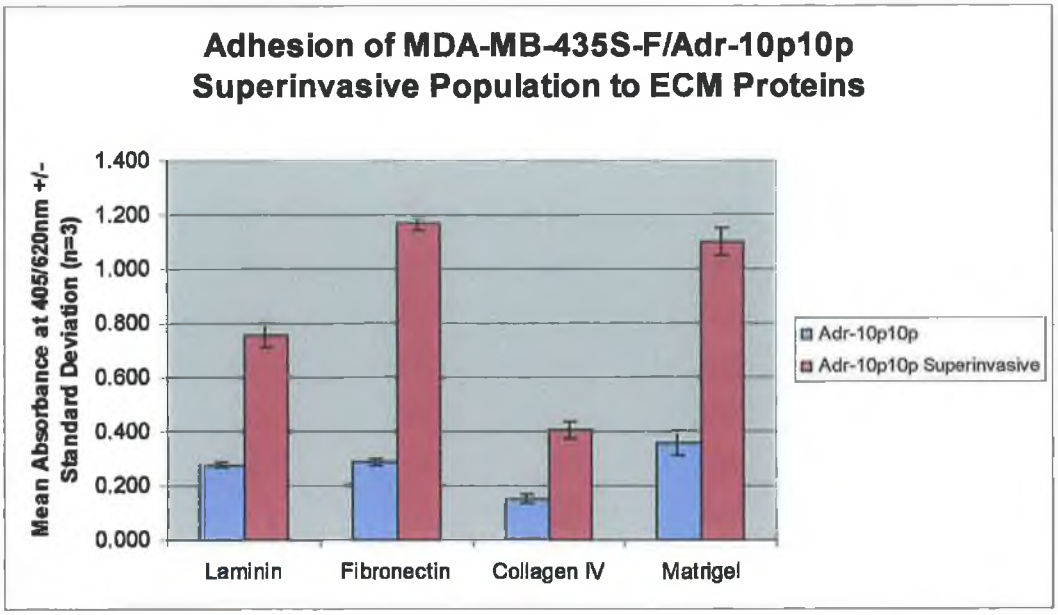

Figure 3.3.16.4.4 Comparison of adhesion of MDA-MB-435S-F/Adr-10p10p superinvasive population to ECM proteins compared to its parental cell line MDA-MB-435S-F/Adr-10p10p

4.0 Discussion

4.1 Characterisation of BT474A, MCF-7 H3 and MDA-MB-435S-F cell lines

The purpose of the thesis was to study the effects of c-erbB-2 levels on chemotherapeutic drug and tamoxifen resistance, expression of drug resistance related genes and on cell invasiveness. Previous studies had indicated that c-erbB-2 overexpression was associated with poor prognosis, increased metastatic potential and resistance to chemotherapy and hormonal therapy (see sections 1.4; 1.5; 1.7).

This was approached from three directions.

1. To study the effect of c-erbB-2 upregulation on the processes described above. This was achieved by the transfection of MCF-7 H3 with c-erbB-2 cDNA
2. To study the effect of c-erbB-2 downregulation on the processes described above and to see if the reverse of that seen in the previous point could be detected. This was achieved by the transfection of BT474A with a c-erbB-2-targeted ribozyme.
3. As c-erbB-2 overexpression was associated with increased drug resistance, a low level c-erbB-2 expressing cell line, MDA-MB-435S-F was chosen for selection with adriamycin and taxol to determine whether c-erbB-2 would play a role in emerging drug resistance.

MCF-7 H3 is a clonal population isolated by Dr. Finbar O'Sullivan (NCTCC, Dublin City University) from the human breast carcinoma cell line MCF-7. MCF-7 H3 expresses normal levels of c-erbB-2 expression and is also estrogen receptor positive (both α and β). BT474A is a clonal population isolated during the course of this thesis from the human breast carcinoma cell line BT474A. BT474A expresses high levels of c-erbB-2 and is also estrogen receptor positive (both α and β). MDA-MB-435S-F is a clonal populations isolated during the course of this thesis from the human breast carcinoma cell line MDA-MB-435S. MDA-MB-435S-F expresses normal levels of c-erbB-2 expression and is estrogen receptor negative.

None of the three cell lines overexpress p-glycoprotein, and their drug resistance profiles are very similar as is shown in Table 4.1. MCF-7 H3 and BT474A express very

low levels of GST π mRNA compared to MDA-MB-435S-F. MDA-MB-435S-F expresses much lower levels of topoisomerase IIα compared to MCF-7 H3 and BT474A. MCF-7 H3 expresses high levels of c-erbB-4 at both the mRNA and protein level.

Drug	**BT474A**	**MCF-7 H3**	**MDA-MB-435S-F**
IC_{50} Taxol LT	1.86 ± 0.05	1.09 ± 0.16	2.12 ± 0.057
IC_{50} Taxol ST	15.6 ± 1.15	9.2 ± 1.0	28.3 ± 1.52
IC_{50} Adriamycin LT	40.3 ± 4.04	19.83 ± 2.3	26.6 ± 1.97
IC_{50} Adriamycin ST	104 ± 4.58	348 ± 2.8	271 ± 3
IC_{50} Carboplatin LT	2.43 ± 0.20	1.75 ± 0.10	
IC_{50} Carboplatin ST	33.0 ± 3.00	42.9 ± 3.4	41.3 ± 1.5
IC_{50} Taxotere ST		6.10 ± 0.17	3.33 ± 0.37
IC_{50} 5-FU LT	0.09 ± 0.012	0.17 ± 0.005	
IC_{50} 5-FU ST	4.86 ± 0.63	6.06 ± 0.11	7.43 ± 0.68
IC_{50} Vincristine ST		73.3 ± 1.52	12.9 ± 1.3

Table 4.1 IC_{50} values for BT474A, MCF-7 H3 and MDA-MB-435S-F.

4.2 The Role of C-erbB-2 in Resistance to Chemotherapy

Overexpression due to gene amplification has been found in 10-40% of breast cancers, although some carcinomas overexpress in the absence of gene amplification (Suo *et al.*, 1998). High levels of c-erbB-2 expression have been shown to correlate strongly with poor prognosis in breast cancer (Verbeek *et al.*, 1998).

An objective of this thesis was to establish a breast cancer cell model for the investigation of the effects of c-erbB-2 expression on resistance to chemotherapeutic drugs and the expression of genes associated with drug resistance. Two breast cancer cell lines were chosen, BT474A and MCF-7 H3. BT474A overexpresses c-erbB-2, while MCF-7 H3 expresses normal levels of c-erbB-2. MCF-7 H3 was transfected with a c-erbB-2 encoding plasmid to upregulate expression of c-erbB-2 (section 3.1). C-erbB-2 expression was not elevated to a great extent at the mRNA level, but was increased at the protein level as shown in section 3.1.3. BT474A was transfected with a c-erbB-2 targeting ribozyme to downregulate expression of c-erbB-2 (section 3.2). The transfection was found to be successful as c-erbB-2 levels were decreased at both the mRNA level and protein level (section 3.2.3). The mutant ribozyme control transfection exhibited no reduction in the expression of c-erbB-2, indicating that the transfection was successful.

Tables 4.2a and 4.2b show the findings of alteration of c-erbB-2 levels of expression in BT474A and MCF-7 H3. The effect of c-erbB-2 expression on drug resistance appears to be cell line dependent. This finding is very similar to Slamon *et al.* (1997) who found that the chemosensitivity profiles resulting from c-erbB-2 transfection observed *in vitro* were cell line specific. There were only two consistent changes in drug resistance exerted by c-erbB-2 expression, the first was a decrease in resistance to adriamycin in short term assays as a result of upregulation of c-erbB-2 in MCF-7 H3, which was mirrored by an increase in resistance to adriamycin in BT474A when c-erbB-2 was downregulated in short term assays (section 3.1.4.1.2; 3.2.4.1.2). Secondly, a decrease in resistance to 5-fluorouracil was observed in long and short term assays as a result of upregulation of c-erbB-2 in MCF-7 H3, which again was mirrored by a increase in resistance to 5-fluorouracil in BT474A when c-erbB-2 was downregulated (section 3.1.4.4.1; 3.1.4.4.2; 3.2.4.4.1; 3.2.4.4.2).

Main Findings in the MCF-7 H3 C-erbB-2 cDNA Transfectants	Methods used
Decreased resistance to adriamycin in long and short term assays	Toxicity assay
Increased resistance to taxol in short term assays only	Toxicity assay
No consistent changes in resistance to carboplatin in long term assays Increased resistance to carboplatin in short term assays	Toxicity assay
Increased resistance to methotrexate in long term assays	Toxicity assay
No significant changes in vincristine, taxotere or 5-fluorouracil ressitance	Toxicity assay
DHFR and topoisomerase IIβ mRNA levels increased	RT-PCR
MDR-1, mrp-4, mrp-5 and GSTπ mRNA expression not detected	RT-PCR
Mrp-1, mrp-2, TS, topoisomerase I and topoisomerase IIα mRNA expression unchanged	RT-PCR

Table 4.2a Summary of findings of the effects of c-erbB-2 upregulation in MCF-7 H3 on chemotherapeutic drug patterns of resistance and expression of a panel of resistance associated genes.

Findings in the BT474A C-erbB-2 Ribozyme Transfectants	Methods used
Decreased resistance to adriamycin in long term assays Increased resistance to adriamycin in short term assays)	Toxicity assay
Increased resistance to taxol in long and short term assays	Toxicity assay
No consistent changes in resistance to carboplatin in long term assays Increased resistance to carboplatin in short term assays	Toxicity assay
Increased resistance to 5-fluorouracil in long and short term assays	Toxicity assay
Increased resistance to methotrexate in long term assays	Toxicity assay
Mrp-2, DHFR, TS, GSTπ topoisomerase I and topoisomerase IIβ mRNA levels increased	RT-PCR
Topoisomerase IIα mRNA levels decreased	RT-PCR
MDR-1 and mrp-4 mRNA expression not detected	RT-PCR
Mrp-1 and mrp-5 mRNA expression unchanged	RT-PCR

Table 4.2b Summary of findings of the effects of c-erbB-2 downregulation in BT474A on chemotherapeutic drug patterns of resistance and expression of a panel of resistance associated genes.

An important observation was the variation in response of the transfectants to a particular drug, depending on whether the toxicity testing assay used was long or short term. Long term toxicity assays involved the determination of the IC_{50} for a particular drug after 7 days drug exposure in 96 well plates. Short term toxicity assays involved the determination of the IC_{50} for a particular drug after 4 hour exposure to the drug, followed by growth in drug-free media for another 7 days in 96 well plates. One might say that the two assays differ in that long term assays reflect the ability of the cells to withstand lengthier exposure to drug, while short term assays reflect the ability of the cells to recover from an acute shock with a high concentration of the drug in question. It should be noted that the half-life of chemotherapy drugs is quite short (approximate range 6-16 hours) in culture medium. It is likely that short term assays reflect what is seen in the clinical setting. The majority of chemotherapy regimes involve a series of exposures to the chemotherapy agent/agents, over a number of weeks, rather than continuous exposure to drug. Downregulation of c-erbB-2 in BT474A resulted in decreased resistance to adriamycin in long term assays, while resistance was increased to adriamycin in short term assays (section 3.2.4.1.1; 3.2.4.1.2). No consistent changes in resistance to carboplatin in long term assays was observed in the BT474A ribozyme transfectants, while increased resistance to carboplatin was observed in short term assays (section 3.2.4.3.1; 3.2.4.3.2). These results suggest that c-erbB-2 is beneficial to BT474A where adriamycin exposure is continuous, but it is not beneficial to BT474A if it receives a high dose of adriamycin. This may explain the findings whereby c-erbB-2 overexpression is linked to better response to high dose adriamycin chemotherapy (Petit *et al.*, 2001). The carboplatin results suggest that c-erbB-2 has no effect on BT474A response to carboplatin where exposure is continuous, and it is not beneficial to BT474A if it receives a high dose of carboplatin. MCF-7 H3 results suggest that c-erbB-2 has no effect on the resistance of MCF-7 H3 to continuous taxol or carboplatin exposure, while c-erbB-2 expression is beneficial to MCF-7 H3 in the case of high doses of taxol or carboplatin (section 3.2.4.2.1; 3.2.4.2.2; 3.2.4.3.1; 3.2.4.3.2). Due to the conflicting effects of c-erbB-2 on resistance to chemotherapeutic agents, it would not be advisable to recommend a particular type of chemotherapeutic drug on the basis of c-erbB-2 status. It is highly likely that c-erbB-2 is one of many proteins in a much larger picture. Until these pathways and receptor combinations are completely elucidated, the role of c-erbb-2 in chemo-resistance, will remain extremly complicated, and difficult to determine.

There are numerous conflicting studies on the effects of c-erbB-2 overexpression on resistance to chemotherapy. In general, these reportes suggest that c-erbB-2 confers ressitance to durugs such as taxol. Transfection of MDA-MB435 human breast cancer cells with c-erbB-2 confers a 5-9-fold increase in taxol resistance (Yu *et al.*, 1996), not linked to p-glycoprotein function (Yu *et al.*, 1998b), due to upregulation of $p21^{Cip1}$, blocking taxol-induced apoptosis in these cells (Yu *et al.*, 1998). In contrast c-erbB-2 overexpression in normal human mammary epithelial cells failed to confer resistance or sensitivity to chemotherapeutic agents (Orr *et al.*, 2000). Transfection of SKOV-3 ovarian cancer cells with an anti-c-erbB-2-targeted ribozyme had no effect on resistance to adriamycin or cisplatin in proliferation assays. In contrast, the sensitivity to taxol was increased approximately 70-fold (Aigner *et al.*, 2000). Ciardiello *et al.* (2000) found that c-erbB-2 transfection of MCF-10A normal human mammary epithelial cells resulted in an increased sensitivity to topoisomerase I- and topoisomerase II-inhibitors, and to platinum-derivatives. The cells were however more resistant to taxol and taxotere.

Harris *et al.* (2001) that Herceptin inhibited the cytotoxicity of adriamycin in c-erbB-2 overexpressing breast cancer cells. This was accompanied by a decrease in topoisomerase IIα protein and activity, suggesting that this is at least one of the mechanisms of change in adriamycin response.

A number of genes involved in drug resistance were examined at the mRNA levels, to determine whether their expression was altered by c-erbb-2 expression, and whether they could explain any of the changes in drug resistance observed in MCF-7 H3 and BT474A. In this thesis, the effect of c-erbB-2 expression on topoisomerase mRNA expression was determined by RT-PCR. C-erbB-2 upregulation in MCF-7 H3 had no effect on the expression of topoisomerase I or topoisomerase IIα mRNA in MCF-7 H3, while topoisomerase IIβ mRNA levels were increased in one of the clonal populations (section 3.1.5.6; 3.1.5.8). This was not consistent with findings for BT474A, as c-erbB-2 downregulation resulted in increased topoisomerase I and topoisomerase IIβ mRNA, while topoisomerase IIα mRNA levels were decreased (section 3.2.5.6; 3.2.5.8). These results are limiting however, as protein expression or enzyme activity were not examined

C-erbB-2 expression appears to have no effect on the regulation of MDR-1, mrp-1, mrp-4, mrp-5 mRNA expression in either cell line as determined by RT-PCR. There is however nothing in the literature to link c-erbB-2 with any of these genes. Mrp-2 mRNA levels increased as a result of c-erbB-2 downregulation in BT474A (section 3.2.5.3). This is a very interesting finding as there are no links in the literature between c-erbB-2 and mrp-2. This may also explain increases in resistance to adriamycin and carboplatin in these cell lines, as shown by short term toxicity assays. Adriamycin is transported by mrp-2 as is cisplatin, an analogue of carboplatin. Therefore it is possible that mrp-2 also transports carboplatin. A next step will be to determine the expression of mrp-2 protein in these cell lines at the protein level, and examine its activity by circumvention assays.

There is no literature linking c-erbB-2 with thymidylate synthase or dihydrofolate reductase. DHFR mRNA levels increased as a result of upregulation of c-erbB-2 in MCF-7 H3 (section 3.1.5.9). However, they also increased in three of the transfectant populations of BT474A as a result of c-erbB-2 downregulation (section 3.2.5.9). TS mRNA levels increased in the c-erbB-2 transfected MCF-7 H3 clones (section 3.1.5.10). Again, TS mRNA levels also increased in BT474A as a result of c-erbB-2 downregulation (section 3.2.5.10).

In this thesis, GST π mRNA was undetectable in MCF-7 H3 (section 3.1.5.11), while it increased in BT474A as a result of c-erbB-2 downregulation (section 3.2.5.11). GST π did not correlate with c-erbB-2 overexpression in intraduct breast carcinomas (Bellamy *et al.*, 1994). There was no association between expression GST π, GST α or GST μ and expression of c-erbB-2 in a series of 74 primary human breast carcinomas (Cairns *et al.*, 1992). In contrast a correlation was found between GST π expression and c-erbB-1 and c-erbB-2 in renal carcinoma cells (Volm *et al.* 1993).

4.3 The Role of C-erbB-2 in Cell Motility, Adhesion, Invasion and Protease Secretion

C-erbB-2 overexpression is known to be associated with invasion and metastasis in human breast cancer (Marx *et al.*, 1990; Quénel *et al.*, 1995; Revillion *et al.*, 1996; Prost *et al.*, 1994; Driouch *et al.*, 1997). A second objective of the establishment of a breast cancer cell model for altering c-erbB-2 expression, was to investigate the role of c-erbB-2 in cell motility, adhesion, invasion and protease secretion.

Findings in the MCF-7 H3 C-erbB-2 cDNA Transfectants	Methods used
Lack of cell motility in parental cell line and c-erbB-2 transfectants	Motility assay
Increased invasion in 2 of 3 clonal transfected populations Decreased invasion in 1 clonal transfected population	Invasion assay
No consistent changes in adhesion to laminin, collagen type IV or matrigel	Adhesion assay
Decreased adhesion of all transfected clonal populations to fibronectin	Adhesion assay
Matrix metalloproteinases secreted by MCF-7 H3 and transfectants	Zymography
Inhibition of MMP and serine proteases activity of BHK, MCF-7 H3 and clonal transfected populations by cysteine and DTT	Zymography
Secretion of serine/cysteine proteases correlate with lack of invasiveness	Zymography

Table 4.3a Summary of findings of the effects of c-erbB-2 upregulation in MCF-7 H3 on cell motility, adhesion, invasion and protease secretion.

C-erbB-2 expression appears to have no effect on cell motility in these cell lines, although it is not possible to be absolutely conclusive on this, as these cell lines do not exhibit motility in the first place (section 3.1.11; 3.2.11). It is very unusual that the cells are invasive but not motile. There is a distinct possibility that motility might be triggered in these cell lines only in the presence of substrates such as the extracellular matrix, when the cell is about to become invasive.

Findings in the BT474A C-erbB-2 Ribozyme Transfectants	Methods used
Lack of cell motility in parental cell line and c-erbB-2 ribozyme transfectants	Motility assay
Decreased invasion in all transfectant populations	Invasion assay
Decreased adhesion of clonal populations to laminin and matrigel	Adhesion assay
Decreased adhesion of pool and clonal populations to collagen type IV	Adhesion assay
Decreased adhesion of pool and three clonal populations to fibronectin	Adhesion assay
Secretion of matrix metalloproteinase by BT474A and ribozyme transfectant, levels of which were reduced in several clonal transfected populations	Zymography

Table 4.3b Summary of findings of the effects of c-erbB-2 downregulation in BT474A on cell motility, adhesion, invasion and protease secretion.

Several studies have shown that c-erbB-2 overexpression results in increased cell motility. Smith *et al.* (2002) reported that the transfection of an ovarian cancer cell line with c-erbB-2, resulted in increased motility, while geldanamycin depletion of c-erbB-2 expression in melanoma cells resulted in decreased motility, accompanied by a loss of c-erbB-2 association with β-catenin. Geldanamycin also stimulated tyrosine dephosphorylation of β-catenin and increased β-catenin/E-cadherin association, resulting in substantially decreased cell motility (Bonvini *et al.*, 2001). Over-expression of c-erbB-2 in MDA-MB-435 cells resulted in increases in mRNA and protein levels of the actin bundling protein fascin. Heightened fascin expression has been observed in other systems to result in greatly increased cell motility. MDA-MB-435 cells over-expressing c-erbB-2 exhibit significantly heightened cellular dynamics and locomotion, while visualization of bundled microfilaments within fixed cells revealed enhanced formation of dendritic-like processes, microspikes and other dynamic actin based structures (Grothey *et al.*, 2000).

C-erbB-2 levels had a profound affect on the invasiveness of BT474A and MCF-7 H3. C-erbB-2 downregulation in BT474A (section 3.2.12) resulted in decreased

invasiveness. This decreased invasiveness was greater in the clonal populations than the pooled population. In MCF-7 H3 c-erbB-2 upregulation resulted in increased invasion in two of the clonal populations, MCF-7 H3/ErbB2-B and MCF-7 H3/ErbB2-C. MCF-7 H3, the parental cell line was only very slightly invasive, while MCF-7 H3/ErbB2-A was not in any way invasive.

Results in the literature suggest that c-erbB-2 overexpression is associated with increased invasiveness. Various groups have transfected both transformed and cancer cell lines with c-erbB-2 to investigate its effect on their metastatic potential. MCF-10A was transfected with c-erbB-2 and Ha-ras, both separately (MCF-10A-H and MCF-10A-E) and in combination (MCF-10A-HE) (Giunciuglio *et al.*, 1995), resulting in the ability to grow in soft agar, increased migration in response to FCM (fibroblast conditioned media) and increased invasion of Matrigel. The MCF10A-HE cells also adopted an invasive stellate growth pattern when plated or embedded in Matrigel, in contrast to the spherical colonies formed by the single transformants MCF10A-H, MCF10A-E, and the parental cells. Expression of MMP-2 was found to elevated while TIMP-2 levels were lower in the transfectants. These results indicate that c-erbB-2 and Ha-ras co-expression can induce a more aggressive phenotype *in vitro*, representative of the malignancy of mammary carcinomas (Giunciuglio *et al.*, 1995).

Transfection of MDA-MB-435 with c-erbB-2 resulted in increased formation of metastatic nodules when injected into the lateral tail veins of 8-week old female ICR-SCID mice, although not larger in size than those formed by the parental cell line. Significantly higher rates of matrigel invasion were also observed. Interestingly, similar to the findings for both the c-erbB-2 cDNA and ribozyme transfectants in this thesis, no increase in motility was seen, in this case using chemoattractants. Similar adhesion ability to the extracellular matrix molecules laminin, fibronectin, collagen IV, vitronectin and Matrigel was observed. They observed higher expression of MMP-2 and MMP-9 in the cultured media of the transfectants, with the greatest expression of both in the highest expression transfectant. C-erbB-2 was not found to effect *in vitro* growth rate, or *in vitro* transforming ability, as measured in soft agar assays (Tan *et al.*, 1997). These findings are very similar to the findings in this thesis.

A study by Roetger *et al.* (1998) analysed disaggregated cells and cell clusters from freshly dissected breast cancer tissues and found that invasive, predominantly clustered

cells from 14 of 23 tumors were positively stained for c-erbB-2 by immunocytochemistry. In four control breast cancer cell lines (SK-BR-3, MCF-7, MDA-MB-468, and MDA-MB-468, the latter transfected with a full-length c-erbB-2 cDNA vector) producing different levels of the c-erbB-2 receptor, the expression level correlated positively with the invasiveness of the cells. They also showed that the invasive cell populations express the metastasis-associated proteins, matrix metalloproteinase MMP-2, CD44, and integrins $\alpha_v\beta_3$ and α_6. Zhang *et al.* (1998) was able to show that c-erbB-2 expression may have a direct effect on the expression of Type IV collagenases (MMP-2 and MMP-9). NIH 3T3 cells were transfected with point mutation activated neu, a mutant analogue of neu, the rat homologue of c-erbB-2. These cells were then treated with emodin and DK-V-47 (a derivative of emodin) which repress the tyrosine kinase activity of c-erbB-2. A consequence of this repression of kinase activity was an inhibition of anchorage dependant (by 55% and 83% respectively) and independent growth, and a decrease in the expression of MMP-2 and MMP-9. Both compounds virtually abolished the ability of the cells to perform in *in vitro* invasion assays.

C-erbB-2 overexpression in human mammary epithelial cells resulted in acquisition of anchorage-independent growth and invasion capabilities, dependent on fibronectin and correlated with the down-regulation of cell surface α4 integrin (Ignatoski *et al.*, 2000). Spencer *et al.* (2000) utilised carcinoma cells depleted of c-erbB-2, but not other ErbB receptor members, to specifically examine the role of c-erbB-2 in carcinoma cell migration and invasion. Cells stimulated with EGF-related peptides show increased invasion of the extracellular matrix, whereas cells devoid of functional c-erbB-2 receptors do not. Expression of the activated rat c-erbB-2/neu oncogene in mouse embryo fibroblast 3T3 cells is sufficient to induce experimental metastases in nude mice (Yu *et al.*, 1992).

The effects of c-erbB-2 upregulation on MCF-7 H3 adhesion were described in section 3.1.13. C-erbB-2 expression had no profound effect of the adhesive properties of MCF-7 H3, with the exception of a reduction in adhesion to fibronectin. However, figure 3.2.13.3 shows that adhesion to fibronectin was also reduced in BT474A after transfection with the c-erbB-2 ribozyme. Therefore this effect is likely to be cell line specific rather than as a result of c-erbB-2 regulation of adhesion. As mentioned c-erbB-2 downregulation in BT474A resulted in decreased adhesion to fibronectin.

Figures 3.2.13.1; 3.2.13.2; 3.2.13.4 shows that c-erbB-2 downregulation resulted in decreased adhesion to laminin, collagen type IV and matrigel. These findings do support the reports in the literature, to the effect that c-erbB-2 overexpression is associated with increased adhesion.

Tumour cells with metastatic propensity secrete more of the laminin α_2 chain than non-metastatic tumour cells do, and laminin-2, which contains the α_2 chain, promotes cell adhesion better than laminin-1. Han *et al.* (1999) found a correlation between the expression of the laminin-2 isoform and the metastatic phenotype in melanoma cells. Cell attachment studies showed that metastatic melanoma cells attached more efficiently to laminin-2 substrates. Studies on integrin expression revealed that the presence of $\alpha_2\beta_1$ integrin correlated with expression of the laminin-2 isoform in metastatic melanoma cells, inducing a specific 185 kD protein tyrosine phosphorylation, identified as c-erbB-2 by immunoprecipitation. These studies suggest that upregulation of expression of the laminin-2 chain correlates with the metastatic phenotype of melanoma cells and provides evidence that specific c-erbB-2 tyrosine phosphorylation may be involved in integrin-mediated signalling during tumour cell invasion and metastasis. Laminin receptors (integrins $\alpha_6\beta_1$ and $\alpha_6\beta_4$) were found to associate directly with c-erbB-2 in carcinoma cell lines and NIH 3T3 transfected with c-erbB-2. Carcinoma cells treated with a monoclonal antibody to the α_6 integrin subunit showed a ligand-dependent increase of c-erbB-2 phosphorylated molecules coprecipitated with integrins and increased DNA synthesis. The interaction between growth factor receptors and integrins was also studied in NIH3T3 cells overexpressing $\alpha_6\beta_4$ receptors and c-erbB-2 protein. Cells overexpressing both receptors, showed enhanced proliferation rates and invasiveness, further suggesting that $\alpha_6\beta_4$ integrin and ErbB-2 receptor interaction might contribute to generate a more malignant phenotype in carcinoma cells (Falcioni *et al.*, 1997).

Evidence exists, that c-erbB-2 effects the expression of metastasis associated proteins such as E-cadherin and β-catenin. The cadherins are a family of transmembrane glycoproteins that mediate cell-cell adhesion, by connecting cells to each other by homophilic interations, in which they bind selectively to identical cadherin types (Liang, 1999). A reduction in E-cadherin expression is found in many breast cancers and is associated with increased invasiveness (D'Souza and Taylor-Papadimitriou, 1994). Disruption of E-cadherin-mediated intercellular adhesion promotes cell

dissociation from the primary cancer nest and the E-cadherin-catenin complex functions as an invasion suppresser system in cancers (Shibata *et al.*, 1996). Overexpression of c-erbB-2 in the human mammary epithelial cell line, MTSV1-7, is associated with reduced ability to undergo morphogenesis *in vitro* and with a decreased level of expression of the E-cadherin and α_2 integrin genes (D'Souza and Taylor-Papadimitriou, 1994; D'Souza *et al.*, 1993). In human gastric cancer TMK-1 cells expressing a N-terminally truncated β-catenin, which binds c-erbB-2 but not E-cadherin, the association between endogenous β-catenin and c-erbB-2 protein was inhibited, suppressing the phosphorylation of β-catenin. These cells exhibited markedly reduced invasiveness *in vitro* and peritoneal metastasis *in vivo* and developed an epithelial morphology (Shibata *et al.*, 1996).

CD44 is a transmembrane glycoprotein that binds hyaluronic acid (HA). CD44 cell surface expression was 4.5 times higher in c-erbB-2 overexpressing mouse fibroblasts, than in the parental cell line. Overexpression of surface CD44s in c-erbB-2 transfected cells results in a dramatic enhancement of HA-mediated cell adhesion. These findings suggest that overexpression of CD44s and up-regulation of CD44s-ankyrin interaction by c-erbB-2 may be one of the pre-requisite steps in regulating tumour cell behavior (Zhu *et al.*, 1996).

Zymography of conditioned media from BT474A shows that this cell line secretes matrix metalloproteinases (MMPs). These MMPs appear to be MMP-2 and MMP-9. C-erbB-2 downregulation in BT474A resulted in decreased secretion of these MMPs. This is similar to the finding of Zhang *et al.* (1998) reported above, as emodin depletion of c-erbB-2 also resulted in decreased expression of MMP-2 and MMP-9. Genistein induced several specific molecular changes in head and neck cancer cells, such as down-regulation of c-erbB-2 expression, down-regulation of MMP-2 and MMP-9 secretion, inhibition of tumour cell invasion and down-regulation of nuclear factor-kappaB DNA binding activity (Alhasan *et al.*, 2001).

O-charoenrat *et al.* (2002) studied the profile of ErbB receptors in head and neck squamous cell carcinomas (HNSCC) to determine whether their expression was associated with clinicopathological features and key molecules involved in angiogenesis and metastasis. They also assessed the impact of expression on survival. This study included 54 cases of primary HNSCC, of which 27 cases showed lymph node

metastasis. HNSCC frequently co-expressed multiple ErbB receptors and showed significant correlations amongst their levels. High expression of c-erbB-1, c-erbB-2 or c-erbB-3 was associated with an infiltrating mode of invasion, nodal metastases and advanced pathological stages. C-erbB-1 and c-erbB-2 levels were strongly correlated (P=0.0004-0.029) with the expression of MMP-2, MMP-7, MMP-9, MMP-10, MMP-11, MMP-13, VEGF-A and VEGF-C whereas the levels of c-erbB-3 and c-erbB-4 showed a weaker correlation (P=0.049-0.01) with some MMPs and VEGF-C. Only nodal metastasis and c-erbB-1 levels were significantly associated with poor outcome in uni- and multi-variate analysis.

Zymography of conditioned media from MCF-7 H3 shows that this cell line secretes, in addition to MMPs, some additional proteases. These proteases not yet identified appear to be serine proteases of approximately, 22, 35, 45, 84 and 130kDa. They are only expressed in MCF-7 H3 and MCF-7 H3/ErbB2-A, with expression greatest in MCF-7 H3/ErbB2-A. It is interesting to note that MCF-7 H3/ErbB2-A is less invasive than MCF-7 H3, and also these bands were not detected in the invasive BT474A and MDA-MB-435S-F. These results were unexpected as previous transfections with c-erbB-2 had resulted in increased secretion of MMPs, especially MMP-2 and MMP-9., in association with increased invasiveness.

Sections 3.1.9.4 and 3.1.9.5 shows that transfection of MCF-7 H3 with c-erbB-2 leads to an increase in the expression of other proteins co-immunoprecipitated with c-erbB-2 or c-erbB-4, suggesting an increase in protein binding to these two receptors, and thus a possible activation of signalling pathways. This also coincides with increases in tyrosine phosphorylated proteins immunoprecipitated by c-erbB-2, 3 and 4, but not 1, as shown in Figure 3.1.9.5. It is possible that some of these proteins upstream of the signalling pathways which exert the effects seen in this thesis. Of special interest would be the isolation of these proteins and their identification, which could lead to a greater understanding of the mechanisms involved in c-erbB-2 receptor signalling. Future work would also include investigation of these phenomenon in the BT474A c-erbB-2 ribozyme transfected cells to determine whether the same proteins are downregulated.

4.4 The Role of c-erbB-2 in Tamoxifen Resistance

The evidence in the literature is conflicting as to whether c-erbB-2 overexpression plays a role in resistance to tamoxifen hormonal therapy. No evidence was found in this thesis for a role for c-erbB-2 in tamoxifen resistance. This may be due to the small changes in expression of c-erbb-2. It is possible that greater alteration in c-erbB-2 expresion may be necessary to have an effect on tamoxifen resistance. C-erbB-2 levels had no effect on the expression of estrogen receptor α protein, while c-erbB-2 overexpression in MCF-7 H3 resulted in increased estrogen receptor β, which was also accompanied by a decrease of estrogen receptor β in c-erbB-2 downregulated BT474A. Estrogen receptor β expression was shown to be significantly up-regulated in a tamoxifen-resistant group of breast cancer patients as compared with a tamoxifen-sensitive group (P = 0.001 by Fisher's exact test) (Speirs *et al.*, 1999). This is interesting as this may indicate a starting point for the development of resistance to tamoxifen as is seen in c-erbB-2 overexpressing patients.

Tsutsui *et al.* (2002) found that c-erbB-2 overexpression in patients with primary breast cancer was associated with reduced disease-free survival and overall survival in patients receiving tamoxifen. It was also associated with decreased estrogen receptor expression. Dowsett *et al.* (2001) evaluated the antiproliferative effects of endocrine therapy in c-erbB-2 positive/ER-positive primary human breast cancer. ER-positive/c-erbB-2 positive primary breast carcinomas show an impeded antiproliferative response to endocrine therapy that nonetheless may vary between individual treatments.

Bieche *et al.* (2001) examined the relation between c-erbB-2 gene expression and the response to adjuvant tamoxifen therapy in a well-defined cohort of 125 ERα positive postmenopausal patients with breast cancer. C-erbB-2 did not persist as an independent prognostic factor in multivariate analysis. Nevertheless, when c-erbB-2 mRNA level was analysed as a continuous variable, the higher the c-erbB-2 mRNA level, the poorer the outcome (P=0.00036). Ellis *et al.* (2001) reported that the aromatase inhibitor letrozole is more effective neoadjuvant endocrine therapy than tamoxifen for c-erbB-1 and/or c-erbB-2 positive, estrogen receptor-positive primary breast cancer (Spigel *et al.*, 2002).

Knoop *et al.* (2001) investigated interactions between adjuvant treatment with tamoxifen and the content of c-erbB-1, c-erbB-2, and p53 in steroid receptor-positive patients. Patients with steroid receptor-positive tumors and positive immunohistochemical staining for c-erbB-1, c-erbB-2 or p53 benefited from treatment with tamoxifen for 1 year. This study did not support the hypothesis that c-erbB-1, c-erbB-2 or p53 status predicts benefit from tamoxifen treatment in estrogen receptor-positive patients with early-stage breast cancer. Stal *et al.* (2000) studied the importance of c-erbB-2 status in early stage postmenopausal breast cancer for patients who participated in a trial of five vs. two years of adjuvant tamoxifen. Overall, c-erbB-2-positive patients had a significantly lower recurrence-free probability than others, 62% at five years as compared to 83%, and showed a significantly decreased breast cancer survival rate (P =0.0007).

Kumar *et al.* (1996) transfected MCF-7 breast cancer cells with a full-length c-erbB-2 cDNA, gaining high expression of c-erbB-2. Transfection led to the upregulation of bcl-2 (2.5-6 fold) compared to the parental or mock-transfected cell lines. Overexpression also led to enhanced expression of bcl-X_L, with no changes in bcl-X_S. No significant changes in levels of bax were seen in the transfectants. The transfection of the MCF-7 cells with c-erbB-2 led to the suppression of tamoxifen induced apoptosis. Benz *et al.* (1992) also transfected MCF-7 cells with c-erbB-2, which were no longer sensitive to tamoxifen. In this thesis transfection of MCF-7 H3 with c-erbB-2 had no effect on tamoxifen sensitivity.

Carlomagno *et al.* (1996) reported that c-erbB-2 positive node-negative patients did not benefit from tamoxifen treatments while those patients that were c-erbB-2 negative did. C-erbB-2 expression was not found to be significantly modified by tamoxifen treatment (Soubeyran *et al.*, 1996). Borg *et al.* (1994) noted a favourable effect of adjuvant tamoxifen on survival for patients with c-erbB-2 negative tumours, while patients who were positive did not benefit from tamoxifen administration. Giai *et al.* (1994) observed that node positive breast cancer patients co-expressing c-erbB-2 and ras had a worse outcome than those patients not co-expressing these oncogenes, when treated with tamoxifen. Wright *et al.* (1992) reported that only 7% of c-erbB-2 positive patients compared to 37% of c-erbB-2 negative patients responded to tamoxifen treatment. The combination of c-erbB-2 and c-erbB-1 appears to have an additive effect in reducing the likelihood of response to tamoxifen, as 0 out of 8 patients benefited. Nicholson *et al.*

(1993) reported that c-erbB-2 expression did not effect response to tamoxifen in a c-erbB-1 negative group of patients, while a significant loss of hormone sensitivity was found in the c-erbB-1 positive group. In contrast Archer *et al.* (1995) found no correlation between c-erbB-2 overexpression and response to tamoxifen therapy.

4.5 Taxol Resistance

For ease of discussion MDA-MB-435S-F shall from here on be referred to as MDA-F, MDA-MB-435S-F/Taxol-10p as Taxol-10p, MDA-MB-435S-F/Taxol-10p4p as Taxol-10p4p, MDA-MB-435S-F/Adr-10p as Adr-10p and MDA-MB-435S-F/Adr-10p10p as Adr-10p10p.

Taxol has demonstrated remarkable antineoplastic effects against a wide range of human tumours, including ovarian, breast, head and neck, small-cell and non-small-cell lung cancers, as well as metastatic melanomas. Studies of taxol-resistant tumour cell lines, have shown that the cellular transport of taxol and its microtubule-binding activity play a major role in the development of resistance to taxol (Pratt *et al.*, 1994).

Findings in the MDA-MB-435S-F taxol resistant variants	**Methods used**
Overexpression of mdr-1 at the RNA but not the protein level	RT-PCR Western Blot
Overexpression of mrp-1 at the RNA and protein level	RT-PCR Western Blot
Decreased expression of mrp-2, topo I, topo IIβ and GST π mRNA, increased expression of TS, topo IIα mRNA.	RT-PCR
Cross resistance to vincristine, taxotere and adriamycin, but not significantly resistant to carboplatin, VP-16 or 5-fluorouracil	Toxicity assay
Increased adriamycin efflux	Adriamycin accumulation assay
Circumvention of adriamycin toxicity by sulindac or verapamil and circumvention of taxol toxicity by verapamil but not sulindac.	Combination assays

Table 4.5 Summary of findings in MDA-MB-435S-F Taxol selected variants

There are numerous studies indicating that $p170^{MDR-1}$ (but not mrp-1 to a significant extent), plays a role in taxol resistance (Reinecke *et al.*, 2000; Mechetner *et al.*, 1998; Parekh *et al.*, 1997; Masenek *et al.*, 1997; Lehnert *et al.*, 1993, Kamazawa *et al.*, 2002). In an attempt to identify the mechanisms of resistance in Taxol-10p and Taxol-10p4p, alterations in the levels of a number of MDR markers were studied in this thesis.

Overexpression of mdr-1 mRNA in the taxol selected variants, Taxol-10p and Taxol-10p4p, was detected by RT-PCR compared to their parental cell line MDA-F (section 3.3.8.1), however western blotting did not reveal an increase at the protein level (section 3.3.9.1). Western blotting and RT-PCR revealed that mrp-1 levels were increased at both the mRNA and protein levels (section 3.3.8.2; 3.3.9.2). Mrp2 mRNA levels were shown by RT-PCR to have decreased with increasing Taxol resistance (section 3.3.8.3). Expression of mrp4 and mrp5 was undetectable by RT-PCR in MDA-F, Taxol-10p and /Taxol-10p4p (section 3.3.8.4; 3.3.8.5). These finding do not correlate with the general observations made in the literature with repsect to taxol resistance, that mdr-1 overexpression plays a role in resistance, while mrp-1 does not. Bhalla *et al.* (1994) described taxol resistant sublines of HL-60 myeloid leukaemia cells (HL-60/Tax100 and HL-60/Tax1000). HL-60/Tax100 and HL-60/Tax1000 displayed crossresistance to taxotere, vincristine and adriamycin, accompanied by increased mdr-1 mRNA and protein expression, circumventable by cyclosporin or verapamil. Decreased accumulation of taxol and daunomycin was also observed. Reinecke *et al.* (2000) compared the effects of taxol in human renal cell carcinoma of different histological types. Mrp-1 was not found to be related to taxol sensitivity, while expression of mdr-1 correlated positively with lack of response to taxol.

Mrp-1 expression was shown by Kamazawa *et al.* (2000) to increase in both KF human ovarian adenocarcinoma cell line and its taxol-resistant variant after exposure to taxol. Vanhoefer *et al.* (1996) investigated the modulatory activity of the novel pyridine analogue PAK-104P, an MRP specific inhibitor, on MRP-mediated resistance to adriamycin in two adriamycin-selected human tumour cell lines, HT1080/DR4 (sarcoma) and HL60/ADR (leukaemia). In cell lines HT1080/DR4 (MRP/lLRP phenotype) and HL60/ADR (MRP phenotype), adriamycin resistance was significantly higher (250-fold and 180-fold, respectively) than that to taxol (6-fold and 9-fold, respectively). With noncytotoxic concentrations of PAK-104P, the reversal of adriamycin resistance was significant but partial in HT1080/DR4 and HL60/ADR cells, whereas complete reversal of taxol resistance was achieved in HL60/ADR cells. This is opposite to the finding of this thesis as sulindac failed to circumvent taxol resistance in MDA-F or any of its taxol and adriamycin variants. The findings of Breuninger *et al.* (1995) were opposite to those of Kamazama *et al.* (2000) and Vanhoefer *et al.* (1996). NIH 3T3 transfection with Mrp-1 conferred resistance to adriamycin, daunorubicin, VP-16, actinomycin D, vincristine and vinblastine, but not taxol.

Adriamycin accumulation assays were performed on these cell lines to determine whether taxol resistance was associated with decreased adriamycin accumulation and increased drug efflux. Section 3.3.5 shows that adriamycin accumulation in Taxol-10p was less than that of the parental cell line), while Taxol-10p4p accumulated more adriamycin. Adriamycin efflux was higher in both cell lines than in MDA-F, with Taxol-10p4p efflux greater than Taxol-10p. These results indicate that increased drug efflux may play a role in adriamycin resistance in these cell lines. By extension efflux may also play a role in taxol resistance in these cell lines, but a taxol accumulation assay was not available for use.

Combination assays were performed to further elucidate mechanisms of resistance to adriamycin and taxol in the MDA-F variants. Verapamil inhibits both MDR-1 function and MRP-1 function. Sulindac inhibits MRP-1 function only. Sulindac and verapamil sensitised MDA-F, Taxol-10p and Taxol-10p4p to adriamycin, with sulindac having the greatest effect in the parental MDA-F cells (section 3.3.6.1; 3.3.6.2), and verapamil in the taxol selected variants (section 3.3.6.3; 3.3.6.4; 3.3.6.5; 3.3.6.6). These results suggest that MRP-1 and MDR-1 play a role in adriamycin resistance in these cell lines, although MDR-1 may have a greater role to play in the MDA-F taxol selected variants. Sulindac failed to circumvent taxol resistance in any of these cell lines (section 3.3.7.2; 3.3.7.4; 3.3.7.6), suggesting that MRP-1 may not transport taxol in these cell lines, while verapamil sensitised Taxol-10p (section 3.3.7.3) and Taxol-10p4p (section 3.3.7.5) to taxol, but had no effect on taxol sensitivity in parental MDA-F cells (section 3.3.7.1).

These results pose a question, why does verapamil circumvent adriamycin resistance in MDA-F, Taxol-10p and Taxol-10p4p, while circumventing taxol resistance in Taxol-10p and Taxol-10p4p, but not in the parental cells? Also if verapamil affects taxol only in taxol-selected cell lines, this would indicate that mdr-1 plays a role in taxol resistance in these cell lines. If this were the case, one would also expect to see large increase in resistance to adriamycin and a large increase in the effect of verapamil on adriamycin sensitivity in the taxol selected cell lines, which is not the case (section 3.3.4.1; 3.3.4.2; 3.3.6.1; 3.3.6.3; 3.3.6.5). It should be noted that, while Mdr-1 mRNA is overexpressed in Taxol-10p and Taxol-10p4p (section 3.3.8.1), it is not overexpressed at the protein level (section 3.3.9.1).

The cross-resistance profile of the MDA-F taxol resistant variants (section 3.3.4.1; 3.3.4.2) illustrates that Taxol-10p and Taxol-10p4p are both cross-resistant to taxotere and vincristine, while only Taxol-10p4p is cross-resistant to adriamycin. They are not resistant to 5-fluorouracil, VP-16 or carboplatin. Taxol resistant cell lines that overexpress mdr-1 are normally cross-resistant to adriamycin, vincristine, vinblastine, VP-16 and show little or no cross resistance to alkylating agents, platinum drugs and antimetabolites. Therefore these taxol-resistant variants do not display a MDR profile consistent with classic mdr-1 conferred drug resistance. As noted in the previous paragraph, mdr-1 overexpression in the taxol-resistant variants appears to be at mRNA level rather than at the protein level.

Neither dihydrofolate reductase mRNA (section 3.3.8.6), glutathine-S-transferase π mRNA (section 3.3.8.7) nor thymidylate synthase mRNA (section 3.3.8.8) levels were found to be significantly altered in MDA-F taxol selected variants. Dihydrofolate reductase does not play any known role in taxol resistance consistent with the findings in this thesis. Longley *et al.* (2001) transfected MDA-MB-435 with thymidylate synthase but found it had no effect on CPT-11, cisplatin, oxaliplatin or Taxol resistance. GST π was downregulated in human colon cancer cell line M7609 and in a M7609 Adriamycin selected variant, by antisense cDNA. The changes in the sensitivity of these transfectants to various anticancer drugs were investigated. Sensitivities to adriamycin, cisplatin, melphalan, and etoposide were increased while, the sensitivities to Taxol, vincristine, 5-fluorouracil, and mitomycin C were not significantly changed. Thus, GST π does not play a role in taxol resistance (Ban *et al.*, 1996).

Levels of topoisomerase I and IIβ mRNA decreased, while topoisomerase IIα mRNA increased with increasing taxol resistance in MDA-F/MDR variants (section 3.3.8.9; 3.3.8.10). This may explain the emergence of increased adriamycin resistance in Taxol-10p4p (section 3.3.4.2), but is unlikely to play a direct role in taxol resistance.

Apart from mdr-1 overexpression, reports have suggested that other mechanisms may be involved in taxol resistance. This includes development of altered α- or β- tubulin isotypes. Taxol is also metabolised by the cytochrome P-450 system and its metabolism may be altered by other drugs affected by this system (Rahman *et al.*, 1994; Martinez C *et al.*, 2002). Consequently, this system may be involved in the mechanism of

resistance to taxol. The sister gene of P-glycoprotein (Spgp) is a liver-specific ATP-binding cassette protein highly related to the P-glycoprotein (Pgp). Spgp is an approximately 170kDa glycosylated plasma membrane protein localised to the canalicular surface of hepatocytes in the rat liver. The expression of Spgp correlates with the differentiation of hepatocytes and is seen only in late liver development. It is not observed in hepatoma cell lines. The physiological function of Spgp in liver is unknown, but it maps to 2q31 in humans, in the vicinity of liver transport disorders for bile acids and cholesterol. Spgp may therefore be involved in some aspect of bile acid or cholesterol metabolism. Spgp transfectants have a low level resistance to Taxol but not to other drugs that form part of the multidrug resistance phenotype. This resistance is reversible by the mdr-1-reversing agents cyclosporin A, PSC833, and verapamil, suggesting a conservation in some functions of Pgps across large evolutionary distance. It is not known whether Spgp plays a role in taxol resistance in cancer cells (Childs *et al.*, 1998). Roy and Horwitz (1985) described a correlation between the presence of a 135kDa phosphoglycoprotein and resistance to taxol. The 135kDa phosphoglycoprotein was isolated from a taxol resistant subline of the macrophage-like cell line J744.2

A taxol-resistant subline, derived from the human ovarian cancer cell line SKOV-3, was established through selection by culture in incrementally increasing taxol concentrations. Comparison of SKOV-3 to SKOV-3TR by differential display identifed a new gene, TRAG-3 (Taxol Resistance Associated Gene- 3). TRAG-3 mRNA was overexpressed in the taxol-resistant cell line SKOV-3TR. DNA and protein analysis revealed that TRAG-3 has no homology to any known cDNAs or proteins. Northern analysis demonstrated that TRAG-3 is overexpressed in the taxol-resistant breast cancer cell line MDA 435TR as well as the adriamycin-resistant multiple myeloma cell lines 8226/DOX40 and 8226/MDR10V. A survey of normal tissue showed minimal or absent TRAG-3 mRNA expression. Screening of a wide variety of cancer cell lines demonstrated TRAG-3 expression in many cell lines derived from different tissue types. In summary, TRAG-3 is a novel gene whose expression is associated with the chemotherapy-resistant and neoplastic phenotype (Duan *et al.*, 1999). Early studies of TRAG-3 revealed overexpression in many carcinoma cell lines including several melanoma lines. Expression of TRAG-3 was present in normal testis but absent in all other tissues. RT-PCR evaluation of TRAG-3 reveals two transcripts in many carcinoma cell lines with sequencing of these products demonstrating the 799 bp TRAG-3

transcript and a second alternatively spliced transcript, TRAG-3 long TRAG-3 maps to band Xq28. TRAG-3 appears to be a novel cancer/testis antigen (Feller *et al.*, 2000).

Apoptotic factors have been implicated in the development of resistance to taxol in carcinoma cell lines. Stable transfection of human ovarian carcinoma cells with survivin cDNA caused a four- to six-fold increase in cell resistance to taxotere and taxol with a concomitant reduction in the apoptotic response to taxol, but did not affect cell sensitivity to cisplatin or oxaliplatin. High levels of survivin protein expression, detected by immunohistochemistry in advanced ovarian carcinomas, were significantly associated with clinical resistance to a taxol/platinum-based regimen but unrelated to tumour shrinkage following cisplatin-including combinations (non-taxol based) (Zaffaroni *et al.*, 2002).

Halder *et al.* (1996) reported that the treatment of prostate cancer cell lines expressing bcl-2 with taxol induced bcl-2 phosphorylation and programmed cell death, whereas treatment of bcl-2-negative prostate cancer cells with taxol did not induce apoptosis. They suggested that these findings supported the use of taxol for the treatment of bcl-2-positive prostate cancers and other bcl-2-positive malignancies, such as follicular lymphoma. Ibrado *et al.* (1996) reported on the effect of bcl-X_L overexpression on resistance to taxol-induced apoptosis. Intracellularly, taxol induces tubulin polymerization and mitotic arrest, followed by apoptosis. High Bcl-xL levels did not affect the microtubular bundling or mitotic arrest due to taxol but significantly inhibited the morphological, flow cytometric, and DNA fragmentation features associated with taxol-induced apoptosis. This resulted in a significant improvement in the survival of taxol-treated cells that possess high Bcl-xL levels.

4.6 Adriamycin Resistance

The most common method of resistance to adriamycin is increased drug efflux due to overexpression of P-glycoprotein. Cells selected for resistance to adriamycin are usually cross resistant to vinca alkaloids and other antibiotics such as actinomycin D. Other cell lines have been found to have increased glutathione peroxidase, glutathione or glutathione S-transferase.

Findings in the MDA-MB-435S-F adriamycin selected variants	**Methods used**
Failure of MDA-MB-435S-F to develop high resistance to adriamycin despite ability to develop resistance to taxol	Toxicity assay
No change in expression of MDR at RNA or protein level	RT-PCR Western Blot
Overexpression of MRP-1 at RNA and protein level	RT-PCR Western Blot
Decreased expression of mrp-2, GST π, TS and topo I mRNA, increased expression of topo IIα mRNA	RT-PCR
Cross resistance to VP-16, vincristine and taxotere, while sensitised to carboplatin, taxol and 5-fluorouracil	Toxicity assay
Increased adriamycin efflux	Adriamycin accumulation assay
Circumvention of adriamycin resistance by sulindac and verapamil, while no circumvention of taxol resistance by verapamil or sulindac detected.	Combination assays

Table 4.6 Summary of findings in MDA-MB-435S-F adriamycin selected variants

Numerous studies have indicated a role for mdr-1, mrp-1, GST π and topoisomerases in adriamycin resistance (Uchiyama-kokubu, *et al.*, 2001; Bader *et al.*, 1998; Yoo *et al.*, 1998; Lee *et al.*, 1996; Kuriyama *et al.*, 1997). In an attempt to identify the mechanisms of resistance in Adr-10p and Adr-10p10p, mRNA expression of a number of MDR markers were studied in this thesis.

MDA-F failed to select for resistance to adriamycin. Adr-10p failed to achieve a significant increase in adriamycin resistance (section 3.3.4.3), although it was significantly resistant to VP-16. Adr-10p10p did have a statistically significant increase in adriamycin resistance (section 3.3.4.4), although it was only a 1.4 fold increase. This cell line was also cross resistant to vincristine (1.61X), VP-16 (2.05X) and Taxotere (1.42X). Both variants were significantly sensitised to taxol and 5-fluorouracil, while only Adr-10p10p was sensitised to carboplatin. It can be concluded that this breast cancer cell line is resistant to selection by adriamycin, but not by taxol. Interestingly, previous work in this lab showed that the breast cell line BT-20 was not selectable for resistance to adriamycin, while MCF-7 was (NicAmhlaoibh, 1997). It may also be of interest that there is a trend here in p53 status in breast cell lines and development of resistance to adriamycin. MCF-7 contains wild type p53, while BT-20 and MDA-MB-435 (the grandparental cell line of MDA-F) both express mutant p53.

A large number of factors play a role in adriamycin resistance. This includes the overexpression of drug pumps such as mdr-1, mrp-1, mrp-2, mrp-3 and LRP (Clynes *et al.*, 1998; Borst *et al.*, 1999; Cui *et al.*, 1999; Young *et al.*, 1999). The cross resistance profiles of Adr-10p and Adr-10p10p, do not indicate a role for mdr-1 in the drug resistance of these cell lines. This confirmed by the lack of detection of any increase in mdr-1 expression at either the mRNA (section 3.3.8.1) or protein level (3.3.9.1) in either of these adriamycin selected variants. Mrp-1 overexpression has been shown to confer resistance to anthracyclines, epipodophyllotoxins and some vinca alkaloids (Clynes *et al.*, 1998). Breuninger *et al.* (1995) transfected NIH 3T3 with Mrp-1 and studied its affect on drug resistance. Mrp-1 overexpression in NIH 3T3 conferred resistance to adriamycin, daunorubicin, etoposide, actinomycin D, vincristine and vinblastine, but not taxol. The increased resistance to adriamycin, VP-16 and vincristine in Adr-10p10p is consistent with an mrp-1 drug resistant phenotype. Western blotting and RT-PCR revealed that mrp-1 levels were increased at both the mRNA and protein level (section 3.3.8.2; 3.3.9.2). As described in section 4.2 adriamycin selected cell lines expressed high levels of mrp-1 (Vanhoefer *et al.*, 1996; Beck *et al.*, 2001). Mrp-2 mRNA expression was reduced in Adr-10p and Adr-10p10p, relative to their parental cell (section 3.3.8.3). This was unexpected as mrp2 is known to confer resistance to adriamycin (Koike *et al.*, 1997; Cui *et al.*, 1999). This may go some way in explaining why MDA-F did not develop adriamycin resistance, as a reduction in mrp-2 expression may have cancelled out any benefits seen by increased mrp-1 expression.

Adriamycin accumulation assays were performed to determine whether the adriamycin selected variants showed changes in adriamycin accumulation or adriamycin efflux. Section 3.3.5 shows that adriamycin accumulation in Adr-10p was greater than the parental cell line (28% more), while Adr-10p10p accumulated the same amount of adriamycin as the parental cell line. Adriamycin efflux was higher in both cell lines than in MDA-F, with almost a 4-fold increase in efflux. These results indicate that the adriamycin selected cell lines have gained increased adriamycin efflux. However the fact still remains that they failed to become highly resistant to adriamycin. It is possible that the increased accumulation of adriamycin in Adr-10p, counteracts the increased efflux in this cell line, and may explain why no increase in adriamycin resistance is observed.

Combination assays performed on these cell line, showed that sulindac and verapamil sensitised MDA-F, Adr-10p and Adr-10p10p to adriamycin. While sulindac had a greater effect on adriamycin sensitivity than verapamil in MDA-F (section 3.3.6.1; 3.3.6.2), the reverse was observed in Adr-10p (section 3.3.6.7; 3.3.6.8) and Adr-10p10p (section 3.3.6.9; 3.3.6.10). This was similar to findings for Taxol-10p (section 3.3.6.3; 3.3.6.4) and Taxol-10p4p (section 3.3.6.5; 3.3.6.6). These results suggest that MRP-1 and mdr-1 play a role in adriamycin sensitivity in these cell lines. No large changes in potency of verapamil or sulindac were observed in Adr-10p (section 3.3.6.7; 3.3.6.8) and Adr-10p10p (section 3.3.6.9; 3.3.6.10). Neither sulindac nor verapamil were capable of circumventing taxol resistance in either the parental (section 3.3.7.2) or any of the adriamycin-resistant variants (section 3.3.7.8; 3.3.7.10). This that the verapamil circumvention of adriamycin toxicity observed was through inhibition of MRP-1 and not MDR-1, as if MDR-1 were present verapamil would also circumvent taxol resistance. Adriamycin-resistant cell lines that express mrp-1 are normally cross-resistant to adriamycin, daunorubicin, VP-16, actinomycin D and vincristine, but not taxol or vinblastine. Mrp-2 resistance profiles are similar to mrp-1 with exception that it also transports cisplatin and vinblastine.

No significant changes in dihydrofolate reductase mRNA levels were observed (section 3.3.8.6), consistent with findings in the literature (Mandelbaum-Shavit and Ramu, 1987;. NicAmhlaoibh *et al.*, 1999). Thymidylate synthase mRNA levels decreased in both Adr-10p and Adr-10p10p (section 3.3.8.8). This correlates well with a decrease in

5-Fluorouracil resistance in these cell lines (section 3.3.4.3; 3.3.4.4). It is unlikely that (section 3.3.4.3; 3.3.4.4) has a direct effect on adriamycin resistance, although correlations have been made between thymidylate synthase expression and failure to respond to adriamycin therapy in human squamous cell lung carcinomas patients (Volm and Mattern, 1992).

No changes in glutathione-S-transferase π mRNA levels were observed in these adriamycin selected variants (section 3.3.8.7). These results differ from those found in the literature. Increased GST π expression is linked to increased adriamycin resistance and is often induced during adriamycin selection. As mentioned in section 4.2, GST π antisense sensitised human colon cancer cell line M7609 to adriamycin, cisplatin, melphalan, and VP-16, but not taxol, vincristine, 5-fluorouracil, or mitomycin C (Ban *et al.*, 1996). Masanek *et al.* (1997) showed that adriamycin selected OAW-42 displayed overexpression of mdr-1, GST π, thymidylate synthase , glutathione peroxidase and c-jun.

Kiura *et al.* (1993) selected the human small cell lung cancer cell line SBC-3 with resulting adriamycin resistance was accompanied by slower growth rate, increased MDR-1 expression, a decrease in intracellular accumulation of Adriamycin, elevation of the intracellular GSH content coupled with GST π levels and a decrease in topoisomerase II activity.

Two types of topoisomerases (Topo I and Topo II) have been distinguished and characterised. Topoisomerase I catalyses the conversion of of the DNA topology by introdicing single strand breaks into the DNA molecule. Topoisomerase II (of which there are two isoforms (IIα of p170 kDa and IIβ of 180 kDa) are able to cleave double stranded DNA and can support more complex interconversions of the DNA topoology by an ATP-dependant strand passage process (Parchment & Pessina, 1998). Levels of topoisomerase I mRNA decreased in response to adriamycin selection (section 3.3.8.9; 3.3.8.11), while levels of topoisomerase IIα mRNA increased as compared to the parental cell line. These results are surprising as increased adriamycin resistance is usually associated with decreased topoisomerase IIα expression (Cole *et al.*, 1991) or activity (De Jong *et al.*, 1990; Deffie *et al.*, 1989), or mutation of topoisomerase IIα (Deffie *et al.*, 1989).

4.7 The Effects of Taxol Selection on Cell Adhesion, Motility and Invasion.

4.7.1 Effects of Taxol Selection on Cell Adhesion

Findings in the MDA-MB-435S-F taxol resistant variants	Methods used
Reduced adherence to laminin	Adhesion Assay
Reduced adherence to fibronectin	Adhesion Assay
Reduced adherence to collagen type IV	Adhesion Assay
Reduced adherence to matrigel	Adhesion Assay
Reduced adherence of Taxol-10p superinvasive population to laminin, fibronectin, collagen type IV and matrigel	Adhesion Assay
Increased adherence of Taxol-10p4p superinvasive population to laminin, fibronectin, collagen type IV and matrigel	Adhesion Assay

Table 4.7.1 Summary of adhesive properties of taxol selected variants of MDA-MB-435S-F.

Taxoids exert a direct effect on cell adhesion by stabilisation of microtubules. Cell adhesion is important in the regulation of cell proliferation, migration, survival, and apoptosis. The major components of cell adhesion are the cadherin family of proteins, α-, β- and γ-catenins, and cytoskeletons. In addition, β-catenin, when associated with adenomatous polyposis coli (APC) protein, an oncosuppressor, is implicated in the regulation of β-catenin/APC-related signaling pathways. To examine the correlation between impairment of cell adhesion events and apoptosis, Ling *et al.* (2001) used human non-small-cell lung cancer H460 and H520 cell lines as models to determine whether taxol-induced apoptosis was associated with disruption of the components of cell adhesion and their functions. Taxol treatment resulted in cells rounding up and losing contact with their neighboring cells, suggesting that the drug does indeed affect cell adhesion and related events. Western blot analysis revealed that taxol caused a time- and concentration-dependent cleavage of β-catenin, γ-catenin, and APC protein, but not α-catenin or E-cadherin. Taxol treatment led to the proteolysis and activation of caspase-3 and -7, but not caspase-1. Furthermore, taxol-induced apoptosis and cleavage

of β-catenin and γ-catenin were inhibited by the pan-caspase inhibitor Z-VAD-FMK and partially inhibited by the caspase-3 inhibitor Z-DEVD-FMK but were not affected by the caspase-1 inhibitor AC-YVAD-CMK. Interestingly, the taxol-induced β-catenin fragment lost its ability to bind to E-cadherin, α-catenin, or APC protein and to serve as a substrate for tyrosine kinase. All their data demonstrate that the caspase-mediated cleavage of β-catenin, γ-catenin, and APC protein might contribute to taxol-induced apoptosis.

These observations suggest that taxol-mediated stabilisation of microtubules and subsequent cell death may be more effective if the tumour is adherent to the extracellular matrix. It may be advantageous to a tumour or cell line to become less adhesive to extracellular matrix components, in order to lessen the effects of taxol on microtubules. In the case of the taxol-selected variants of MDA-F, they are considerably less adhesive to laminin, fibronectin, collagen type IV and matrigel (sections 3.3.14.1; 3.3.14.2; 3.3.14.3; 3.3.14.4). If the cell is less adherent, then taxol will be unable to induce events such as observed by Ling *et al.* (2001). Bershadsky *et al.* (1996) also studied the disruption of microtubules by nocodazole or vinblastine, without the addition of external growth factors in serum-starved Swiss 3T3 cells. In matrix-adherent, serum-starved Swiss 3T3 cells, the system of focal adhesions and actin bundles is poorly developed, and the level of tyrosine phosphorylation of FAK and paxillin is low. A number of growth factors rapidly stimulate tyrosine phosphorylation of these proteins and the assembly of focal adhesions and actin bundles. Growth factors and adhesion to the ECM are both necessary for the subsequent transition of cells to the S-phase of the cell cycle. Vinblastine and nocodazole induced the rapid assembly of focal adhesions and microfilament bundles, tyrosine phosphorylation of FAK and paxillin, and subsequent enhancement of DNA synthesis. All these effects required cell adhesion to the ECM and do not occur when cells are plated on substrates coated with poly-L-lysine or concanavalin A. Inhibitors of tyrosine phosphorylation and cell contractility also eliminate the effects of microtubule disruption on adhesion-dependent signal transduction. In ECM-attached cells, microtubule disruption activates the integrin-dependent signalling cascade, which leads to the assembly of matrix adhesions and the induction of DNA synthesis. The increase in cell contractility is an indispensable intermediate step in this signalling process.

The effectiveness of chemotherapeutic drug is severely limited by expression of intrinsic resistance in some patients and by acquired resistance in others. Kerbel *et al.* (1996) hypothesised that the resistance of solid tumors, including breast cancer, can be expressed at the prototissue/multicellular level, and that this "multicellular resistance" can be minimized or reversed by the appropriate use of so-called "anti-adhesive" agents. It is well known that monolayer cultures of tumour cells including murine breast cancer are generally much more intrinsically chemosensitive than the same cells grown as solid tumors *in vivo*. However, the relative resistance of solid tumors can often be recapitulated in tissue culture simply by growth of the tumour cells as three dimensional multicellular spheroids. There are cases where this is also true with respect to acquired drug resistance. This "multicellular resistance" could be due to such factors as insufficient drug penetration, a reduced growth fraction, or a decreased sensitivity to drug induced apoptosis mediated by cell-cell interaction survival signals. The relative intrinsic resistance of intact murine EMT-6 mouse mammary carcinoma spheroids can be significantly reversed by the anti-adhesive (disaggregating) effects of hyaluronidase. Moreover, this novel method of chemosensitization appears to depend on increased recruitment of disaggregated cells into the cycling pool, thus rendering them more sensitive to a cell cycle dependent drug such as cyclophosphamide. The reduced growth fraction observed in spheroids appears to be due to a marked cell contact-dependent upregulation of the cyclin dependent kinase inhibitor, p27Kipl.

If one of the mechanisms of action of taxol is to reduce the adhesiveness of tumour cells to their tumour mass there by increasing the surface area available to the drug, and reducing cell-cell interactions which might be advantageous to the tumour cells, it is possible that tumour cells may develop resistance to taxol, through loss of adhesiveness, thereby eliminating one of the mechanisms of taxol action.

4.7.2 Effects of Taxol Selection on Cell Motility

Findings in the MDA-MB-435S-F taxol resistant variants	Methods used
Decreased motility of Taxol-10p compared to parental cell line	Motility Assay
Decreased motility of Taxol-10p4p compared to parental cell line	Motility Assay

Table 4.7.2 Summary of motility properties of taxol selected variants of MDA-MB-435S-F.

Taxol treatment at non-lethal levels in general leads to decreased cell motility (Stracke *et al.*, 1993; Liao *et al.*, 1995; Belotti *et al.*, 1996). Motility assays for MDA-F and its taxol resistant variants showed that Taxol-10p and Taxol-10p4p were considerably less motile then their parental cell line (section 3.12.1). This may be as a direct result of exposure to taxol which inhibits motility, after which the subsequent cell population did not recover, or due to the development of reduced motility so that taxol is no longer able to target components involved in motility.

Taxol, which stabilises microtubules, decreases stimulated-motility of the human tumour cell line, A2058. Taxol had an inhibitory effect on adherence, with adhesion to gelatin being greater affected than adhesion to tissue culture plastic or laminin. This suggests that, in these tumour cells, taxol stabilisation of microfilaments inhibits both motility and adherence (Stracke *et al.*, 1993).

The effect of taxol on the morphological changes induced by hepatocyte growth factor/scatter factor (HGF/SF) in MDCK cells were studied. The results suggest that there are two components in the response to HGF/SF: (a) activation of the extension of lamellae leading to cell spreading; and (b) reorganisation of microtubules leading to polarisation of cell shape. The latter response is highly sensitive to taxol. HGF/SF induced spreading in taxol-treated MDCK cells but these cells retained a non-polarized discoid shape and a pattern of actin microfilament bundles characteristic of the untreated cells. Taxol did not prevent HGF/SF-induced migration of cells in Boyden chambers but completely inhibited the outgrowth of multicellular strands and tubules from cell aggregates in collagen gels. These results show that enhanced lamella formation in response to HGF/SF without polarisation of cell shape is sufficient to induce cell motility. In contrast, microtubule-dependent polarisation is essential for complex morphogenetic responses such as tubulogenesis in collagen gels (Dugina *et al.*, 1995). These results again suggest that taxol action is enhanced when cells are adhered to an extracellular type substrate.

Liao *et al.* (1995) measured the rate of locomotion of NRK fibroblasts migrating into an *in vitro* wound, before and after treatment with different concentrations of nocodazole to generate cells with different levels of microtubules. A comparison of the locomotion rate measurements with the microtubule level measurements indicated that over half of

the cell locomotion rate could be blocked by nocodazole without significantly affecting microtubule levels in the cell; the remaining locomotion rate was reduced proportionally to microtubule levels. This suggests that low concentrations of nocodazole interfere with microtubule dynamics and thus, microtubule dynamics are critical for the maximal speed of cell locomotion. Analogous effects of taxol and vinblastine on cell locomotion further supported this notion: at concentrations that reportedly cause little change in the level of microtubules, taxol and vinblastine also dramatically decreased the rate of locomotion of NRK cells.

Belotti *et al.* (1996) studied the effect of taxol on the adhesive and motility properties of human ovarian carcinoma cell lines. Taxol significantly inhibited the motility of OVCAR 5, SK-OV-3, and HOC-1OTC ovarian carcinoma cell but did not affect the adhesion of these cells to the subendothelial matrix. The association between inhibition of motility and cytotoxic activity was investigated using an A2780 subclone (1A9) and three taxol-resistant variants (designated 1A9/PTX22, 1A9/PTX10, and 1A9/PTX18). Although taxol did not significantly affect the adhesion to subendothelial matrix of the sublines, it completely inhibited their migration. Inhibition of migration was similar in 1A9 cells and the resistant sublines. Taxol inhibited motility induced by soluble attractant (chemotaxis) and immobilised attractant (haptotaxis). Inhibition of cell motility occurred in the absence of an antiproliferative effect, because higher concentrations of taxol were required to inhibit tumour cell. These data show that taxol is a potent inhibitor of ovarian carcinoma cell motility and that this activity is independent of its cytotoxic activity.

The effect of taxol on endothelial cell functions and on angiogenesis was studied by Belotti *et al.* (1996). *In vivo*, non-lethal concentrations of taxol significantly inhibited the angiogenic response induced by tumour cell supernatant embedded in a pellet of reconstituted basement membrane (Matrigel) injected s.c. into C57BL/6N mice. *In vitro*, it inhibited endothelial cell proliferation, motility, invasiveness, and cord formation on Matrigel in a dose-dependent manner. This data indicates that taxol has a strong anti-angiogenic activity, a property that might contribute to its antineoplastic activity *in vivo*.

Migrating cells are polarised with a protrusive lamella at the cell front followed by the main cell body and a retractable tail at the rear of the cell. The lamella terminates in ruffling lamellipodia that face the direction of migration. Ballestrem *et al.* (2000)

studied the contribution of microtubules to cell motility by time-lapse video microscopy on green fluorescence protein-actin- and tubulin-green fluorescence protein-transfected melanoma cells. Treatment of cells with either the microtubule-disrupting agent nocodazole or with the stabilising agent taxol showed decreased reversible ruffling and lamellipodium formation. Although ruffling and lamellipodia were formed without microtubules, the microtubular network was needed for advancement of the cell body and the subsequent retraction of the tail. The formation of lamellipodia occurs via actin polymerisation independently of microtubules, but microtubules are required for cell migration, tail retraction, and modulation of cell adhesion.

4.7.3 Affects of Taxol Selection on Cell Invasion

Findings in the MDA-MB-435S-F taxol resistant variants	**Methods used**
Novel finding of thesis - Development of a two tiered invasive phenotype not present in the parental cell line (1) Invasion of matrigel to underside of invasion chamber (2) Detachment of cells from underside of invasion chamber and reattachment to bottom of 24-well plate (only in taxol selected and adriamycin selected variants – see section 4.5)	Invasion Assay
No changes observed secretion of MMP-2 or MMP9 in Taxol-10p or Taxol-10p4p compared to parental cell line	Zymography

Table 4.7.3 Summary of invasion properties of taxol selected variants of MDA-MB-435S-F.

Initially invasion assays indicated no major changes in the invasiveness of Taxol-10p or Taxol-10p4p compared to MDA-F (section 3.3.13.1). It actually appeared that the cell lines were less invasive which would have been similar to reports of the effects of taxol on cell invasion as seen in the literature (Stearns and Wang, 1992; Terzis *et al.*, 1997; Westerlund *et al.*, 1997; Sgadari *et al.*, 2000; Liu *et al.*, 1998). It was then observed that the taxol selected variants had developed the ability to invade to the underside of the invasion chamber and then detach from the bottom and reattach to the bottom of the 24

well plate. It was thought that this phenomenon might be linked to the vastly reduced adhesiveness of these cells to components of the extracellular matrix (section 3.3.14). This could be an indication that taxol selects for a more aggressive invasive phenotype, which may appear to be overall less invasive, but selects for cells capable of invading further, and perhaps with a greater survival rate. No changes in the secretion of MMP-2 or MMP-9 were observed in these cell lines (section 3.3.15), however it has not yet been investigated whether there is a reduction in the tissue inhibitors of matrix metalloproteinases in these variants.

While some reports indicate that taxol increases motility and invasion, they are very few (Silbergeld *et al.*, 1995; Welch *et al.*, 1989), the majority of reports indicate that that taxol exposure has an inhibitory effect on invasion and metastasis. Stearns and Wang (1992) reported that taxol blocked processes essential for prostate tumour cell (PC-3 ML) invasion and metastases. Abnormal bundling of microtubules in a dosage-dependent manner, was observed upon treatment with taxol, accompanied by inhibition of secretion of the 72kDa and 92 kDa type IV collagenases and 57kDa gelatinase, and inhibition of invasion of Matrigel in Boyden chamber chemotactic studies. More importantly, studies in SCID mice demonstrated that taxol (50 to 250 mg/m^2/day) blocked the establishment, growth, and long-term survival of PC-3 ML cells. Verschueren *et al.* (1994) also reported on the inhibition by taxol of BW-O-Li1, a T-lymphoma cell line that forms metastases in various organs after injection into syngeneic mice, motility and invasion.

In contrast Silbergeld *et al.* (1995) evaluated *in vitro* chemosensitivity of glioblastoma to Taxol and the affect of Taxol on glioblastoma cell locomotion. Five human glioblastomas and the C6 rat glioma, were exposed to taxol (0-250 nM) and suspended in agar in capillary tubes. All six cell lines demonstrated sensitivity to Taxol (LD50 1 nM to > 250 nM). Increasing Taxol concentration caused increased locomotion in all six cell lines ($p < 0.0001$). These findings suggested that the clinical use of Taxol for glioblastoma may slow the growth of bulk disease, but may also lead to increased tumour invasion. Terzis *et al.* (1997) tested taxol for its anti-migrational, anti-invasive and anti-proliferative effect on two human glioma cell lines (GaMg and D-54Mg) grown as multicellular tumour spheroids. Both cell lines showed a dose-dependent growth and migratory response to taxol. Taxol also proved to be remarkably effective in

preventing invasion in a co-culture system in which tumour spheroids were confronted with fetal rat brain cell aggregates.

Westerlund *et al.* (1997) studied the effect of the taxol on a human ovarian cancer cell line (Ovcar-3). Ovcar-3 cell attachment, migration and *in vitro* invasion were significantly decreased after taxol treatment ($P = 0.02$, $P < 0.01$ and $P = 0.001$, respectively) whereas no alteration in the secretion of latent MMP-2 was noted. However, the intracellular localisation of the immunoreactive protein for MMP-2 was altered in response to taxol treatment. Interestingly, taxol increased the appearance of TIMP-2 protein in culture medium ($P = 0.002$) but did not change the expression of mRNA for TIMP-2 in Ovcar-3 cells. These data show that taxol is an effective suppressor of Ovcar-3 cell invasion. It inhibits attachment and migratory activities of the cells and also causes a release of TIMP-2 protein into the tissue culture medium.

Sgadari *et al.* (2000) investigated the mechanisms of taxol activity in Kaposi's sarcoma (KS), an angioproliferative disease. Using a model of experimental KS induced by the inoculation of KS-derived spindle cells in nude mice and primary cultures of KS spindle cells, they found that taxol promoted regression of KS lesions *in vivo* and that it blocked the growth, migration, and invasion of KS cells *in vitro*. Furthermore, taxol treatment promoted apoptosis and down-regulated Bcl-2 protein expression in KS cells *in vitro* and in KS-like lesions in mice. These results suggest that taxol interferes with KS by down regulating Bcl-2 antiapoptotic effect. Liang *et al.* (2001) reported that the selection of RPMI 2650 with taxol had no effect on the invasiveness of the cell line, while selection with melphalan resulted in a cell line with increased invasiveness.

Myoung *et al.* (2001) investigated the inhibitory effects of taxol and thalidomide on the growth of oral squamous cell carcinoma (OSCC) xenotransplanted into nude mice. Taxol showed an inhibitory effect on the growth of transplanted human OSCC and reduced the immunohistochemical expression of VEGF and CD31 and VEGF mRNA ($P<0.01$). Thalidomide also lowered remarkably VEGF expression ($P<0.01$) and CD31 ($P<0.01$) as well as VEGF mRNA ($P<0.05$), but it did not show statistically significant inhibitory effect on the tumour growth. These results suggest that the growth of human OSCC is not simply dependent on VEGF-induced angiogenesis and that anti-angiogenic therapy alone is not likely to be effective for the treatment of OSCC, but might be regarded as an adjuvant chemotherapeutic strategy.

Liu *et al.* (1998) reported on the antitumour and anti-invasion activities of taxol, harringtonine, homoharringtonine (harringtonine and its derivative homoharringtonine are ester-containing anti-leukemic alkaloids isolated from the tree *Cephalotaxus harringtonia*) and camptothecin on highly metastatic melanoma B16-BL6 and human fibrosarcoma HT-1080 cells. Results demonstrated that taxol, harringtonine, homoharringtonine and camptothecin exhibited significant inhibition of cell growth of B16-BL6 and HT-1080 cells. Taxol, harringtonine and homoharringtonine were also found to be effective for the inhibition of cell invasion and migration of B16-BL6 cells, but camptothecin showed basically no effect at the indicated concentration. Welch *et al.* (1989) studied the effects of chemotherapeutic drug pre-treatment on the invasiveness of cell lines demonstrating low and high invasive and metastatic potentials. Cells were treated with drug for 48 hours prior to invasion assays, at non-cytotoxic levels. Of these, vincristine, colcemid and colchicine inhibited invasion but taxol did not.

4.8 The Effects of Adriamycin Selection on Cell Adhesion, Motility and Invasion.

4.8.1 Affects of Adriamycin Selection on Cell Adhesion

Findings in the MDA-MB-435S-F adriamycin selected variants	Methods used
Reduced adherence to laminin	Adhesion Assay
Reduced adherence to fibronectin	Adhesion Assay
Reduced adherence to collagen type IV	Adhesion Assay
Reduced adherence to matrigel	Adhesion Assay
Increased adherence of/Adr-10p superinvasive population to laminin, fibronectin, collagen type IV and matrigel	Adhesion Assay
Increased adherence of Adr-10p10p superinvasive population to laminin, fibronectin, collagen type IV and matrigel	Adhesion Assay

Table 4.8.1 Summary of adhesive properties of adriamycin-selected variants of MDA-MB-435S-F.

Similar to the taxol-selected variants, the adriamycin-selected variants of Adr-10p and Adr-10p10p exhibited decreased adhesion to laminin (section 3.3.14.1), collagen type IV (section 3.3.14.2), fibronectin (section 3.3.14.3) and matrigel (section 3.3.14.1). The reduction in adhesion was greatest for fibronectin and laminin). These reductions in adhesion to ECM proteins were not as great as for the taxol-selected variants.

Tumour cell adhesion to the extracellular matrix (ECM) is closely linked with tumour cell invasion and metastasis. Repesh *et al.* (1993) demonstrated that low levels of adriamycin can inhibit the invasion of highly metastatic K1735-M2 mouse melanoma cells *in vitro* through a reconstituted basement membrane extract. Adriamycin-induced inhibition of melanoma cell invasion occurred at levels of the drug (i.e. 1 ng/ml) that did not inhibit tumour cell growth, suggesting that the observed inhibition in tumour cell invasion was not due to the well-documented ability of adriamycin to interfere with DNA and/or RNA synthesis. Rather, these studies indicated that adriamycin-induced

inhibition of melanoma cell invasion was accompanied by a corresponding decrease in the ability of adriamycin-treated tumour cells to migrate in response to several isolated ECM components including fibronectin, laminin and basement membrane (type IV) collagen. The decreased migration of adriamycin-treated tumour cells was not accompanied by a decrease in the adhesion or spreading of the adriamycin-treated cells on substrata coated with these ECM components. Instead, adriamycin-treated cells actually exhibited a slightly increased propensity (compared to untreated control cells) to adhere on fibronectin-, laminin-, and type IV collagen-coated substrata. Additionally, adriamycin treatment caused a dramatic increase in focal contact formation by these melanoma cells, as assessed by fluorescent microscopy of actin and vinculin. The findings of Repesh *et al.* (1993) suggest that decreased invasion is accompanied by decreased motility and increased adhesion.

4.8.2 Effects of Adriamycin Selection on Cell Motility

Findings in the MDA-MB-435S-F adriamycin selected variants	Methods used
Increased motility of Adr-10p compared to parental cell line	Motility Assay
Decreased motility of Adr-10p10p compared to Adr-10p, but levels similar to grandparental cell line MDA-F	Motility Assay

Table 4.8.2 Summary of motility of adriamycin selected variants of MDA-MB-435S-F.

From these results there does not appear to be a direct link in our system to the motility of Adr-10p and Adr-10p10p and their adhesion to ECM proteins.

Drug-resistance is critical in treating malignant tumours. Little study has been done on the biological changes in tumour cell activity in the course of acquiring drug-resistance. Hikawa *et al.* (2000) used a glioma cell line to study changes in cell adhesion and invasion on acquiring drug-resistance. Human glioma culture cell line IN157 was used to establish the cell lines resistant to VP-16, vincristine and adriamycin. Expressions of integrin α_2, α_3, α_5, and β_1, neuronal cell adhesion molecule (NCAM) and MMPs were examined by flow cytometry. In drug-resistant cells, integrin expression was enhanced and NCAM expression was reduced. Adhesions to the extracellular matrix (ECM)

proteins (laminin, fibronectin or type IV collagen) were studied. The adhesive ability of all cell lines increased in a concentration-dependent manner. Adhesion of drug-resistant cells was significantly stronger than that of IN157. The cell invasion of drug-resistant cell lines to the basal membrane was significantly lower than that of IN157. The cell invasion of IN157 was significantly suppressed by adding anti-NCAM antibody. In the case of IN157 with the acquisition of drug-resistance, an increase in the expression of integrins may have enhanced the adhesion to ECM proteins. This finding may be concerned with the decreased activity of drug-resistant cell lines in invading the basement membrane. NCAM expression in drug-resistant cell lines was reduced and anti-NCAM antibody abated invasion of IN157, suggesting that NCAM is involved in IN157 invasion.

4.8.3 Affects of Adriamycin Selection on Cell Invasion

Findings in the MDA-MB-435S-F adriamycin resistant variants	**Methods used**
Development of a two tiered invasive phenotype not present in the parental cell line (1) Invasion of matrigel to underside of invasion chamber (2) Detachment of cells from underside of invasion chamber and reattachment to bottom of 24-well plate (only in taxol selected and adriamycin selected variants – see section 4.4)	Invasion Assay
No changes observed in the secretion of MMP-2 or MMP9 in Adr-10p or Adr-10p10p compared to parental cell line	Zymography

Table 4.8.3 Summary of invasion of adriamycin selected variants of MDA-MB-435S-F.

Similar to results for the taxol selected variants of MDA-F, initially invasion assays indicated no major changes in the invasiveness of Adr-10p or Adr-10p10p compared to MDA-F (section 3.3.13.1). Again it appeared that the cell lines were less invasive than the parental MDA-F, and even less invasive than the taxol-selected variants. It was again observed that similar to the taxol selected variants, Adr-10p and Adr-10p10p had developed the ability to invade to the underside of the invasion chamber and then detach from the bottom and reattach to the bottom of the 24 well plate. Again this

phenomenon coincided with vastly reduced adhesiveness of these cells to components of the extracellular matrix (section 3.3.14). This could be an indication that adriamycin and taxol selection, selects for more aggressive invasive phenotypes, which appear overall to be less invasive, but selects for cells capable of invading further, and perhaps with a greater survival rate. Again no changes in the secretion of MMP-2 or MMP-9 were observed in these cell lines (section 3.3.15), however it has not yet been investigated whether there is a reduction in the tissue inhibitors of matrix metalloproteinases in these variants.

As mentioned in the previous paragraph, selection of MDA-F with adriamycin or taxol appears to generate a more invasive phenotype in this cell line, characterised by the ability of the cells to detach from the bottom of the invasion chamber and relocate to the bottom of the 24-well plate. In order to investigate this further it was decided to isolate three populations from invasion assays of MDA-F and its selected variants. The three populations were those cells that had not invaded, those that had and those that had also relocated to the bottom of the 24-well plate. The purpose of this study was to see if there were variations in the morphology, motility, invasiveness and adhesiveness of these populations, and to determine if particular cell populations were in a particular stage of invasiveness, due to their inability to proceed further, or just because the other cells had "got there first" or had been in a different physiolgical state, for example in a different phase of the cell cycle. The results of these experiments are presented in section 3.3.16.

Analysis of these populations revealed no major difference in their morphology. An observation was made that they displayed decreased cell contact inhibition. The superinvasive populations displayed increased motility in comparison to both the invasive and non-invasive subpopulations, in all cases except for Taxol-10p4p subpopulations. In Adr-10p-SI and Adr-10p10p-SI this increase was most apparent, these are very motile populations. Invasion showed with the exception of Taxol-10p4p that non-invasive populations were less invasive than invasive populations, while the superinvasive populations were the most invasive. The most invasive populations proved to be Adr-10p-SI and Adr-10p10p-SI. There appears to be a link in these cell lines between motility and invasion. The Taxol-10p-SI population is less adhesive than its parental cell line Taxol-10p which in turn is less adhesive than the grandparental cell line MDA-F to laminin, fibronectin, collagen type IV and matrigel Taxol-10p4p-SI,

Adr-10p-SI and Adr-10p10p-SI superinvasive populations are more adhesive than their individual parental cell lines, which in turn are less adhesive than the parental cell line MDA-F to laminin, fibronectin, collagen tyoe IV and matrigel. The superinvasive populations of Adriamycin selected origin are more adhesive to ECM proteins than those of taxol selected origin. This is also similar to their ability to perform in motility assays and invasion assays, but is dissimilar to the link between invasion and adhesion in their parental populations.

The findings of this thesis are opposite to those of Hikawa *et al.* (2000) in that increased resistance to adriamycin and taxol lead to a more aggressive invasive pheonotype (section 3.3.13.2). However these findings are similar in that Hikawa *et al.* (2000) found that decreased invasion was accompanied by increased adhesion to laminin, fibronectin or type IV collagen. The findings of this thesis were that more aggressive invasiveness was accompanied by decreased adhesion to laminin, fibronectin, collagen type IV and matrigel (section 3.3.13.2; 3.3.14).

Rintoul *et al.* (2002) studied the role of extracellular matrix in regulation of drug resistance in small-cell lung cancer (SCLC). They hypothesised that factors within the local environment of SCLC cells could provide a survival signal or block a death signal, thereby accounting for the protection of SCLC cells from chemotherapy-induced apoptosis. They showed that, *in vivo*, SCLC cells are surrounded by an extensive stroma of extracellular matrix (ECM) at both primary and metastatic sites which contain, among other proteins, fibronectin, laminin and collagen IV. Furthermore, adhesion of SCLC cells to fibronectin, laminin and collagen IV through β1 integrins enhanced tumorigenicity and conferred resistance to apoptosis induced by standard chemotherapeutic agents, including VP-16, cisplatin and adriamycin. Adhesion to ECM proteins stimulated protein tyrosine kinase (PTK) activity in both untreated and etoposide-treated cells. This effect could be completely blocked by a selective PTK inhibitor or by a function-blocking β1 integrin antibody. PTK activation was found to block chemotherapy-induced activation of the death protease caspase-3 and, hence, apoptosis. Adhesion to ECM or treatment with a PTK inhibitor did not affect etoposide inhibition of topoisomerase II. Thus adhesion to ECM through β1 integrins protects SCLC cells from chemotherapy-induced caspase-3 activation and apoptosis by activating PTK signalling downstream of DNA damage. Survival of tumour cells

attached to ECM within this microenvironment could explain the local recurrence of SCLC and other tumours that is often seen clinically after chemotherapy.

Adhesion of U937 human histiocytic lymphoma cells to fibronectin provided a survival advantage with respect to damage induced by the topoisomerase II inhibitors mitoxantrone, adriamycin and VP-16. Cellular adhesion by means of β1 integrins resulted in a 40% to 60% reduction in mitoxantrone- and etoposide-induced DNA double-strand breaks. When the mechanisms regulating the initial drug-induced DNA damage were examined, a β1 integrin-mediated reduction in drug-induced DNA double-strand breaks was found to correlate with reduced topoisomerase II activity and decreased salt-extractable nuclear topoisomerase IIβ protein levels. Confocal studies showed changes in the nuclear localisation of topoisomerase IIβ; however, alterations in the nuclear-to-cytoplasmic ratio of topoisomerase IIβ in fibronectin-adhered cells were not significantly different. Higher levels of topoisomerase IIβ-associated DNA binding were observed in fibronectin-adhered cells than in cells in suspension. Together, these data suggest that topoisomerase IIβ is more tightly bound to the nucleus of fibronectin-adhered cells. Thus, fibronectin adhesion by means of β1 integrins appears to protect U937 cells from initial drug-induced DNA damage by reducing topoisomerase II activity secondarily to alterations in the nuclear distribution of topoisomerase IIβ. (Hazlehurst *et al.*, 2001). Similar findings were also reported by Damiano *et al.* (1999).

These results do not correlate with the findings of this thesis, as the taxol and adriamycin selected variants are less adhesive to the ECM proteins tested, but exhibit increased resistance (section 3.3.14). Of further interest would be the examination of the drug resistance of MDA-F, MDA-F/Taxol-10p, MDA-F/Taxol-10p4p, MDA-F/Adr-10p and MDA-F/Adr-10p10p, while in the presence of various extracellular matrix components. Does adhesion to, for example laminin, increase the resistance of the cells to taxol or adriamycin. This is a potential avenue for future work.

Another mechanism whereby tumour cells may become increasingly invasive, is by the alteration in the expression of proteins regulating cell-cell adhesion. In a study by Molinari *et al.* (2002) the phenotypic alterations that are associated with the acquisition of the multidrug-resistant phenotype in tumour cells, together with drug transporter overexpression, were investigated in human melanoma cells. The expression of cell

adhesion molecules was analysed in a panel of multidrug-resistant melanoma cell lines (M14Dx) showing different degrees of resistance to adriamycin and different levels of the expression of the drug transporter P-glycoprotein. In particular, expression of intercellular adhesion molecule-1, CD44, very late activation antigen $\alpha_5\beta_1$ and $\alpha_2\beta_1$ was determined by flow cytometry in the different resistant cell lines. A progressive downregulation of all the adhesion molecules examined was revealed in M14Dx cells, in parallel with an increasing level of expression of the drug transporter P-glycoprotein. These results also raise a question about the role of P-glycoprotein in the invasive and metastatic behaviour of tumour cells.

E-cadherin-mediated cell-cell adhesion plays a crucial role in intercellular communication, which is related to the regulation of cell proliferation, differentiation, and apoptosis. Decreased expression of MUC1 can induce E-cadherin-mediated cell-cell adhesion in human breast cancer cell lines proliferating in suspension without aggregation. Using such a cell line (YMB-S) Yang *et al.* (1999) observed the effects of adriamycin on cell-cell adhesion and expression of E-cadherin-catenin complex and MUC1. The cells showed E-cadherin-mediated cell-cell adhesion after 48 h exposure to 0.4 μM/l adriamycin, accompanied by increases in E-cadherin and β-catenin and a decrease in MUC1 mRNA and protein levels. In immunohistochemical analysis, β-catenin protein in untreated cells showed diffuse cytoplasmic localization, whereas β-catenin in treated cells was present in cytoplasm with a clear submembranous localisation, indicating that increased β-catenin mainly bound with E-cadherin, participating in cell-cell adhesion.

A number of questions arise from the findings of this thesis and those of other investigators. Is P-glycoprotein directly involved in the downregulation of these cell adhesion molecules? It should be noted that the taxol selected variants display the lowest levels of adhesion (section 3.3.14) and also overexpress mdr-1 mRNA (section 3.3.8.1). It would be beneficial in future work following this thesis to look at the expression of cell adhesion molecules also including the cadherin, catenin and actin families in the adriamycin and taxol selected variants of MDA-F. Finally it would be interesting to see whether adhesion of MDA-F and its variants to ECM proteins, would result in increased resistance to chemotherapeutic drugs.

4.9 Long and Short Term Toxicity Assays

In this thesis both long and short term assays were performed for a number of different chemotherapeutic drugs. In the MDA-F MDR selectants it was found that the increase in resistance to taxol was greater in short term than in long term assays (section 3.3.4.5; 3.3.4.6). This was similar to the findings of (Tuohey, *et al.* 2000). Transfection of the cell line 2008 with MRP1, MRP2 and MRP3 resulted in greater resistance in short term than long term assays for adriamycin, methotrexate, taxol and taxotere. Kool *et al.* (1999) and Hooijberg *et al.* (1999) reported that transfected 2008 MRP1, 2008 MRP2 and 2008 MRP3 showed a marked level of resistance to the polyglutamatable antifolate, methotrexate. These results were obtained by short term assays, but not in long term assays. They suggested that this was due to fact that methotrexate is polyglutamated after entering the cell, a form which is very effective at inhibiting dihydrofolate reductase. Polyglutamatation is slow and after short term exposure, cells with good efflux pumps can pump out monoglutamate methotrexate efficiently, thereby accumulating less methotrexate, rendering the cells more resistant.

In the MCF-7 H3 c-erbB-2 transfected variants, resistance to taxol was also greater in short than in long term assays (section 3.1.4.2). This trend was also observed for carboplatin in these cell lines (3.1.4.3). No such trend was observed for adriamycin, taxotere, 5-fluorouracil or vincristine. The BT474A c-erbB-2-ribozyme transfected cell lines yielded very unexpected results. In adriamycin toxicity assays, the ribozyme-transfected variants, were sensitised to adriamycin in long term assays, but were actually resistant in short term assays. A similar trend was observed for carboplatin in that the ribozyme variants displayed no changes in resistance in long term assays but were resistant in short term assays. The reason behind these results has yet to be determined.

As mentioned in section 4.2 these two assays differ in that long term assays reflect the ability of the cells to withstand lengthier exposure to drug, while short term assays reflect the ability of the cells to recover from an acute shock with a high concentration of the drug in question. It is therefore possible that different mechanism of resistance to drug exposure come into play in these two assays, such as detoxification systems and apoptosis resistance factors. This is an area for future study.

4.10 Conclusions

The establishment of a model to investigate the effects of upregulation of c-erbB-2 by cDNA transfection and the downregulation by ribozyme transfection on chemotherapeutic drug sensitivity, *in vitro* invasion, and expression of a range of mRNA and proteins was a major part of this thesis.

Conclusions with Respect to the Effect of C-erbB-2 on Drug Resistance and Expression of a Panel of Resistance Associated Genes

1. C-erbB-2 upregulation in MCF-7 H3 c-erbB-2 cDNA transfectants resulted in decreased resistance to adriamycin in long and short term assays, while c-erbB-2 downregulation in BT474A- ribozyme transfectants resulted in decreased resistance in long term assay, but increased resistance in short term assays.
2. C-erbB-2 upregulation in MCF-7 H3 c-erbB-2 cDNA transfectants resulted in increased resistance to taxol in short term assays only, while c-erbB-2 downregulation in BT474A- ribozyme transfectants resulted in increased resistance in long and short term assays. These apparently contradictory results indicate the importance of different cell backgrounds in determining the phenotypic effects of a single gene.
3. C-erbB-2 upregulation in MCF-7 H3 c-erbB-2 cDNA transfectants resulted in decreased resistance to carboplatin in long term assays, but increased resistance in short term assays, while c-erbB-2 downregulation in BT474A ribozyme transfectants also resulted in decreased resistance to carboplatin in long term assays, but increased resistance in short term assays.
4. C-erbB-2 upregulation in MCF-7 H3 c-erbB-2 cDNA transfectants resulted in decreased resistance to 5-Fluorouracil in long and short term assays for two clonal transfectants, but increased resistance in the remaining transfectant, while c-erbB-2 downregulation in BT474A- ribozyme transfectants resulted in increased resistance in long and short term assays for several of the clonal transfectants.
5. C-erbB-2 upregulation in MCF-7 H3 c-erbB-2 cDNA transfectants resulted in increased resistance to methotrexate in long term assays, while c-erbB-2 downregulation in BT474A ribozyme transfectants also resulted in increased resistance long term assays.

6. No significant changes in vincristine or taxotere were observed in MCF-7 H3 c-erbB-2 cDNA
7. MDR-1, mrp-1, mrp-4 and mrp-5 mRNA were not not affected by c-erbB-2 expression.
8. Mrp-2 mRNA levels was inversely associated with c-erbB-2 expression.
9. Topoisomerase I and topoisomerase IIα mRNA expression were unaltered in MCF-7 H3 transfectants, while topoisomerase IIβ mRNA expression decreased. Topoisomerase IIα and topoisomerase IIβ mRNA expression were unaltered in BT474A transfectants, while topoisomerase I mRNA expression increased. These changes in topoisomerases were inconsistent between the two cell systems and therefore are unlikely to play a role in c-erbB-2 mediated resistance.
10. DHFR, TS and GSTπ mRNA levels were not found to play an obvious role in c-erbB-2 mediated drug resistance.

Conclusions With Respect to the Effects of C-erbB-2 Expression on Other ErbB Receptors

1. C-erbB-1 expression was unaltered by c-erbB-2 downregulation at both the mRNA and protein levels in BT474A ribozyme transfectants, while c-erbB-1 increased at the mRNA level, but not the protein in MCF-7 H3 cDNA transfectants.
2. C-erbB-3 protein expression was increased by c-erbB-2 upregulation and decreased by c-erbB-2 down regulation. C-erbB-3 levels appear to be linked to c-erbB-2 levels.
3. C-erbB-4 expression was unaltered by c-erbB-2 downregulation at the mRNA level, while c-erbB-4 was decreased at both the mRNA and protein levels in MCF-7 H3 cDNA transfectants.

Conclusions With Respect to the Effects of C-erbB-2 Expression on Tamoxifen resistance and Estrogen Receptor Expression

1. C-erbB-2 was not found to influence tamoxifen resistance or estrogen receptor α expression. Interestingly, though, it did regulate estrogen receptor β expression. The effect of this is not known.

Conclusions With Respect to the Effects of C-erbB-2 Expression on Cell Growth, Motility, Invasiveness and Adhesiveness

1. C-erbB-2 upregulation resulted in increased invasion, while its downregulation had the opposite effect. It is interesting to note that while these cell lines are invasive they do not display any motility.
2. C-erbB-2 upregulation in MCF-7 H3 had no effect on adhesion to laminin, collagen type IV or matrigel, but did result in decreased adhesion to fibronectin. C-erbB-2 downregulation BT474A resulted in decreased adhesion to fibronectin laminin, collagen type IV and matrigel.
3. MCF-7 H3 secretes a serine proteases which seems to be associated with a lack of invasion, since it is expressed in MCF-7 H3 and MCF-7 H3/ErbB2-A, but not in the invasive MCF-7 H3/ErbB2-B, MCF-7 H3/ErbB2-C, MDA-MB-435S-F or BT474A. C-erbB-2 upregulation in this cell line abolishes its expression. The ell line also secretes MMPs. BT474A also secretes MMPs, which appear to decrease with decreasing c-erbB-2 levels.

The establishment and characterisation of novel taxol- and adriamycin-resistant variants of MDA-MB-435S-F with interesting cross-resistance patterns and invasion related properties is a major achievement of this thesis. Of particular interest was the novel finding that the taxol- and adriamycin-selected variants had developed a two step invasive phenotype. This later achievement was a major novel achievement of this thesis. For ease of discussion MDA-MB-435S-F shall from here on be referred to as MDA-F, MDA-MB-435S-F/Taxol-10p as Taxol-10p, MDA-MB-435S-F/Taxol-10p4p as Taxol-10p4p, MDA-MB-435S-F/Adr-10p as Adr-10p and MDA-MB-435S-F/Adr-10p10p as Adr-10p10p.

Conclusions with Respect to Drug Resistance and ErbB Receptor Status

1. Taxol resistant variants of the human breast cancer cell line MDA-F are readily selectable on treatment with taxol, but selection with adriamycin in slower and more difficult.
2. Taxol selection of MDA-F yields a cross-resistance pattern whereby the cells become resistant to taxol, taxotere and vincristine, and to a lesser extent to adriamycin.
3. This cross-resistance pattern suggests the involvement of microtubule alteration in the development of taxol resistance.

4. Taxol selection does not alter sensitivity of MDA-F to VP-16, 5-fluorouracil or carboplatin. This may indicate that taxol in combination with 5-fluorouracil, carboplatin or VP-16 may be an effective combination in the treatment of breast cancer. Also patients who develop resistance to taxol chemotherapy may benefit from one of these drugs.
5. Adriamycin resistance in MDA-F is slow to develop and even then developed to only a low level. Adriamycin selection results in cross-resistance to VP-16, vincristine and taxotere.
6. Adriamycin selection sensitises the cells to taxol, 5-fluorouracil and carboplatin. Again this may indicate that adriamcyin in combination with these drugs may be an effective combination in the treatment of breast cancer, or a means to treat adriamycin resistant cancer.
7. The MRP family does not appear to play a significant role in taxol resistance our system, while it does play a role in adriamycin resistance. Mrp-1 is induced by taxol and adriamycin selection, but is not involved in taxol resistance, as sulindac does not circumvent taxol resistance. Sulindac is capable of circumventing adriamycin resistance in the parental, taxol-selected and adriamycin-selected variants. There is no significant difference in its ability to circumvent adriamycin in any of the cell lines and therefore it is unlikely that mrp-1 plays a major role in the development of resistance to adriamycin in MDA-F. Rather it is likely that mrp-1 is a part of its intrinsic resistance. Mrp-2 mRNA appears to be reduced by adriamycin and taxol selection, this may explain to some extent why there is no major change in adriamycin circumvention by sulindac, as mrp-2 transports adriamycin. Mrp-4 and mrp-5 are not expressed by MDA-F, or any of its taxol selected or adriamycin selected variants.
8. MDR-1 mRNA expression was increased in response to taxol but not to adriamcyin selection.
9. MDR-1 protein levels were unchanged in either the taxol- or the adriamycin-selected variants.
10. Verapamil circumvention of taxol and adriamycin does not follow expectedpatterns in the taxol-selected variants of MDA-F. Verapamil circumvents adriamycin resistance equally in the parental and taxol-selected variants, while only circumventing taxol resistance in the taxol-selected variants, but not in the parental cells. This may suggest involvement of a mdr-1 like pump.
11. All the resistant variants display increased adriamycin accumulation

12. As expected dihydrofolate reductase, and thymidylate synthase do not appear to play any major role in the development of resistance to taxol or adriamycin. One side effect of adriamycin selection is a reduction in the expression of thymidylate synthase mRNA perhaps resulting in the sensitisation of Adr-10p10p to 5-FU. Interestingly unlike what is generally reported in the literature levels of GST π decreased with both adriamycin and taxol selection.
13. Taxol and adriamycin selection have a definite effect on the expression of ErbB receptors in MDA-F. C-erbB-1 is induced at the protein, but not at mRNA level by both taxol and adriamycin selection. C-erbB-2 expression at the protein level is not induced by taxol or adriamycin selection, although its expression is reduced at the mRNA level. C-erbB-3 protein expression is downregulated hugely in response to adriamycin and taxol selection, while c-erbB-4 mRNA is increased in the more taxol resistant variant and is increased by adriamycin selection. C-erbB-4 protein expression was undetectable in these cell lines.
14. Topoisomerase I and IIβ were induced by taxol and adriamycin selection.

Conclusions With Respect to Cell Growth, Motility, Invasiveness and Adhesiveness

1. Selection of MDA-F with taxol and adriamycin leads to reduced growth rates.
2. Selection of MDA-F with taxol and adriamycin leads to reduced motility for taxol selected variants while the motility of MDA-F is unaffected by adriamycin selection.
3. Taxol and adriamycin selection of MDA-F results in a two staged invasive phenotype. *In vitro* invasion is generally measured as the ability of cells to travel through a layer of matrigel and then through 8μM pores in a multiwell plate insert – Cell invasiveness is proportional to the number of cells on the underside of the insert. It was discovered in this thesis a more aggressive phenotype whereby the cells are able to detach after invasion of the matrigel and movemnet through the pores and to then reattach to the bottom of the 24 well plate in which the invasion chamber sits. This is not accompanied by a change in MMP secretion, but is accompanied by reduced adhesion to laminin, and matrigel, and especially fibronectin and collagen type IV. Interestingly while MDA-F was most adhesive to fibronectin, all the MDR variants of MDA-F are most adherent to matrigel.

As a result of the two stage invasive phenotype observed in the MDA-F adriamycin and taxol selected variants, nine cell populations were isolated from invasion assays. They

were entitled non-invasive, invasive and superinvasive depending on the area of isolation. The **non-invasive populations (NI)** referred to cells that had not invaded through the matrigel (5 lines isolated from parental, adriamycin selected and taxol selected cell lines). The **invasive populations (I)** referred to cells that had invaded through the matrigel and were attached to the bottom of the insert (5 lines isolated from parental, adriamycin selected and taxol selected cell lines). The **superinvasive populations (SI)** referred to cells that had invaded through the matrigel and relocated to the bottom of the 24-well plate (4 lines isolated from the adriamycin selected and taxol selected cell lines). The member of cell lines is 4 in the final group because the parental cell lines were incapable of the 2-step invasion.

Conclusions for the Morphology, Motility, Invasiveness and Adhesiveness of the Non-invasive, invasive, and Superinvasive Populations Were

1. No changes in morphology were observed.
2. The SI populations displayed increased motility in comparison to both the I and NI subpopulations, in all cases except for Taxol-10p4p subpopulations. In Adr-10p-SI and Adr-10p10p-SI this increase was most apparent, these are very motile populations.
3. Invasion showed with the exception of Taxol-10p4p that NI populations were less invasive than I populations, while the SI populations were the most invasive. The most invasive populations proved to be Adr-10p-SI and Adr-10p10p-SI. There appears to be a link in these cell lines between motility and invasion.
4. The Taxol-10p-SI population is less adhesive than its parental cell line Taxol-10p which in turn is less adhesive than the grandparental cell line MDA-F to laminin, fibronectin, collagen tyoe IV and matrigel
5. Taxol-10p4p-SI, Adr-10p-SI and Adr-10p10p-SI superinvasive populations are more adhesive than their individual parental cell lines, which in turn are less adhesive than the parental cell line MDA-F to laminin, fibronectin, collagen type IV and matrigel.
6. The superinvasive populations of Adriamycin selected origin are more adhesive to ECM proteins than those of taxol selected origin. This is also similar to their ability to perform in motility assays and invasion assays, but is dissimilar to the link between invasion and adhesion in their parental populations.

4.11 Future Work

1. Investigation of the role of other ErbB family members (alone and in combination) in drug resistance and invasion by stable or transient transfection of ErbB cDNAs and ribozymes
2. Application of DNA arrays and proteomic approaches to determine genes under the control of ErbB receptors.
3. Further investigation of the lack of motility displayed by BT474A and MCF-7 H3 is necessary. Despite the fact that these cell lines are invasive, they failed to perform in motility assays. This raises the following question, do these cell lines only exhibit motility in the presence of ECM proteins, but not when attached to plastic, as is the case for most cells in culture. Assays could be designed to observe the motility of these cell lines on plastic, membranes and ECM proteins.
4. The role of estrogen receptor β also needs to be further investigated in these cell lines, involving cDNA transfection and its effect on estrogen response, tamoxifen and ErbB expression.
5. Investigation of mechanism involved in taxol transport in MDA-MB-435S-F/Taxol-10p and MDA-MB-435S-F/Taxol-10p4p. Clearly taxol resistance in circumvented by verapamil in the taxol selected variants, but not in the parental cells or the adriamycin selected variants, despite the fact that adriamycin resistance is circumvented by verapamil in all five variants of MDA-MB-435S-F. This raises the question as to why are these cell lines not also resistant to Adriamycin and VP-16 (also substrates of P-glycoprotein). Indeed is there a novel transporter protein expressed here specific for vincristine, taxol and taxotere? Would the same effect be seen with verapamil and taxotere or vincristine? Future work would involve combination assays of verapamil with taxotere and vincristine and epirubicin, to determine if their resistance can be circumvented by verapamil. If so, are they also circumvented by other specific p-glycoprotein inhibitors? If not, what particular part of p-glycoprotein do these inhibitors work on? This may give an insight into structural differences between p-glycoprotein and any novel mdr-type protein.
6. DNA arrays and proteomics are a possible avenue to begin to search for any novwlgenes/proteins involved in taxol resistance. Gene profiling and 2-D electrophoresis/MS of possible novel proteins isolated may help to yield a clue as to the type or identity of proteins involved.

7. Judging by the cross-resistance profiles of MDA-MB-435S-F/Taxol-10p and MDA-MB-435S-F/Taxol-10p4p, the expression and taxol-binding profiles of α-tubulins and β-tubulins need to be studied.
8. Investigation of the inability of MDA-MB-435S-F to develop resistance to adriamycin, while being able to develop resistance to taxol. Does this also apply to other members of the anthracycline family? Is there an X factor that prevents development of resistance? Comparison of gene arrays of other adriamycin selected cell lines with these selectants, and MDA-MB-435S-F selected with other anthracyclines could be a place to start.
9. Despite decreased accumulation of adriamycin in MDA-MB-435S-F/Taxol-10p, MDA-MB-435S-F/Taxol-10p4p, MDA-MB-435S-F/Adr-10p and MDA-MB-435S-F/Adr-10p10p, they display little or no increase in resistance to adriamycin. It is necessary to investigate further whether other mechansims of adriamycin resistance are downregulated thus reversing any advantage increased efflux may have on the cells. GST activity and topoisomerase protein expression/activity would be a place to begin.
10. Identification of specific MMPs and TIMPs expressed by the MDA-MB-435S-F variants.
11. Further investigation of subpopulations with different invasive potential of MDA-MB-435S-F and its variants isolated from invasion assays.
    - Protease secretion
    - ErbB receptor profiles
    - Expression of integrins, cadherins, catenins and α-actin
12. As c-erbB-3 protein levels are drastically reduced in taxol- and adriamycin- selected variants, c-erbB-3 cDNA transfection into MDA-MB-435S-F may show whether c-erbB-3 plays a role in the observations made in these variants. C-erbB-1 and 4 are other candidates for this also, while c-erbB-2 levels were unchanged by taxol or adriamycin selection, and therefore may not be as interesting.
13. Finally its is desirable to pulse select a panel of breast cancer cell lines to determine whether these observations are common to breast cell lines or unique to MDA-MB-435S-F.

5.0 Bibliography

5.1 Bibliography

Aaronson SA. (1991) Growth factors and cancer. Science, 254, 1146-53

Ahmad A, Hart IR. (1997) Mechanisms of metastasis. Crit Rev Oncol Hematol, 26, 163-73

Aigner, A., Hsieh, S.S., Malerczyk, C., Czubayko, F. (2000) Reversal of HER-2 over-expression renders human ovarian cancer cells highly resistant to taxol. Toxicology, 144, 221-8

Al Moustafa, A.E., Alaoui-Jamali, M., Paterson, J. and O'Connor-McCourt, M. (1999) Expression of P185erbB-2, P160erbB-3, P180erbB-4, and heregulin alpha in human normal bronchial epithelial and lung cancer cell lines. Anticancer Res, 19, 481-6

Alhasan, S.A., Aranha, O., Sarkar, F.H. (2001) Genistein elicits pleiotropic molecular effects on head and neck cancer cells. Clin Cancer Res, 7, 4174-81

Archer, S.G., Eliopoulos, A., Spandidos, D., Barnes, D., Ellis, I.O., Blamey, R.W., Nicholson, R.I. and Robertson, J.F. (1995) Expression of ras p21, p53 and c-erbB-2 in advanced breast cancer and response to first line hormonal therapy. Br J Cancer. 72, 1259-66.

Aziz, S.A., Pervez, S., Khan, S., Kayani, N., Rahbar, M.H. (2002) Epidermal growth factor receptor (EGFR) as a prognostic marker: an immunohistochemical study on 315 consecutive breast carcinoma patients. J Pak Med Assoc, 52, 104-10

Bader P, Fuchs J, Wenderoth M, von Schweinitz D, Niethammer D, Beck JF. (1998) Altered expression of resistance associated genes in hepatoblastoma xenografts incorporated into mice following treatment with adriamycin or cisplatin. Anticancer Res, 18, 3127-32

Ballestrem, C., Wehrle-Haller, B., Hinz, B. and Imhof, B.A. (2000) Actin-dependent lamellipodia formation and microtubule-dependent tail retraction control-directed cell migration. Mol Biol Cell, 11, 2999-3012

Ban, N., Takahashi, Y., Takayama, T., Kura, T., Katahira, T., Sakamaki, S. and Niitsu, Y. (1996) Transfection of glutathione S-transferase (GST)-π antisense complementary DNA increases the sensitivity of a colon cancer cell line to adriamycin, cisplatin, melphalan, and etoposide. Cancer Res, 56, 3577-82.

Baselga, J., Norton, L., Albanell, J., Kim,Y.M., Mendelsohn, J. (1998) Recombinant humanized anti-HER2 antibody (Herceptin) enhances the antitumor activity of paclitaxel and doxorubicin against HER2/neu overexpressing human breast cancer xenografts. Cancer Res, 58, 2825-31

Baselga, J., Seidman, A.D., Rosen, P.P., Norton, L. (1997) HER2 overexpression and paclitaxel sensitivity in breast cancer: therapeutic implications. Oncology (Huntingt), 11, (3 Suppl 2), 43-8

Beck, J.F., Brugger, D., Brischwein, K., Liu, C., Bader, P., Niethammer, D., Gekeler, V. (2001) Anticancer drug-mediated induction of multidrug resistance-associated genes and protein kinase C isozymes in the T-lymphoblastoid cell line CCRF-CEM and in blasts from patients with acute lymphoblastic leukemias. Jpn J Cancer Res, 92, 896-903

Beerli, R.R. and Hynes, N.E. (1996) Epidermal growth factor-related peptides activate distinct subsets of erbB receptors and differ in their biological activities. J Biol Chem, 271, 6071-6076.

Bei, R., Pompa, G., Vitolo, D., Moriconi, E., Ciocci, L., Quaranta, M., Frati, L., Kraus, M.H., Muraro, R. (2001) Co-localization of multiple ErbB receptors in stratified epithelium of oral squamous cell carcinoma. J Pathol, 195, 343-8

Bellamy, C.O. and Harrison, D.J. (1994) Evaluation of glutathione S-transferase π in non-invasive ductal carcinoma of breast. Br J Cancer, 69, 183-5

Belotti, D., Rieppi, M., Nicoletti, M.I., Casazza, A.M., Fojo, T., Taraboletti, G. and Giavazzi, R. (1996) Paclitaxel (Taxol(R)) inhibits motility of paclitaxel-resistant human ovarian carcinoma cells. Clin Cancer Res, 2, 1725-30

Benz, C.C., Scoff, G.K., Sarup, J.C., Johnson, R.M., Tripathy, D., Coronado, E., Shepard, H.M. and Osbourne, C.K. (1992) Estrogen-dependant, tamoxifen resistant tumourigenic growth in MCF-7 cells transfected with HER2/neu. Breast Cancer Res Treat, 24, 85-95.

Bershadsky, A., Chausovsky, A., Becker, E., Lyubimova, A., Geiger, B. (1996) Involvement of microtubules in the control of adhesion-dependent signal transduction. Curr Biol, 6, 1279-89

Bhalla, K., Huang, Y., Tang, C., Self, S., Ray, S., Mahoney, M.E., Ponnathpur, V., Tourkina, E., Ibrado, A.M., Bullock G. (1994) Characterization of a human myeloid leukemia cell line highly resistant to taxol. Leukemia, 8, 465-75

Bieche, I., Toamsetto, C., Regnier, C.H., Moog-Lutz, C., Rio, M.C. and Lidereau, R. (1996) Two distinct amplifed regions involved in human primary breast cancer. Cancer Res, 56, 3886-3890.

Bobrow, L.G., Millis, R.R., Happerfield, L.C. and Gullick, W.J. (1997) C-erbB-3 protein expression in ductal carcinoma *in situ* of the breast. Eur J Cancer, 33, 1846-50.

Bonvini, P., An, W.G., Rosolen, A., Nguyen, P., Trepel, J., Garcia de Herreros, A., Dunach, M. and Neckers, L.M. (2001) Geldanamycin abrogates ErbB2 association with proteasome-resistant beta-catenin in melanoma cells, increases beta-catenin-E-cadherin association, and decreases beta-catenin-sensitive transcription. Cancer Res, 61, 1671-7.

Borg, A., Baldetorp, B., Ferno, M., Killander, D., Olsson, H., Ryden, S. and Sigurdsson, H.. (1994) ErbB-2 amplification is associated with tamoxifen resistance in steroid-receptor positive breast cancer. Cancer Lett, 81, 137-144.

Borst P, Evers R, Kool M, Wijnholds J. (1999) The multidrug resistance protein family. Biochim Biophys Acta, 1461, 347-57

Bottini, A., Berruti, A., Bersiga, A., Brunelli, A., Brizzi, M.P., Marco, B.D., Cirillo, F., Bolsi, G., Bertoli, G., Alquati, P., Dogliotti, L. (1996) Effect of neoadjuvant chemotherapy on Ki67 labelling index, c-erbB-2 expression and steroid hormone receptor status in human breast tumours. Anticancer Res, 16, 5B, 3105-10

Brabender, J., Danenberg, K.D., Metzger, R., Schneider, P.M., Park, J., Salonga, D., Holscher, A.H., Danenberg, P.V. (2001) Epidermal growth factor receptor and HER2-neu mRNA expression in non-small cell lung cancer is correlated with survival. Clin Cancer Res, 7, 1850-5

Breuninger, L.M., Paul, S., Gaughan, K., Miki, T., Chan, A., Aaronson, S.A., Kruh, G.D. (1995) Expression of multidrug resistance-associated protein in NIH/3T3 cells confers multidrug resistance associated with increased drug efflux and altered intracellular drug distribution. Cancer Res, 55, 5342-7

Cabral F, Barlow SB. (1989) Mechanisms by which mammalian cells acquire resistance to drugs that affect microtubule assembly. FASEB J, 3, 1593-9

Cairns, J., Wright, C., Cattan, A.R., Hall, A.G., Cantwell, B.J., Harris, A.L., Horne, C.H. (1992) Immunohistochemical demonstration of glutathione S-transferases in primary human breast carcinomas. J Pathol, 166, 19-25

Carlomagno, C., Perrone, F., Gallo, C., De Laurentiis, M., Lauria, R., Morabito, A., Pettinato, G., Panico, L., D'Antonio, A., Bianco, R. and De Placido, S. (1996) C-erbB2 overexpression decreases the benefit of adjuvant tamoxifen in early-stage breast cancer without axillary lymph node metastasis. J Clin Oncol, 14, 2702-2708.

Carraway III, K.L. and Burden, S.J. (1995) Neuregulins and their receptors. Curr Opin Neurobiol, 5, 606-612.

Chen, X., Yeung, T.K., Wang, Z. (2000) Enhanced drug resistance in cells coexpressing ErbB2 with EGF receptor or ErbB3. Biochem Biophys Res Commun, 277, 757-63

Childs, S., Yeh, R.L., Hui, D. and Ling, V. (1998) Taxol resistance mediated by transfection of the liver-specific sister gene of P-glycoprotein. Cancer Res, 58, 4160-7.

Chow, N.H., Chan, S.H., Tzai, T.S., Ho, C.L., Liu, H.S. Expression profiles of ErbB family receptors and prognosis in primary transitional cell carcinoma of the urinary bladder. Clin Cancer Res, 7, 1957-62

Christianson, T.A., Doherty, J.J., Lin, Y.J., Ramsey, E.E., Holmes, R., Keenan, E.J. and Clinton, G.M. (1998) NH_2-terminally truncated HER-2/neu protein: Relationship with shedding of the extracellular domain and with prognostic factors in breast cancer. Cancer Res, 58, 5123-5129.

Ciardiello F, Caputo R, Pomatico G, De Laurentiis M, De Placido S, Bianco AR, Tortora G. (2000) Resistance to taxanes is induced by c-erbB-2 overexpression in human MCF-10A mammary epithelial cells and is blocked by combined treatment with an antisense oligonucleotide targeting type I protein kinase A. Int J Cancer, 85, 710-5

Cirisano, F.D. and Karlan, B.Y. (1996) The role of the HER2/neu oncogene in gynecological cancers. J Soc Gynecol Invest, 3, 99-105.

Clynes M, Daly C, NicAmhlaoibh R, Cronin D, Elliott C, O'Connor R, O'Doherty T, Connolly L, Howlett A, Scanlon K. (1998) Recent developments in drug resistance and apoptosis research. Crit Rev Oncol Hematol, 28, 181-205

Cohen, B.D., Kiener, P.A., Green, J.M., Foy, L., Fell, H.P. and Zhang, k. (1996) The relationship between human epidermal growth-like factor receptor expression and cellular transformation in NIH3T3 cells. J Biol Chem, 271, 30897-30903.

Cole SP, Chanda ER, Dicke FP, Gerlach JH, Mirski SE. (1991) Non-P-glycoprotein-mediated multidrug resistance in a small cell lung cancer cell line: evidence for decreased susceptibility to drug-induced DNA damage and reduced levels of topoisomerase II. Cancer Res, 51, 3345-52

Cole SP, Downes HF, Mirski SE, Clements DJ. (1990) Alterations in glutathione and glutathione-related enzymes in a multidrug-resistant small cell lung cancer cell line. Mol Pharmacol, 37, 192-7

Cui Y, Konig J, Buchholz JK, Spring H, Leier I, Keppler D. (1999) Drug resistance and ATP-dependent conjugate transport mediated by the apical multidrug resistance protein, MRP2, permanently expressed in human and canine cells. Mol Pharmacol, 55, 929-37

Curran S, Murray GI. (2000) Matrix metalloproteinases: molecular aspects of their roles in tumour invasion and metastasis. Eur J Cancer, 36, 13 Spec No, 1621-30

D'Souza, B. and Taylor-Papadimitriou, J. (1994) Overexpression of erbB2 in human mammary epithelial cells signals inhibition of transcription of E-cadherin gene. Proc Nat. Acad Sci, 91, 7202-7206.

D'Souza, B., Berdichevsky, F., Kyprianou, N. and Taylor-Papadimitriou, J. (1993) Collagen-induced morphogenesis and expression of the α_2 integrin subunit is inhibited in c-erbB-2 transfected human mammary epithelial cells. Oncogene, 8, 1797-1806.

Damiano, J.S., Cress, A.E., Hazlehurst, L.A., Shtil, A.A. and Dalton, W.S. (1999) Cell adhesion mediated drug resistance (CAM-DR): role of integrins and resistance to apoptosis in human myeloma cell lines. Blood , 93, 1658-67.

de Jong S, Zijlstra JG, de Vries EG, Mulder NH. (1990) Reduced DNA topoisomerase II activity and drug-induced DNA cleavage activity in an adriamycin-resistant human small cell lung carcinoma cell line. Cancer Res,50, 304-9

Deffie AM, Batra JK, Goldenberg GJ. (1989) Direct correlation between DNA topoisomerase II activity and cytotoxicity in adriamycin-sensitive and -resistant P388 leukemia cell lines. Cancer Res, 49, 58-62

Dieras, V., Beuzeboc, P., Laurence, V., Pierga, J.Y., Pouillart, P. (2001) Interaction between Herceptin and taxanes. Oncology, 61, Suppl 2, 43-9

Dittadi, R., Calderazzo, F., Cabrelle, A., Di Fresco, S., Gion, M. and Chieco-Bianchi, L. (1996) C-erbB2/Neu protein expression, DNA ploidy and S phase in breast cancer. Cell Prolif, 29, 403-412.

Dowsett, M., Harper-Wynne, C., Boeddinghaus, I., Salter, J., Hills, M., Dixon, M., Ebbs, S., Gui, G., Sacks, N., Smith, I. HER-2 amplification impedes the antiproliferative effects of hormone therapy in estrogen receptor-positive primary breast cancer. Cancer Res, 61, 8452-8

Driouch, K., Champeme, M.H., Beuzelin, M., Bieche, I. And Lidereau, R. (1997) Classical gene amplifications in human breast cancer are not associated with distant solid metastases. Bt J Cancer, 76, 784-787.

Duan, Z., Feller, A.J., Toh, H.C., Makastorsis, T. and Seiden, M.V. (1999) TRAG-3, a novel gene, isolated from a taxol-resistant ovarian carcinoma cell line. Gene, 229, 75-8.

Dugina, V.B., Alexandrova, A.Y., Lane, K., Bulanova, E. and Vasiliev, J.M. (1995) The role of the microtubular system in the cell response to HGF/SF. J Cell Sci, 108, 1659-67

Elledge R.M., Green, S., Ciocca, D., Pugh, R., Allred, D.C., Clark, G.M., Hill, J., Ravsin, P., O'Sullivan, J., Martino, S. and Osbourne, C.K. (1998) HER-2 expression and response

to tamoxifen in estrogen receptor-positive breast cancer: A southwest oncology group study. Clin Cancer Res, 4, 7-12.

Ellis, M.J., Coop, A., Singh, B., Mauriac, L., Llombert-Cussac, A., Janicke, F., Miller, W.R., Evans, D.B., Dugan, M., Brady, C., Quebe-Fehling, E., Borgs, M. (2001) Letrozole is more effective neoadjuvant endocrine therapy than tamoxifen for ErbB-1- and/or ErbB-2-positive, estrogen receptor-positive primary breast cancer: evidence from a phase III randomized trial. J Clin Oncol, 19, 3808-16

Esteva, F.J., Valero, V., Booser, D., Guerra, L.T., Murray, J.L., Pusztai, L., Cristofanilli, M., Arun, B., Esmaeli, B., Fritsche, H.A., Sneige, N., Smith, T.L., Hortobagyi, G.N. (2002) Phase II study of weekly docetaxel and trastuzumab for patients with HER-2-overexpressing metastatic breast cancer. J Clin Oncol, 20, 1800-8

Evans C (1991) The Metastatic Cell, ed. By Evans C. Chapman and Hall, 100-321.

Falcioni, R., Antonini, A., Nistico, P., Di Stefano, S., Crescenzi, M., Natali, P.G., Sacchi, A. (1997) Alpha 6 beta 4 and alpha 6 beta 1 integrins associate with ErbB-2 in human carcinoma cell lines. Exp Cell Res, 236, 76-85

Feller, A.J., Duan, Z., Penson, R., Toh, H.C.and Seiden, M.V. (2000) TRAG-3, a novel cancer/testis antigen, is overexpressed in the majority of melanoma cell lines and malignant melanoma. Anticancer Res, 20, 4147-51.

Ferrero JM, Ramaioli A, Largillier R, Formento JL, Francoual M, Ettore F, Namer M, Milano G. (2001) Epidermal growth factor receptor expression in 780 breast cancer patients: a reappraisal of the prognostic value based on an eight-year median follow-up. Ann Oncol, 12, 841-6

Ferrero, J.M., Ramaioli, A., Largillier, R., Formento, J.L., Francoual, M., Ettore, F., Namer, M., Milano, G. (2001) Epidermal growth factor receptor expression in 780 breast cancer patients: a reappraisal of the prognostic value based on an eight-year median follow-up. Ann Oncol, 12, 841-6

Formenti, S.C., Spicer, D., Skinner, K., Cohen, D., Groshen, S., Bettini, A., Naritoku, W., Press, M., Salonga, D., Tsao-Wei, D., Danenberg, K., Danenberg, P. (2002) Low HER2/neu gene expression is associated with pathological response to concurrent paclitaxel and radiation therapy in locally advanced breast cancer. Int J Radiat Oncol Biol Phys, 52, 397-405

Fountzilas, G., Tsavdaridis, D., Kalogera-Fountzila, A., Christodoulou, C.H., Timotheadou, E., Kalofonos, C.H., Kosmidis, P., Adamou, A., Papakostas, P., Gogas, H., Stathopoulos, G., Razis, E., Bafaloukos, D., Skarlos, D. (2001) Weekly paclitaxel as first-line chemotherapy and trastuzumab in patients with advanced breast cancer. A Hellenic Cooperative Oncology Group phase II study. Ann Oncol, 12, 1545-51

Francis PA, Kris MG, Rigas JR, Grant SC, Miller VA. (1995) Paclitaxel (Taxol) and docetaxel (Taxotere): active chemotherapeutic agents in lung cancer. Lung Cancer, 12, Suppl 1, S163-72

Funayama, T., Nakanishi, T., Takahashi, K., Taniguchi, S., Takigawa, M. and Matsumura, T. (1998) Overexpression of c-erbB-3 in various stages of human squamous cell carcinomas. Oncology, 55, 161-7.

Furger, C., Fiddes, R.J., Quinn, D.I., Bova, R.J., Daly, R.J. and Sutherland, R.L. (1998) Granulosa cell tumours expresss c-erbB-4 and aresensitive to the cytotoxic action of Heregulin-β2/PE40. Cancer Res, 58, 1773-1778.

Gamett, D.C., Pearson, G., Cerione, R.A. and friedberg, I. (1997) Secondary dimerisation between members of the epidermal growth factor receptor family. J Biol Chem, 272, 12052-12056.

Genestier L, Paillot R, Quemeneur L, Izeradjene K, Revillard JP. (2000) Mechanisms of action of methotrexate. Immunopharmacology, 47, 247-57

Giai, M., Roagna, R., Ponzone, R., De Bortoli, M., Dati, C. and Sismondi, P. (1994) Prognostic and predictive relevance of c-erbB-2 and ras expression in node positive and negative breast cancer. Anticancer Res, 14, 1441-50.

Giani, C., Casalini, P., Pupa, S.M., De Vecchi, R., Ardini, E., Colnaghi, M.I., Giordano, A. and Menard, S. (1998) Increased expression of c-erbB-2 in hormone dependent breast cancer cells inhibits cell growth and induces differentiation. Oncogene, 17, 425-432.

Gidding CE, Kellie SJ, Kamps WA, de Graaf SS. (1999) Vincristine revisited. Crit Rev Oncol Hematol, 29, 267-87

Gilbertson R, Hernan R, Pietsch T, Pinto L, Scotting P, Allibone R, Ellison D, Perry R, Pearson A, Lunec J. (2001) Novel ERBB4 juxtamembrane splice variants are frequently expressed in childhood

Gilmour, L.M., Macleod, K.G., McCaig, A., Gullick, W.J., Smyth, J.F. and Langdon, S.P. (2001) Expression of erbB-4/HER-4 growth factor receptor isoforms in ovarian cancer. Cancer Res, 61, 2169-76

Giunciuglio, D., Culty, M., Fassina, G., Masiello, L., Melchiori, A., Paglialunga, G., Arand, G., Ciardiello, F., Basolo, F. and Thompson, E.W. (1995) Invasive phenotype of MCF10A cells overexpressing c-Ha-ras and c-erbB-2 oncogenes. Int J Cancer, 63, 815-822.

Gottesman MM, Pastan I. (1993) Biochemistry of multidrug resistance mediated by the multidrug transporter. Annu Rev Biochem, 62, 385-427

Graber, H.U., Friess, H., Kaufmann, B., Willi, D., Zimmermann, A., Korc, M. and Buchler, M.W. (1999) ErbB-4 mRNA expression is decreased in non-metastatic pancreatic cancer. Int J Cancer, 84, 24-7

Graus-Porta, D., Beerli, R.R., Daly, J.M. and Hynes, N.E. (1997) ErbB-2, the preferred hetrodimerization partner of all ErbB receptors, is a mediator of lateral signaling. EMBO, 16, 1647-1655.

Grothey, A., Hashizume, R., Ji, H., Tubb, B.E., Patrick, C.W. Jr, Yu, D., Mooney, E.E. and McCrea, P.D. (2000) C-erbB-2/ HER-2 upregulates fascin, an actin-bundling protein associated with cell motility, in human breast cancer cell lines. Oncogene, 19, 4864-75.

Guerra-Vladusic, F.K., Scott, G., Weaver, V., Vladusic, E.A., Tsai, M.S., Benz, C.C., Lupu, R. (1999) Constitutive expression of Heregulin induces apoptosis in an erbB-2 overexpressing breast cancer cell line SKBr-3. Int J Oncol, 15, 883-92

Gum, R., Wang, S., Lengyel, E., Yu, D, Hung, M., Juarez, J. and Boyd, D. (1995) Up-regulation of urokinase-type plasminogen activator expression by the HER2/neu proto-oncogene. Anticancer Res, 15, 1167-1172.

Guy, C.T., Webster, M.A., Schaller, M., Parsons, T.J., Cardiff, R.D. and Muller, W.J. (1992) Expression of the neu protooncogene in the mammary epithelium of transgenic mice induces metastatic disease. Proc Natl Acad Sci USA, 89, 10578-10582.

Haber M, Burkhart CA, Regl DL, Madafiglio J, Norris MD, Horwitz SB. (1995) Altered expression of M beta 2, the class II beta-tubulin isotype, in a murine J774.2 cell line with a high level of taxol resistance. J Biol Chem, 270, 31269-75

Haldar, S., Chintapalli, J. and Croce, C.M. (1996) Taxol induces bcl-2 phosphorylation and death of prostate cancer cells. Cancer Res, 56, 1253-5

Hamilton, A., Larsimont, D., Paridaens, R., Drijkoningen, M., van de Vijver, M., Bruning, P., Hanby, A., Houston, S., Treilleux, I., Guastalla, J.P., Van Vreckem, A., Sylvester, R., Piccart, M. (2000) A study of the value of p53, HER2, and Bcl-2 in the prediction of response to doxorubicin and paclitaxel as single agents in metastatic breast cancer: a companion study to EORTC 10923. Clin Breast Cancer, 1, 233-40

Han, J., Jenq, W., Kefalides, N.A. (1999) Integrin alpha2beta1 recognizes laminin-2 and induces C-erb B2 tyrosine phosphorylation in metastatic human melanoma cells. Connect Tissue Res, 40, 283-93

Hande KR. (1998) Etoposide: four decades of development of a topoisomerase II inhibitor. Eur J Cancer, 34, 1514-21

Harris, L.N., Yang, L., Liotcheva, V., Pauli, S., Iglehart, J.D., Colvin, O.M. and Hsieh, T.S. (2001) Induction of topoisomerase II activity after ErbB2 activation is associated with a differential response to breast cancer chemotherapy. Clin Cancer Res, 7, 1497-504

Harris, L.N., Yang, L., Tang, C., Yang, D., Lupu, R. (1998) Induction of sensitivity to doxorubicin and etoposide by transfection of MCF-7 breast cancer cells with heregulin beta-2. Clin Cancer Res, 4, 1005-12

Haugen, D.R., Akslen, L.A., Varhaug, J.E. and Lillehaug, J.R. (1996) Expression of c-erbB-3 and c-erbB-4 proteins in papillary thyroid carcinomas. Cancer Res, 56, 1184-8.

Hazlehurst, L.A., Valkov, N., Wisner, L., Storey, J.A., Boulware, D., Sullivan, D.M. and Dalton, W.S. (2001) Reduction in drug-induced DNA double-strand breaks associated with beta1 integrin-mediated adhesion correlates with drug resistance in U937 cells. Blood, 98, 1897-903.

Hijazi, M.M., Thompson, E.W., Tang, C., Coopman, P., Torri, J.A., Yang, D., Mueller, S.C. and Lupu, R. (2000) Heregulin regulates the actin cytoskeleton and promotes invasive properties in breast cancer cell lines. Int J Oncol, 17, 629-41.

Hikawa, T., Mori, T., Abe, T. and Hori, S. (2000) The ability in adhesion and invasion of drug-resistant human glioma cells. J Exp Clin Cancer Res, 19, 357-62.

Himelstein BP, Canete-Soler R, Bernhard EJ, Muschel RJ. (1994) Induction of fibroblast 92 kDa gelatinase/type IV collagenase expression by direct contact with metastatic tumor cells. J Cell Sci, 107, 477-86.

Hong, R.L., Spohn, W.H., Hung, M.C. (1999) Curcumin inhibits tyrosine kinase activity of p185neu and also depletes p185neu. Clin Cancer Res, 5, 1884-91

Hooijberg JH, Broxterman HJ, Kool M, Assaraf YG, Peters GJ, Noordhuis P, Scheper RJ, Borst P, Pinedo HM, Jansen G. (1999) Antifolate resistance mediated by the multidrug resistance proteins MRP1 and MRP2. Cancer Res, 59, 2532-5

Horan, T., Wen, J., Arakawa, T., Liu, N., Brankow, D., Hu, S., Ratzkin, H. and Philo, J.S. (1995) Binding of neu differentiation factor with the extralcellular domain of Her2 and Her3. J Biol Chem, 270, 24604-24608.

Hortobagyi GN. (1997) Anthracyclines in the treatment of cancer. An overview. Drugs, 54, Suppl 4, 1-7

Hung, M.C. and Lau, Y.K. (1999) Basic science of HER-2/neu: A review. Semin Oncol, 26, (4 Suppl 12), 51-99.

Ibrado, A.M., Huang, Y., Fang, G. and Bhalla, K. (1996) Bcl-xL overexpression inhibits taxol-induced Yama protease activity and apoptosis. Cell Growth Differ, 7, 1087-94.

Ignatoski, K.M., Maehama, T., Markwart, S.M., Dixon, J.E., Livant, D.L., Ethier, S.P. ERBB-2 overexpression confers PI 3' kinase-dependent invasion capacity on human mammary epithelial cells. Br J Cancer, 82, 666-74

Ito A, Nakajima S, Sasaguri Y, Nagase H, Mori Y. (1995) Co-culture of human breast adenocarcinoma MCF-7 cells and human dermal fibroblasts enhances the production of matrix metalloproteinases 1, 2 and 3 in fibroblasts. Br J Cancer, 71, 1039-45.

Jarvinen, T.A., Holli, K., Kuukasjarvi, T., Isola, J.J. (1998) Predictive value of topoisomerase IIalpha and other prognostic factors for epirubicin chemotherapy in advanced breast cancer. Br J Cancer, 77, 2267-73

Jarvinen, T.A., Tanner, M., Rantanen, V., Barlund, M., Borg, A., Grenman, S., Isola, J. (2000) Amplification and deletion of topoisomerase IIalpha associate with ErbB-2

amplification and affect sensitivity to topoisomerase II inhibitor doxorubicin in breast cancer. Am J Pathol, 156, 839-47

Jones, J.L., Royall, J.E., Walker, R.A. (1996) E-cadherin relates to EGFR expression and lymph node metastasis in primary breast carcinoma. Br J Cancer, 74, 1237-41

Kamazawa, S., Kigawa, J., Minagawa, Y., Itamochi, H., Shimada, M., Takahashi, M., Sato, S., Akeshima, R. and Terakawa, N. (2000) Cellular efflux pump and interaction between cisplatin and paclitaxel in ovarian cancer cells. Oncology, 59, 329-35

Kerbel, R.S., St Croix, B., Florenes, V.A., Rak, J. (1996) Induction and reversal of cell adhesion-dependent multicellular drug resistance in solid breast tumors. Hum Cell, 9, 257-64

Kim,R, Osaki, A., Toge, T. (2001) Pharmacokinetic and biochemical analysis in the treatment of weekly paclitaxel in relapsed breast cancer. Oncol Rep, 8, 171-6

Kiura, K., Ohnoshi, T., Tabata, M., Shibayama, T. and Kimura, I. (1993) Establishment of an adriamycin-resistant subline of human small cell lung cancer showing multifactorial mechanisms of resistance. Acta Med Okayama, 47, 191-7.

Knoop, A.S., Bentzen, S.M., Nielsen, M.M., Rasmussen, B.B., Rose, C. (2001) Value of epidermal growth factor receptor, HER2, p53, and steroid receptors in predicting the efficacy of tamoxifen in high-risk postmenopausal breast cancer patients. J Clin Oncol, 19, 3376-84

Knowlden, J.M., Gee, J.M., Seery, L.T., Farrow, L., Gullick, W.J., Ellis, I.O., Blamey, R.W., Robertson, J.F. and Nicholson, R.I. (1998) C-erbB-3 and c-erbB-4 expression is a feature of the endocrine responsive phenotype in clinical breast cancer. Oncogene, 17, 1949-1957.

Konecny, G., Fritz, M., Untch, M., Lebeau, A., Felber, M., Lude, S., Beryt, M., Hepp, H., Slamon, D. and Pegram, M. (2001) HER-2/neu overexpression and *in vitro*

chemosensitivity to CMF and FEC in primary breast cancer. Breast Cancer Res Treat, 69, 53-63

Kool M, van der Linden M, de Haas M, Scheffer GL, de Vree JM, Smith AJ, Jansen G, Peters GJ, Ponne N, Scheper RJ, Elferink RP, Baas F, Borst P. (1999) MRP3, an organic anion transporter able to transport anti-cancer drugs. Proc Natl Acad Sci U S A, 96, 6914-9

Krajewski, S., thor, A.D., Edgerton, S.M., Moore II, D.H., Krajewska, M. and Read, J.C. (1997) Analysis of Bax and Bcl-2 expression in p53-immunopositive breast cancers. Clin Cancer Res, 3, 199-208.

Kumar, R., Mandal, M., Lipton, A., Harvey, H. and Thompson, C.B. (1996) Overexpression of HER2 modulates Bcl-2, Bcl-X_L and tamoxifen in human MCF-7 breast cancer cells. Clin Cancer Res, 2, 1215-1219.

Kuriyama M, Tsutsui K, Tsutsui K, Ono Y, Tamiya T, Matsumoto K, Furuta T, Ohmoto T. (1997) Induction of resistance to etoposide and adriamycin in a human glioma cell line treated with antisense oligodeoxynucleotide complementary to the messenger ribonucleic acid of deoxyribonucleic acid topoisomerase II alpha. Neurol Med Chir (Tokyo, 37, 655-61

Lai, G.M., Moscow, J.A., Alvarez, M.G., Fojo, A.T. and Bates, S.E. (1991) Contribution of glutathione and glutathione-dependent enzymes in the reversal of adriamycin resistance in colon carcinoma cell lines. Int J Cancer, 49, 688-95.

Lauwaet T, Oliveira MJ, Mareel M, Leroy A. (2000) Molecular mechanisms of invasion by cancer cells, leukocytes and microorganisms. Microbes Infect, 2, 923-31

Lebwohl D, Canetta R. (1998) Clinical development of platinum complexes in cancer therapy: an historical perspective and an update. Eur J Cancer, 34, 1522-34

Lee WP, Lee CL, Lin HC. (1996) Glutathione S-transferase and glutathione peroxidase are essential in the early stage of adriamycin resistance before P-glycoprotein overexpression in HOB1 lymphoma cells. Cancer Chemother Pharmacol, 38, 45-51

Lee, J.C., Wang, S.T., Chow, N.H., Yang, H.B. (2002) Investigation of the prognostic value of coexpressed erbB family members for the survival of colorectal cancer patients after curative surgery. Eur J Cancer, 38, 1065-71

Lehnert M, Emerson S, Dalton WS, de Giuli R, Salmon SE. (1993) *In vitro* evaluation of chemosensitizers for clinical reversal of P-glycoprotein-associated Taxol resistance. : J Natl Cancer Inst Monogr, 15, 63-7

Li, Y., Bhuiyan, M., Alhasan, S., Senderowicz, A.M., Sarkar, F.H. (2000) Induction of apoptosis and inhibition of c-erbB-2 in breast cancer cells by flavopiridol. Clin Cancer Res, 6, 223-9

Li, Y., Bhuiyan, M., Sarkar, F.H. (1999) Induction of apoptosis and inhibition of c-erbB-2 in MDA-MB-435 cells by genistein. Int J Oncol, 15, 525-33

Liang Y, Meleady P, Cleary I, McDonnell S, Connolly L, Clynes M. (2001) Selection with melphalan or paclitaxel (Taxol) yields variants with different patterns of multidrug resistance, integrin expression and *in vitro* invasiveness. Eur J Cancer, 37, 1041-52

Liang, Y. (1999) Investigation of multidrug resistance and invasion in human cancer cell lines. PhD thesis, DCU, Glasnevin, Dublin 9.

Liao, G., Nagasaki, T. and Gundersen, G.G. (1995) Low concentrations of nocodazole interfere with fibroblast locomotion without significantly affecting microtubule level: implications for the role of dynamic microtubules in cell locomotion. J Cell Sci, 108, 3473-83

Ling, Y., Zhong, Y., Perez-Soler, R. (2001) Disruption of cell adhesion and caspase-mediated proteolysis of beta- and gamma-catenins and APC protein in paclitaxel-induced apoptosis. Mol Pharmacol, 59, 593-603

Liu, E., Thor, A., He, M., Barcos, M., Ljung, B.M. and Benz, C. (1992) The HER2 (c-erbB-2) oncogene is amplifed in *in situ* carcinomas of the breast. Oncogene, 7, 1027-1032.

Liu, H., Lei, X. and Han, R. (1998) Anti-invasion activity of several plant-originated anticancer drugs with different mechanism of action. Yao Xue Xue Bao, 33, 18-21

Longley, D.B., Ferguson, P.R., Boyer, J., Latif, T., Lynch, M., Maxwell, P., Harkin, D.P. and Johnston, P.G. (2001) Characterization of a thymidylate synthase (TS)-inducible cell line: a model system for studying sensitivity to TS- and non-TS-targeted chemotherapies. Clin Cancer Res, 7, 3533-9.

Mader RM, Muller M, Steger GG. (1998) Resistance to 5-fluorouracil. Gen Pharmacol, 31, 661-6

Mandelbaum-Shavit, F. and Ramu, A. (1987) Dihydrofolate reductase activity in adriamycin and methotrexate sensitive and resistant P388 leukemia cells. Cell Biol Int Rep, 11, 389-96.

Markogiannakis, E., Georgoulias, V., Margioris, A.N., Zoumakis, E., Stournaras, C. and Gravanis, A. Estrogens and glucocorticoids induce the expression of c-erbB-2/neu receptor in Ishikawa human endometrial cells. Life Sci, 61, 1083-1095.

Martinez, C., Garcia-Martin, E., Pizarro, R.M., Garcia-Gamito, F.J., Agundez, J.A. (2002) Expression of paclitaxel-inactivating CYP3A activity in human colorectal cancer: implications for drug therapy. Br J Cancer, 87, 681-6

Marx, D., Schauer, A., Reiche, C., May, A., Ummenhofer, L., Reles, A., Rauschecker, H., Sauer, R. and Schumacher, M. (1990) C-erbB2 expression in correlation to other biological parameters of breast cancer. J Cancer Res Clin Oncol, 116, 15-20.

Masanek, U., Stammler, G. and Volm, M. (1997) Messenger RNA expression of resistance proteins and related factors in human ovarian carcinoma cell lines resistant to doxorubicin, taxol and cisplatin. Anticancer Drugs, 8, 189-98.

Maurer, C.A., Friess, H., Kretschmann, B., Zimmermann, A., Stauffer, A., Baer, H.U., Korc, M., and Buchler, M.W. (1998) Increased expression of erbB3 in colorectal cancer is associated with concomitant increase in the level of erbB2. Hum Pathol, 29, 771-7.

Mechetner E, Kyshtoobayeva A, Zonis S, Kim H, Stroup R, Garcia R, Parker RJ, Fruehauf JP. (1998) Levels of multidrug resistance (MDR1) P-glycoprotein expression by human breast cancer correlate with *in vitro* resistance to taxol and doxorubicin. Clin Cancer Res, 4, 389-98

Merimsky, O., Issakov, J., Bickels, J., Kollender, Y., Flusser, G., Soyfer, V., Schwartz, I., Inbar, M. and Meller, I. (2002) ErbB-4 expression in limb soft-tissue sarcoma: correlation with the results of neoadjuvant chemotherapy. Eur J Cancer, 38, 1335-42

Meyer, T. and Hart, I.R. (1998) Mechanisms of tumour metastasis. Eur J Cancer, 34, 214-221.

Molinari, A., Calcabrini, A., Meschini, S., Marra, M., Stringaro, A., Toccacieli, L., Cianfriglia, M. and Arancia, G. (2002) What is the relationship between P-glycoprotein and adhesion molecule expression in melanoma cells? Melanoma Res, 12, 109-14.

Montgomery, R.B., Guzman, J., O'Rourke, D.M., Stahl, W.L. (2000) Expression of oncogenic epidermal growth factor receptor family kinases induces paclitaxel resistance and alters beta-tubulin isotype expression. J Biol Chem, 275, 17358-63

Myoung, H., Hong, S.D., Kim, Y.Y., Hong, S.P. and Kim, M.J. (2001) Evaluation of the anti-tumor and anti-angiogenic effect of paclitaxel and thalidomide on the xenotransplanted oral squamous cell carcinoma. Cancer Lett, 163, 191-200

Nguyen, D.M., Chen, A., Mixon, A., Schrump, D.S. (1999) Sequence-dependent enhancement of paclitaxel toxicity in non-small cell lung cancer by 17-allylamino 17-demethoxygeldanamycin. J Thorac Cardiovasc Surg, 118, 908-15

NicAmhlaoibh, R., Heenan, M., Cleary, I., Touhey, S., O'Loughlin, C., Daly, C., Nunez, G.,Scanlon, K.J. and Clynes, M. (1999) Altered expression of mRNAs for apoptosis-modulating proteins in a low level multidrug resistant variant of a human lung carcinoma cell line that also expresses mdr1 mRNA. Int J Cancer, 82, 368-76.

Nicholson, R.I., Gee, J.M., Harper, M.E. (2001) EGFR and cancer prognosis. Eur J Cancer, 37, Suppl 4, S9-15

Nicholson, R.I., McClelland, R.A., Finlay, P., Eaton, C.L., Gullick, W.J., Dixon, A.R., Robertson, J.F., Ellis, I.O. and Blamey, R.W. (1993) Relationship between EGF-R, c-erbB-2 protein expression and Ki67 immunostaining in breast cancer and hormone sensitivity. Eur J Cancer. 29A, 1018-23.

O-charoenrat, P., Rhys-Evans, P., Court, W.J., Box, G.M., Eccles, S.A. (1999) Differential modulation of proliferation, matrix metalloproteinase expression and invasion of human head and neck squamous carcinoma cells by c-erbB ligands. Clin Exp Metastasis, 17, 631-9

O-charoenrat, P., Rhys-Evans, P.H., Archer, D.J, Eccles, S.A. (2002) C-erbB receptors in squamous cell carcinomas of the head and neck: clinical significance and correlation with matrix metalloproteinases and vascular endothelial growth factors. Oral Oncol, 38, 73-80

Ochiai, A., Akimoto, S., Kanai, Y., Shibata, T., Oyama, T., Hirohashi, S. (1994) c erbB-2 gene product associates with catenins in human cancer cells. Biochem Biophys Res Commun, 205, 73-8

O'Dwyer, P.J., Benson, A.B. 3rd. (2002) Epidermal growth factor receptor-targeted therapy in colorectal cancer. Semin Oncol, 29, (5 Suppl 14), 10-7

Olayioye, M.A., Graus-Porta, D., Beerli, R.R., Rohrer, J., Gay, B. And Hynes, N.E. (1998) ErbB-1 and ErbB-2 acquire distinct signaling properties dependant on their dimerization partner. Molecular and Cellular Biology, 18, 5042-5051.

Oldham, E.A., Li, C., Ke, S., Wallace, S., Huang, P. (2000) Comparison of action of paclitaxel and poly(L-glutamic acid)-paclitaxel conjugate in human breast cancer cells. Int J Oncol, 16, 125-32

Ooi, A., Kobayashi, M., Mai, M. And Nakanishi, I. (1997) Amplification of c-erbB-2 in gastric cancer: Detection in formalin-fixed, paraffin-embedded tissue by fluorescence *in situ* hybridisation. Laboratory Investigations, 78, 345-351.

Orr, M.S., O'Connor, P.M., Kohn, K.W. (2000) Effects of c-erbB2 overexpression on the drug sensitivities of normal human mammary epithelial cells. J Natl Cancer Inst, 92, 987-94

Osmak, M., Kapitanovic, S., Vrhovec, I., Beketic-Oreskovic, L., Jernej, B., Eljuga, D., Skrk, J. (1997) Characterization of human breast adenocarcinoma SK-BR-3 cells resistant to doxorubicin. Neoplasma, 44, 157-62

Paik, S., Bryant, J., Park, C., Fisher, B., Tan-Chiu, E., Hyams, D., Fisher, E.R., Lippman, M.E., Wickerham, D.L. and Wolmark, N. (1998) ErbB-2 and response to doxorubicin in patients with axillary node-positive, hormone receptor-negative breast cancer. J Natl Cancer Inst, 90, 1361-1370.

Paik, S., Bryant, J., Tan-Chiu, E., Yothers, G., Park, C., Wickerham, D.L. and Wolmark, N. (2000) HER2 and choice of adjuvant chemotherapy for invasive breast cancer: National Surgical Adjuvant Breast and Bowel Project Protocol B-15. J Natl Cancer Inst, 92, 1991-8

Parekh H, Wiesen K, Simpkins H. (1997) Acquisition of taxol resistance via P-glycoprotein- and non-P-glycoprotein-mediated mechanisms in human ovarian carcinoma cells. Biochem Pharmacol, 53, 461-70

Parkes, H.C., Lillycrop, K., Howell, A. And Craig, R.K. (1990) C-erbB-2 mRNA expression in human breast tumours: comparison with c-erbB-2 DNA amplification and correlation with prognosis. Br J Cancer, 61, 39-45.

Pegram MD, Finn RS, Arzoo K, Beryt M, Pietras RJ, Slamon DJ. (1997) The effect of HER-2/neu overexpression on chemotherapeutic drug sensitivity in human breast and ovarian cancer cells. Oncogene, 15, 537-47

Pegram, M., Hsu, S., Lewis, G., Pietras, R., Beryt, M., Sliwkowski, M., Coombs, D., Baly, D., Kabbinavar, F., Slamon, D. (1999) Inhibitory effects of combinations of HER-2/neu antibody and chemotherapeutic agents used for treatment of human breast cancers. Oncogene, 18, 2241-51

Petit, T., Borel, C., Ghnassia, J.P., Rodier, J.F., Escande, A., Mors, R. and Haegele, P. (2001) Chemotherapy response of breast cancer depends on HER-2 status and anthracycline dose intensity in the neoadjuvant setting. Clin Cancer Res, 7, 1577-81

Pfeiffer, P., Clausen, P.P., Andersen, K. and Rose, C. (1996) Lack of prognostic significance of epidermal growth factor receptor and the oncoprotein $p185^{HER-2}$ in patients with systemically untreated non-small-cell lung cancer: an immunohistochemical study on cryosections. Br J Cancer, 74, 86-91.

Prenzel N, Fischer OM, Streit S, Hart S, Ullrich A. (2001) The epidermal growth factor receptor family as a central element for cellular signal transduction and diversification. Endocr Relat Cancer, 8, 11-31

Prost, S., Lê, M.G., Douc-Rasy, S., Ahomadegbe, J.C., Spielmann, M., Guérin, M. and Riou, G. (1994) Association of c-erbB2 gene amplification with poor prognosis in non-inflammatory breast carcinomas but not in carcinomas of the inflammatory type. Int J Cancer, 58, 763-768.

Puricelli, L., Proiettii, C.J., Labriola, L., Salatino, M., Balana, M.E., Ghiso, J.A., Lupu, R., Pignataro, O.P., Charreau, E.H., Bal de Kier Joffe, E., Elizalde, P.V. (2002) Heregulin inhibits proliferation via ERKs and phosphatidyl-inositol 3-kinase activation but regulates urokinase plasminogen activator independently of these pathways in metastatic mammary tumor cells. Int J Cancer, 100, 642-53

Quénel, N., Wafflart, J., Bonichon, F., de Mascarel, I., Trojani, M., Durand, M., Avril, A. and Coindre, J.M. (1995) The prognostic value of c-erbB2 in primary breast carcinomas: A study of 942 cases. Breast Cancer Res Treat, 35, 283-291.

Quinn, C.M., Ostrowski, J.L., Lane, S.A., Loney, D.P., Teasdale, J. and Benson, F.A. (1994) C-erbB-3 protein expression in human breast cancer: comparison with other tumour variables and survival. Histopathology, 25, 247-52.

Rahman, A., Korzekwa, K.R., Grogan, J., Gonzalez, F.J. and Harris, J.W. (1994) Selective biotransformation of taxol to 6 alpha-hydroxytaxol by human cytochrome P450 2C8. Cancer Res, 54, 5543-6.

Rajkumar, T. and Gullick, W.J. (1994) The type I growth factor receptors in human breast cancer. Breast Cancer Res Treat, 29, 3-9.

Rajkumar, T., Gooden, C.S., Lemoine, N.R. and Gullick, W.J. (1993) Expression of the c-erbB-3 protein in gastrointestinal tract tumours determined by monoclonal antibody RTJ1. J Pathol, 170, 271-8.

Reinecke, P., Schmitz, M., Schneider, E.M., Gabbert, H.E., Gerharz, C.D. (2000) Multidrug resistance phenotype and paclitaxel (Taxol) sensitivity in human renal carcinoma cell lines of different histologic types. Cancer Invest, 18, 614-25

Repesh, L.A., Drake, S.R., Warner, M.C., Downing, S.W., Jyring, R., Seftor, E.A., Hendrix, M.J. and McCarthy, J.B. (1993) Adriamycin-induced inhibition of melanoma cell invasion is correlated with decreases in tumor cell motility and increases in focal contact formation. Clin Exp Metastasis. 11, 91-102.

Revillion, F., Hebbar, M., Bonneterre, J. and Peyrat, J.P. (1996) Plasma c-erbB2 concentrations in relation to chemotherapy in breast cancer patients. Eur J Cancer, 32A, 231-234.

Rintoul, R.C. and Sethi, T. (2002) Extracellular matrix regulation of drug resistance in small-cell lung cancer. Clin Sci (Lond), 102, 417-24.

Robertson, K.W., Reeves, J.R., Smith, G., Keith, W.N., Ozanne, B.W. and Cooke, T.G. (1996) Quantification of epidermal growth factor reeptor ans c-erbB-2 in human breast cancer. Cancer Res, 56, 3823-3830.

Roetger, A., Merschjann, A., Dittmar, T., Jackisch, C., Barnekow, A. and Brandt, B. (1998) Selection of potentially metastatic subpopulations expressing c-erbB-2 from breast cancer tissue by use of an extravasation model. Am J Pathol, 153, 1797-1806.

Roy SN, Horwitz SB. (1985) A phosphoglycoprotein associated with taxol resistance in J774.2 cells. Cancer Res, 45, 3856-63

Sakorafas GH, Krespis E, Pavlakis G. (2002) Risk estimation for breast cancer development; a clinical perspective. Surg Oncol, 10, 183-92

Sawyer, C., Hiles, I., Page, M., Crompton, M. and Dean, C. (1998) Two erbB-4 transcripts are expressed in normal breast and in most breast cancers. Oncogene, 17, 919-24

Scoccia, B., Lee, Y.M., Niederberger, C. and Ilekis, J.V. (1998) Expression of the ErbB family of receptors in ovarian cancer. J Soc Gynecol Investig, 5, 161-5

Seidman, A.D., Fornier, M.N., Esteva, F.J., Tan, L., Kaptain, S., Bach, A., Panageas, K.S., Arroyo, C., Valero, V., Currie, V., Gilewski, T., Theodoulou, M., Moynahan, M.E., Moasser, M., Sklarin, N., Dickler, M., D'Andrea, G., Cristofanilli, M., Rivera, E., Hortobagyi, G.N., Norton, L., Hudis, C.A. (2001) Weekly trastuzumab and paclitaxel therapy for metastatic breast cancer with analysis of efficacy by HER2 immunophenotype and gene amplification. J Clin Oncol, 19, 2587-95

Sgadari, C., Toschi, E., Palladino, C., Barillari, G., Carlei, D., Cereseto, A., Ciccolella, C., Yarchoan, R., Monini, P., Sturzl, M. and Ensoli, B. (2000) Mechanism of paclitaxel activity in Kaposi's sarcoma. J Immunol, 165, 509-17

Shibata, T., Ochiai, A., Kanai, Y., Akimoto, S., Gotoh, M., Yasui, N., Machinami, R. and Hirohashi, S. (1996) Dominant negative inhibition of the association between β-catenin and c-erbB-2 by N-terminally deleted β-catenin suppresses the invasion and metastasis of cancer cells. Oncogene, 13, 883-889.

Silbergeld, D.L., Chicoine, M.R. and Madsen, C.L. (1995) *In vitro* assessment of Taxol for human glioblastoma: chemosensitivity and cellular locomotion. Anticancer Drugs, 6, 270-6.

Sjostrom, J., Collan, J., von Boguslawski, K., Franssila, K., Bengtsson, N.O., Mjaaland, I., Malmstrom, P., Ostenstad, B., Wist, E., Valvere, V., Bergh, J., Skiold-Petterson, D., Saksela, E., Blomqvist, C. (2002) C-erbB-2 expression does not predict response to docetaxel or sequential methotrexate and 5-fluorouracil in advanced breast cancer. Eur J Cancer, 38, 535-42

Skovsgaard T, Nielsen D, Maare C, Wassermann K. (1994) Cellular resistance to cancer chemotherapy. Int Rev Cytol, 156, 77-157

Slamon, D.J., Leyland-Jones, B., Shak, S., Fuchs, H., Paton, V., Bajamonde, A., Fleming, T., Eiermann, W., Wolter, J., Pegram, M., Baselga, J. and Norton, L. (2001) Use of chemotherapy plus a monoclonal antibody against HER2 for metastatic breast cancer that overexpresses HER2. N Engl J Med, 344, 783-92

Sleijfer, S., Asschert, J.G., Timmer-Bosscha, H., Mulder, N.H. (1998) Enhanced sensitivity to tumor necrosis factor-alpha in doxorubicin-resistant tumor cell lines due to down-regulated c-erbB2. Int J Cancer, 77, 101-6

Sloane, B.F. (1990) Cathepsin B and cystatins: evidence for a role in cancer progression. Semin Cancer Biol, 1, 137-52.

Smith, B.D., Smith, G.L., Carter, D., DiGiovanna, M.P., Kasowitz, K.M., Sasaki, C.T., Haffty, B.G. (2001) Molecular marker expression in oral and oropharyngeal squamous cell carcinoma. Arch Otolaryngol Head Neck Surg, 127, 780-5

Smith, V., Hobbs, S., Court, W., Eccles, S., Workman, P. and Kelland, L.R. (2002) ErbB2 overexpression in an ovarian cancer cell line confers sensitivity to the HSP90 inhibitor geldanamycin. Anticancer Res, 22, 1993-9.

Soubeyran, I., Quénel, N., Mauriac, L., Durand, M., Bonichon, F. and Coindre, J.M. (1996) Variation of hormonal receptor, pS2, c-erbB2 and GSTp contents in breast carcinomas under tamoxifen: a study of 74 cases. Br J Cancer, 73, 735-743.

Speirs V, Malone C, Walton DS, Kerin MJ, Atkin SL. (1999) Increased expression of estrogen receptor beta mRNA in tamoxifen-resistant breast cancer patients. Cancer, 59, 5421-4

Speirs, V., Malone, C., Walton, D.S., Kerin, M.J., Atkin, S.L. (1999) Increased expression of estrogen receptor beta mRNA in tamoxifen-resistant breast cancer patients. Cancer Res, 59, 5421-4

Spencer, K.S., Graus-Porta, D., Leng, J., Hynes, N.E., Klemke, R.L. (2000) ErbB2 is necessary for induction of carcinoma cell invasion by ErbB family receptor tyrosine kinases. J Cell Biol, 148, 385-97

Spigel, D.R., Burstein, H.J. (2002) HER2 overexpressing metastatic breast cancer. Curr Treat Options Oncol, 3, 163-74

Srinivasan, R., Poulsom, R., Hurst, H.C. and Gullick, W.J. (1998) Expression of the c-erbB-4/HER4 protein and mRNA in normal human fetal and adult tissues and in a survey of nine solid tumour types. J Pathol, 185, 236-245.

Stal, O., Borg, A., Ferno, M., Kallstrom, A.C., Malmstrom, P., Nordenskjold, B. (2000) ErbB2 status and the benefit from two or five years of adjuvant tamoxifen in postmenopausal early stage breast cancer. Ann Oncol, 11, 1545-50

Stearns, M. E. and Wang, M. (1992) Taxol blocks processes essential for prostate tumor cell (PC-3 ML) invasion and metastases. Cancer Res, 52, 3776-81.

Storkel, S., Reichert, T., Reiffen, K.A., Wagner, W. (1993) EGFR and PCNA expression in oral squamous cell carcinomas--a valuable tool in estimating the patient's prognosis. Eur J Cancer B Oral Oncol, 29B, 273-7

Stracke, M.L., Soroushm M., Liottam L.A. and Schiffmannm E. (1993) Cytoskeletal agents inhibit motility and adherence of human tumor cells. Kidney Int, 43, 151-7

Suo, Z., Emilsen, E., Tveit, K.M. and Nesland, J.M. (1998) Type I protein kinases in benign and malignant breast cancers. Histopathology, 33, 514-521.

Suo, Z., Risberg, B., Kalsson, M.G., Willman, K., Tierens, A., Skovlund, E., Nesland, J.M. (2002) EGFR family expression in breast carcinomas. c-erbB-2 and c-erbB-4 receptors have different effects on survival. J Pathol, 196, 17-25

Suo, Z., Yang, H., Mei, Q., Skovlund, E., Cui, J., Nesland, J.M. (2001) Type 1 protein tyrosine kinases in Chinese breast carcinomas: a clinicopathologic study. Int J Surg Pathol, 9, 177-87

Suzuki, T., Anderegg, B., Ohkawa, T., Irie, A., Engebraaten, O., Halks-Miller, M., Holm, P.S., Curiel, D.T., Kashani-Sabet, M., Scanlon, K.J. (2000) Adenovirus-mediated ribozyme targeting of HER-2/neu inhibits *in vivo* growth of breast cancer cells. Gene Ther, 7, 241-8

Tan, M., Grijalva, R., Yu, D. (1999) Heregulin beta1-activated phosphatidylinositol 3-kinase enhances aggregation of MCF-7 breast cancer cells independent of extracellular signal-regulated kinase. Cancer Res, 59, 1620-5

Tan, M., Jing, T., Lan, K.H., Neal, C.L., Li, P., Lee, S., Fang, D., Nagata, Y., Liu, J., Arlinghaus, R., Hung, M.C., Yu, D. (2002) Phosphorylation on tyrosine-15 of p34(Cdc2) by ErbB2 inhibits p34(Cdc2) activation and is involved in resistance to taxol-induced apoptosis. Mol Cell, 9, 993-1004

Tan, M., Yao, J. and Yu, D. (1997) Overexpression of the c-erbB-2 gene enhanced intrinsic metastasis potential in human breast cancer cells without increasing their transforming abilities. Cancer Res, 57, 1199-1205.

Terzis, A.J., Thorsen, F., Heese, O., Visted, T., Bjerkvig, R., Dahl, O., Arnold, H. and Gundersen, G. (1997) Proliferation, migration and invasion of human glioma cells exposed to paclitaxel (Taxol) *in vitro*. Br J Cancer, 75, 1744-52

Todd, D.M., Miller, J.M., Rubin, A.D. and DeBari, V.A. (1992) Amplification of the c-erbB-2 oncogene in breast cancer and its relationship to estrogen and progesterone receptors. Diagn Oncol, 2, 313-317.

Touhey S, O'Connor R, Plunkett S, Maguire A, Clynes M. (2002) Structure-activity relationship of indomethacin analogues for MRP-1, COX-1 and COX-2 inhibition. identification of novel chemotherapeutic drug resistance modulators. Eur J Cancer, 38, 1661-70

Towbin, H., Staehelin, T. and Gordon, J. (1979) Electrophoretic transfer of proteins from polyacrylamide gels to nitrocellulose sheets: procedures and some applications. Proc Natl Acad Sci USA, 76, 4350-4354.

Tsai, C.M., Levitzki, A., Wu, L.H., Chang, K.T., Cheng, C.C., Gazit, A. and Perng R.P. (1996) Enhancement of chemosensitivity by tyrphostin AG825 in high-p185^{neu} expressing non-small cell lung cancer cells. Cancer Res, 56, 1068-1074.

Tsutsui, S., Ohno, S., Murakami, S., Hachitanda, Y., Oda, S. (2002) Prognostic value of epidermal growth factor receptor (EGFR) and its relationship to the estrogen receptor status in 1029 patients with breast cancer. Breast Cancer Res Treat, 71, 67-75

Tzahar, E., Pinkas-Kramarski, R., Moyer, J.D., Klapper, L.N., Alroy, I., Levkowitz, G., Shelly, M., Henis, S., Eisenstein, M., Ratzkin, B.J., Sela, M., Andrews, G.C. and Yarden, Y. (1997) Bivalence of EGF-like ligands drives the ErbB signaling network. EMBO, 16, 4938-4950.

Uchiyama-Kokubu N, Watanabe T. (2001) Establishment and characterization of adriamycin-resistant human colorectal adenocarcinoma HCT-15 cell lines with multidrug resistance. Anticancer Drugs, 12, 769-79

Vafa, A., Zhang, Y., Sikes, R.A., Marengo, S.R. (1998) Overexpression of p185erbB2/neu in the NbE prostatic epithelial cell line increases cellular spreading and the expression of integrin alpha6beta1. Int J Oncol, 13, 1191-7

Vaishampayan U, Parchment RE, Jasti BR, Hussain M. (1999) Taxanes: an overview of the pharmacokinetics and pharmacodynamics. Urology, 54, 6A Suppl, 22-9

Van Poznak, C., Tan, L., Panageas, K.S., Arroyo, C.D., Hudis, C., Norton, L., Seidman, A.D. (2002) Assessment of molecular markers of clinical sensitivity to single-agent taxane therapy for metastatic breast cancer. J Clin Oncol, 20, 19-26

Vanhoefer, U., Cao, S., Minderman, H., Toth, K., Scheper, R.J., Slovak, M.L. and Rustum, Y.M. (1996) PAK-104P, a pyridine analogue, reverses paclitaxel and doxorubicin resistance in cell lines and nude mice bearing xenografts that overexpress the multidrug resistance protein. Clin Cancer Res, 2, 369-77

Vargas-Roig, L.M., Gago, F.E., Tello, O., Martin de Civetta, M.T., Ciocca, D.R. (1999) c-erbB-2 (HER-2/neu) protein and drug resistance in breast cancer patients treated with induction chemotherapy. Int J Cancer, 84, 129-34

Verbeek, B.S., Adriaansen-Slot, S.S, Vroom, T.M., Beckers, T. and Rijksen, G. (1998) Overexpression of EGFR and c-erbB2 causes enhanced cell migration in human breast cancer cells and NIH3T3 fibroblasts. FEBS Letters, 425, 145-150.

Vered, M., Braunstein, E., Buchner, A. (2002) Immunohistochemical study of epidermal growth factor receptor in adenoid cystic carcinoma of salivary gland origin. Head Neck, 24, 632-6

Verschueren, H., Dewit, J., De Braekeleer, J., Schirrmacher, V. and De Baetselier, P. (1994) Motility and invasive potency of murine T-lymphoma cells: effect of microtubule inhibitors. Cell Biol Int 18, 11-9

Vincent-Salomon, A., Carton, M., Freneaux, P., Palangie, T., Beuzeboc, P., Mouret, E., de Cremoux, P., Coue, O., Zafrani, B., Nicolas, A., Clough, K., Fourquet, A., Pouillart, P., Sastre-Garau, X. (2000) ERBB2 overexpression in breast carcinomas: no positive correlation with complete pathological response to preoperative high-dose anthracycline-based chemotherapy. Eur J Cancer, 36, 586-91

Volm, M. and Mattern, J. Expression of topoisomerase II, catalase, metallothionein and thymidylate-synthase in human squamous cell lung carcinomas and their correlation with doxorubicin resistance and with patients' smoking habits. Carcinogenesis, 13, 1947-50.

Volm, M., Kastel, M., Mattern, J., Efferth, T. (1993) Expression of resistance factors (P-glycoprotein, glutathione S-transferase-pi, and topoisomerase II) and their interrelationship to proto-oncogene products in renal cell carcinomas. Cancer, 71, 3981-7

Wani MC, Taylor HL, Wall ME, Coggon P, McPhail AT. (1971) Plant antitumor agents. VI. The isolation and structure of taxol, a novel antileukemic and antitumor agent from Taxus brevifolia. J Am Chem Soc, 93, 2325-7

Waterman, H., Sabanai, I., Geiger, B. and Yarden, Y. (1998) Alternative intracellular routing of ErbB receptors may determine signaling potency. J Biol Chem, 273, 13819-27.

Welch, D.R., Lobl, T.J., Seftor, E.A., Wack, P.J., Aeed, P.A., Yohem, K.H., Seftor, R.E., Hendrix, M.J. (1989) Use of the Membrane Invasion Culture System (MICS) as a screen for anti-invasive agents. Int J Cancer, 43, 449-57

Wells, C.A., McGregor, I.L., Makunura, C.N., Yeomans, P. and Davies, J.D. (1995) Apocrine adenosis: A precursor of aggressive breast cancer? J Clin Pathol, 48, 737-742.

Westerlund, A., Hujanen, E., Hoyhtya, M., Puistola, U. and Turpeenniemi-Hujanen, T. (1997) Ovarian cancer cell invasion is inhibited by paclitaxel. Clin Exp Metastasis, 15, 318-28

Wiechen, K., Karaaslan, S. and Dietel, M. (1999) Involvement of the c-erbB-2 oncogene product in the EGF-induced cell motility of SK-OV-3 ovarian cancer cells. Int J Cancer, 83, 409-14.

Wilding J, Vousden KH, Soutter WP, McCrea PD, Del Buono R, Pignatelli M. (1996) E-cadherin transfection down-regulates the epidermal growth factor receptor and reverses the invasive phenotype of human papilloma virus-transfected keratinocytes. Cancer Res, 56, 5285-92

Woesner, B.J. Jr. (1991) Matrix metalloproteinases and theeeir inhibitors in connective tissue remodelling. FASEB J, 5, 2145-54.

Wright, C., Nicholson, S., Angus, B., Sainsbury, J.R., Farndon, J., Cairns, J., Harris, A.L. and Horne, C.H. (1992) Relationship between c-erbB-2 protein product expression and response to endocrine therapy in advanced breast cancer. Br J Cancer. 65, 118-121.

Xu, F., Yu, Y., Le, X.F., Boyer, C., Mills, G.B., Bast, R.C. Jr. (1999) The outcome of heregulin-induced activation of ovarian cancer cells depends on the relative levels of HER-2 and HER-3 expression. Clin Cancer Res 5, 3653-60

Xu, F.J., Stack, S., Boyer, C., O'Briant, K., Whitaker, R., Mills, G.B., Yu, Y.H., Bast, R.C. Jr. (1997) Heregulin and agonistic anti-p185(c-erbB2) antibodies inhibit proliferation but increase invasiveness of breast cancer cells that overexpress p185(c-erbB2): increased invasiveness may contribute to poor prognosis. Clin Cancer Res, 3, 1629-34

Yang, S.Z., Kohno, N., Kondo, K., Yokoyama, A., Hamada, H., Hiwada, K. and Miyake, M. (1999) Adriamycin activates E-cadherin-mediated cell-cell adhesion in human breast cancer cells. Int J Oncol, 15, 1109-15.

Yoo YD, Kang S, Kang YK. (1998) Cellular resistance to adriamycin conferred by enhanced Rb expression is associated with increased MDR1 expression. Biochem Biophys Res Commun, 249, 6-10

Young LC, Campling BG, Voskoglou-Nomikos T, Cole SP, Deeley RG, Gerlach JH. (1999) Expression of multidrug resistance protein-related genes in lung cancer: correlation with drug response. Clin Cancer Res, 5, 673-80

Yu D, Liu B, Jing T, Sun D, Price JE, Singletary SE, Ibrahim N, Hortobagyi GN, Hung MC. (1998B) Overexpression of both p185c-erbB2 and p170mdr-1 renders breast cancer cells highly resistant to taxol. Oncogene , 16, 2087-94

Yu, D., Hamada, J., Zhang, H., Nicolson, G.L., Hung, M.C. (1992) Mechanisms of c-erbB2/neu oncogene-induced metastasis and repression of metastatic properties by adenovirus 5 E1A gene products. Oncogene, 7, 2263-70

Yu, D., Jing, T., Liu, B., Yao, J., Tan, M., McDonnell, T.J., Hung, M.C. (1998) Overexpression of ErbB2 blocks Taxol-induced apoptosis by upregulation of p21Cip1, which inhibits p34Cdc2 kinase. Mol Cell, 2, 581-91

Yu, D., Liu, B., Jing, T., Sun, D., Price, J.E., Singletary, S.E., Ibrahim, N., Hortobagyi, G.N. and Hung, M.C. (1998) Overexpression of both $p185^{c\text{-}erbB2}$ and $p170^{mdr\text{-}1}$ renders breast cancer cells highly resistant to taxol. Oncogene, 16, 2087-2094.

Yu, D., Liu, B., Tan, M., Li, J., Wang, S.S. and Hung, M.C. (1996) Overexpression of c-erbB-2/neu in breast cancer cells confers increased resistance to Taxol via MDR-1 independent mechanisms. Oncogene, 13, 1359-1365.

Yu, H., Levesque, M.A., Khosravi, M.J., Papanastasiou-Diamandi, A., Clark, G.M. and Diamandis, E.P. (1996) Associations between insulin-like growth factors and their binding proteins and other prognostic indicators in breast cancer. Br J Cancer, 74, 1242-1247.

Zaffaroni, N., Pennati, M., Colella, G., Perego, P., Supino, R., Gatti, L., Pilotti, S., Zunino, F., Daidone, M.G. (2002) Expression of the anti-apoptotic gene survivin correlates with taxol resistance in human ovarian cancer. Cell Mol Life, 59, 1406-12

Zhang, L., Lau, Y.K., Xi, L., Hong, R.L., Kim, D., Chen, C.F., Hortobagyi, G.N., Chang, C.J. and Hung, M.C. (1998) Tyrosine kinase inhibitors, emodin and its derivative repress HER2/neu-induced cellular transformation and metastasis-associated properties. Oncogene, 16, 2855-2863.

Zhang, L., Lau, Y.K., Xia, W., Hortobagyi, G.N., Hung, M.C. (1999) Tyrosine kinase inhibitor emodin suppresses growth of HER-2/neu-overexpressing breast cancer cells in athymic mice and sensitizes these cells to the inhibitory effect of paclitaxel. Clin Cancer Res, 5, 343-53

Zhu, D., Bourguignon, L. (1996) Overexpression of CD44 in pl85(neu)-transfected NIH3T3 cells promotes an up-regulation of hyaluronic acid-mediated membrane-cytoskeleton interaction and cell adhesion. Oncogene, 12, 2309-1

Zwick E, Bange J, Ullrich A. (2001) Receptor tyrosine kinase signalling as a target for cancer intervention strategies. Endocr Relat Cancer, 8, 161-73

Appendix A – Molecular Weights of Chemotherapeutic Agents Used in This Thesis

Drug	Molecular Weight
Adriamycin	543
Taxol	853
Taxotere	808
Methotrexate	454
Carboplatin	371
5-Fluorouracil	130
VP-16	588
Vincristine	824

Appendix B - Abbreviations

Ab	-	Antibody
ABC	-	ATP Binding Cassette
AMP	-	Adenosine Monophosphate
ATP	-	Adenosine-triphosphate
ATCC	-	American Tissue Culture Collection
BSA	-	Bovine Serum Albumin
cDNA	-	Complementary DNA
Da	-	Daltons
DEPC	-	Diethyl Pyrocarbonate
DHFR	-	Dihydrofolate reductase
DMEM	-	Dulbecco's Minimum Essential Medium
DMSO	-	Dimethyl sulfoxide
DNase	-	Deoxyribonuclease
DNA	-	Deoxyribonucleic Acid
dNTP	-	Deoxynucleotide triphosphate (N= A, C, T, G or U)
DTT	-	Dithiothreitol
ECM	-	Extracellular matrix
EDTA	-	Ethylene diamine tetracetic acid
FCS	-	Fetal Calf Serum
GSH	-	Glutathione
GST	-	Glutathione-S-Transferase
GS-X Pump	-	GSH-conjugate export carrier
HEPES	-	N-[2-Hydroxyethyl]piperazine-N'-[2-ethanesulphonic acid]
H-SFM	-	Ham's F12 Serum Free Medium
IC_{50}	-	Inhibitory Concentration 50%
Ig	-	Immunoglobulin
IMS	-	Industrial Methylated Spirits
LRP	-	Lung Resistance-related Protein
MAb	-	Monoclonal Antibody
MDR	-	Multiple Drug Resistance
MRP	-	Multidrug Resistance-associated Protein
MEM	-	Minimum Essential Medium
min	-	Minute(s)

MMLV-RT	-	Moloney Murine Leukemia Virus-Reverse Transcriptase
mRNA	-	Messenger RNA
Mr marker	-	Molecular Weight Marker
NCTCC	-	National Cell & Tissue Culture Centre
NSCLC	-	Non-Small Cell Lung Carcinoma
OD	-	Optical Density
Oligos	-	Oligonucleotides
P	-	Passage
PBS A	-	Phosphate Buffered Saline A
PEG	-	Polyethylene Glycol
PCR	-	Polymerase Chain Reaction
P-gp	-	P-glycoprotein
PKA	-	cAMP-dependant protein kinase
RNA	-	Ribonucleic Acid
RNase	-	Ribonuclease
RPA	-	RNase protection assay
RNasin	-	Ribonuclease Inhibitor
rpm	-	Revolution(s) Per Minute
RT-PCR	-	Reverse Transcriptase-PCR
Rz	-	Ribozyme
SCLC	-	Small Cell Lung Carcinoma
SDS	-	Sodium Doedecyl Sulphate
sec(s)	-	Second(s)
TBE	-	Tris-boric acid-EDTA buffer
TBS	-	Tris Buffered Saline
TE	-	Tris-EDTA
Topo I	-	Topoisomerase I
Topo IIα	-	Topoisomerase IIα
Topo IIβ	-	Topoisomerase IIβ
TEMED	-	N, N, N', N'-Tetramethyl-Ethylenediamine
Tris	-	Tris(hydroxymethyl)aminomethane
TS	-	Thymidylate Synthase
UHP	-	Ultra high pure water
v/v	-	volume/volume
w/v	-	weight per volume